ZooKeys 809: 1–14 (2018)
doi: 10.3897/zookeys.809.30087
http://zookeys.pensoft.net

RESEARCH ARTICLE

A peer-reviewed open-access journal
ZooKeys
Launched to accelerate biodiversity research

Phylogenetic and morphological discord indicates introgressive hybridisation in two genera of Australian millipedes (Diplopoda, Polydesmida, Paradoxosomatidae)

Peter Decker[1]

1 *Senckenberg Museum of Natural History Görlitz, Am Museum 1, 02826 Görlitz, Germany*

Corresponding author: *Peter Decker* (peter.decker@senckenberg.de)

Academic editor: *Pavel Stoev* | Received 26 September 2018 | Accepted 26 November 2018 | Published 19 December 2018

http://zoobank.org/E0ED437A-8C99-45C2-B444-802D626E985F

Citation: Decker P (2018) Phylogenetic and morphological discord indicates introgressive hybridisation in two genera of Australian millipedes (Diplopoda, Polydesmida, Paradoxosomatidae). ZooKeys 809: 1–14. https://doi.org/10.3897/zookeys.809.30087

Abstract

Discord between molecular and morphological datasets was observed in two pairs of species of Australian millipedes in the family Paradoxosomatidae using morphological and molecular phylogenetic analysis (mitochondrial COI rDNA and 16 rRNA, and nuclear 28S rRNA). Close to the presumed distributional boundary between *Pogonosternum nigrovirgatum* (Carl, 1912) and *Pogonosternum jeekeli* Decker, 2017, near Dargo in Central Gippsland, Victoria, *Pogonosternum* specimens were collected which are phylogenetically closer to *P. jeekeli* in COI and 16S sequences, but are morphologically closer to *P. nigrovirgatum.* At Mount Osmond, Adelaide, South Australia, eight morphologically typical *Somethus castaneus* (Attems, 1944) specimens were collected are phylogenetically closer to *S. castaneus* in 28S genealogy, but three of the eight are closer to *S. lancearius* Jeekel, 2002 in COI genealogy. These two cases are discussed in terms of hybridisation, past introgressive hybridisation events and aberrant morphology.

Keywords

Aberrant morphology, Arthropoda, COI, hybridisation, introgression, Myriapoda, 16S, 28S

Introduction

While many cases of hybridisation in plants, fungi and animals are well known (Alix et al. 2017, Crossman et al. 2016, Ottenburghs et al. 2016, Stukenbrock 2016, Yazicioglu et al. 2016), examples in millipedes are scarce. Pedroli-Christen and Scholl (1990) studied a hybrid zone between the two chordeumatidans *Rhymogona cervina* (Verhoeff, 1910) and *Rhymogona silvatica* (Rothenbühler, 1899) in the Swiss Alps. However, later revisions (Pedroli-Christen and Scholl 1996; Scholl and Pedroli-Christen 1996) placed both nominal species within *R. montivaga* (Verhoeff, 1894), either as a synonym (*R. silvatica*) or as a subspecies (*R. cervina*).

In Illinois, United States, the monotypic polydesmidan *Illiniurus beattyi* Shear, 1968 was later described as "transitional" in gonopod structure between *Euryurus leachii* Gray, 1832 and *Auturus evides* Bollman, 1887, both of which occur near the *I. beattyi* type locality (Jorgensen 2009). Later searches of the area for *I. beattyi* were unsuccessful, and Jorgensen (2009) was unable to determine whether the one known male of *I. beattyi* was a hybrid of *E. leachii* and *A. evides*, or simply an aberrant individual of one of these two euryurid species.

The introduction of genes from the gene pool of one species into that of another during hybridization, especially near species boundaries, is called introgressive hybridisation and can affect nuclear or mitochondrial DNA (Harper and Hart 2007, Harrison and Larson 2014, Toews and Brelsford 2012). Introgressive hybridisation has not yet been reported in the class Diplopoda.

Two cases of disagreement between relationships inferred from morphological similarity and molecular phylogenetics were observed in recent taxonomic studies of the Australian paradoxosomatid genera *Pogonosternum* Jeekel, 1965 (Decker 2016a, Decker et al. 2017) and *Somethus* Chamberlin, 1920 (Decker 2016b). These two cases are described here in detail and discussed with regard to hybridisation, past introgressive hybridisation events and aberrant morphology.

Materials and methods

Specimen collection and preservation

Pogonosternum cf. *nigrovirgatum* (Carl, 1912) "Dargo": 7 males, 1 female, 1 juvenile (NMV K-12202, K-13866, K-13867, K-13474, K-13868, SMNG VNR018276, VNR018277) were collected by hand in forest on Dargo Road, SSW of Dargo, central Gippsland, Victoria, 37.595S, 147.193E by P. Decker, K. Voigtländer and R. Mesibov on 14 August 2014.

Somethus castaneus (Attems, 1944): specimens were collected by hand at two localities in Mount Osmond Reserve, Adelaide, South Australia by P. Decker and K. Voigtländer : 1 male (SMNG VNR016973) and 3 females (SAM OM2149, SMNG VNR016975 and VNR016976) on a southwestern slope (34.969S, 138.654E, 27 Au-

gust 2014, site number S110), and 5 males (SAM OM2138, SAM registration in progress, SMNG VNR018275) and 1 female (SMNG VNR018274) on a northern slope (34.962S, 138.659E, 23 August 2014, site number S90).

Specimens were killed and stored in 95% ethanol, with a change of ethanol after 1–2 months. One male of *Somethus castaneus* from Mt. Osmond (SAM OM2138) was found dead in the field. DNA was not obtained from this specimen. The material is deposited in the Museums Victoria, Melbourne, Victoria, Australia (**NMV**), the South Australian Museum, Adelaide, Australia (**SAM**) and the Senckenberg Museum of Natural History Görlitz, Görlitz, Germany (**SMNG**).

Illustrations

Preserved specimens were imaged with a Leica Z6 Apo stereo microscope and Leica DFC420 camera. Focus-stacked images were assembled from 25–40 source images using the software package Leica Application Suite 4.5. All images were later edited using Adobe Photoshop CS4 and assembled into plates. The distribution maps were created with ArcMap 10.

Molecular analysis

DNA was extracted from 2–4 legs from each of four male *Pogonosternum* cf. *nigrovirgatum* "Dargo" and nine *Somethus castaneus* specimens from Mt Osmond (Table 1). Total genomic DNA was extracted using a Qiagen DNAeasy Blood & Tissue kit following the standard protocol with an incubation of tissue for 48h. Glom primer cocktail pairs (Decker 2016a, 2016b, Macek et al. 2014) were used to sequence a 618 bp fragment of the mitochondrial cytochrome *c* oxidase subunit I (COI) gene. Primer pairs 28S D1a (Fw) and 28S D3b (Rv) (Dell'Ampio et al. 2009) were used to amplify 1225 bp of the D2 fragment and adjacent areas of D1 and D3 on the nuclear 28S ribosomal RNA gene. Primer pairs 16Sar (Fw) (5'-CGCCTGTTTAACAAAAACAT-3') and 16Sbr (Rv) (5'-CCGGTCTGAACTCAGATCACGT-3') (Simon et al. 1994) were used to sequence a 566 bp fragment of the large-subunit ribosomal RNA (16S) gene. For PCR protocol and all primer sequences (COI, 16S, 28S) see Decker (2016a, 2016b). Fragments were sequenced in both directions by the BiK-F Laboratory Centre, Frankfurt, Germany. All obtained sequences were checked with BLAST in GenBank and no contamination was apparent. The sequences were aligned by hand in ClustalX ver. 1.83 (Chenna et al. 2003) and uploaded to GenBank (Table 1). In addition, 41 previously published (Decker 2016a for more information) sequences for five *Pogonosternum* species *P. nigrovirgatum*, *Pogonosternum adrianae* Jeekel, 1982, *Pogonosternum laetificum* Jeekel, 1982, *Pogonosternum jeekeli* Decker, 2017, and *Pogonosternum montanum* Decker, 2017 (COI: Genbank accession numbers KU745235–KU745274, KT948680; 16S: KU745194–KU745234) were used for the phylogenetic analysis of the *Pogonosternum*

Table 1. Site numbers, localities, GenBank accession numbers and repository accession numbers for all specimens analysed. NMV = Museum Victoria, Melbourne, Victoria, Australia; SAM = South Australian Museum, Adelaide, Australia; SMNG = Senckenberg Museum of Natural History Görlitz, Görlitz, Germany; SA = South Australia; VIC = Victoria.

Species	Site No.	Locality	Sex	GenBank Acc. No. COI	GenBank Acc. No. 16S	GenBank Acc. No. 28S	Voucher
Somethus castaneus	S110-1	SA, Mt. Osmond, SW slope	male	KT948668		KT964470	SMNG VNR016973
	S110-2	SA, Mt. Osmond, SW slope	female	MK170142		MK142784	SAM OM2149
	S110-3	SA, Mt. Osmond, SW slope	female	MK170143		MK142785	SMNG VNR016975
	S110-4	SA, Mt. Osmond, SW slope	female	MK170144		MK142786	SMNG VNR016976
	S90-1	SA, Mt. Osmond, N slope	male	MK170145		MK142787	SAM
	S90-2	SA, Mt. Osmond, N slope	male	MK170146		MK142788	SAM
	S90-3	SA, Mt. Osmond, N slope	male	MK170147		MK142789	SAM
	S90-4	SA, Mt. Osmond, N slope	female	MK170148		MK142790	SMNG VNR018274
	S90-5	SA, Mt. Osmond, N slope	male	MK170149		MK142791	SMNG VNR018275
Pogonosternum nigrovirgatum	Dargo-1	VIC, SSW of Dargo	male	MK170150	MK170154		NMV K-12202
	Dargo-2	VIC, SSW of Dargo	male	MK170151	MK170155		NMV K-13866
	Dargo-3	VIC, SSW of Dargo	male	MK170152	MK170156		SMNG VNR018276
	Dargo-4	VIC, SSW of Dargo	male	MK170153	MK170157		SMNG VNR018277

cf. *nigrovirgatum* "Dargo" sequences. For the molecular analysis of *Somethus castaneus* "Mt Osmond" sequences the following published (Decker 2016b for more information) sequences were included: 16 COI sequences for the five *Somethus* species *S. castaneum*, *Somethus inflatus* (Jeekel, 2002), *Somethus lancearius* Jeekel, 2002, *Somethus scopiferus* Jeekel, 2002, and *Somethus grossi* Jeekel, 1985 (GenBank accession numbers KT948655–56, KT948658, KT948662–70, KT948672–76) and 15 28S sequences of the four species *S. castaneum*, *S. inflatus*, *S. lancearius*, and *S. grossi* (GenBank accession numbers KT964457–58, KT964457). *Archicladosoma magnum* Jeekel, 1984 (KT948681) was used as outgroup. Primary homologisation problems in the 16S rRNA sequences of the *Pogonosternum* dataset arose because of the highly variable expansion loops. As a result, selected alignment positions (272–297) were excluded from the 16S rRNA dataset. COI and 16S sequences were combined in *Pogonosternum* as a single dataset and incongruence assessed between them with the incongruence length difference (ILD) test (Farris et al. 1994) implemented as the partition homogeneity test in PAUP* version 4.0b10 using a full heuristic search, 10 random taxon addition replicates, tree-bisection-reconnection (TBR) branch swapping, and with MaxTrees set to 100 (Swofford 2002). The best-fit model of nucleotide substitution for the individual COI and 16S dataset was determined by MrModelTest 2 (Nylander 2004).

Phylogenetic hypothesis was inferred for COI+16S, COI and 28S by using the maximum likelihood method conducted in MEGA6 (Tamura et al. 2011). The phylogenetic trees with the highest log likelihood (COI+16S: -5141; COI: -2565; 28S: -2328) are shown (Figs 3, 5). Initial trees for the heuristic search were obtained by applying the neighbour-joining method to a matrix of pairwise distances estimated using the Maximum Composite Likelihood (MCL) approach (Tamura et al. 2004). A discrete Gamma distribution was used to model evolutionary rate differences among sites (five categories (+G, parameter = COI+16S: 0.6793; COI: 0.1017; 28S: 0.0500)). The bootstrap consensus tree inferred from 1000 replicates (Felsenstein 1985) is here used as the best estimate of the phylogeny of each of the analysed taxa (Figs 3, 5). Mean uncorrected pairwise distances between terminals (transformed into percentages) were determined using MEGA6 (Tamura et al. 2011).

Results

Molecular analysis

The final alignments consisted of 618 bp of COI mtDNA and 1206 bp of 28S rRNA in *Somethus*, and 1158 bp for COI+16S in *Pogonosternum*. Individual alignments are available upon request from the author. The best-fit model of nucleotide substitution selected using MrModelTest 2 was the General Time Reversible model with gamma distribution and proportion of invariant sites (Nei and Kumar 2000) for the individual COI and 16S dataset. The trees constructed from individual genes did not show significant conflicts in topology (nodes different among trees with support > 70% in ML) and no significant incongruence among the three genes was revealed by the ILD test ($P > 0.81$ in all of the pairwise comparisons), and the sequences were concatenated into a dataset comprised 1158 characters for phylogenetic analysis in *Pogonosternum*.

Morphology and sequence analysis of *Pogonosternum* cf. *nigrovirgatum* "Dargo"

Pogonosternum nigrovirgatum and *P. jeekeli* are very similar in somatic morphology, and the "Dargo" form agrees with both species in size, colouration, spiracle morphology and form of the leg pair 2 coxa in females. The "Dargo" form (Fig. 1) agrees with typical *P. nigrovirgatum* (Fig. 2) in having an elongated gonopod femorite and differs from *P. jeekeli* in gonopods (Fig. 3) and male tarsal and tibial brushes only on leg pairs 1–7. See also Decker et al. (2017) for a detailed (re)description of *P. nigrovirgatum* and *P. jeekeli* and the considerable gonopod variability in these species as well as Decker 2016a for phylogeographic distribution of similar gonopod morphology. However, the four sequenced "Dargo" males are all phylogenetically closer to *P. jeekeli* in the combined COI and 16S dataset and form a well-supported group (Fig. 3; bootstrap value 98% and with uncorrected percent difference of 2.4%), and appear

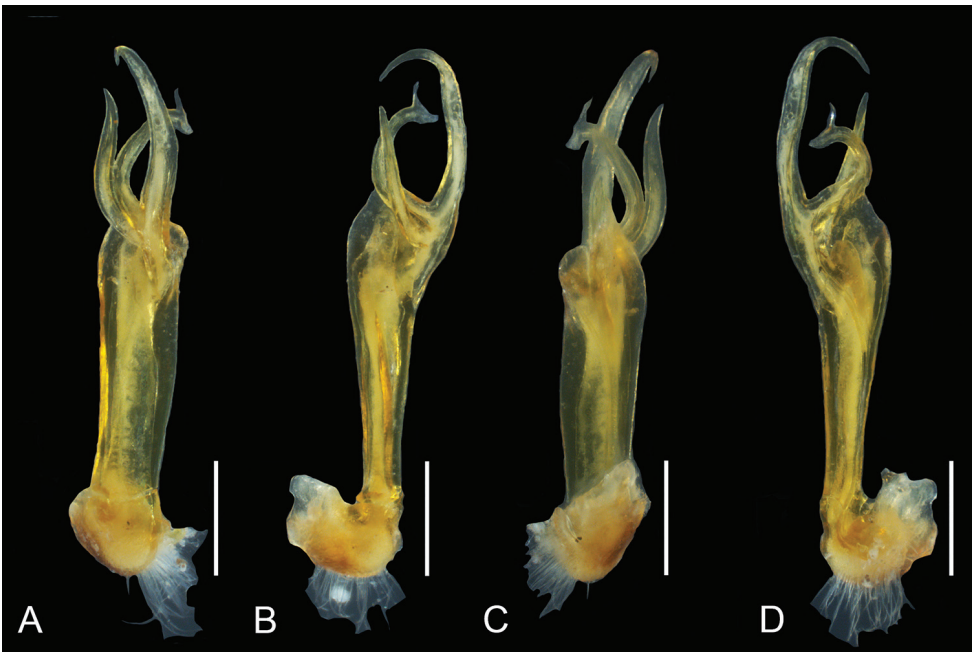

Figure 1. *Pogonosternum* cf. *nigrovirgatum* "Dargo", male, right gonopod (NMV K-12202). **A** Posterior view **B** Lateral view **C** Anterior view **D** Mesal view. Abbreviations: *fp1* = femoral process 1; *fp2* = femoral process 2; *lp* = lateral process; *prof* = prolongation of femorite; *S* = solenomere; *F* = femorite. Scale bar: 0.5 mm.

in the tree next to a population of *P. jeekeli* from northeastern Tasmania. The Dargo collection site is close to the observed species distribution boundary between *P. jeekeli* and *P. nigrovirgatum* (Fig. 4).

Morphology and sequence analysis of *Somethus castaneus* from Mount Osmond

All six male specimens from Mt Osmond fully agree in gonopod morphology with *S. castaneus* and lack a medial prefemoral process (Decker 2016b). In the 28S phylogenetic analysis, all nine sequenced specimens (uncorrected p-distance of 0–0.08%) occur within a clade of *S. castaneus* and are closest to specimens from Onkaparinga, Horsnell Gully Conservation Park, and Brownhill Creek Recreation Park (Fig. 5). In the COI analysis (Fig. 5), three specimens from the northern slope of Mt Osmond (site S90) and three from the southwestern slope (site S110) occur with *S. castaneus* from Morialta Conservation Park, Brownhill Creek Recreation Park, Horsnell Gully Conservation Park, and Belair National Park (uncorrected p-distances 0.3–1.1%).

However, two specimens from site S90 and one from site S110 form a separate, well-supported clade (100% bootstrap support) within *Somethus*, with genetic p-distances of 4.8–6.9% to *S. lancearius*, 5.3–6.9% to *S. castaneus* and 7.2–8.8 % to *S. inflatus*. The two Mt Osmond localities are in the centre of the *S. castaneus* distribution (Fig. 6).

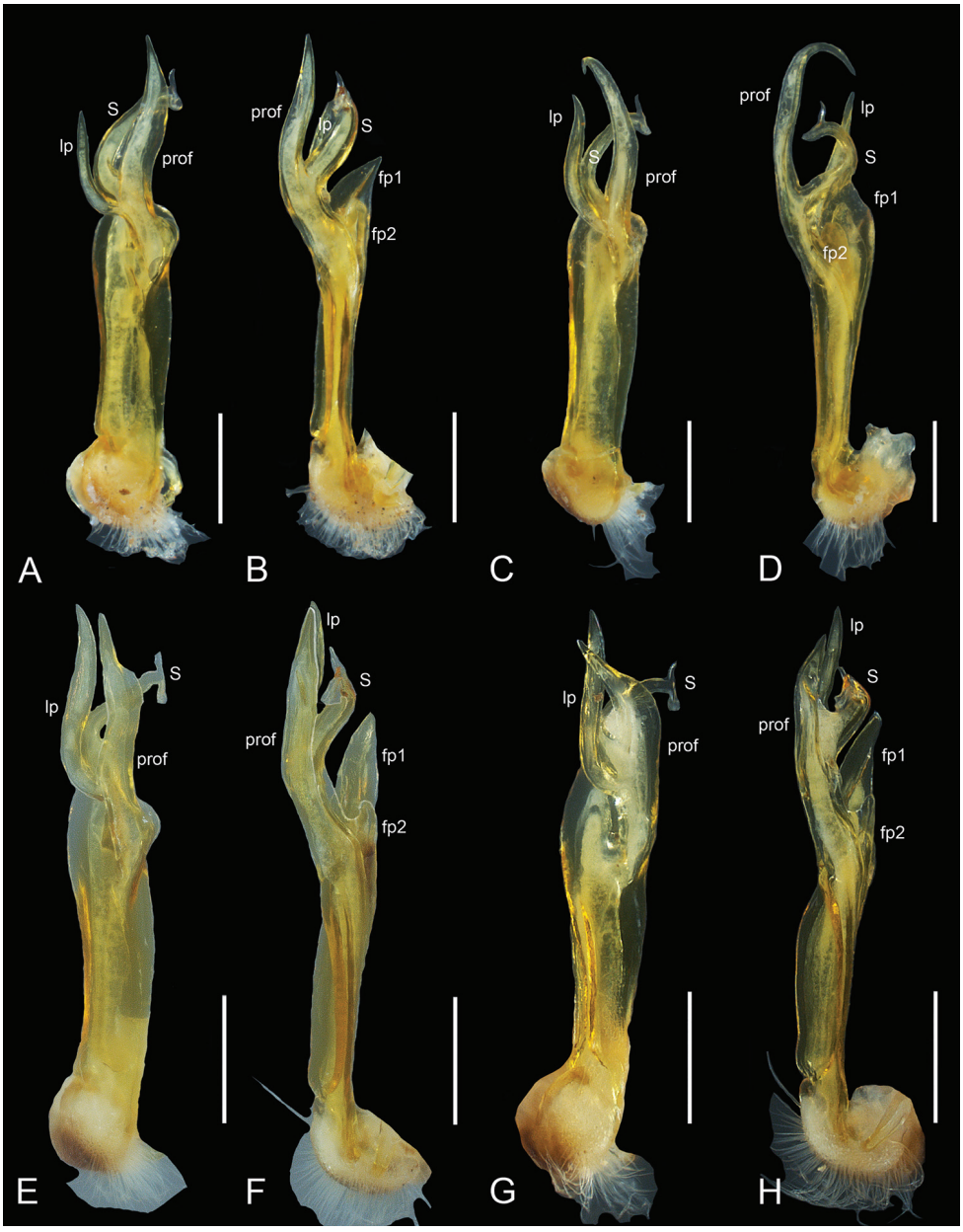

Figure 2. *Pogonosternum nigrovirgatum* (Carl, 1902), ♂, right gonopod. **A, B** AMS KS96017 Ferntree Gully **C, D** NMV K-10248 from Sandringham and Brighton. *Pogonosternum jeekeli* Decker, sp. n., ♂, right gonopod **E, F** NMV K-10252 from Dyer Creek **G, H** NMV K-10250 from Bemm River. **A, C** Posterior view **B, D** Mesal view. Scale bar: 0.5 mm.

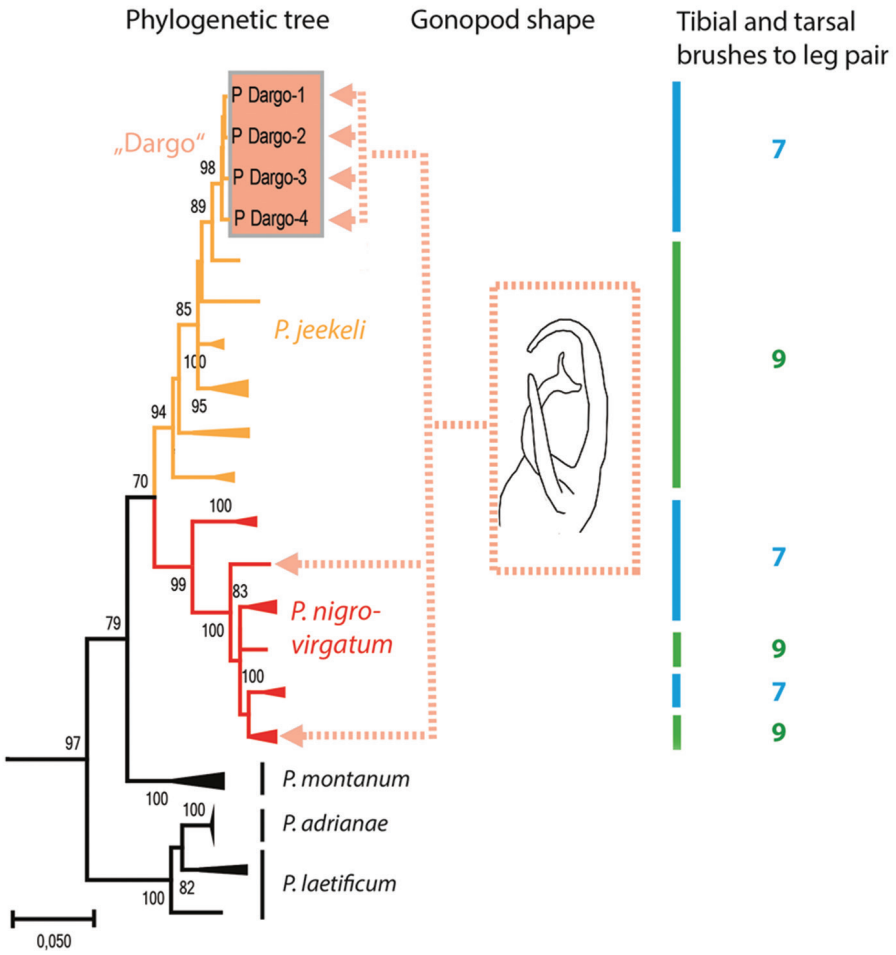

Figure 3. Bootstrap consensus tree for the combined mt COI+16S dataset in *Pogonosternum*; maximum likelihood, 1000 bootstrap replicates. Coloured dotted lines indicate specimens with similar gonopod morphology. Coloured bars indicate last male leg pairs with tibial and tarsal brushes (leg pair 7 = blue, leg pair 9 = green).

Discussion

Pogonosternum cf. *nigrovirgatum* "Dargo"

Despite the clear phylogenetic placement of this form within *P. jeekeli* as indicated by COI+16S gene trees (Fig. 3), the gonopod morphology of the seven Dargo specimens is closest to that of *P. nigrovirgatum*. In addition, tibial and tarsal brushes in the Dargo males extend only to leg pair 7, whereas in *P. jeekeli* the brushes reach leg pair 9 (74 studied males, Decker et al. 2017). In *P. nigrovirgatum* male brushes typically extend to leg pair 7, and infrequently to leg pair 9 in the area around Port Philip Bay.

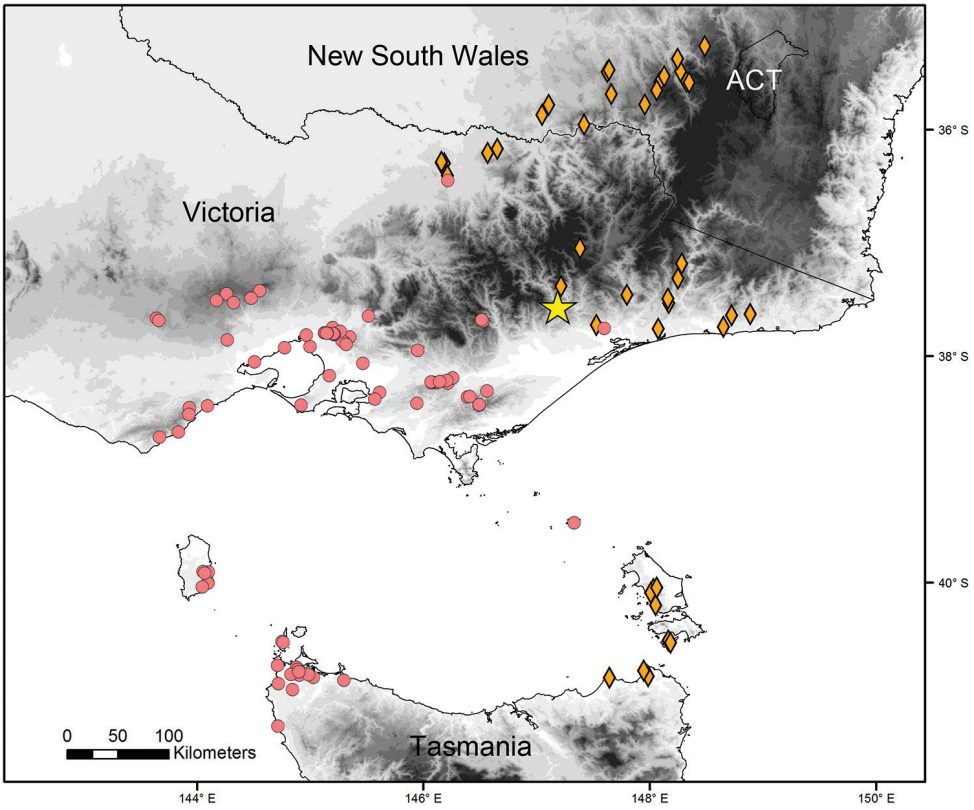

Figure 4. Distribution map of *Pogonosternum nigrovirgatum* (red circles), *P. jeekeli* (orange diamonds) and *P.* cf. *nigrovirgatum* "Dargo" (yellow star) in southeastern Australia. Abbreviation: ACT = Australian Capital Territory.

Pogonosternum nigrovirgatum and *P. jeekeli* form a sister clade (Decker 2016a) and the Dargo site is located close to the presumed boundary between the species (Fig. 4). The observed discordance between morphology and genetics could be the result of introgressive hybridisation of *P. jeekeli* and *P. nigrovirgatum*, resulting in a *P. nigrovirgatum*-type gonopod phenotype but a *P. jeekeli* mitochondrial COI and 16S genotypes. Furthermore, the finding of seven discordant males with a *P. nigrovirgatum*-type gonopod shows that the form is not the result of a developmental aberration in an individual within a *P. jeekeli* population. Another possibility is that *P.* cf. *nigrovirgatum* "Dargo" is simply a local variant of *P. jeekeli*, a species which is known to have variable gonopods in a genus that exhibits high gonopod variability (Decker 2016a, Decker et al. 2017). However, *P. jeekeli* is the only *Pogonosternum* species with tibial and tarsal brushes always ranging to leg pair 9. In contrast, brushes to leg pair 7 are found in *P. adrianae* Jeekel, 1982, *P. montanum* Decker, 2017, most males of *P. nigrovirgatum* and some males of *P. laetificum* Jeekel, 1982. This leg pair 7 limit is observed in four out of the five species in the genus *Pogonosternum* and likely to be plesiomorphic. Thus the hypothetical local variation in *P. jeekeli* resulting in the "Dargo" phenotype would

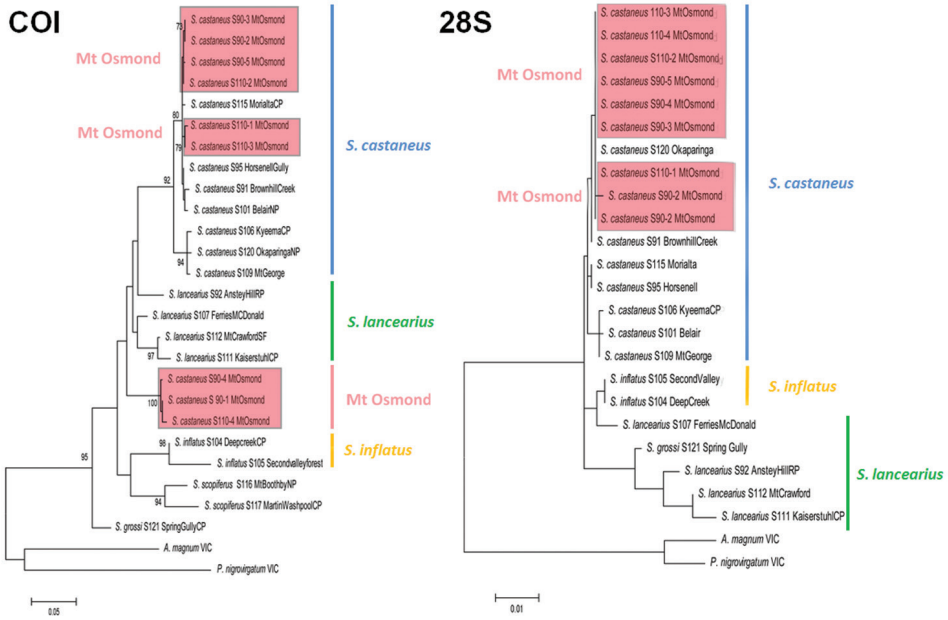

Figure 5. COI and 28S bootstrap consensus trees for *Somethus* species; maximum likelihood, 1000 bootstrap replicates.

involve both a change in gonopod morphology and a regression from apomorphy or common distribution of tibial and tarsal brushes in *P. jeekeli*. However, the author favours the hypothesis that two closely related *Pogonosternum* species have undergone introgressive hybridisation in an area of range overlap near Dargo. To distinguish between hypotheses of introgression versus gene tree lineage sorting, further gene sampling and analysis is needed of *Pogonosternum* individuals near the Dargo site and along near the presumed distribution boundary between *P. nigrovirgatum* and *P. jeekeli*. In addition, sampling of *P. jeekeli* and *P. nigrovirgatum* far from sympatry are needed.

Somethus castaneus from Mount Osmond

Somethus castaneus was sampled for sequencing at 13 localities covering most of the known species range, and genetic variability was shown to be low (up to 3.8% in uncorrected p-distances in COI) with three phylogenetic lineages (Decker 2016b). The morphologically typical *S. castaneus* from Mt Osmond, in the centre of the species range, includes three individuals whose COI sequences are not close to those of either the other *S. castaneus*, *S. inflatus* or *S. lancearius*, although they are slightly closer to those of *S. lancearius* (in % bp difference). *Somethus lancearius* is distributed in the north-eastern and eastern part of the Adelaide Hills, with some scattered, possibly introduced, occurrences of *S. castaneus* within its distributional area. The closest record of *S. lancearius* is about 17 km from Mt Osmond. Genetic variability within *S. lancearius* from five sampled localities is 1.6–5.8% (in uncorrected p-distances in COI) and with unique haplotypes that cor-

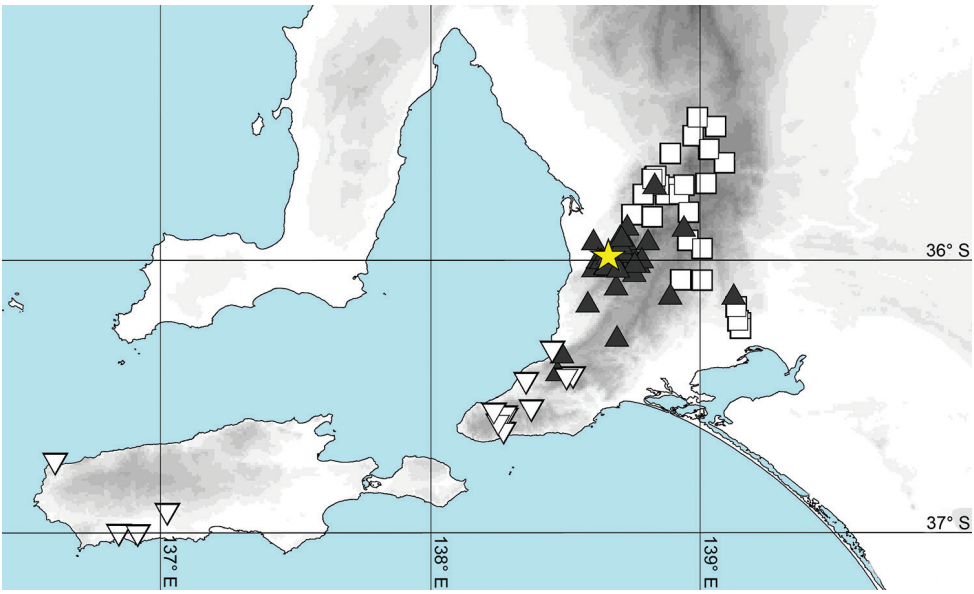

Figure 6. Map of South Australia and southern Mt Lofty Ranges showing localities for *Somethus* species: *S. castaneus* (filled triangle), *S. inflatus* (open triangle), *S. lancearius* (square), and *S. castaneus* from Mt. Osmond (yellow star).

respond to geographical areas (Decker 2016b). Widespread sampling of this species is no longer possible, as natural vegetation has largely been cleared within its range and *S. lancearius* is now restricted to scattered conservation areas and tiny remnants.

Several of the paratypes of *S. inflatus* were collected in the Adelaide suburb of Glen Osmond, near Mt Osmond, in 1969 (Jeekel 2002). These paratypes appear to have been lost and could not be compared with recently collected *S. inflatus* (Decker 2016b), and no *S. inflatus* have since been found on Mt Osmond. *S. inflatus* is distributed to the southwest of Adelaide on the Fleurieu Peninsula and on Kangaroo Island (Fig. 6). Jeekel's *S. inflatus* paratypes might represent a non-permanent introduction.

The three discordant *S. castaneus* found on Mt Osmond might be evidence for past introgression of mitochondrial DNA following hybridisation with another South Australian *Somethus* species. Alternatively, the anomalous individuals might represent a distinct and distantly related *S. castaneus* lineage which is either naturally occurring on Mt Osmond or introduced from another locality within the Adelaide Hills. There is no support for both hypotheses, but it seems that the likelihood of the presence (or former existence) on Mt Osmond of the in COI and 28S variable *S. lancearius* or *S. inflatus* is higher than that of a fourth distinct COI and 28S lineage in *S. castaneus*.

Future investigations with additional molecular markers and more individuals of from *S. lancearius* may not assist in clarifying the situation, as much of the former genetic variation of *S. lancearius* has probably been lost due to habitat loss and local extinctions. If the missing paratypes of *S. inflatus* are found in future, it might be possible to extract DNA and obtain sequences from them which could reveal whether *S. inflatus* in the Mt Osmond area has contributed mitochondrial COI to the local *S. castaneus* population.

Conclusion

The results presented here suggest that introgressive hybridisation may have occurred in the paradoxosomatid millipede genera *Pogonosternum* and *Somethus* in southeastern Australia. With the increasing use of molecular data in taxonomy and in barcoding projects, similar cases are likely to be found elsewhere. Interestingly, no evidence of introgressive hybridisation was found in more than 2000 COI sequences from Central European millipedes during the German Barcoding of Life Project (GBOL) (Wesener, Spelda, Reip, Decker pers. comm.). The phenomenon may be rare, or limited to narrow parapatric zones, as appears to be the case in *Pogonosternum*.

Acknowledgments

For loans of material I am very grateful to Kate Sparks (formerly at SAM), Peter Lillywhite and Catriona McPhee (NMV). Also sincere thanks to Karin Voigtländer (SMNG), Ulrich Burkhardt (SMNG), and Thomas Wesener (Bonn) for technical advice as well as interesting discussions. I am very grateful to Robert Mesibov (West Ulverstone), Meike Schuppenhauer (SMNG), Paul Marek (Blacksburg), and Henrik Enghoff (Copenhagen) for their helpful and constructive comments on earlier versions of the manuscript. The field trip of the author to Australia 2014 was financially supported by the 'Förderkreis Naturkundemuseum Görlitz'.

References

Alix A, Gérard PR, Schwarzacher T, Heslop-Harrison JS (2017) Polyploidy and interspecific hybridization: partners for adaptation, speciation and evolution in plants. Annals of Botany 120(2): 183–194. https://doi.org/10.1093/aob/mcx079

Chenna R, Sugawara H, Koike T, Lopez R, Gibson TJ, Higgins DG, Thompson JD (2003) Multiple sequence alignment with the Clustal series of programs. Nucleic Acids Research 31: 3497–3500. https://doi.org/10.1093/nar/gkg500

Crossman CA, Taylor EB, Barrett-Lennard LG (2016) Hybridization in the Cetacea: widespread occurrence and associated morphological, behavioral, and ecological factors. Ecology and Evolution 6(5): 1293–1303. https://doi.org/10.1002/ece3.1913

Decker P (2016a) Phylogenetic analysis of the Australian trans-Bass Strait millipede genus *Pogonosternum* (Carl, 1912) (Diplopoda, Polydesmida, Paradoxosomatidae) indicates multiple glacial refugia in southeastern Australia. ZooKeys 578: 15–31. https://10.3897/zookeys.578.8052

Decker P (2016b) Integrative taxonomic revision of the polymorphic flat-millipede genera *Oncocladosoma* and *Somethus* in South Australia (Diplopoda: Polydesmida: Paradoxosomatidae). Invertebrate Systematics 30(3): 201–218. https://doi.org/10.1071/IS15047

Decker P, Mesibov R, Voigtländer K, Xylander WER (2017) Revision of the Australian millipede genus *Pogonosternum* Jeekel, 1965, with descriptions of two new species (Diplopoda, Polydesmida, Paradoxosomatidae). European Journal of Taxonomy 259: 1–34. https://doi.org/10.5852/ejt.2017.259

Dell'Ampio E, Szucsich NU, Carapelli A, Frati F, Steiner G, Steinacher A, Pass G (2009) Testing for misleading effects in the phylogenetic reconstruction of ancient lineages of hexapods: influence of character dependence and character choice in analyses of 28S rRNA sequences. Zoologica Scripta 38(2): 155–170.

Farris JS, Källersjö M, Kluge AG, Bult C (1994) Testing the significance of incongruence. Cladistics 10(3): 315–319. https://doi.org/10.1111/j.1096-0031.1994.tb00181.x

Felsenstein J (1985) Confidence limits on phylogenies: an approach using the bootstrap. Evolution 39: 783. https://doi.org/10.2307/2408678

Harper FM, Hart MW (2007) Morphological and phylogenetic evidence for hybridisation and introgression in a sea star secondary contact zone. Invertebrate Biology 126: 373–384. https://doi.org/10.1111/j.1744-7410.2007.00107.x

Harrison RG, Larson EL (2014) Hybridisation, introgression, and the nature of species boundaries. Journal of Heredity 105 (S1): 795–809. https://doi.org/10.1093/jhered/esu033

Jeekel CAW (2002) Millipedes from Australia, 14:A third contribution to South Australian Paradoxosomatidae (Diplopoda, Polydesmida). Myriapod Memoranda 5: 60–77.

Jorgensen MC (2009) A new species of *Euryurus* from southern Alabama and remarks on the status of *Illiniurus beattyi* Shear (Diplopoda Polydesmida Euryuridae). The Great Lakes Entomologist 42 (1–2): 80–90.

Macek O, Bartel D, Szucsich N, Pass G (2014) Cocktails and pills: A COI primer cocktail for pill millipedes. In: Tuf IH, Tajovský K (Eds) 16th International Congress of Myriapodology. Book of Abstracts. Institute of Soil Biology, BC ASCR & Faculty of Science, Palacký University, Olomouc, 50.

Nei M, Kumar S (2000) Molecular Evolution and Phylogenetics. Oxford University Press, Oxford, 352 pp.

Nylander JAA (2004) MrModeltest v2. Program distributed by the author. Evolutionary Biology Centre, Uppsala University.

Ottenburghs J, van Hooft P, van Wieren SE, Ydenberg RC, Prins HHT (2016) Hybridization in geese: a review. Frontiers in Zoology 13(20). https://doi.org/10.1186/s12983-016-0153-1

Pedroli-Christen A, Scholl A (1990) Ecological and genetic studies on parapatric *Rhymogona silvatica* Roth. and *R. cervina* Verh. Diplopoda Craspedosomatidae) with special reference to hybrid populations in a zone of contact. Revue suisse de zoologie 97: 349–359. https://doi.org/10.5962/bhl.part.79741

Pedroli-Christen A, Scholl A (1996) *Rhymogona* (Diplopoda: Craspedosomatidae) un genre monospécifique. Deuxième partie: Révision basée sur les résultats morphologiques, génétriques et faunistiques. In: Geoffroy J-J, Mauriès J-P, Nguyen Duy-Jacquemin M (Eds) Acta Myriapodologica. Mémoires du Muséum national d'histoire naturelle, N. S. 169: 53–60.

Scholl A, Pedroli-Christen A (1996) The taxa of *Rhymogona* (Diplopoda: Craspedosomatidae): a ring species. Part one: genetic analysis of population structure. In: Geoffroy J-J, Mauriès J-P, Nguyen Duy-Jacquemin M (Eds) Acta Myriapodologica. Mémoires du Muséum national d'histoire naturelle, N. S. 169: 45–51.

Simon C, Frati F, Beckenbach A, Crespi B, Liu H, Flook P (1994) Evolution, weighting, and phylogenetic utility of mitochondrial gene sequences and a compilation of conserved polymerase chain reaction primers. Annals of the Entomological Society of America 87: 651–701. https://doi.org/10.1016/j.ympev.2008.11.025

Stukenbrock EH (2016) The role of hybridization in the evolution and emergence of new fungal llant pathogens. phytopathology 106(2): 104–112. https://doi.org/10.1094/PHYTO-08-15-0184-RVW

Swofford DL (2002) PAUP*: Phylogenetic analysis using parsimony (*and other methods). v.4.0b10. Sinauer & Associates, Sunderland, Massachusetts. https://doi.org/10.1111/j.0014-3820.2002.tb00191.x

Tamura K, Nei M, Kumar S (2004) Prospects for inferring very large phylogenies by using the neighbor-joining method. Proceedings of the National Academy of Sciences 101: 11030–11035. https://doi.org/10.1073/pnas.0404206101

Tamura K, Peterson D, Peterson N, Stecher G, Nei M, Kumar S (2011) MEGA5: molecular evolutionary genetics analysis using maximum likelihood, evolutionary distance, and maximum parsimony methods. Molecular Biology and Evolution 28: 2731–2739. https://doi.org/10.1093/molbev/msr121

Toews DPL, Brelsford A (2012) The biogeography of mitochondrial and nuclear discordance in animals. Molecular Ecology 21: 3907–3930. https://doi.org/10.1111/j.1365-294X.2012.05664.x

Yazicioglu B, Reynolds J, Kozák P (2016) Different aspects of reproduction strategies in crayfish: A review. Knowledge and Management of Aquatic Ecosystems 417(33). https://doi.org/10.1051/kmae/2016020

ZooKeys 809: 15–29 (2018)
doi: 10.3897/zookeys.809.29058
http://zookeys.pensoft.net

RESEARCH ARTICLE

A peer-reviewed open-access journal
ZooKeys
Launched to accelerate biodiversity research

Notes on the genus *Indocnemis* Laidlaw, 1917 in Vietnam with description of *Indocnemis marijanmatoki* sp. n. (Odonata, Zygoptera, Platycnemididae)

Quoc Toan Phan[1]

1 *Center for Entomology and Parasitology Research, Institute of Research and Training of Medicine, Biology and Pharmacy, Duy Tan University, 3 Quang Trung, Da Nang, Vietnam*

Corresponding author: *Quoc Toan Phan* (pqtoan84@gmail.com)

Academic editor: *Jan van Tol* | Received 13 August 2018 | Accepted 14 November 2018 | Published 19 December 2018

http://zoobank.org/5B887472-95E1-4E0D-8ED5-3A3428FF36ED

Citation: Phan QT (2018) Notes on the genus *Indocnemis* Laidlaw, 1917 in Vietnam with description of *Indocnemis marijanmatoki* sp. n. (Odonata, Zygoptera, Platycnemididae). ZooKeys 809: 15–29. https://doi.org/10.3897/zookeys.809.29058

Abstract

Indocnemis marijanmatoki **sp. n.** (holotype ♂, 12°07'10.0"N, 108°5'51.0"E, 1503 m a.s.l., Hon Ba Nature Reserve, Nha Trang city, Khanh Hoa Province, central Vietnam) is described based on both sexes. The morphological variation of *Indocnemis orang* (Förster in Laidlaw, 1907) is discussed and its distribution in Vietnam updated.

Keywords

Indocnemis, new species, Odonata, Platycnemididae, Vietnam

Introduction

Laidlaw (1917) established the genus *Indocnemis* characterized it as having the "wing relatively broad and rounded, [with] 3 cells between the quadri-lateral and sub-nodal. Reticulation on the fore-wing not so dense (not more than 250 cells on the hind-wing)". This was based on a single male of *Indocnemis kempi* from Assam, India, and according to Laidlaw (1917), this male has a blue antehumeral stripe on the synthorax and the appendages are entirely black. In 1917, Laidlaw thought that *I. kempi* might

be congeneric with *Trichocnemis orang* Förster, 1907. In 1931, he transferred *T. orang* to the genus *Indocnemis* after examining the type specimen and several other specimens of from Malaysia and Thailand (Laidlaw 1931); he also suggested that his Assamese *I. kempi* might be a synonym of *I. orang.* He wrote that "young males appear to have a narrow blue band on either side of the dorsum of the synthorax", but "in adult male, the blue stripe of the dorsum of the synthorax seems to widen considerably, so as to form a large oblong-oval mark extending inwards almost to the mid-dorsal carina". The change from a narrow dorsal tripe on the synthorax in young to a large shield in adult specimens has never been confirmed in the field in Vietnam, where immature males have similar large shields as adults, but of a pale yellow colour (Kompier in. litt.). Moreover, no case of expanding pale elements of the pattern with age are known in Odonata, although their reduction with age is common. Therefore, it seems possible that Laidlaw (1931) based his discussion on specimens of both forms. It requires further examination of the Malaysian and Thai specimens used in Laidlaw's (1931) description to establish whether there truly is a change in these characters with maturation. Asahina (1985) downgraded *I. kempi* to a synonym of *I. orang* and showed that males from Assam have a narrow stripe on the dorsum of the synthorax (Asahina 1985: 9, fig. 30). However, in 1997 Asahina stated "Now I am changing my previous idea (1985a), in which *kempi* (1917) was synonymized with *orang* (1907), though the former was recognized as a large-sized form of the latter." Asahina (1997) concluded that the genus *Indocnemis* consisted of only one species*, I. orang*, which has two forms differing in size: the first form (forma *orang*), originally described from Perak, Malaysia (measurements of males: abdomen 46–47 mm, hind wing 32–34 mm) is smaller than the second form (forma *kempi,* based on specimens from Assam and Tam Dao National Park, northern Vietnam) (measurements of males: abdomen 51–57 mm, hind wing 35–38 mm) (Laidlaw 1917, 1931; Asahina 1985, 1997). *Indocnems orang* forma *kempi* in Tam Dao also has a broader thoracic stripe than the population in Cuc Phuong (Asahina 1997).

Dijkstra et al. (2013) pointed out that the two genera *Indocnemis* and *Coeliccia* Kirby are paraphyletic. *Indocnemis* differs from *Coeliccia* by the anal crossing (Ac) ending on the anal bridge vein, not on the wing margin (Asahina 1997). However, several specimens in my collection of, for instance, *Coeliccia cyanomelas* (Fig. 35) do not have the Ac ending at the wing margin, just like *Indocnemis* (see also Wilson and Reels 2003). Therefore, this character cannot be used to consistently separate the two genera. Wilson and Reels (2003) provided another character of the genus *Indocnemis*: the presence of four cells between the discoidal cell and the nervure descending from the subnode, whereas *Coeliccia* has just three cells. However, some *I. orang* specimens have only three cells (Fig. 32) and some *Coeliccia* species have four cells (Fig. 33) or two cells (Figs 34–35). Wilson and Reels (2003) stated that this character was also variable and that some *ambigua* only had three cells. Therefore, these venational characters are variable, even within a species, and there is no basis on which to distinguish the genera *Indocnemis* and *Coeliccia.* Although Wilson and Reels (2003) transferred *Coeliccia ambigua* Asahina, 1997 to the genus *Indocnemis*, their interpretation has not been accepted in several later publications (e.g. Phan and Kompier 2016; Kosterin and

Kompier 2017; Phan and Tran 2018). Moreover, the genital ligula of *C. ambigua* is structurally simple and unlike the two *Indocnemis* species discussed here. Therefore, I retain the original combination of *C. ambigua* and do not list this species in the genus *Indocnemis* in this paper.

I do not intend here to synonymize the genus *Indocnemis* with *Coeliccia,* but I do not think the current distinction is valid (see also Dijkstra et al. 2013). The taxonomic relationships between these two genera may be solved in the future based on further molecular analysis. Here I characterise the morphological variation of the widespread species *I. orang* in Vietnam and describe a second member of the genus, *I. marijanmatoki* sp. n. I place the new species in the genus *Indocnemis* in view of its great similarity to *I. orang* by the structure of the appendages and the genital ligula of the male, and the body coloration of both sexes. *Indocnemis marijanmatoki* sp. n. differs from *I. orang* by the shape of its cerci and female prothorax structures.

Material and methods

Specimens of *Indocnemis orang* used for comparing with the new species were collected on the same date and location, Hon Ba Nature Reserve of Khanh Hoa Province (km 19, 12°06'49.3"N, 108°59'37.3"E, 418 m a.s.l.) as the types of *I. marijanmatoki* sp. n. The habitus of holotype and the female paratype were photographed with a Nikon D3300 digital camera and Nikon AFS DX Micro Nikkor 85 mm f/3.5G ED VR lens. Photographs in nature were taken with a Nikon D3300 digital camera with Nikon AF Micro 200 mm f4D IF-ED lens. Other colour photographs were taken with an Axiocam Erc 5s camera on Zeiss Stemi 508 stereomicroscope. Illustrations were made with Adobe Photoshop 7.0.

Morphological nomenclature used for damselfly structures follows Phan and Kompier (2016). Preparation of specimens follows standard practice as for instance described in Paulson (2018).

Abbreviations:

S1–10	abdominal segments 1 to 10;	**FW**	forewing;
Px	postnodal crossveins;	**a.s.l**	above sea level.
HW	hindwing;		

Results

All examined mature males of *Indocnemis orang* have synthoracic dorsal stripes covering most of mesepisternum and black cerci with blue marks dorsally (Fig. 24), that agree with the forma *kempi,* but only specimens from Bach Ma National Park have the same large body size (male: abdomen 55–57 mm, hind wing 37–38 mm) of this form as described by Asahina (1997). Measurements of others specimens fall within the size range of *I. orang* forma *orang* (male: abdomen 46–50 mm, hind wing 35–36 mm). As the males of Viet-

namese populations of *I. orang* display considerable variation in body size among different individuals, this alone does not seem a sound basis to divide them into two forms as in Asahina's interpretation. Most of examined males of Vietnamese *I. orang* in this paper are similar to those in photos of *I. orang* taken in Malaysia by Choong (2018), Meghalaya, India by Joshi et al. (2018) or Thailand by Farrell (2018) in respect of the large dorsal shield on the synthorax and very dark cerci, which are entirely black or black with blue mark dorsally. Wilson and Reels (2003) also pointed out that Asahina's (1997) treatment did not make it clear whether Vietnamese specimens of *I. orang* should be assigned to formae *orang* or *kempi*. There is the population, probably unique, of *I. orang* in Cuc Phuong that is consistent with the original description of *I. orang* forma *kempi* in having its synthorax displaying a dorsal stripe, not a shield (Fig. 9) although its cerci are pale yellow (Fig. 10). Therefore, I maintain the division of Vietnamese *I. orang* into two forms on the basis of the difference of the body coloration pattern of the mature male as follows:

Indocnemis orang forma *orang*: Large shield-shaped stripe on synthorax (Figs 8, 23), cerci black with blue marks dorsally (becoming entirely black after acetone treatment) (Fig. 24). Throughout the species' range.

Indocnemis orang forma *kempi*: Narrow stripe on synthorax (Fig. 9), cerci pale yellow (Fig. 10). Cuc Phuong National Park.

The population of *I. orang* in Tam Dao, as reported by Asahina (1997), also should be transferred into the forma *orang* (not *kempi*) based on the shield-like oval mark on the synthorax (Asahina 1997: 33, figs 66, 67).

Indocnemis orang (Förster in Laidlaw, 1907) forma *orang*

Figures 1–4, 8, 17–20, 23, 24, 29, 30, 32

Examined specimens. 1 mature male, Pia Oac National Park, Cao Bang Prov., 16 May 2015; 1 mature female, Xuan Son National Park, Phu Tho Prov., 15 September 2015; 1 mature female, Vu Quang National Park, Ha Tinh Prov., 07 April 2015; 6 mature males, 5 mature females, Bach Ma National Park, Thua Thien Hue Prov., 27 June 2017; 1 mature male, 1 mature female, Sao La Nature Reserve, A Luoi District, Thua Thien Hue Prov., 18 September 2015; 1 mature male, 3 mature females, Deo Lo Xo, Phuoc Son District, Quang Nam Province, 05 August 2017; 3 mature males, 1 mature female, Nam Giang District, Quang Nam Prov., 25 May 2017; 1 mature male, 1 mature female, Bhalee, Tay Giang District, Quang Nam Prov., 18 September 2015; 1 mature male, 2 mature females, Ba Na Nature Reserve, Da Nang city, 25 May 2015; 1 mature male, Kon Chu Rang Nature Reserve, Gia Lai Prov., 11 March 2017; 1 mature male, Dak Roong, K'Bang District, Gia Lai Prov., 24 May 2018; 1 mature female, Chu Mom Ray National Park, Kon Tum Prov., 22 May 2017; 3 mature males, 1 mature female, Chu Yang Sin National Park, Dak Lak Prov., 19 May 2018; 1 mature male, Mang Canh, Kon Plong District, Kon Tum Prov., 22 September 2015; 1 mature male, 1 immature male, Maria pass, Bao Loc District, Lam Dong Prov., 16 March 2016; same location, 1 immature male, 3 mature female, 22 April 2016; 1 mature male, same location, 11 May 2017; 3 mature males, 1 immature male, 1

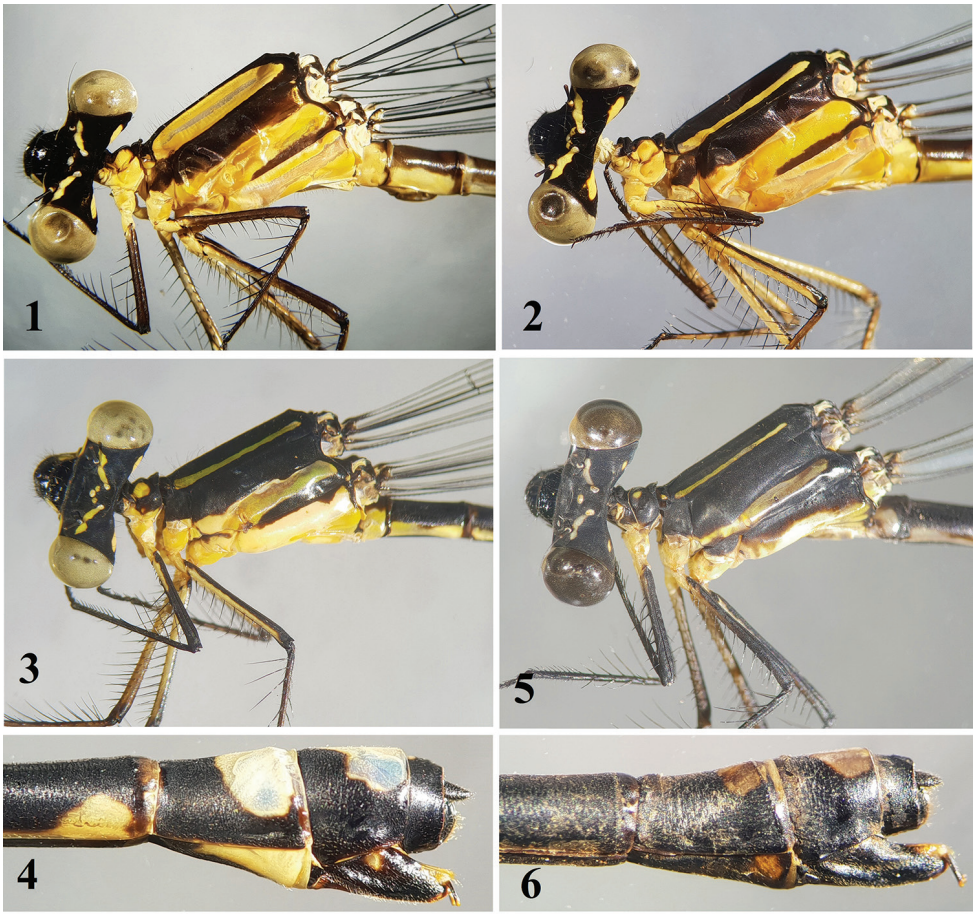

Figures 1–6. *Indocnemis orang*, **1–4** forma *orang* & **5, 6** forma *kempi*. **1** immature male, Hon Ba **2** immature female, Hon Ba **3, 4** head, thorax and abdominal tip of mature female, Phuoc Son **5, 6** head, thorax and abdominal tip of mature female, Cuc Phuong.

immature female, km19, Hon Ba Nature Reserve, Khanh Hoa Prov., 16 April 2017; 1 mature female, same location, 08 May 2015. All materials were collected by the author. 2 mature females, Kon Ka Kinh National Park, Gia Lai Prov., 6 April 2018, To Van Quang leg.

Remarks. All examined immature males of *Indocnemis orang* forma *orang* differ from the mature specimens by the following characters: middle lobe of prothorax is mostly yellowish (Fig. 1) but this mark reduced to a very small dot on either side or absent in mature males (Fig. 23); large dorsal shield on synthorax yellow, not purple as in mature males (Fig. 1); metepimeron entirely yellowish (Fig. 1) but largely black in mature males (Fig. 23); dorsal S9–10 and whole appendages pale yellowish, whereas cerci are black with blue marks dorsally in mature males (Fig. 24). The immature females are very similar to mature ones except that dorsal head stripes and yellow spots in either side of middle lobe of prothorax broader and antehumeral stripe is yellow, not blue as in mature females (Figs 2, 3).

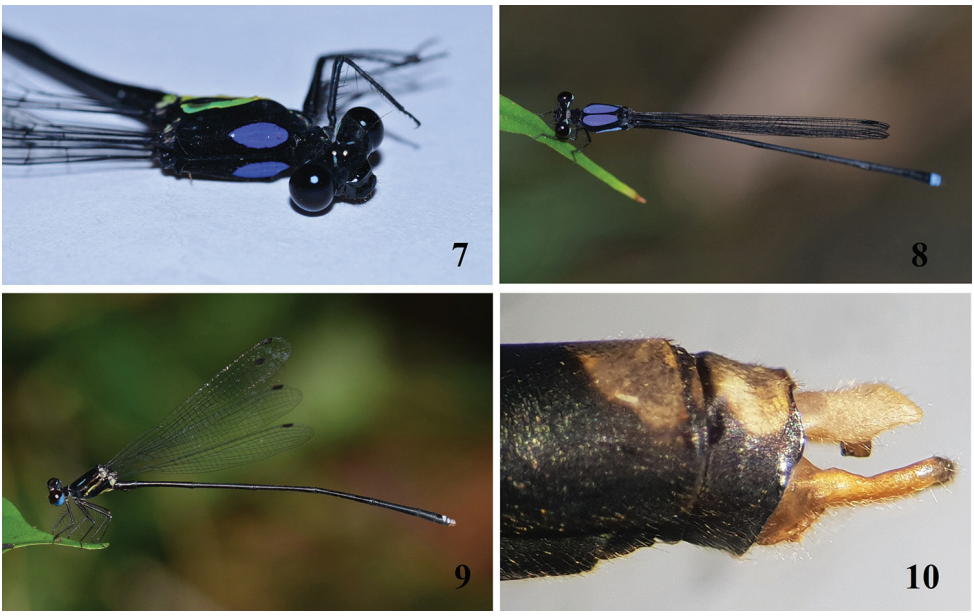

Figures 7–10. *Indocnemis* spp. **7** *I. marijanmatoki* sp. n., ♂ from Kon Ka Kinh National Park, photographed by Mr To Van Quang **8** *I. orang* ♂ in nature, Nam Giang, Quang Nam **9, 10** Habitus and appendages of *I. orang* ♂, Cuc Phuong National Park, photographed by the author.

Indocnemis orang (Förster in Laidlaw, 1907) forma *kempi*

Figures 5, 6, 9, 10

Examined specimens. 1 mature male, 1 mature female, Cuc Phuong National Park, Ninh Binh Prov., 25 June 2018, Q.T. Phan leg.

Remarks. Asahina (1997) did not describe the colour of the dorsal stripes on synthorax of his *orang* forma *kempi* from Cuc Phuong. I can now confirm that the dorsal stripe of the mature living male of this form in Cuc Phuong is blue (Fig. 9). Asahina (1997) also did not mention the pale yellowish appendages of the males from Cuc Phuong (Fig. 10). Females of the two forms *orang* and *kempi* can be separated by their body pattern: the yellow spot on the middle lobe of prothorax and lateral stripes on synthorax in forma *kempi* are smaller (Fig. 5) than those in forma *orang* (Fig. 3); the bluish markings on dorsal S9–10 in forma *kempi* are smaller and in forma *orang*; and S8 is black, without yellow marks as in forma *orang* (Figs 4, 6). In female forma *kempi* in Cuc Phuong, the structure of the posterior lobe of the prothorax is the same as in the female of forma *orang*.

Distribution. *Vietnam*: Vinh Phuc (Tam Dao National Park), Ninh Binh (Cuc Phuong National Park), Thua Thien Hue (Bach Ma National Park), Lam Dong (Bao Loc District) [Do and Dang 2007], Ha Noi (Ba Vi National Park) [Kompier 2018], Cao Bang (Pia Oac National Park), Phu Tho (Xuan Son National Park), Ha Tinh (Vu

Quang National Park), Quang Nam (Phuoc Son and Tay Giang Districts), Gia Lai (Kon Chu Rang Nature Reserve and Kon Ka Kinh National Park), Dak Lak (Chu Yang Sin National Park), Kon Tum (Kon Plong District and Chu Mom Ray National Park) and Khanh Hoa Provinces (Hon Ba Nature Reserve); *Laos*: Luang Prabang, Oudomxay and Xiang Khouang Provinces [Yokoi and Souphanthong 2014]; *Thailand*: Khao Ram Rome Moutain, Nakhon Si Thammarat Province [Laidlaw 1931], Petchaburi (Nam Nao National Park), Phang Nga (Khao Lak) and Chantaburi Provinces (Khao Soi Dao National Park) [Noppadon Makbun pers. comm.]; *China*: Fujian, Guangdong, Fukien, Sichuan and Guangxi Provinces [Asahina 1985, Wilson and Reels 2003]; *Malaysia*: Perak [Laidlaw 1931] and Cameron Highlands [Asahina 1985]; *India*: Assam and Sikkim [Asahina 1985, Laidlaw 1917], *Bangladesh*: ? [Subramanian 2010].

***Indocnemis marijanmatoki* sp. n.**
http://zoobank.org/83FEE544-10B1-4754-A678-9ACD521AF85D
Figures 7, 11, 12, 13–16, 21, 22, 25–28, 31

Type specimens. Holotype. A mature male, folded wings in triangular envelope. Original label: "*Indocnemis marijanmatoki* sp. n., Hon Ba Nature Reserve, Nha Trang city, Khanh Hoa Province, Vietnam (12°07'10.0"N, 108°5'51.0"E, 1503 m a.s.l.), T.odo.16041705, Q.T. Phan leg", "HOLOTYPE" [red handwritten label]. **Paratypes.** 1 mature male, 1 mature female, same date, location and collector as the holotype. All type specimens are deposited in the Zoological Collection of Duy Tan University, Da Nang city, Vietnam.

Other specimens examined. Two mature males, collected in a small stream on the main route to the top of the Kon Ka Kinh Mountain (14°19'83.5"N, 108°24'31.9"E, 1450 m a.s.l), Dak Hro village, Dak Roong commune, K'Bang District, Gia Lai Province, 09 April 2018, To Van Quang leg.

Etymology. *Marijanmatoki*, a noun in the genitive case, after Marijan Matok (born 28 March 1972) of Ulm-Söflingen, Germany, in appreciation of his support of the author's odonatological research in Vietnam through the International Dragonfly Fund.

Diagnosis. The new species differs from *I. orang* with a combination of the following characters: in the male, the marking on dorsum of synthorax is small, shield-shaped; S9–10 entirely black; cerci short, of the length as S10, without a robust basal spine; paraproct entirely black. In the female, the posterior pronotal lobe of the prothorax is rather small, semicircular-shaped.

Description of holotype. *Head* (Fig. 21). Labrum, genae, mandible and postclypeus shining black; anteclypeus dark brown. Antennae black except paler apical part of first and second segments. Top of head matte black with two long stripes adjacent to median ocellus running towards the base of the antennae and two water drop-shaped yellow spots just posterior to postoccipital lobes.

Thorax (Fig. 21). Prothorax entirely black. Synthorax black with a large oval-shaped marking and another tiny stripe in mesepisternum. The large marking blue in

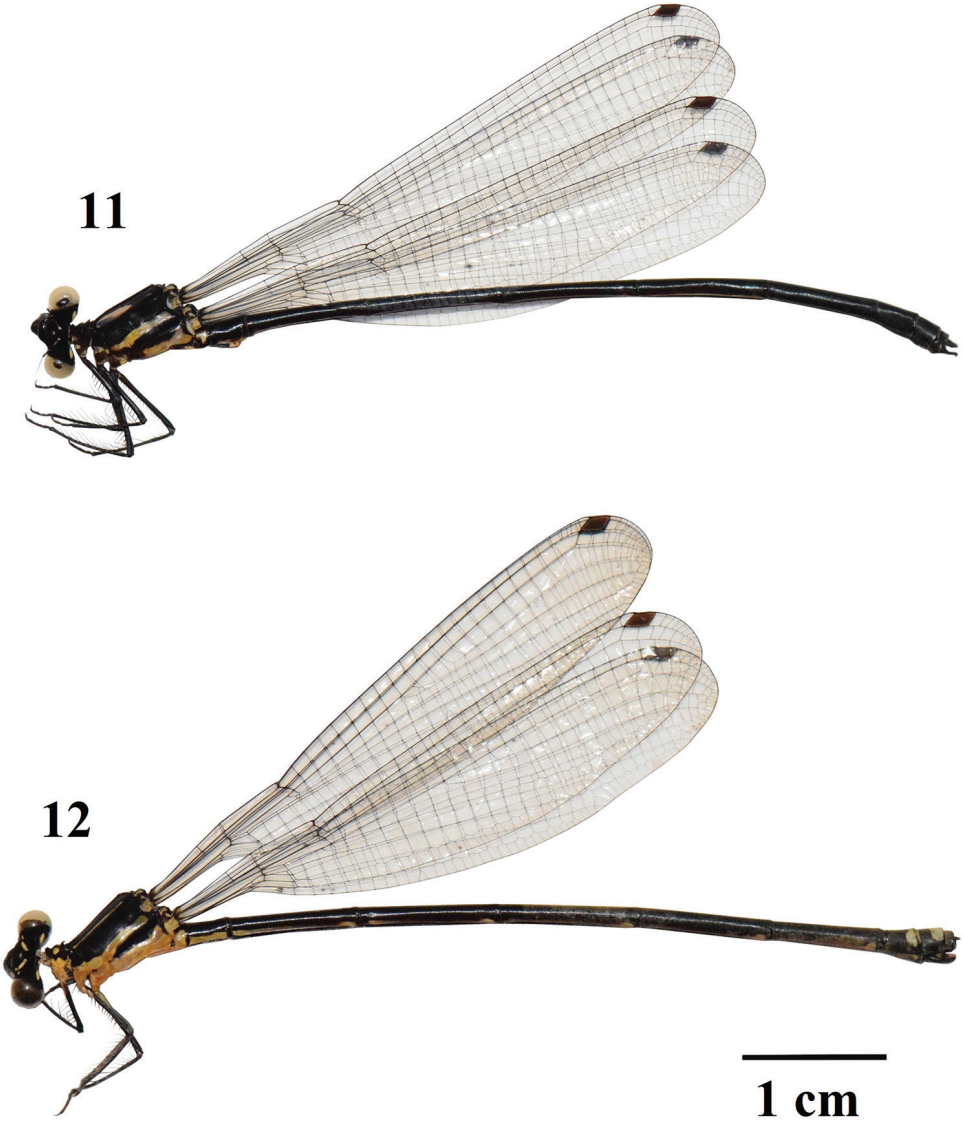

Figures 11–12. Habitus of *Indocnemis marijanmatoki* sp. n. **11** Holotype male **12** Paratype female.

life, but becoming pale yellow surrounding a smaller blue part after acetone treatment. Mesepimeron black, metepisternum black with a large yellow stripe adjacent to meso-coxa and covering spiracle, interrupted before end of segment. A large yellow marking covering most of metepimeron.

Legs (Fig. 21). Coxae pale brown. Femora and tibiae black. Tarsi and armature brown.

Wings (Fig. 31) hyaline with black venation, 24 and 20 Px in FW and HW, respectively. Pterostigma brown, covering 2 underlying cells.

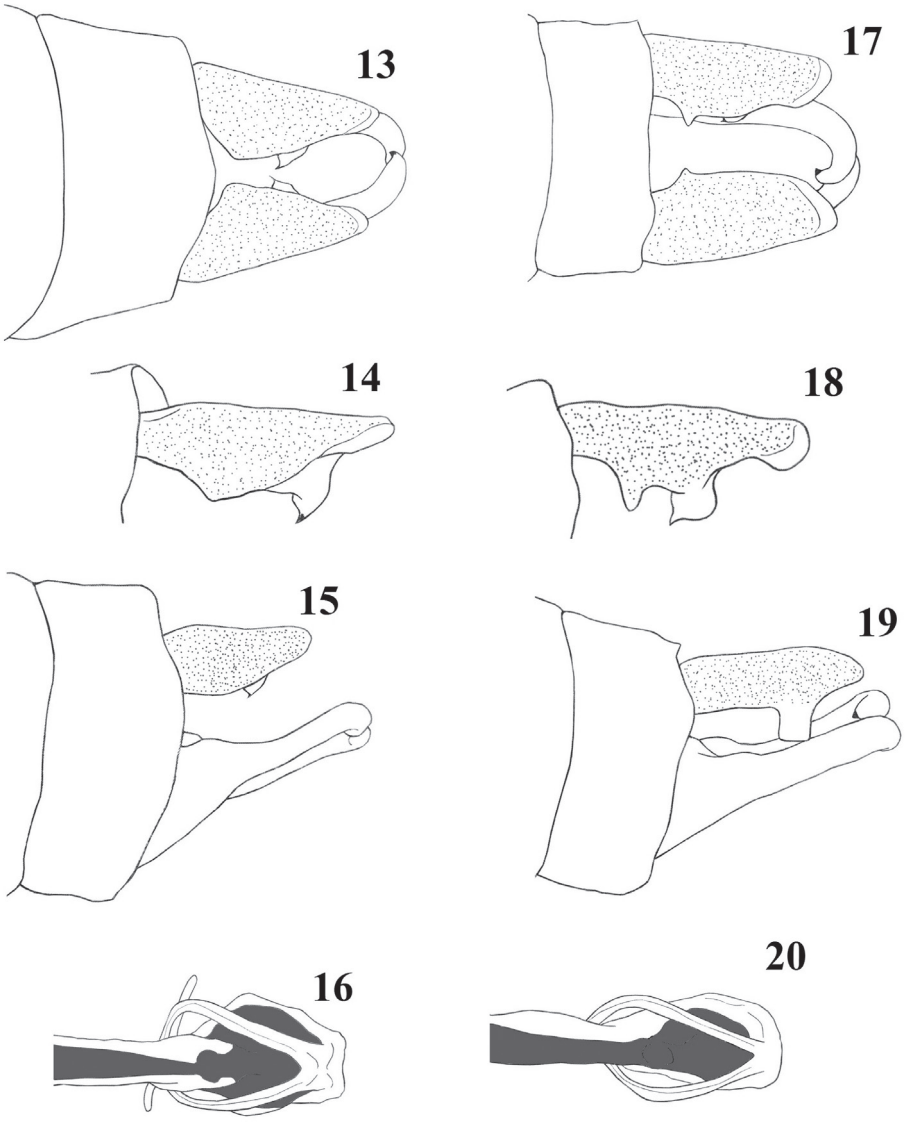

Figures 13–20. *Indocnemis* spp. ♂. **13–16** *I. marijanmatoki* sp. n., holotype ♂ and **17–20** *I. orang* (km19, Hon Ba Nature Reserve) **13, 17** appendages, dorsal view **14, 18** right cerci, oblique-dorsal view **15, 19** appendages, lateral view **16, 20** genital ligula, dorsal view.

Abdomen (Figs 11, 22). Segments entirely black excluded a large yellow marking laterally in S1 and ventral yellow line on S2 and a small whitish lateral spot on S10.

Genital ligula (Fig. 16) structurally simple with two long flagella.

Anal appendages (Figs 13–15, 22) black, except for dorso-apical margin of cerci, which are pale yellow. Cerci bearing a large ventral tooth near the apical portion. In lateral view,

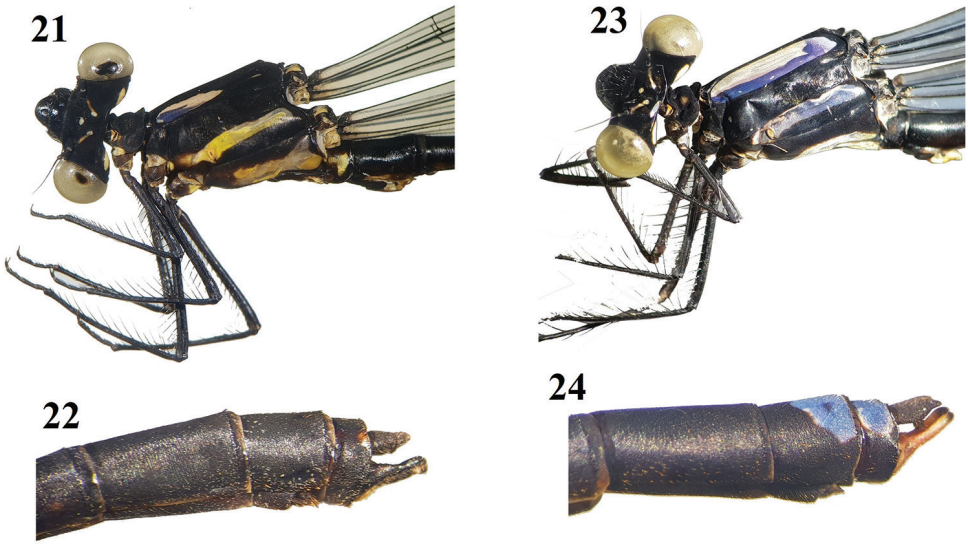

Figures 21–24. *Indocnemis* spp. ♂. **21, 22** *I. marijanmatoki* sp. n., holotype ♂ **23, 24** *I. orang* (km19, Hon Ba Nature Reserve). **21, 23** Head & thorax **22, 24** tip of abdomen.

cerci as long as S10; in dorsal view, cercus narrowing distally and slightly pointed at apex. Paraproct longer than cercus, its tip directed medially and ending in a black tooth.

Measurements. HW 41 mm; abdomen (incl. appendages) 55 mm.

Variation in paratype male. The paratype male differs from the holotype as follows: the blue marking on the mesepisternum slightly larger; the yellow marking in metepimeron not extending to the margin of metinfraepisternum as in the holotype; ventro-lateral S2 without yellow band and the pale marking on S10 bigger than in the holotype. In one male from Kon Ka Kinh National Park, cerci longer than S10, reaching the level of paraproct as in *I. orang*. Measurements ranges of hind wing 40 mm and abdomen (incl. appendages) 52 mm.

Description of female. *Head* (Figs 25, 26). Labrum and postclypeus shining black; anteclypeus brownish; mandible and genae yellow, the lower margin of genae black. Dorsal head side matt black, ocelli pale yellow, there are two long stripes adjacent to ocellus and nearby two oval yellow spots. Posterior side of head black with two yellow spots as in male.

Thorax (Figs 12, 27, 28). Prothorax black, except two large oval spots at sides of middle pronotal lobe of pronotum; lower part of propleuron yellowish. Posterior pronotal lobe well developed, but only half as wide as middle lobe, rounded (Figs 27, 28). Mesepisternum black with a long and narrow antehumeral stripe; mesepimeron black, metepisternum black with a large yellow stripe, rounded at the end and covering spiracle and metathoracic cross sutures; this mark connected to yellow part of metepimeron and metinfraepisternum.

Legs. Coxae and trochanter yellowish. Femora black with yellow marks at base. Tibia, tarsus and armature black.

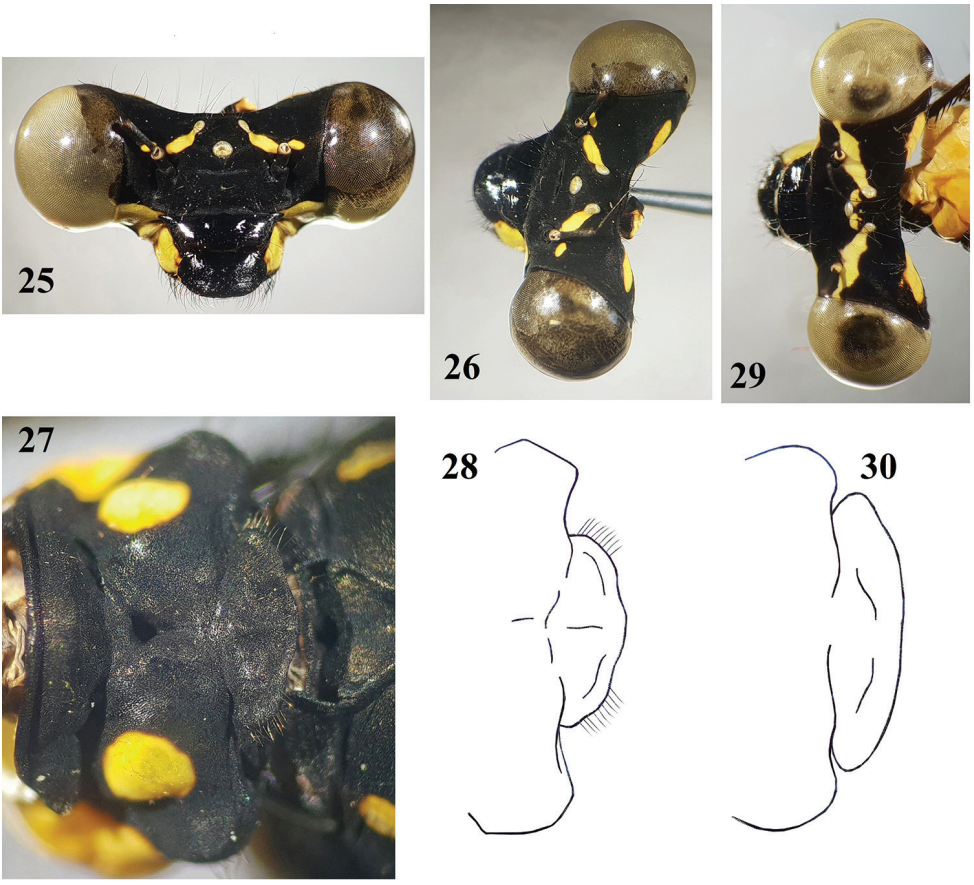

Figures 25–30. *Indocnemis* spp. ♀. **25–28** *I. marijanmatoki* sp. n. and **29, 30** *I. orang* (km19, Hon Ba Nature Reserve) **25** head, frontal view **26, 28** head, oblique-dorsal view **27** prothorax, dorsal view **29, 30** posterior lobe of prothorax, dorsal view.

Wings. Hyaline, 23–24 and 20 Px in FW and HW, respectively. Pterostigma brown, covering 1.5–2 cells.

Abdomen (Fig. 12). S1 black with a large lateral yellow spot; S2–3 with a yellow latero-ventral band; S4 with two tiny yellow spots at segment margins; S5–7 with a tiny yellow spot at ventral-apical margin of each segment; S8–9 black with a large bluish marking dorso-apically on each segment; S10 black. Cerci black, ovipositor black with small yellow spot anteriorly and dorsally at apex.

Measurements. HW 41 mm; abdomen (incl. appendages) 55 mm.

Habitat and ecology. At the type locality, the new species was found at a narrow (2–3 m wide), shallow stream with sandy bottom. Specimens were collected in April, which otherwise is early for other dragonflies and damselflies, so only *Anotogaster* sp. was found at the same stream. At the two localities where the new species was found, *I. marijanmatoki* sp. n. and *I. orang* occur at quite different elevations. The new spe-

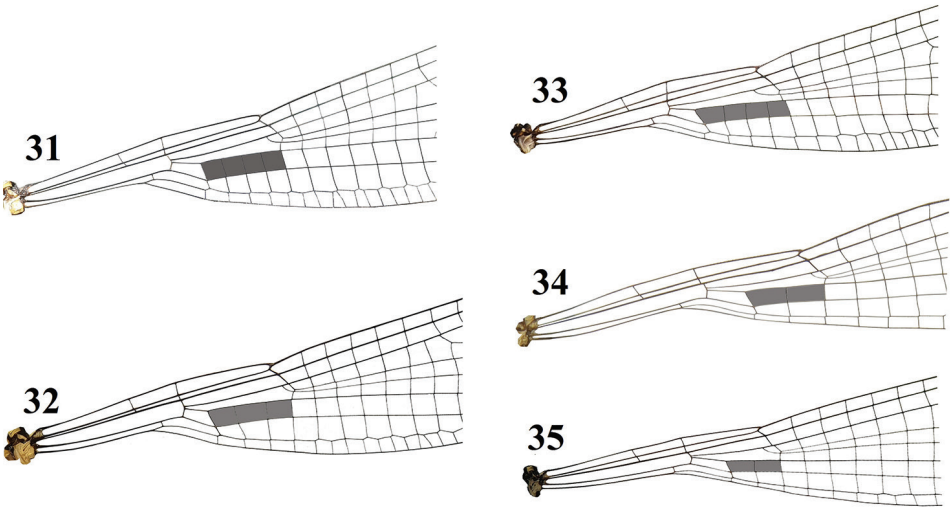

Figures 31–35. *Indocnemis* spp. and *Coeliccia* spp., base of hind wing. The brownish cells indicated the number of cells between discoidal cell and the nervure descending from the subnode **31** *I. marijanmatoki* sp. n., holotype male **32** *I. orang,* male (Km 19, Hon Ba Nature Reserve) **33** *C. ambigua,* female (Ba Be National Park, Bac Kan Prov., 6.vii.2015, Hoang Vu Tru leg.) **34** *C. mingxiensis*, male (Bach Ma National Park, Thua Thien Hue Prov., 27.vi.2017, Q.T. Phan leg.) **35** *C. cyanomelas,* male (Bach Ma National Park, Thua Thien Hue Prov., 27.vi.2017, Q.T. Phan leg.).

cies occurs at very high elevations, from 1,400–1,500 m a.s.l., while *I. orang* is usually found in the areas ranging from 300–600 m a.s.l.

Discussion. In the male, the cerci of *Indocnemis marijanmatoki* sp. n. are relatively short, as long as S10 and lack a robust basal spine (Figs 13–15), while in *I. orang*, the cerci are 1.5 times the length of S10 and have a robust basal spine (Figs 17–19); the paraprocts of *I. marijanmatoki* sp. n. are entirely black (Fig. 22), but those of *I. orang* are yellowish (Fig. 24); the dorsum of S9–10 of *I. marijanmatoki* is black (Fig. 22), while strikingly marked with blue in *I. orang* (Fig. 24); and finally, the bluish dorsal stripe extends above the mesepimeron, covering most of the mesepisternum in *I. orang* (Figs 8, 23) but is reduced to a smaller shield-shaped mark and another tiny oval spot in *I. marijanmatoki* (Figs 7, 21). Females of both species are very similar in appearance but differ clearly in the shape of the posterior lobe of the prothorax. In *I. marijanmatoki* sp. n., this structure is prominent, but clearly less wide and semicircular in shape (Fig. 28), whereas it is much wider in *I. orang* (Fig. 30). The yellow stripe on the dorsum of the head of all examined specimens of *I. orang* extends to the margin of the compound eyes (Fig. 29), just like in Thai (Asahina 1985: 8, fig. 27) and Indian specimens (Asahina 1997: 9, fig. 32), while these are divided into two stripes, never touching the margin of the compound eye (Fig. 26) in *I. marijanmatoki* sp. n.

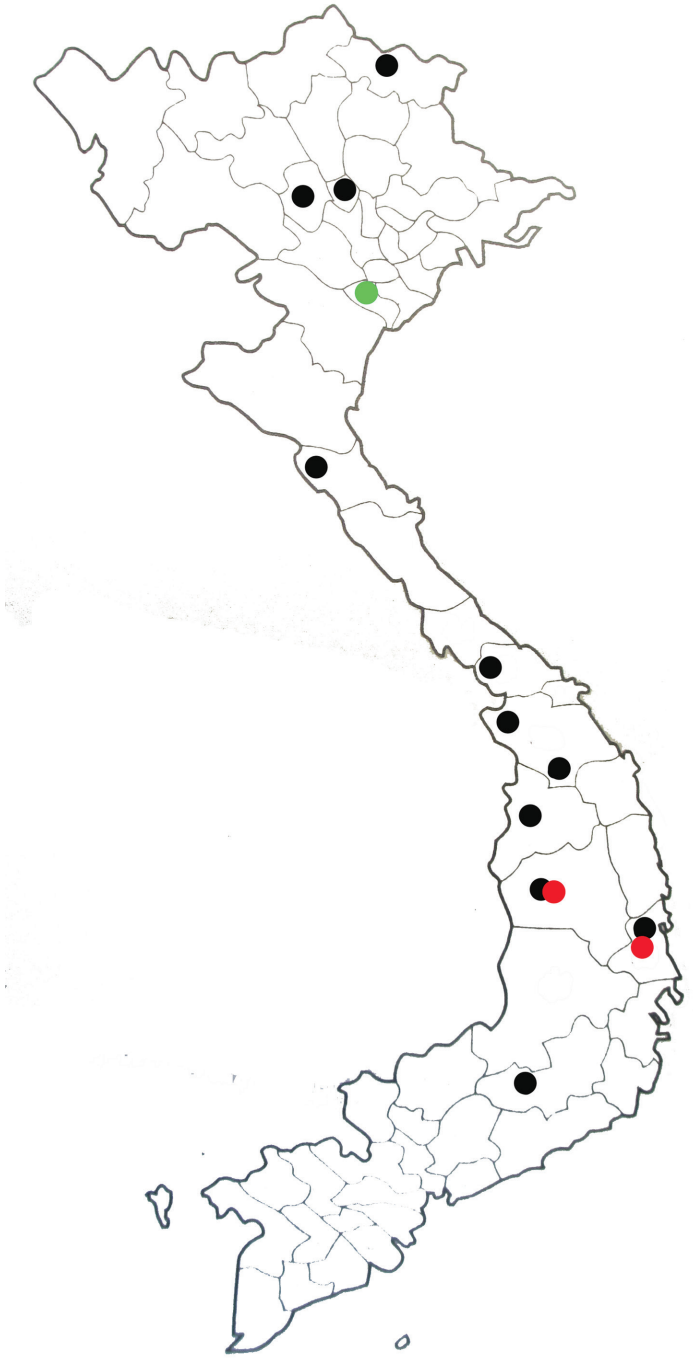

Figure 36. Provincial distribution map of *Indocnemis marijanmatoki* (●), *I. orang* forma *orang* (●) and *I. orang* forma *kempi* (●) in Vietnam based on Do and Dang 2007) and this study.

Acknowledgements

I am sincerely grateful to the following people: Mr Tom Kompier for revising and improving earlier drafts of the manuscript; Dr Oleg E. Kosterin, Dr Keith D.P. Wilson, and Dr Jan van Tol for reviewing, revising the manuscript; Mr To Van Quang (Southern Institute of Ecology, Vietnam Academy of Science and Technology) for providing specimens; Mr Noppadon Makbun for providing information on the distribution of *Indocnemis orang* in Thailand; Dr Le Nguyen Bao (Provost of Duy Tan University) for supporting fieldwork; Mr Pham Anh Tuan (Duy Tan University) for his help during fieldwork and the directorate of Hon Ba Nature Reserve for providing support and permission; and finally the IDEA WILD Foundation for supporting the purchase of the Micro Nikkor lens used in this study.

My fieldwork was partly funded by the International Dragonfly Fund and the Nagao Natural Environment Foundation, Japan to the author via the project entitled "Assessment of species diversity and conservation status of stream-dwelling damselflies (Odonata: Calopterygoidea) in Vietnam".

References

Asahina S (1985) A list of the Odonata recorded from Thailand. Part V. Platycnemididae 2 (*Calicnemia* and *Indocnemis*). Chô Chô 8(1): 2–12.

Asahina S (1997) Records of the northern Vietnamese Odonata taken by the expedition members from the National Science Museum, Tokyo. 5: Coenagrionidae, Protoneuridae, Platycnemididae. Bulletin of the National Science Museum, Tokyo (A) 23: 17–34.

Choong CY (2018) Odonata of Peninsular Malaysia. http://odonata-malaysia.blogspot.com/2010/11/indocnemis-orang.html [accessed 4 April 2018]

Dijkstra KDB, Kalkman VJ, Dow RA, Stokvis FR, van Tol J (2013) Redefining the damselfly families: a comprehensive molecular phylogeny of Zygoptera (Odonata). Systematic Entomology 39(1): 68–96. https://doi.org/10.1111/syen.12035

Farrell D (2018) Dragonflies and Damselflies of Thailand. http://thaiodonata.blogspot.com/2011/03/indocnemis-orang.html [accessed 4 April 2018]

Joshi S, Dawn P, Roy PK, Kunte K (2018) Odonata of India, v. 1.10. Indian Foundation for Butterflies. http://www.indianodonata.org/sp/309/Indocnemis-orang [accessed 4 April 2018]

Kompier T (2018) Dragonflies and Damselflies of Vietnam. http://odonatavietnam.blogspot.com/search/label/Indocnemis [accessed 4 April 2018]

Kosterin OE, Kompier T (2017) *Coeliccia rolandorum* sp. n. from eastern Cambodia and southern Vietnam, the eastern relative of *C. kazukoae* Asahina, 1984 (Odonata: Platycnemididae). Zootaxa 4341(4): 509–527. https://doi.org/10.11646/zootaxa.4341.4.4

Laidlaw FF (1917) A list of the dragonflies recorded from the Indian Empire with special reference to the collection of the Indian Museum. Part II. The family Agrioninae. Records of the Indian Museum 13: 321–348. https://doi.org/10.5962/bhl.part.5864

Laidlaw FF (1931) A list of the dragonflies (Odonata) of the Malay Peninsula with descriptions of new species. Journal of the Federated Malay Museums 16: 175–233.

Paulson DR (2018) Collecting Dragonflies (Odonata) and Maintaining a Collection. https://www.pugetsound.edu/academics/academic-resources/slater-museum/biodiversity-resources/dragonflies/collecting-preserving-specim [accessed 4 April 2018]

Phan QT, Kompier T (2016) Description of two new species of *Coeliccia* from Vietnam (Odonata: Platycnemididae). Zootaxa 4196(3): 407–414. https://doi.org/10.11646/zootaxa.4196.3.4

Phan QT, Tran TTT (2018) Description of *Coeliccia phamiha* sp. n. from central Vietnam (Odonata: Platycnemididae). International Journal of Odonatology 21(1): 45–53. https://doi.org/10.1080/13887890.2017.1419885

Subramanian KA (2010) *Indocnemis orang*. The IUCN Red List of Threatened Species 2010. e.T167459A6351350. https://doi.org/10.2305/IUCN.UK.2010-4.RLTS.T167459A6351350.en [accessed 4 April 2018]

Wilson KDP, Reels GT (2003) Odonata of Guangxi Zhuang autonomous region, China, Part I: Zygoptera. Odonatologica 32(3): 237–279.

Yokoi N, Souphanthong V (2014) A List of Lao Dragonflies. Privately published by the first author, 110 pp.

ZooKeys 809: 31–39 (2018)
doi: 10.3897/zookeys.809.30647
http://zookeys.pensoft.net

RESEARCH ARTICLE

A peer-reviewed open-access journal
ZooKeys
Launched to accelerate biodiversity research

A new species of the genus *Deinodryinus* Perkins (Hymenoptera, Dryinidae) from the USA

Stefano Speranza[1], Massimo Olmi[2], Adalgisa Guglielmino[1], Mario Contarini[1]

1 *Department of Agriculture and Forest Sciences (DAFNE), University of Tuscia, Viterbo, Italy* **2** *Tropical Entomology Research Center, Viterbo, Italy*

Corresponding author: *Adalgisa Guglielmino* (guglielm@unitus.it)

Academic editor: *Michael Ohl* | Received 17 October 2018 | Accepted 20 November 2018 | Published 19 December 2018

http://zoobank.org/453BD4A0-1DEE-4490-84FB-6BAA780B8B6E

Citation: Speranza S, Olmi M, Guglielmino A, Contarini M (2018) A new species of the genus *Deinodryinus* Perkins (Hymenoptera, Dryinidae) from the USA. ZooKeys 809: 31–39. https://doi.org/10.3897/zookeys.809.30647

Abstract

A new species of *Deinodryinus* Perkins, 1907, is described from the USA, Texas: *D. bimaculatus* **sp. n.** Morphologically the new species is similar to *D. masneri* (Olmi, 1984), but it is distinguished by the head lacking a frontal line and the forewing crossed by two dark transverse bands; in *D. masneri* the head shows a conspicuous frontal line and the forewing is hyaline and without dark transverse bands.

Keywords

Chrysidoidea, Anteoninae, Texas, Buescher State Park, *Deinodryinus bimaculatus*, *Deinodryinus masneri*, taxonomy, key

Introduction

Dryinidae (Hymenoptera: Chrysidoidea) are parasitoids and often also predators of leafhoppers, planthoppers and treehoppers (Hemiptera, Auchenorrhyncha) (Guglielmino et al. 2013). They comprise 16 subfamilies, 50 genera and more than 1800 world species (Olmi and Xu 2015; Tribull 2015).

One of the most common genera of this family is *Deinodryinus* Perkins, 1907, belonging to the subfamily Anteoninae. *Deinodryinus* species are parasitoids of leafhoppers belonging to the Cicadellidae (Guglielmino et al. 2013; Olmi and Virla 2014;

Olmi and Xu 2015). As in almost all dryinids, females of *Deinodryinus* have a chelate protarsus. Chelae are used to capture and restrain the host during oviposition and host feeding (Olmi 1984, 1994).

According to Olmi (1984, 1987), in the Nearctic region, the genus *Deinodryinus* includes four species. In 2017 the authors examined a further new species collected in Texas. It is described below.

Material and methods

The description follows the terminology used by Olmi (1984), Guglielmino et al. (2017b, 2018) and Olmi and Virla (2014). The measurements reported are relative, except for the total length (head to abdominal tip, without the antennae), which is expressed in millimeters. In the descriptions, POL is the distance between the inner edges of the lateral ocelli; OL is the distance between the inner edges of a lateral ocellus and the median ocellus; OOL is the distance from the outer edge of a lateral ocellus to the compound eye; OPL is the distance from the posterior edge of a lateral ocellus to the occipital carina; TL is the distance from the posterior edge of an eye to the occipital carina.

The term "metapectal-propodeal complex" is here used in the sense of Kawada et al. (2015). It corresponds to the term "metathorax + propodeum" sensu Olmi (1984), Xu et al. (2013), Olmi and Virla (2014) and Olmi and Xu (2015). The terms "metapostnotum" and "first abdominal tergum" sensu Kawada et al. (2015), used here, correspond to the terms "dorsal surface of propodeum" and "posterior surface of propodeum", *sensu* Olmi (1984), Xu et al. (2013), Olmi and Virla (2014) and Olmi and Xu (2015).

The types of all Nearctic species of *Deinodryinus* were examined. The material studied in this paper is deposited in the collection of the Department of Entomology, Texas A&M University, College Station, Texas, USA (TAMU).

The description of the new species is based on the study of only a single specimen. The authors are aware that descriptions of new taxa should normally be based on more individuals. However, Dryinidae are so rare that it is uncommon to collect more than one specimen of each species. In addition, on the basis of the experience and knowledge of the authors, the new species is sufficiently delimited by unique characters to justify its description.

Results

Genus *Deinodryinus* Perkins, 1907

Deinodryinus Perkins, 1907: 45.

Type species. *Deinodryinus paradoxus* Perkins, 1907, designated by Muesebeck and Walkley (1951).

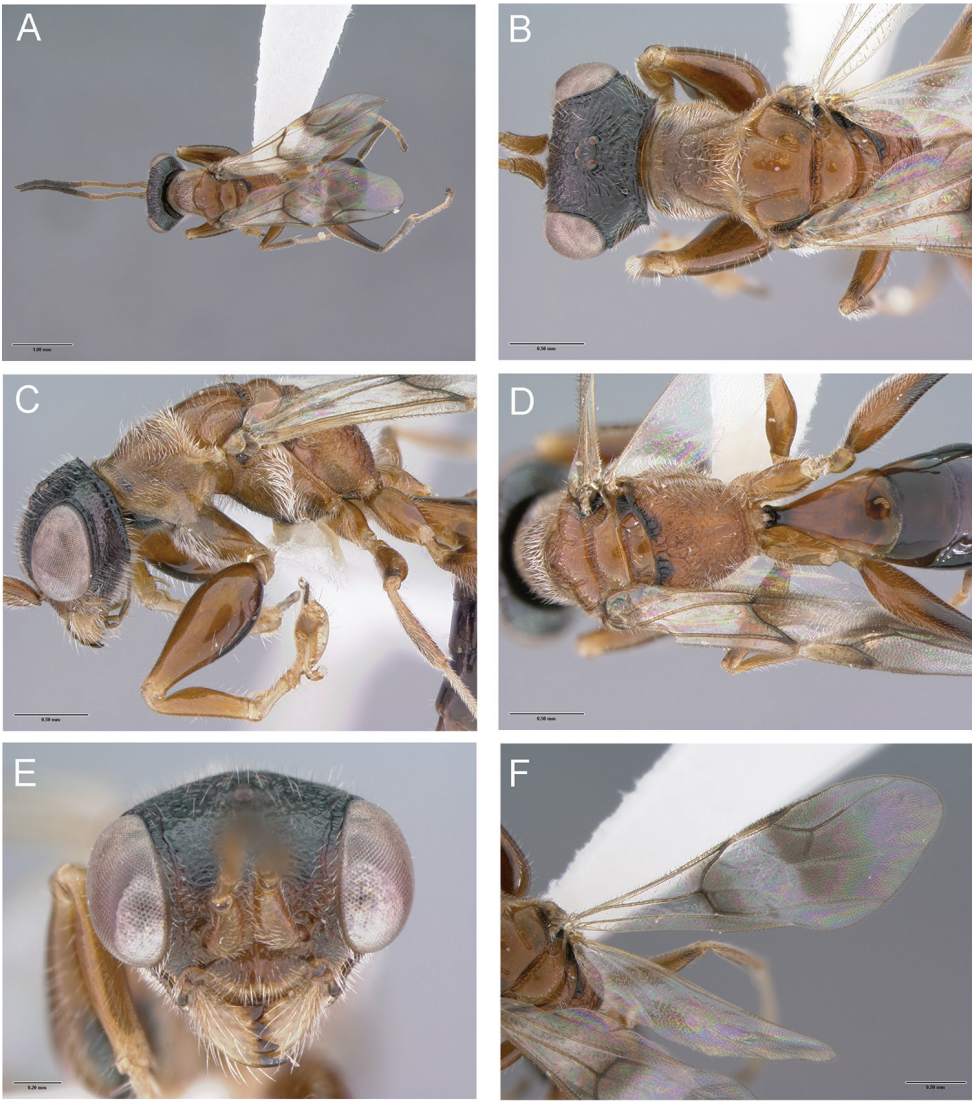

Figure 1. *Deinodryinus atriventris* (Cresson), female from Ohio, Columbus: **A** habitus in dorsal view **B** head and mesosoma in dorsal view **C** head and mesosoma in lateral view **D** metapectal-propodeal complex in dorsal view **E** head in frontal view **F** forewing.

Diagnosis. Female (Fig. 1): Macropterous or micropterous; palpal formula 6/3; occipital carina complete; vertex of head frequently with two strong oblique keels connecting posterior ocelli to occipital carina; pronotum with distinct anterior collar and posterior disc; in macropterous females forewing usually with distal part of stigmal vein longer than proximal part, less frequently as long as, or shorter than proximal part; enlarged claw with inner proximal prominence not bearing bristles, with one or two bristles or peg-like hairs located further distally than proximal prominence; tibial

spurs 1/1/2. Male: Macropterous (even with micropterous female); palpal formula 6/3; vertex of head frequently with two strong oblique keels connecting posterior ocelli to occipital carina; antennal hairs usually much longer than breadth of segments, less frequently shorter than breadth of segments; forewing usually with distal part of stigmal vein longer than proximal part, less frequently as long as, or shorter than proximal part; forewing usually with pterostigma four, or more than four, times as long as broad; paramere without dorsal process, usually with one more-or-less large inner branch wrapping penis, less frequently with one reduced inner branch; tibial spurs 1/1/2.

***Deinodryinus bimaculatus* sp. n.**
http://zoobank.org/229725A4-497A-40D7-AE11-3ED7BCE6D7AB
Fig. 2

Diagnosis. Female with head not provided with two oblique keels connecting posterior ocelli to occipital carina (Fig. 2B); head without frontal line (Fig. 2B); forewing with two dark transverse bands (Fig. 2C); metapectal-propodeal complex strongly reticulate rugose, mainly on metapostnotum (Fig. 2D).

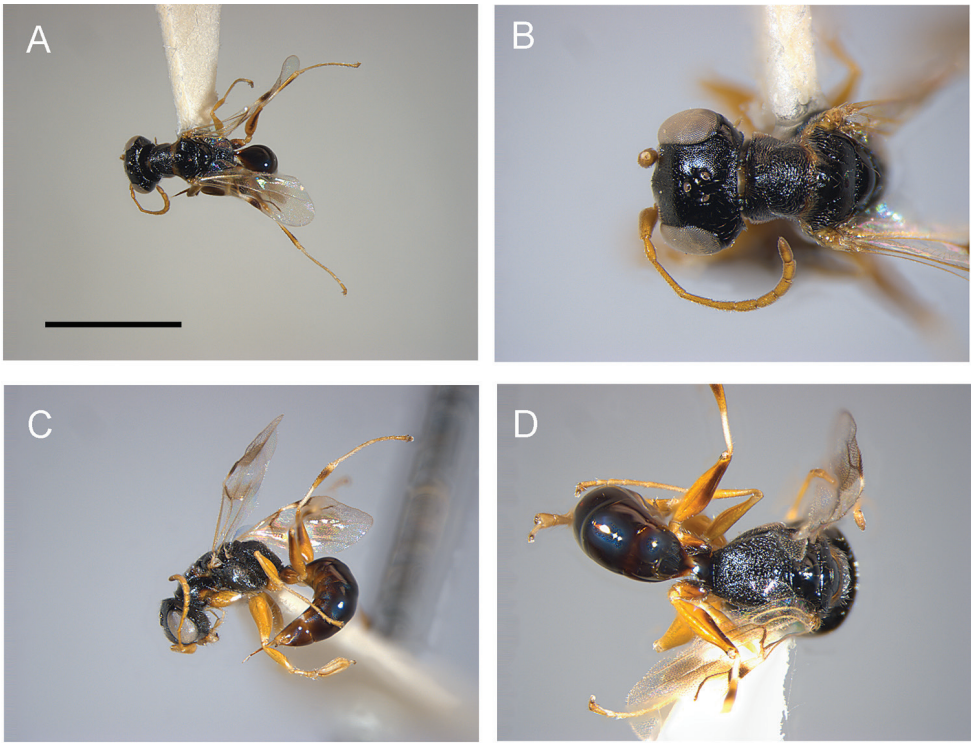

Figure 2. *Deinodryinus bimaculatus* sp. n., female holotype: **A** habitus in dorsal view **B** head, pronotum and mesoscutum in dorsal view **C** habitus in lateral view **D** metapectal-propodeal complex in dorsal view. Scale bars: 2.09 mm (**A**), 0.95 mm (**B**), 1.50 mm (**C**), 0.99 mm (**D**).

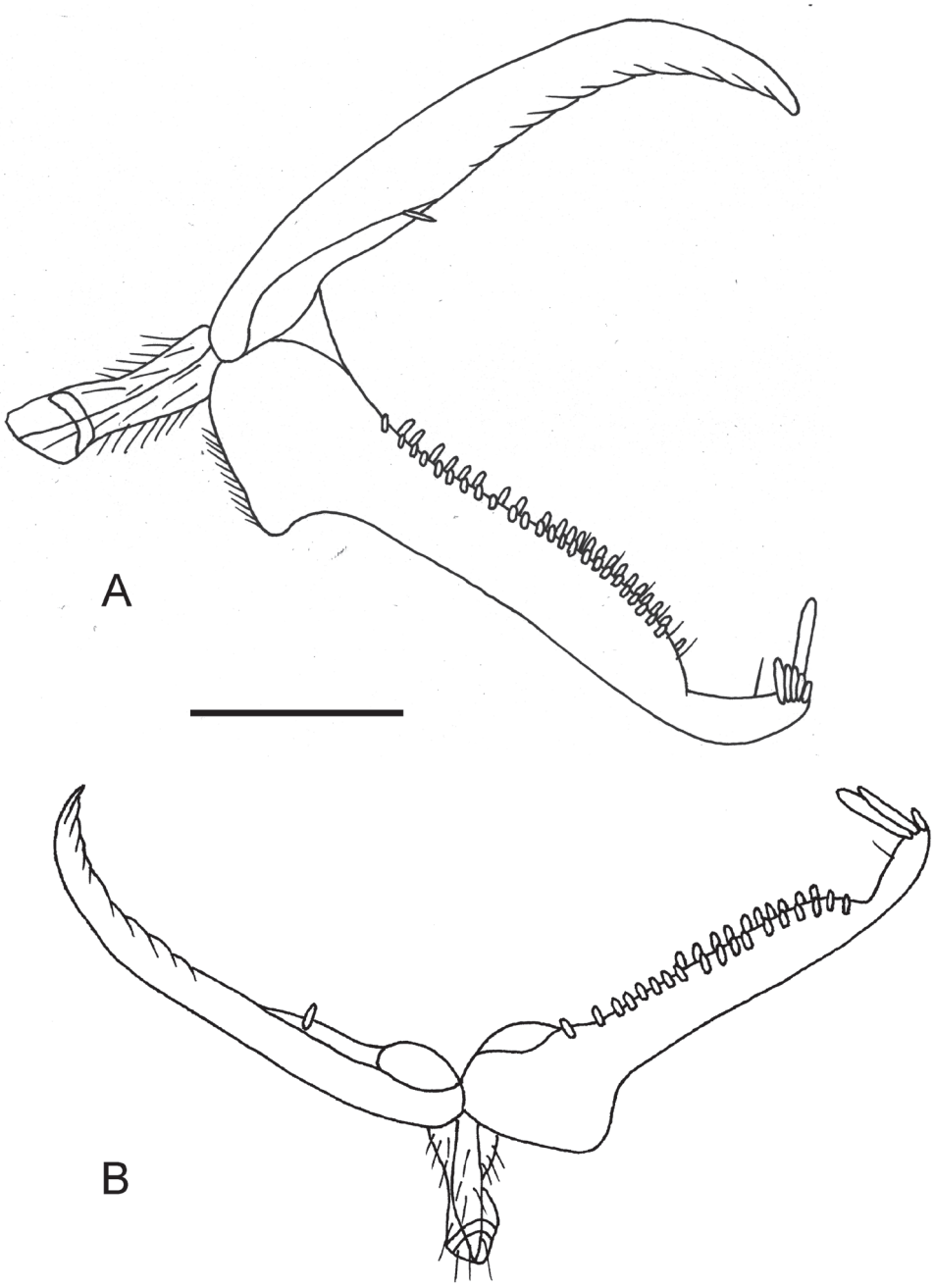

Figure 3. *Deinodryinus bimaculatus* sp. n., female holotype: **A** chela **B** *Deinodryinus masneri* (Olmi), female from California, Tulare Co., Clough's Cave; chela. Scale bars: 0.08 mm (**A**), 0.12 mm (**B**).

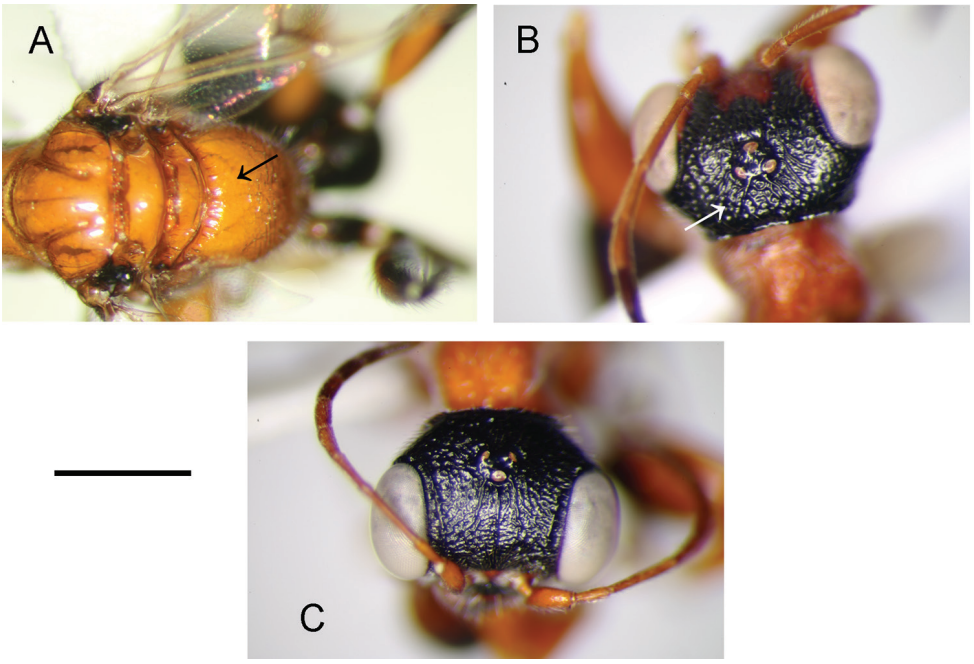

Figure 4. *Deinodryinus paradoxus* Perkins: female from Arizona, Madera Canyon: **A** mesosoma in dorsal view **C** head in dorsal view. *Deinodryinus atriventris* (Cresson), female from Kentucky, Herndon Farm: **B** head in dorsal view. Scale bars: 0.84 mm (**A**), 0.61 mm (**B**), 0.59 mm (**C**).

Description. Female. Fully winged (Fig. 2). Length 2.4 mm. Head black, except mandible, clypeus and gena testaceous. Antenna testaceous, except antennomere 10 slightly darkened. Mesosoma black, except anterior, posterior and lateral margins of pronotum testaceous. Metasoma brown. Legs testaceous, except metacoxa partly brown, club of metafemur and metatibia with brown spot. Antenna clavate. Antennomeres in following proportions: 9:5:10:7:5:5:5:5:5:6. Head dull, granulate (Fig. 2B). Frontal line absent. Occipital carina complete. Head without oblique keels connecting posterior ocelli to occipital carina (Fig. 2B). POL = 3; OL = 3; OOL = 5; OPL = 6; TL = 6. Greatest breadth of lateral ocelli shorter than OPL (2:6). Pronotum shiny, punctate, unsculptured among punctures, sculptured by many transverse striae, with posterior surface about as long as mesoscutum. Mesoscutum shiny, very slightly granulate, mainly on lateral regions. Notauli incomplete (Fig. 2B), reaching approximately 0.6 × length of mesoscutum. Mesoscutellum and metanotum shiny, unsculptured. Metapectal-propodeal complex dull, reticulate rugose and granulate, without transverse or longitudinal keels (Fig. 2D). Metapostnotum and first abdominal tergum not separated by transverse keel. Forewing hyaline, with two dark transverse bands (Fig. 2D). Distal part of stigmal vein longer than proximal part (8:6). Protarsomeres in following proportions: 7:3:4:10:18. Enlarged claw (Fig. 3) with one bristle situated further distally than proximal prominence. Protarsomere 5 (Fig. 3) with two rows of about 46 lamellae and distal apex provided

with approximately six lamellae, among which one much longer than others. Tibial spurs 1/1/2.

Male. Unknown.

Material examined. Holotype: female, USA: Texas, Bastrop Co., Buescher State Park, 29.iv–10.v.1990, R. Wharton leg. (TAMU).

Hosts. Unknown.

Distribution. USA (Texas).

Etymology. The species is named *bimaculatus* (adjective formed by the prefix "bi-" meaning "two" + the Latin adjective "maculatus", meaning "spotted"), because its forewing shows two dark transverse bands.

Remarks. On the basis of the morphological characters indicated in the above diagnosis, *D. bimaculatus* is similar to *D. masneri* (Olmi, 1984), but it differs because the head has no frontal line (frontal line present in *D. masneri*) and the forewing has two dark transverse bands (no dark bands in *D. masneri*). Following the description of the new species, the key to the females of Nearctic *Deinodryinus* published by Olmi (1984) can be revised as follows:

1 Metapectal-propodeal complex strongly reticulate rugose, mainly on metapostnotum (Figs 1D, 2D) **2**

– Metapectal-propodeal complex not reticulate rugose; metapostnotum surface mainly smooth, except some slight irregular keels (Fig. 4A) **4**

2 Vertex of head with two complete keels connecting posterior ocelli to occipital carina (Fig. 4B); occasionally keels incomplete (Fig. 1B) ..... ***D. atriventris* (Cresson)**

– Vertex of head without two oblique keels connecting posterior ocelli to occipital carina (Fig. 2B) **3**

3 Head with frontal line; forewing hyaline, without dark transverse bands..... ***D. masneri* (Olmi)**

– Head without frontal line (Fig. 2B); forewing with two dark transverse bands (Fig. 2C)..... ***D. bimaculatus* sp. n.**

4 Face mostly smooth, except few irregular keels near clypeus..... ***D. quercicolus* Perkins**

– Face completely sculptured by irregular keels (Fig. 4C)..... ***D. paradoxus* Perkins**

Conclusion

Olmi (1984, 1987) listed in the Nearctic region the following four species of *Deinodryinus*: *D. atriventris* (Cresson, 1872), known from Canada, Mexico and USA; *D. masneri* (Olmi, 1984), *D. paradoxus* Perkins, 1907, and *D. quercicolus* Perkins, 1907, known from Mexico and USA. Following the above description, *D. bimaculatus* sp. n., from Texas, is added to the previous lists.

The genus *Deinodryinus* comprises now 163 species (including the new species hereby described), recorded in all the zoogeographic regions, except Antarctica. In the Neotropical region, 112 species are known (Olmi and Virla 2014). In the other regions the number of known species is fewer: nine species in the Oriental region (Xu et al. 2013), seven species in the Palaearctic region (unpublished data), 28 species in the Afrotropical region (unpublished data), two species in the Australian region (Olmi 1991); and five species in the Nearctic region (according to the present paper).

The most common Nearctic species of *Deinodryinus* is *D. atriventris*. One of the authors (MO) reared this species in 2002 in New York state (surroundings of Geneva, Ontario Co.) from *Gyponana cacumina* DeLong and *Gyponana lamina* DeLong (Cicadellidae, Gyponinae), well known vectors of phytoplasmas (Hill and Sinclair 2000) (**New host record**; no other hosts are known). The hosts of other Nearctic species of *Deinodryinus* are unknown (Guglielmino et al. 2013). Records of hosts in the genus *Deinodryinus* are very rare. Previously, the unique records were those of Guglielmino et al. (2013, 2017a). They quoted the following hosts: in Italy, *Laburrus quadratus* (Forel) (Cicadellidae, Deltocephalinae) as host of *Deinodryinus hispanicus* (Olmi, 1991); in South Africa, *Colistra parvulus* (Linnavuori) (Cicadellidae, Deltocephalinae) as host of *Deinodryinus danielssoni* Olmi, 1998; in Namibia, *Aconurella compta* (Naudé), *Exitianus nanus* (Distant) and *Exitianus okahandia* Ross (Cicadellidae, Deltocephalinae) as hosts of *Deinodryinus paulyi* (Olmi, 1987).

Acknowledgements

Many thanks to Prof. James B. Woolley and Dr Karen Wright (Texas A&M University, College Station, USA) for the loan of the specimen described in the present paper. The authors are very grateful to Prof. Maurizio Biondi (University of L'Aquila, Italy) for the multifocal pictures of the new species. Many thanks to Dr. Huayan Chen (Ohio State University) for permission to publish his photos of *Deinodryinus atriventris* (Fig. 1). The authors are grateful to Dr. Clayton Corréa Gonçalves (Instituto Nacional de Pesquisas de Amazônia, Manaus, Brazil) for the identifications of *Gyponana* species hosts of *Deinodryinus atriventris*. Many thanks to Mr. Massimo Vollaro (University of Tuscia, Viterbo) for his photos of *Deinodryinus atriventris* and *paradoxus* (Fig. 4) and Prof. James B. Woolley for his review of the English language of the present paper. We thank two anonymous referees and the subject editor Michael Ohl for their valuable comments and suggestions. This research was carried out in the frame of the MIUR (Italian Ministry for Education, University and Research) initiative "Department of excellence" (Law 232/2016) and partially supported by the European Commission under the Grant Agreement number 774571 (project PANTHEON – "Precision farming of hazelnut orchards").

References

Guglielmino A, Olmi M, Bückle C (2013) An updated host-parasite catalogue of world Dryinidae (Hymenoptera: Chrysidoidea). Zootaxa 3740: 1–113. https://doi.org/10.11646/zootaxa.3740.1.1

Guglielmino A, Olmi M, Marletta A, Bückle C (2017a) Larval morphology of three species of Anteoninae (Hymenoptera, Dryinidae). Zootaxa 4320: 470–486. https://doi.org/10.11646/zootaxa.4320.3.4

Guglielmino A, Olmi M, Marletta A, Speranza S (2017b) Description of the first species of *Gonadryinus* Olmi (Hymenoptera, Dryinidae) from the Afrotropical region. Zootaxa 4238: 440–444. https://doi.org/10.11646/zootaxa.4238.3.11

Guglielmino A, Olmi M, Marletta A, Speranza S (2018) Discovery of the first species of *Dryinus* Latreille (Hymenoptera: Dryinidae) from Burmese amber. Zootaxa 4394: 443–448. https://doi.org/10.11646/zootaxa.4394.3.10

Hill GT, Sinclair WA (2000) Taxa of Leafhoppers Carrying Phytoplasmas at Sites of Ash Yellows Occurrence in New York State. Plant Disease 84(2): 134–138. https://doi.org/10.1094/PDIS.2000.84.2.134

Kawada R, Lanes GO, Azevedo CO (2015) Evolution of metapostnotum in flat wasps (Hymenoptera, Bethylidae): implications for homology assessments in Chrysidoidea. PLoS ONE 10(10): e0140051. https://doi.org/10.1371/journal.pone.0140051

Muesebeck CFW, Walkley LM (1951) Family Dryinidae. In: Muesebeck CFW, Krombein KV, Townes HK (Eds) Hymenoptera of America North of Mexico. Synoptic catalogue. U.S. Department of Agriculture, Agriculture Monograph, 2, Washington, D.C., 1034–1043.

Olmi M (1984) A revision of the Dryinidae (Hymenoptera). Memoirs of the American Entomological Institute 37: i–xii + 1–1913.

Olmi M (1987) New species of Dryinidae (Hymenoptera, Chrysidoidea). Fragmenta Entomologica 19: 371–456.

Olmi M (1991) Supplement to the revision of the world Dryinidae (Hymenoptera Chrysidoidea). Frustula entomologica (NS) 12[1989]: 109–395.

Olmi M (1994) The Dryinidae and Embolemidae (Hymenoptera: Chrysidoidea) of Fennoscandia and Denmark (Fauna Entomologica Scandinavica 30). E.J. Brill, Leiden, Netherlands, 100 pp.

Olmi M, Virla EG (2014) Dryinidae of the Neotropical Region (Hymenoptera: Chrysidoidea). Zootaxa 3792: 1–534. https://doi.org/10.11646/zootaxa.3792.1.1

Olmi M, Xu Z (2015) Dryinidae of the Eastern Palaearctic region (Hymenoptera: Chrysidoidea). Zootaxa 3996: 1–253. https://doi.org/10.11646/zootaxa.3996.1.1

Perkins RCL (1907) Parasites of leaf-hoppers. Report of Work of the Experiment Station of the Hawaiian Sugar Planters' Association, Division of Entomology, Bulletin No. 4: 5–59.

Tribull CM (2015) Phylogenetic relationships among the subfamilies of Dryinidae (Hymenoptera, Chrysidoidea) as reconstructed by molecular sequencing. Journal of Hymenoptera Research 45: 15–29. https://doi.org/10.3897/JHR.45.5010

Xu Z, Olmi M, He J (2013) Dryinidae of the Oriental region (Hymenoptera: Chrysidoidea). Zootaxa 3614: 1–460. https://doi.org/10.11646/zootaxa.3614.1.1

ZooKeys 809: 41–47 (2018)
doi: 10.3897/zookeys.809.30742
http://zookeys.pensoft.net

RESEARCH ARTICLE

A peer-reviewed open-access journal
ZooKeys
Launched to accelerate biodiversity research

First record of *Odontosphaeropyx* Cameron, 1910 from the Oriental Region with description of a new species from Thailand (Hymenoptera, Braconidae, Cheloninae)

Donald L.J. Quicke[1,2], Buntika A. Butcher[1,2]

1 *Integrative Ecology Laboratory, Department of Biology, Faculty of Science, Chulalongkorn University, Phayathai Road, Pathumwan, BKK 10330, Thailand* **2** *Center of Excellence in Entomology: Bee Biology, Diversity of Insects and Mites, Chulalongkorn University, Phayathai Road, Pathumwan, BKK 10330, Thailand*

Corresponding author: *Buntika A. Butcher* (buntika.a@chula.ac.th)

Academic editor: *C. van Achterberg* | Received 22 October 2018 | Accepted 8 November 2018 | Published 19 December 2018

http://zoobank.org/04AD4CA5-2DBB-4A62-BAAE-18D2333F8645

Citation: Quicke DLJ, Butcher BA (2018) First record of *Odontosphaeropyx* Cameron, 1910 from the Oriental Region with description of a new species from Thailand (Hymenoptera, Braconidae, Cheloninae). ZooKeys 809: 41–47. https://doi.org/10.3897/zookeys.809.30742

Abstract

Odontosphaeropyx matasi Quicke & Butcher, **sp. n.** from Thailand is described and illustrated. The new species represents the first known record of *Odontosphaeropyx* from outside of the Afrotropical Region. A key is provided to separate it from the apparently closely related *O. flavifasciatus* Zettel, 1990, with which it shares almost identical colouration, very different from the other five known species.

Keywords

Cheloninae, parasitoid, Afrotropical, Oriental, range extension, new taxon

Introduction

The Cheloninae is a large cosmopolitan subfamily of ovo-larval parasitoids of Lepidoptera (Shaw and Huddleston 1991, Quicke 2015). It is dominated in terms of numbers of species by three genera, *Ascogaster* Wesmael, 1835, *Chelonus* Panzer, 1806, and *Phanerotoma* Wesmael, 1838, which are collectively represented by more than 1500 described species (Yu et al. 2016). However, worldwide another 16 genera (including

the Adeliini) are known, most with more restricted geographic distributions and often known from only a few species and specimens (Zettel 1990, He et al. 1994, Kittel and Austin 2014). The Odontosphaeropygini Zettel 1990 (= Pseudophanerotomini Zettel 1990, synonymized by Braet et al. 2014) are a monotypic tribe with six included species, all in *Odontosphaeropyx* Cameron, and all from the Afrotropical region (Kittel et al. 2016). Here we report the discovery of the first species from outside of Africa and describe a new species of *Odontosphaeropyx* of Thailand.

The discovery of the new species was the result of the extensive TIGER (Thailand Inventory Group for Entomological Research) programme which sampled insects in 25 national parks in Thailand over a three-year period, 2006–2008 (see http://sharkeylab.org/tiger). This programme yielded many thousands of braconid wasp specimens. Among these we discovered two specimens of a relatively large-bodied chelonine, with a single clypeal tooth, fore wing vein (RS+M)a arising from vein 1-M well removed from parastigma, forewing vein m-cu joining (RS+M)a basal to 2RS, and with a pair of transverse sutures on the carapace. Initial generic identification based on the known Asian fauna was problematic, so we used the key to world genera and tribes of Zettel (1990) and obtained a clear identification as *Odontosphaeropyx* which was previously known from six described species, all from sub-Saharan Africa and Madagascar (Braet et al. 2014).

Materials and methods

Terminology follows van Achterberg (1988) except for wing venation nomenclature which follows Sharkey and Wharton (1997); see also fig. 2.2 in Quicke (2015) for comparison of wing venation naming systems.

Specimens were imaged using an Olympus SXZ16 microscope with automated multiple image capture at pre-set focal levels using an Olympus DP72 camera, and image combination using the Cell^D image processing system.

Collection abbreviations: **CUMZ** (Collection of the Insect Museum, Chulalongkorn University Museum of Natural History, Bangkok); **QSBG** (Queen Sirikit Botanic Gardens, Chiang Mai, Thailand.

Species description

***Odontosphaeropyx matasi* Quicke & Butcher, sp. n.**
http://zoobank.org/23D59C0D-8E85-4921-91CA-22A2D48E0F7A
Fig. 1

Type material. Holotype male, THAILAND: Kamphaeng Phet Mae Wang NP, 3–10.ix.2007, 1306 m, C Puluk, A Inpuang, T2812 (QSBG). **Paratype** male, same data as holotype (CUMZ).

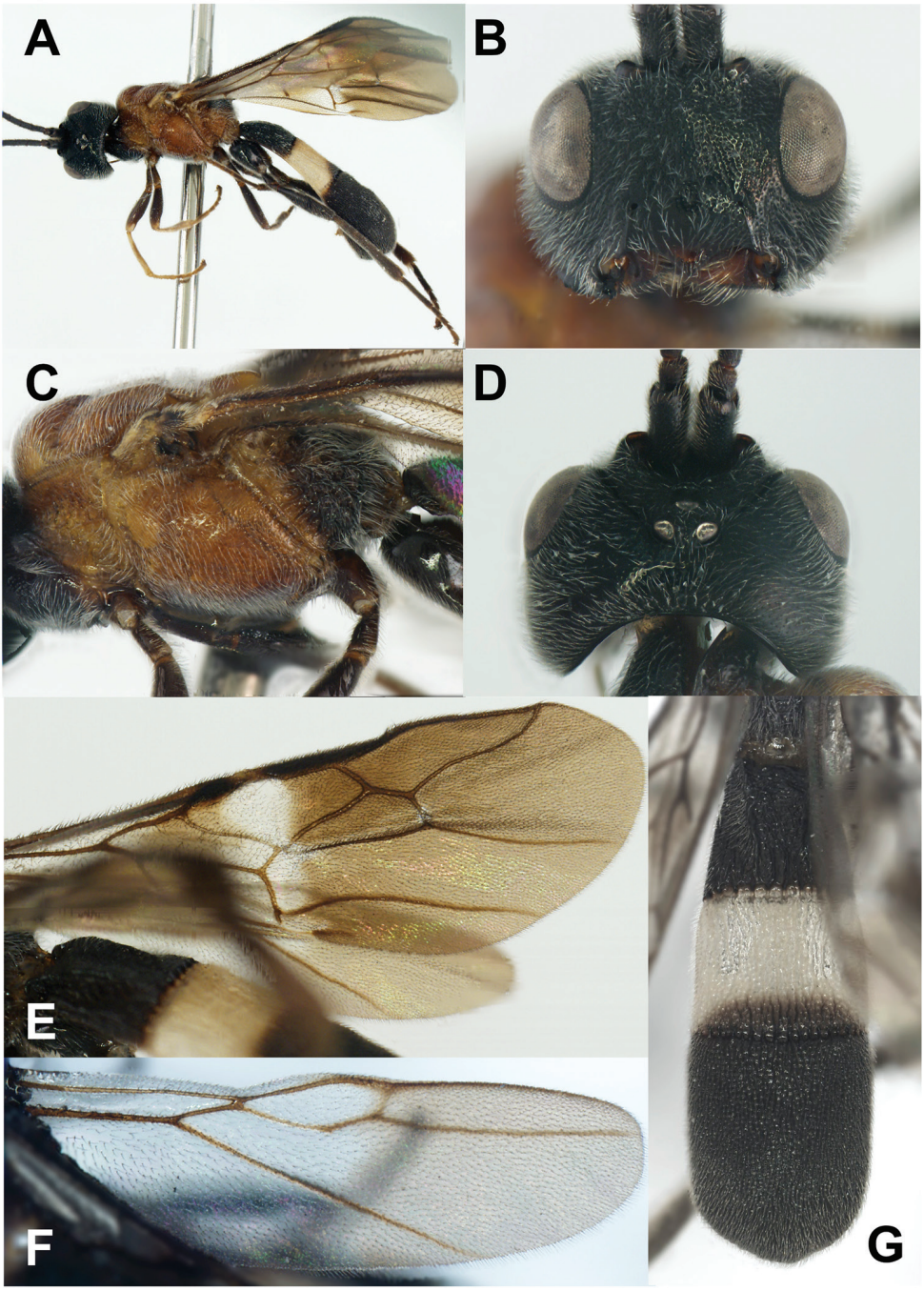

Figure 1. *Odontosphaeropyx matasi* sp. n., males. **A** holotype, habitus lateral view **B** holotype, head, front view **C** paratype, mesosoma, lateral view **D** holotype, head, dorsal view **E** paratype, fore wing **F** holotype, hind wing **G** paratype, metasoma, dorsal view.

Diagnosis. The new species can be distinguished from all other *Odontosphaeropyx* species in having the combination of an orange thorax, a largely black metasoma with white-banded 2nd tergite, and fore wing vein 3RSa longer than r-rs.

Description. Length of body 7.2 mm, of fore wing 6.0 mm and of antenna 6.2 mm. Antenna with 38 flagellomeres. Penultimate flagellomere 1.8× longer than wide. First flagellomere 1.3× longer than 2nd; 3.3× longer than wide. Scapus with 'v'-shaped notch on outer apical margin. Antennal sockets distinctly above level of top of eye. Width of head 1.3× length of head in lateral view. Eyes 2.0× taller than wide in frontal view; glabrous. Width of head: height of eye: width of face = 2.6: 1.0: 1.6. Face and clypeus with dense setiferous punctation. Intertentorial distance 2.0× tentorio-ocular distance. Clypeus produced into a strong median tooth. Length of temple 1.3× length of eye in dorsal view. Frons demarked by a sharply-defined elevation running from front of eye straight to and around stemmaticum; with a crescent-shaped ridge in front of anterior ocellus. Occipital carina complete.

Notauli deeply impressed, foveate-crenulate, the area between them on posterior half of mesoscutum depressed (lower than lateral lobes) and evenly strongly rugose. Scutellar sulcus curved, deep and with 4–6 strong crenulae between outer pair. Mesopleuron and mesosternum with small, dense, setiferous punctures, the cuticle between the punctures shiny. Median area of metanotum with complete mid-longitudinal carina. Propodeum with distinct apophyses, a wide medial groove bordered by irregular carinae and transversed by a ladder-like set of carinae superimposed on rugose background.

Fore wing. Vein 1CUb 3.1× longer than 1CUa. Lengths of veins r-rs: 3RSa: 3RSb = 1.0: 1.3: 4.9.

Length of fore femur: tibia: tarsus = 1.0: 1.50: 1.30. Length of hind femur: tibia: tarsus = 1.0: 1.25: 1.15. Hind femur 4.4× longer than maximally deep. Claws with a pectin of two teeth.

Metasoma 2.8× longer than maximally wide. First tergite with strong, though somewhat irregular, dorsal carinae that almost meet the posterior margin of the tergite. Sutures between the three carapace segments well developed.

Coloration. Head, palps, propleuron, ventromedial part of mesosternum, metapleuron (mostly), propodeum, metasoma except most of second tergite, legs except fore tibia black; fore tibia cream-coloured; 2nd metasomal tergite except medio-posteriorly, white. Wings hyaline with a pale brown cross-band at level of parastigma and pale brown distally from slightly beyond base of pterostigma.

Female. Not known.

Biology. Not known.

Variation. Paratype. Vein 1CUb 3.3× longer than 1CUa. Lengths of veins r-rs: 3RSa: 3RSb = 1.0: 1.25: 4.8. Otherwise almost identical to holotype.

Etymology. Named after Mr Matas Srisabye, late friend, triathlete, Thai National Team athlete (water polo) and running coach of BAB.

Remarks. In the key to *Odontosphaeropyx* species by Braet et al. (2014), which was modified after the one by Zettel (1990), this new species falters at couplet 1 because it has fore wing vein 3RSa longer than r-rs but has the metasoma more than 2.6× longer than wide. The only described species with similar colouration (orange thorax and

largely black metasoma with white-banded 2nd tergite) is *O. flavifasciatus* Zettel, 1990, which is known from Nigeria (type locality) and Democratic Republic of Congo. The two species may be separated using the following amended couplet:

1 Fore wing vein 3RSa longer than r-rs; mesopleuron punctate; fore wing vein 1CUb approximately 3× longer than 1CUa; fore tibia cream-coloured .... ***O. matasi* sp. n.**

– Fore wing vein 3RSa shorter than r-rs; mesopleuron strongly foveate-rugose; fore wing vein 1CUb approximately 2× longer than 1CUa; fore tibia black .. ..***O. flavifasciatus***

In addition to the description and drawings of the holotype of *O. flavifasciatus* [as *Pachychelonus flavofasciatus* Zettel] given in Zettel (1990: figs 3–9), Braet et al. (2012: figs 48–51) provide photographs of a specimen from Democratic Republic of Congo, and further images of the holotype are on the WaspWeb web site housed at the Iziko institution (http://www.waspweb.org/) (accessed 30 September 2018).

Discussion

The increasing use of Malaise traps in diverse countries is resulting in major range extensions of many braconid taxa (e.g., Sharkey 2004, Tan et al. 2010, Sharkey and Braet 2012, Kittel and Austin 2013, Butcher et al. 2016, Ranjith et al. 2017). Given this, together with the relative paucity of studies on SE Asian Braconidae, it is not too surprising that a principally Afrotropical genus also occurs there. Until 2016 only 373 Braconidae species had been recorded from Thailand (Yu et al. 2016) of which 199 belong to the Rogadinae (largely by BA Butcher and collaborators) and 70 to the Agathidinae (largely as a result of Mike Sharkey's studies). Material for both of these groups mainly originated from the TIGER (Thailand Inventory Group for Entomological Research) project. Since much of the TIGER material has yet to be systematically investigated taxonomically, with most braconid subfamilies hardly investigated, it is likely that the Thai braconid fauna will eventually be found to be several times larger than the current total.

Acknowledgements

We are grateful to the Rachadaphiseksomphot Fund, Graduate School, Chulalongkorn University, for the award of a Senior Postdoctoral Fellowship to DLJQ, Center of Excellence in Biodiversity (BDC). Office of Higher Education Commission (BDC-PG2-160007) to BAB. The Animal Systematics Research Unit, Department of Biology, Faculty of Science, Chulalongkorn University, kindly allowed us to use their Cell^D imaging facility. The specimens were collected as part of the TIGER research programme funded by NSF Grant Number: DEB-0542864.

References

Braet Y, Rousse P, Sharkey MJ (2012) New data on African Cheloninae (Hymenoptera, Braconidae) show a strong biogeographic signal for taxa with spined propodea. Zootaxa 3385: 1–32.

Braet Y, van Noort S, Kittel RN (2014) New species of the 'rare' genera *Dentigaster* Zettel, 1990 and *Odontosphaeropyx* Cameron, 1910 (Hymenoptera, Braconidae: Cheloninae). Austral Entomology 54: 197–209. https://doi.org/10.1111/aen.12112

Brues CT (1924) Some South African parasitic Hymenoptera of the families Evaniidae, Braconidae, Alysiidae, and Plumariidae in the South African Museum with a catalogue of the known species. Annals of the South African Museum 19: 1–150.

Brues CT (1926) Studies on Ethiopian Braconidae with a catalogue of the African species. Proceedings of the American Academy of Arts and Sciences 61: 206–436. https://doi.org/10.2307/20026158

Butcher BA, Quicke DLJ, Santhosh S, Ranjith AP (2016) Major extensions of range of two genera of the parasitic wasp subtribe Facitorina (Braconidae: Rogadinae: Yeliconini) with new generic synonymy. ZooKeys 584: 109–120. https://doi.org/10.3897/zookeys.584.7815

Cameron P (1910) On some African species of the subfamilies Exothecinae, Aphrastobraconinae, Cheloninae, Doryctinae, Cardiochilinae and Microgasterinae in the Royal Berlin Zoological Museum. Zeitschrift für Naturwissenschaft 81: 433–450.

De Saeger H (1948) Cardiochilinae et Sigalphinae (Hymenoptera: Apocrita) Fam. Braconidae. Exploration du Parc National Albert. Mission G.F. de Witte 53: 1–272.

He JH, Chen XX, van Achterberg C (1994) *Siniphanerotomella* gen. nov., a new genus of the subfamily Cheloninae Nees (Hymenoptera: Braconidae) from China. Zoologische Mededelingen 68(17): 191–195.

Kittel RN, Austin AD (2013) Remarkable range extension of the previously monotypic braconid genus *Wushenia* Zettel (Hymenoptera: Braconidae: Cheloninae), with description of a second species from Australia. Zootaxa 3694: 486–492. https://doi.org/10.11646/zootaxa.3694.5.6

Kittel RN, Austin AD (2014) Synopsis of Australian chelonine wasps (Hymenoptera: Braconidae: Cheloninae) with description of two new genera. Austral Entomology 53: 183–202. https://doi.org/10.1111/aen.12070

Kittel RN, Austin AD, Klopfstein S (2016) Molecular and morphological phylogenetics of chelonine parasitoid wasps (Hymenoptera: Braconidae), with a critical assessment of divergence time estimations. Molecular Phylogenetics and Evolution 101: 224–241. https://doi.org/10.1016/j.ympev.2016.05.016

Quicke DLJ (2015) Biology, systematics, evolution and ecology of braconid and ichneumonid parasitoid wasps. Wiley Blackwell, Chichester, 681 pp.

Ranjith AP, Santhosh S, Nasser M (2017) Range extension of the rare braconine genus, *Lyricibracon* Quicke (Hymenoptera: Braconidae), with the description of a new species from India. Zootaxa 4227(3): 422–430. https://doi.org/10.11646/zootaxa.4227.3.8

Sharkey MJ (2004) Afrotropical-North American disjunct distribution of *Minanga* (Hymenoptera: Braconidae) with the description of a new species and first record for the New

World. Annals of the Entomological Society of America 97: 1198–1203. https://doi.org/10.1603/0013-8746(2004)097[1198:AADDOM]2.0.CO;2

Sharkey MJ, Wharton RA (1997) Morphology and terminology. In: Wharton RA, Marsh PM, Sharkey MJ (Eds) Identification manual to the New World genera of Braconidae. Special Publication of the International Society of Hymenopterists 1: 19–37.

Sharkey MJ, Braet Y (2012) New species of the rare genera *Dentigaster* Zettel, 1990 (Hymenoptera, Braconidae, Cheloninae) and *Minanga* Cameron, 1906 (Sigalphinae) from French Guiana. Journal of Hymenoptera Research 25(3): 93–102.

Shaw MR, Huddleston T (1991) Classification and biology of Braconid wasps (Hymenoptera: Braconidae). Handbooks for the Identification of British Insects 7(11): 1–126.

Tan JL, He J-H, Chen XX (2010) The genus *Minanga* Cameron (Hymenoptera: Braconidae) in China, with description of a new subgenus and species. Annals of the Entomological Society of America 103(3): 360–365. https://doi.org/10.1603/AN10001

van Achterberg C (1988) Revision of the subfamily Blacinae Foerster (Hymenoptera, Braconidae). Zoologische Verhandelingen, Leiden 249: 1–324.

Yu DS, van Achterberg C, Horstmann K (2016) Taxapad 2016, Ichneumonoidea 2015. Database on flash-drive. www.taxapad.com, Nepean, Ontario.

Zettel H (1990) Eine Revision der Gattungen der Cheloninae (Hymenoptera, Braconidae) mit Beschreibungen neuer Gattungen und Arten. Annalen des Naturhistorischen Museums in Wien 91: 147–196.

ZooKeys 809: 49–54 (2018)
doi: 10.3897/zookeys.809.31162
http://zookeys.pensoft.net

RESEARCH ARTICLE

A peer-reviewed open-access journal
ZooKeys
Launched to accelerate biodiversity research

A new species of *Catapiestus* Perty, 1831 from China (Coleoptera, Tenebrionidae, Cnodalonini)

Shulin Yang[1,2], Juan Guo[1]

1 *School of Life Sciences, Guizhou Normal University, Guiyang, Guizhou China* **2** *Research Center for Karst Caves, Guizhou Normal University, Guiyang, Guizhou China*

Corresponding author: *Shulin Yang* (s.yang@gznu.edu.cn)

Academic editor: *W. Schawaller* | Received 5 November 2018 | Accepted 20 November 2018 | Published 19 December 2018

http://zoobank.org/9ACEA321-5AC5-4A78-A37B-B9E05668CA4F

Citation: Yang S, Guo J (2018) A new species of *Catapiestus* Perty, 1831 from China (Coleoptera, Tenebrionidae, Cnodalonini). ZooKeys 809: 49–54. https://doi.org/10.3897/zookeys.809.31162

Abstract

A new species of the genus *Catapiestus* Perty, 1831 (Coleoptera, Tenebrionidae, Cnodalonini), *C. bispinosus*, is described from Leigonsan National Nature Reserve, Leishan County, Guizhou, China. The identification key by Lang and Ren for the species of *Catapiestus* is modified.

Keywords

darkling beetle, Guizhou, taxonomy, southwest China

Introduction

Catapiestus Perty, 1831 is a genus in the tribe Cnodalonini (Coleoptera, Tenebrionidae), with twelve species recorded from south and southeast Asia and China; only four species were previously known from China. The species have quite uniform strongly flattened body form and coloration, and scarce or no apparent external sexual dimorphism (Lang and Ren 2009). Morphological differentiation of the species mainly depends on features of the pronotum (e.g., shape, lateral serration pattern, presence or absence of mid-longitudinal groove) and number of teeth or denticles of profemora (Lang and Ren 2009). A new species of the genus is described herein based on specimens collected from the Leigongshan National Nature Reserve, Leishan County, Guizhou, China.

Materials and methods

Specimens were collected with six level Lindgren funnel traps which used ethanol as the lure and glycol as the killing and preserving agent in the collection bottles. Specimens were glued on pinned paper points. Labels were handwritten in Chinese. The type material is preserved in the School of Life Sciences, Guizhou Normal University, Guiyang, China (**GZNULS**). An AmScope SM-4TZ stereo microscope was used for specimen observation and dissection. Photographs were taken with a Canon EOS 6D digital camera with EOS MP-E 65 lenses.

Taxonomy

***Catapiestus bispinosus* sp. n.**
http://zoobank.org/F117D549-B08A-4746-A05A-68EB6ED7B46A
Figures 1–3

Type locality. *Holotype*, ♂, China, Guizhou Province, Leishan County, Leigongshan National Nature Reserve, 26°22'25"N, 108°11'58"E, 23.VI.2017, border of broad-leaf forest and Chinese white pine (*Pinus armandii* Franch) forest, leg. S. Yang. *Paratypes*, 1♂, China, Guizhou Province, Leishan County, Leigongshan National Nature Reserve, 26°22'29"N, 108°11'54"E, 19.VIII.2011, broad-leaf forest, leg. S. Yang; 1♀, China, Guizhou Province, Leishan County, Leigongshan National Nature Reserve, 26°22'25"N, 108°11'58"E, 2.VIII.2017, border of broad-leaf forest and Chinese white pine (*Pinus armandii* Franch) forest, leg. Yaokui Yang and Gugangzu Yang.

Type specimens. ***Holotype***, ♂, glued on pinned paper point, with genitalia in a separate microvial. Original label (slash, "/", represents new line): "中国 贵州 雷山/雷公山 八公里入口处 下一/26°22'25"N, 108°11'58"E / 2017.VI.23 / 杨书林采 [handwritten label]" (translation: China, Guizhou, Leishan / Leigongshan, Entrance at 8km Lower #1 / 23.VI.2017 / leg. Shulin Yang), "HOLOTYPE: / *Catapiestus bispinosus* Yang & Guo / ♂ [handwritten on red label]". ***Paratypes***, 1♂, glued on pinned paper point, with genitalia in a separate microvial. Original label (slash, "/", represents new line): "中国 贵州 雷山 / 雷公山 生态定位点 / 26°22'29"N, 108°11'54"E / 2011.VIII.19 / 杨书林采 [handwritten label]" (translation: China, Guizhou, Leishan / Leigongshan Eco-monitoring site / 19.VIII.2011 / leg. Shulin Yang), "PARATYPE:/ *Catapiestus bispinosus* Yang & Guo / ♂ [handwritten on red label]". 1♀, glued on pinned paper point. Original label (slash, "/", represents new line): "中国 贵州 雷山/雷公山 八公里入口处 下一 / 26°22'25"N, 108°11'58"E / 2017.VIII.2 / 杨耀奎 杨光祖 采 [handwritten label]" (translation: China, Guizhou, Leishan /Leigongshan, Entrance at 8km Lower #1 / 26°22'25"N, 108°11'58"E / 2.VIII.2017 / leg. Yaokui Yang and Gugangzu Yang), "PARATYPE:/ *Catapiestus bispinosus* Yang & Guo / ♀ [handwritten on red label]".Type specimens deposited in School of Life Sciences, Guizhou Normal University (GZNULS).

Figure 1. Habitus of *C. bispinosus*, male, dorsal view.

Figure 2. Femora of *C. bispinosus*, male, ventral view.

Differential Diagnosis. The new species *C. bispinosus* sp. n. has two distinctive teeth on profemora. *Catapiestus clavipes* Lang & Ren, 2009, which also has two teeth on profemora, differs from *C. bispinosus* sp. n by larger size and different shape, and tooth positions of profemora. The profemora of *C. bispinosus* are nearly parallel-sided, not expanded at base, the larger tooth is situated at apex, and a small tooth is located at the base of profemora (Figs 1, 2). The profemora of *C. clavipes* are expanded at base with a large tooth at the base and a small tooth at apex. Aedeagus of *C. bispinosus* is more rounded in lateral view and gradually widening from apex to base while aedeagus of *C. clavipes* is nearly parallel-sided in basal half of parameres and phallobase.

Description. Male (Fig. 1): Body broad, flat, length 12.98–13.14 mm, width 4.02–4.1 mm. Integument dark brown to black. Head, pronotum, and elytra densely punctured, ventral head and pro-thorax, and abdomen weakly punctured and wrinkled.

Head: broad, trapezoidal, constricted at base to cylindrical neck. *Labrum* transverse, densely punctured and with sparsely short hairs, margin nearly rounded, with dense hairs. *Clypeus* broad, frontal slightly concave, lateral corners rounded. Outer edges of *gena* raised at antennal insertions. Fronto-clypeal suture visible as a lineal ridge, fronto-genal sulcus indistinct. Interocular space 4× eye width. *Antennae* not reaching beyond middle of pronotum when extended backwards, pedicel and 3–5th antennomeres nearly conical, 6–11th antennomeres clavate with shape transition from nearly triangular of the 6th to oval of the last antennomere.

Thorax: *pronotum* transverse, raised, and with mid-longitudinal sulcus, glossy with sparse small shallow punctures in inner half, outer half inclined toward lateral margins with dense large deep punctures; anterior margin slightly concave; lateral margins arched, widest nearly at middle, serrate with 5 to 6 blunt teeth; base nearly straight with narrow ridge. *Propleura* densely punctured, pro-sternal process also punctured, gradually widening, trapezoidal, base angles acute, mesepisterna and mesepimera with denser but shallower punctures. *Scutellum* nearly semicircular, with sparse small shallow punctures.

Elytra nearly parallel; *epipleura* reaching apex, not glossy as other part; scutellary striole short, with 4–6 punctures; each elytron with nine punctured striae, 1st and 2nd, 3rd and 4th, 5th and 6th connected at base, respectively; intervals between 5th and 6th, and

Figure 3. Aedeagus of *C. bispinosus*, male, left to right: ventral view, dorsal view and lateral view. Scale bar: 1 mm.

6th and 7th striae carinate, carina of interval between 6th and 7th striae starting at elytral base and ending at basal 2/5 of elytral length, where carina of interval between 5th and 6th striae starting. The two carinae connected, sometimes weakly, at basal 2/5 of elytra, forming a longitudinal plica on elytron.

Legs: slender with dense punctures; anterior side of ventral profemur slightly extended and ridged with two teeth, one smaller near basal third and one larger near apex. Meso- and metafemora with only one tooth on ventral anterior side of each femur near apex, larger on metafemura (Figs 1, 2).

Abdomen: densely and coarsely punctured, first three ventrites with longitudinal winding wrinkles.

Male genitalia: aedeagus nearly spindle shaped in dorsal view, arcuate in lateral view, ratio of width to length 1:5, ratio of parameres to phallobase nearly 3:5 (Fig 3).

Female, no apparent external sexual dimorphism except body slightly smaller, length 12.66 mm, width 3.74 mm.

Etymology. The name of the new species refers to two spine-like teeth on each profemur.

Distribution. China: Guizhou, Leishan, Leigongshan.

Discussion. The range of *Catapiestus* in China has a distributional gap between Yunnan and Fujian provinces below 30°N in southern China. The discovery of *C. bispinosus* in Guizhou province presents a range extension for the genus and a provision for new species and distribution records of the genus in the area of southern China between Guizhou and Fujian provinces.

Modified couplets to the key to *Catapiestus* by Lang and Ren (2009)

The couplets 2 and 3 of the key to *Catapiestus* by Lang and Ren (2009) should be modified as follows to receive *C. bispinosus* sp. n.

2	Profemur with 2 teeth	**2a**
–	Profemur with 1 or 3 teeth or denticles	**3**
2a	Profemur strongly expanded at base, with 1 large tooth at widest point, 1 small tooth at apex	***C. clavipes***
–	Profemur not expanded at base, nearly parallel-sided, with 1 small tooth at base and 1 large tooth at apex	***C. bispinosus***
3	Profemur with only 1 tooth in front margin	**5**
–	Profemur with 3 denticles	***C. mediocris***

Acknowledgements

The study was funded by Guizhou Science and Technology Department (Grant No. 黔科合SY字 [2013]3170 and 黔科合J字LKS[2011]38号 to Shulin Yang, and 黔科合J字LKS[2012]21号to Juan Guo), Guizhou Human Resources and Social Security Department [黔6人项目资助合同(2013)12号] and National Science Foundation of China (31360435) to Shulin Yang. We thank the subject editor, Wolfgang Schawaller, and the two reviewers, Ottó Merkl and Kiyoshi Ando, for their help in improving this manuscript.

References

Lang JT, Ren GD (2009) A review of the genus *Catapiestus* Perty, 1831 (Coleoptera: Tenebrionidae: Cnodalonini) with descriptions of two new species from China. Caucasian Entomological Bulletin 5(2): 195–199.

Perty JAM (1831) Observationes nonnullae in Coleoptera Indiae orientalis. Mich. Lindauer, Monachii, 44 pp. [1 pl.]

ZooKeys 809: 55–77 (2018)
doi: 10.3897/zookeys.809.29032
http://zookeys.pensoft.net

RESEARCH ARTICLE

A peer-reviewed open-access journal
ZooKeys
Launched to accelerate biodiversity research

Skeleton and musculature of the male abdomen in Tanyderidae (Diptera, Nematocera) of the Southern Hemisphere

Olga G. Ovtshinnikova[1], Tatiana V. Galinskaya[2,3], Elena D. Lukashevich[4]

1 *Zoological Institute, Russian Academy of Sciences, Universitetskaya nab., 1, St. Petersburg 199034, Russia* **2** *Department of Entomology, Faculty of Biology, Lomonosov Moscow State University, Leninskie gory 1–12, Moscow 119234, Russia* **3** *Scientific-Methodological Department of Entomology, All-Russian Plant Quarantine Center, Pogranichnaya 32, Bykovo, Moscow region 140150, Russia* **4** *Borissiak Paleontological Institute of Russian Academy of Sciences, Profsoyuznaya st., 123, Moscow 117647, Russia*

Corresponding author: *Tatiana V. Galinskaya* (nuha1313@gmail.com)

Academic editor: *Vladimir Blagoderov* | Received 11 August 2018 | Accepted 2 November 2018 | Published 19 December 2018

http://zoobank.org/D00683C7-C5D0-4CF6-A361-DEB457EA2650

Citation: Ovtshinnikova OG, Galinskaya TV, Lukashevich ED (2018) Skeleton and musculature of the male abdomen in Tanyderidae (Diptera, Nematocera) of the Southern Hemisphere. ZooKeys 809: 55–77. https://doi.org/10.3897/zookeys.809.29032

Abstract

The structure of the male terminalia and their musculature of species of tanyderid genera *Araucoderus* Alexander, 1929 from Chile and *Nothoderus* Alexander, 1927 from Tasmania are examined and compared with each other and with published data on the likely relatives. The overall pattern of male terminalia of both genera is similar to those of most Southern Hemisphere genera, with simple curved gonostyli, lobe-like setose parameres, and setose cerci inconspicuous under the epandrium. Both genera have terminalia similarly rotated by 180° (and 90° as an intermediate stage); rotation may be either clockwise or counter-clockwise. However, the similar patterns are realized differently: segment VIII is the decreased and asymmetrical due to completely membranose tergite VIII in *Nothoderus* (the first record of such modification in Tanyderidae), but narrow and symmetrical in *Araucoderus*. Accordingly, pregenital muscles are very different between the genera. Based on localization of muscle attachment sites, the hypandrial origin of the stripe between gonocoxites is shown in both genera, and entire membranization of tergite VIII and partial membranization of hypoproct is shown in *Nothoderus*. Tanyderidae are characterized by highly specialized sclerites and muscles of male terminalia and provide no evidence of relationship with previously studied members of Psychodidae, Blephariceridae and Ptychopteridae.

Keywords
crane flies, rotation, terminalia, genitalia, morphology, *Araucoderus*, *Nothoderus*

Introduction

Tanyderidae, or primitive crane flies, are a small ancient nematocerous family with amphitropical distribution and higher recent diversity in the Southern Hemisphere (Eskov and Lukashevich 2015). Only 18 extinct and extant genera (most of them monotypic) are described in the family, which has been known since the Early Jurassic (Ansorge 1994, Skibińska et al. 2014). In the 19th century tanyderids were described in the family Ptychopteridae, but now the family is usually considered to be close to Psychodidae (Crampton 1926, Alexander 1927, Shcherbakov et al. 1995, Krzemiński et al. 2013); however, some current authors consider it to be closely related to Ptychopteridae (Hennig 1973, Wood and Borkent 1989, Oosterbroek and Courtney 1995) or Blephariceridae (Lambkin et al. 2013; Ptychopteridae were not included in the analysis). Close relationships between Tanyderidae, Blephariceridae and Psychodidae was recently inferred from DNA phylogeny (Bertone et al. 2008, Wiegmann et al. 2011) and possible closeness of Tanyderidae and Psychodidae was inferred from DNA phylogeny of Psychodidae (Curler and Moulton 2012).

The family is important for understanding of the history of the order, but remains insufficiently studied. Male genitalia of some extant genera have been described or drawn with varying degrees of detail; both genera from the Northern Hemisphere: *Protoplasa* Osten-Sacken, 1860 and *Protanyderus* Handlirsch, 1909; and most of genera from the Southern Hemisphere: *Peringueyomyina* Alexander, 1921, *Mischoderus* Handlirsch, 1909, *Araucoderus* Alexander, 1929, *Eutanyderus* Alexander, 1928, *Nothoderus* Alexander, 1927 and *Neoderus* Alexander, 1927 (Alexander 1927, 1928, Williams 1933, Colless and McAlpine 1970, Savchenko 1971, 1974, 1978, Borkent and Sinclair 2012, Madriz and Courtney 2016, Madriz 2017, Madriz et al. 2018). Only *Peringueyomyina*, *Araucoderus* and *Neoderus* were described in sufficient detail. Musculature of the terminalia has never been examined in the family.

Among the likely relatives, musculature has been examined in the blepharicerid, *Edwardsina gigantea* Zwick, 1977 (Zwick 1977), the ptychopterid, *Ptychoptera lacustris* Meigen, 1830 (Just 1973) and the psychodids, *Phlebotomus garnhami* Heisch, Guiggsberg & Teesdale, 1956 (Just 1973), *P. papatasi* (Scopoli, 1786) (Jobling 1987), *Pericoma* sp. (Hennig 1936) and *Pneumia palustris* (Meigen, 1804) (as *Pericoma palustris* in Just 1973). All examined psychodids are members of more derived subfamilies (Phlebotominae and Psychodinae), whereas musculature for members of basal subfamilies has not yet been described. Additionally, the data of different authors are usually difficult to compare, because a uniform nomenclature of muscles is lacking; moreover, figures of Jobling (1987) are not accompanied by any descriptions. Therefore, as the first step for further comparison, a table with the presumed homology of musculature among families was compiled (Table 1). Recently a similar attempt of homologization was undertaken for other families of Diptera (Spangenberg et al. 2012).

Study of the musculature is helpful not only for specifying the functions of genital sclerites, but also for revealing the homology of some poorly traced structures (Ovtshinnikova and Yeates 1998, Ovtshinnikova and Galinskaya 2016b, 2017, Galinskaya et al. 2018). Based on morphogenetical regularities formulated by Matsuda (1976) and verified by Ovtshinnikova (1989) and Friedrich and Beutel (2008), characters associated with muscles are confirmed to be more stable than those associated with sclerites and therefore can be used successfully in phylogenetic studies; morphological series of different species are especially productive for such studies.

The purpose of this study was to investigate the skeleton and musculature of the male genitalia of two genera of Tanyderidae from the Southern Hemisphere. The muscles and sclerites of the male abdomen of *Nothoderus australiensis* (Alexander, 1922) from Tasmania and the muscles of the male abdomen of *Araucoderus gloriosus* (Alexander, 1920) from Chile are described for the first time.

Material and methods

This study is based on males of Tanyderidae collected in *Nothofagus*-dominated forests in Chile and Tasmania by D. Shcherbakov and E. Lukashevich in 2014 and 2015. Specimens studied herein will be deposited in the Zoological Institute RAS, St-Petersburg, Russia. Additional specimens are deposited in the National Museum of Natural History, Santiago, Chile (*Araucoderus*) and Tasmanian Museum and Art Gallery, Hobart, Australia (*Nothoderus*).

Scanning electron micrographs of uncoated and coated males were taken with a Tescan Vega microscope using backscattered electron (BSE) and secondary electron (SE) detectors.

The terminology of the male genital sclerites mainly follows Cumming and Wood (2009) with additions on structure of the parameres made by Madriz and Courtney (2016). Description of sclerites of *Nothoderus australiensis* in this study is modeled on the description of *Araucoderus gloriosus* from the study of Madriz and Courtney (2016).

The muscular systems of male genitalia were studied by manually dissecting the material (preserved fresh in 70% alcohol) with microknives in water under a Leica MZ9^5 stereomicroscope. The pictures were taken using the image capture function of the Leica MZ9^5 trinocular head and subsequently processed. The male terminalia muscles were classified into several groups: muscles of the epandrial complex, muscles of the hypandrial complex, tergosternal muscles, and pregenital muscles. The muscles were numbered according to the classification previously accepted by Ovtshinnikova with the following modifications *M21* = *M3*, *M29* = *M7* and *M32* = *M23* based on homologization of muscles (Ovtshinnikova 2000).

List of abbreviations: *aed* – aedeagus; *cerc* – cercus; *ej apod*– ejaculatory apodeme; *ep* – epandrium; *goncx* – gonocoxite; *gonst* – gonostylus; *hypd* – hypandrium; *hypp* – hypoproct; *ISM* – abdominal intersegmental sternal muscles; *ITM* – abdominal intersegmental tergal muscles; *lepr* – lateral ejaculatory process; *M1–M33* – pregenital

and genital muscles; *pm db* – dorsal bridge of paramere; *pm dme* – dorsomedial element of paramere; *pm gbl* – paramere lobe at gonocoxite base; *pm lme* – lateromedial element of paramere; *spm sac* – sperm sac; *st* – sternite; *tes* – testis; *th* – thorax; *tg* – tergite; *TSM* – abdominal tergosternal muscles.

Results

Family Tanyderidae Osten-Sacken, 1880
Subfamily Tanyderinae Osten-Sacken, 1880

The subfamily includes nine extant and five extinct genera with relatively short gonopods. Musculature of male terminalia is here examined for only two members of the subfamily.

Tanyderidae are characterized by abdominal segments with intersegmental tergal (*ITM*), intersegmental sternal (*ISM*) and tergosternal (*TSM*) muscles and by pregenital muscles (*M18*, *M19*). Male genital muscles of Tanyderidae are classified into several groups: tergosternal muscles (*M5*); muscles of the hypandrial complex (3 pairs of ejaculator muscles *M23*, *M30*, *M31*; aedeagal muscle *M1+2*; 2 pairs of gonostylar muscles *M27*, *M28*); muscles of the epandrial complex (muscles *M3*, connecting epandrium with hypoproct (=X sternite); muscles *M7*, connecting hypoproct with cerci).

Araucoderus gloriosus (Alexander, 1920)

Figures 1A, B, 2–4

Material. Chile, *Nothofagus*-dominated forest, on riparian vegetation. Alerce Andino National Park: Lenca River, 340 m asl (41°30'S, 72°37'W), 6–8.i.2014, 12–18.i.2015, D.E. Shcherbakov, E.D. Lukashevich, 8 males; Puyehue National Park: Anticura River near Anticura Waterfall, 400 m asl (40°40'S, 72°10'W), 14.i.2014, E.D. Lukashevich, 1 male; Chanlefu River at Aguas Calientes, 470 m asl (40°44'S, 72°18'W), 16.i.2014, D.E. Shcherbakov, 1 male; Huerquehue Natianal Park: near Tiquilco Lake, 780 m asl, (39°10'S, 71°44'W), 22.xii.2014, E.D. Lukashevich, 1 male; near La Junta, Rio Palena, 70 m asl, (43°49'S, 72°21'W), 5.i.2015, E.D. Lukashevich, 1 male. The specimens will be deposited in the Zoological Institute RAS, St-Petersburg, Russia.

Exoskeleton. The male terminalia were described in great detail by Madriz and Courtney (2016), so here we describe only the muscles; scanning electron micrographs of genitalia are published for comparison purposes (Figure 1A, B).

Musculature. *Thoracic muscles.* One pair of tergal muscles, connecting thorax and medial part of tergite I; one pair of sternal muscles, connecting thorax and anterolateral margin of sternite II (Figure 2C).

Abdominal muscles. One pair of long intersegmental tergal muscles *ITM1* connecting medial part of tergite I and medial part of tergite II (Figure 2C). Segments I–VII

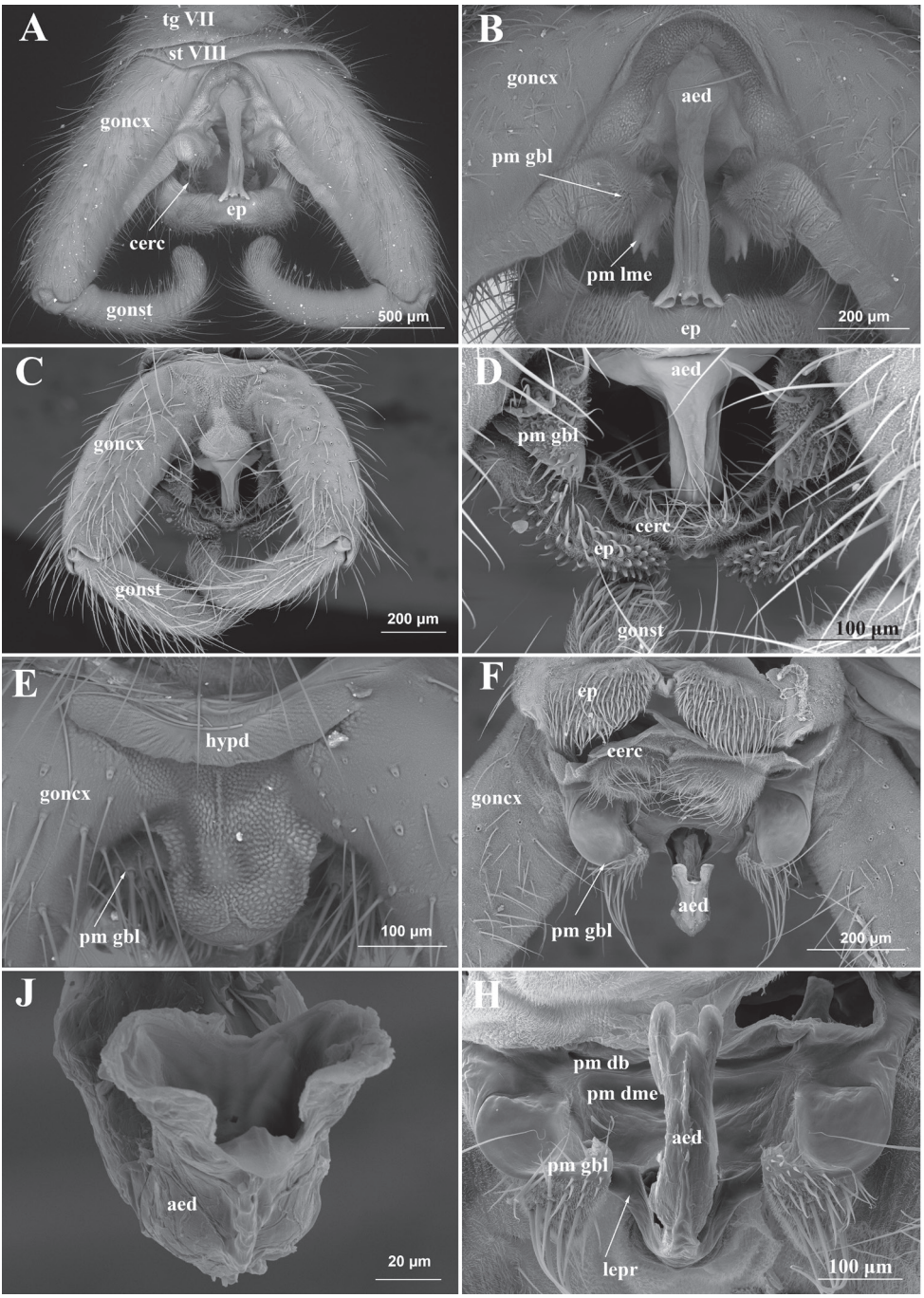

Figure 1. SEM images of male genitalia of Tanyderidae. **A–B** *Araucoderus gloriosus* (uncoated, BSE; Chile, Alerce Andino), dorsal view **C–H** *Nothoderus australiensis* **C–E** dorsal view (uncoated, BSE; Tasmania, Mystery Creek Cave) **F–H** ventral view (coated, SE; Tasmania, Lake Saint Clair).

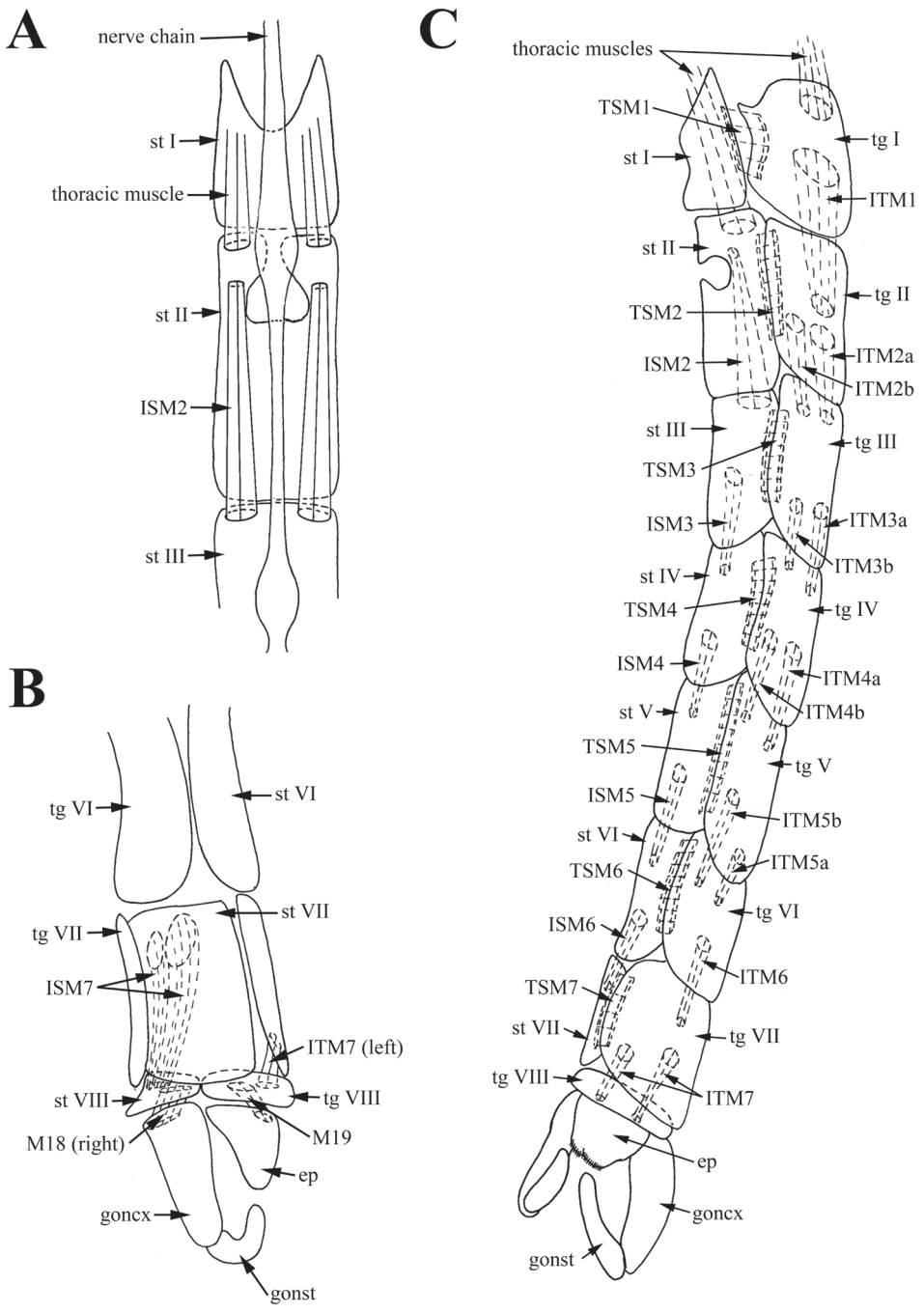

Figure 2. Male of *Araucoderus gloriosus*. **A** sternites, inner view **B** tip of abdomen, right lateral view **C** abdomen, left lateral view.

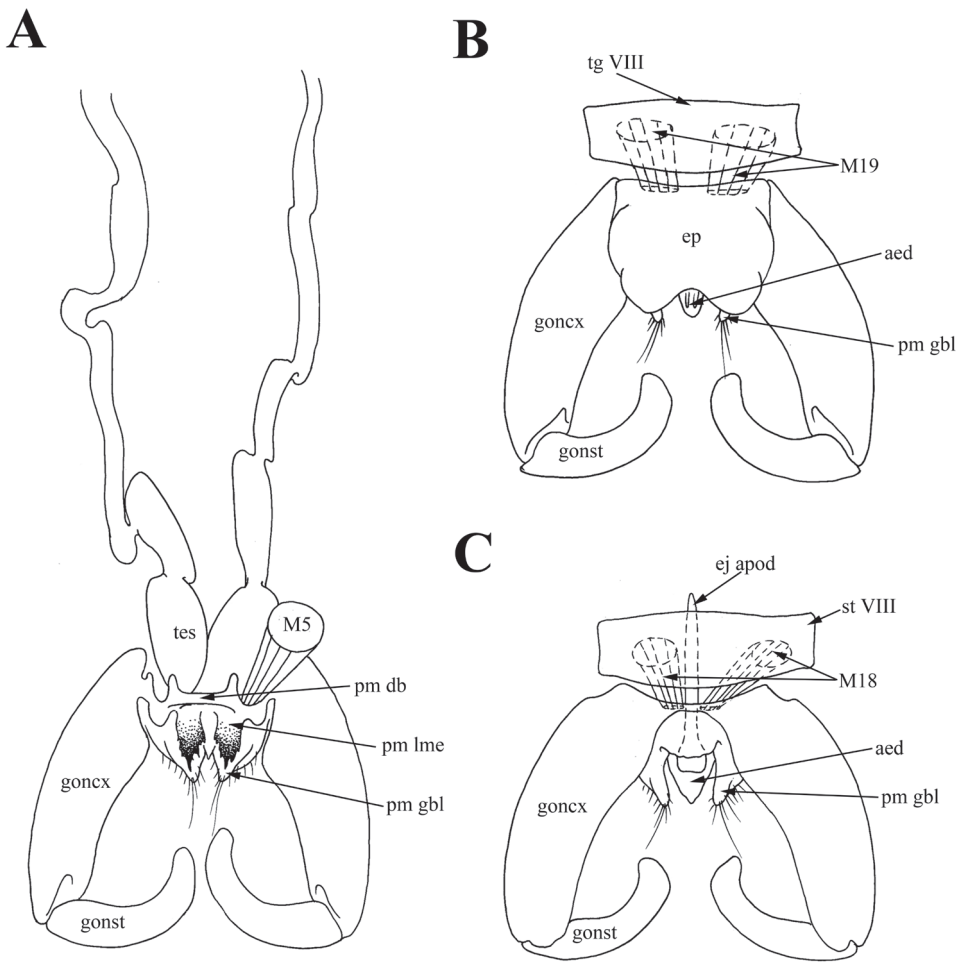

Figure 3. Male of *Araucoderus gloriosus*. **A** genitalia, inner view **B** genitalia, ventral view **C** genitalia, dorsal view.

with wide, short tergosternal muscles (*TSM1–TSM7*) (Figure 2C). One pair of long symmetrical intersegmental sternal muscles *ISM2* passing from anterior third of sternite II to anterior margin of sternite III. Two pairs of long symmetrical intersegmental tergal muscles (*ITM2a,b*) passing from posterior half of tergite II to anterior margin of tergite III; medial ITM2a slightly thinner and longer, lateral *ITM2b* slightly stronger but shorter (Figure 2A, C). Intersegmental tergal and sternal muscles on segments III–V with similar attachment sites as intersegmental muscles of segments II–III (Figure 2C). One pair of intersegmental tergal muscles *ITM6* extending from tergite VI to tergite VII. One pair of intersegmental sternal muscles *ISM6* extending from sternite VI to sternite VII. Intersegmental muscles *ITM6* and *ISM6* thinner than intersegmental muscles of previous segments; posterior sites of attachment of muscles *ITM6* and *ISM6* slightly displaced counterclockwise due to terminalia rotation (Figure 2C). One pair of

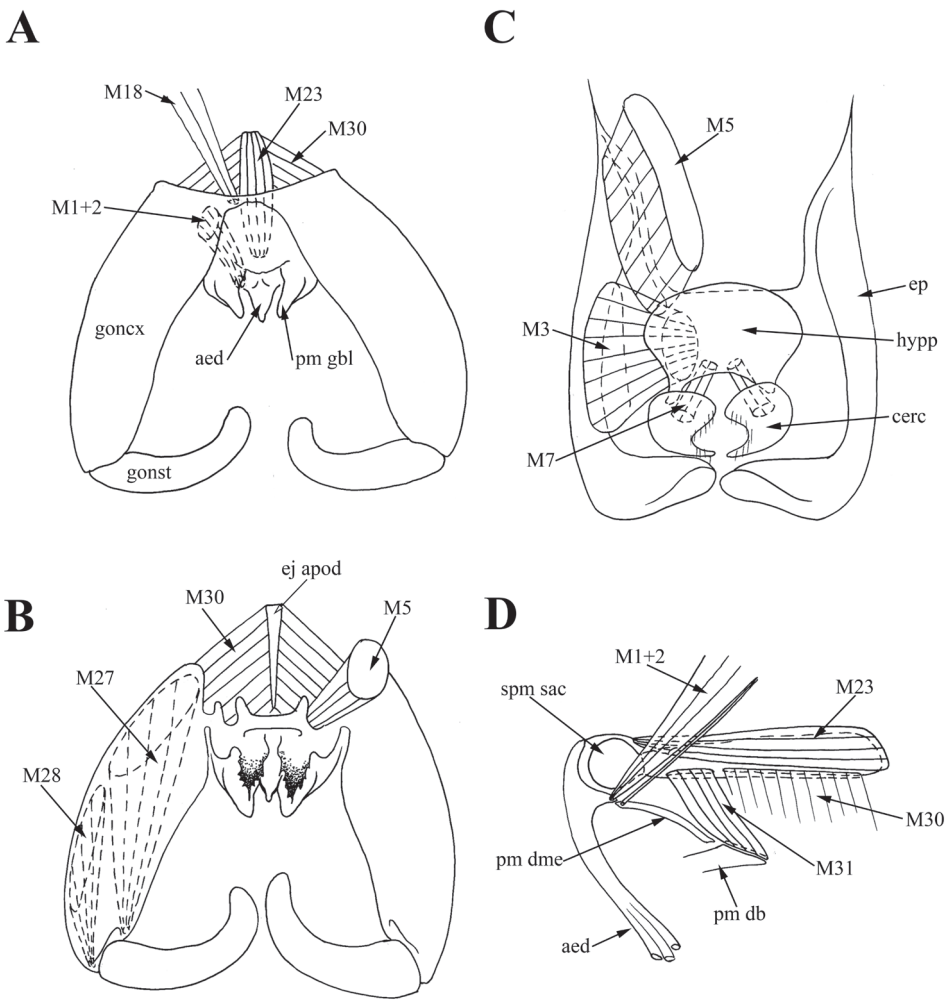

Figure 4. Male of *Araucoderus gloriosus*. **A** genitalia, dorsal view **B** genitalia, inner view **C** epandrium, inner view **D** aedeagal complex, lateral view.

long asymmetrical muscles *ISM7* extending from middle of anterior part of sternite VII to left anterior margin of sternite VIII; posterior sites of attachment of muscles *ISM7* displaced counterclockwise due to terminalia rotation (Figure 2B). Tergite VIII situated on left side of abdomen. One pair of asymmetrical muscles *ITM7* extending from tergite VII to tergite VIII. Right muscle *ITM7* long, extending from middle of tergite VII to posterior part of tergite VIII. Left muscle *ITM7* short, extending from posterior margin of tergite VII to posterior part of tergite VIII. Posterior sites of attachment of muscles *ITM7* displaced counterclockwise due to terminalia rotation (Figure 2B, C).

Pregenital muscles. Paired short asymmetrical muscles *M18*: right muscle *M18* long, connecting middle of right side of sternite VIII to narrow sclerotized stripe or

hypandrium between gonocoxite bases; left wide short muscle *M18* connecting middle of left side of sternite VIII to narrow sclerotized stripe between gonocoxite bases (Figures 2B, 3C). Narrow sclerotized stripe between gonocoxite bases interpreted as hypandrium according to attachment sites of muscles *M18*. Paired short, wide and slightly asymmetrical muscles *M19* extending from center of tergite VIII to anterior margin of epandrium (Figure 3B).

Tergosternal muscles. Paired, wide symmetrical *M5* connecting anterolateral parts of epandrium to lateral thickenings of dorsal bridge of paramere in the point of connection of *pm db* with gonocoxites (= gonocoxal apodeme) (Figures 3A, 4B, C). Lateral thickenings of dorsal bridge of paramere interpreted as gonocoxites according to attachment sites of muscles *M5*.

Muscles of the hypandrial complex. Paired long retractors *M1+2* extending from anterior edges of gonocoxites to aedeagal condyle, and several muscle filaments of *M1+2* extending from anterior edges of gonocoxites to posterior margin of dorsomedial element of paramere *pm dme* (Figure 4A, D). Paired long *M23* extending from posterior edge of ejaculatory apodeme (dorsally) to membrane near aedeagus (Figure 4A, D). Paired wide protractors *M30* extending from anterior half of ejaculatory apodeme (laterally) to anterior margin of gonocoxites (Figure 4A, B, D). Paired retractors *M31* extending from posterior part of ejaculatory apodeme to medial part of dorsal bridge of paramere *pm db* (Figure 4D). Paired long wide *M27* extending from anterior part of gonocoxites to ligament near anterior margin of gonostyli (Figure 4B). Paired long wide *M28* extending from medial part of gonocoxites to condyle of gonostyli (Figure 4B).

Muscles of the epandrial complex. Paired short wide *M3* extending from most of inner epandrium surface to hypoproct (X sternite) (Figure 4C). Paired thin *M7* extending from posterolateral parts of hypoproct to cerci (Figure 4C).

***Nothoderus australiensis* (Alexander, 1922)**

Figures 1C–H, 5, 6

Material. Tasmania, *Nothofagus*-dominated forest, on riparian vegetation. Lake Saint Clair National Park (42°6'S, 146°9'E), 7.xii.2015, D.E. Shcherbakov, 2 males; Mystery Creek Cave (43°28'S, 146°51'E), 13.xii.2015, D.E. Shcherbakov, E.D. Lukashevich, 4 males. The specimens will be deposited in the Zoological Institute RAS, St-Petersburg, Russia.

Exoskeleton. Abdomen: tergite I about 0.6 times as long as tergite II, sternite I about 0.3 times as long as sternite II (Figure 5). Segments II–VII well developed. Terminalia with 160–180° rotation of through segments VII–IX, with segment VIII rotated about 80–90°. Segment VIII reduced to one small sclerite situated dorsally (Figure 5B). Gonocoxites and gonostyli pubescent with long setae. Gonocoxites narrowly contiguous at base, divergent from each other at origin, each nearly cylindrical, tapered slightly toward apex (Figures 1C, 5, 6A). Gonostylus cylindrical, about 4/5 length of gonocoxite, slightly tapered at apex, curved medially, with dense macrosetae

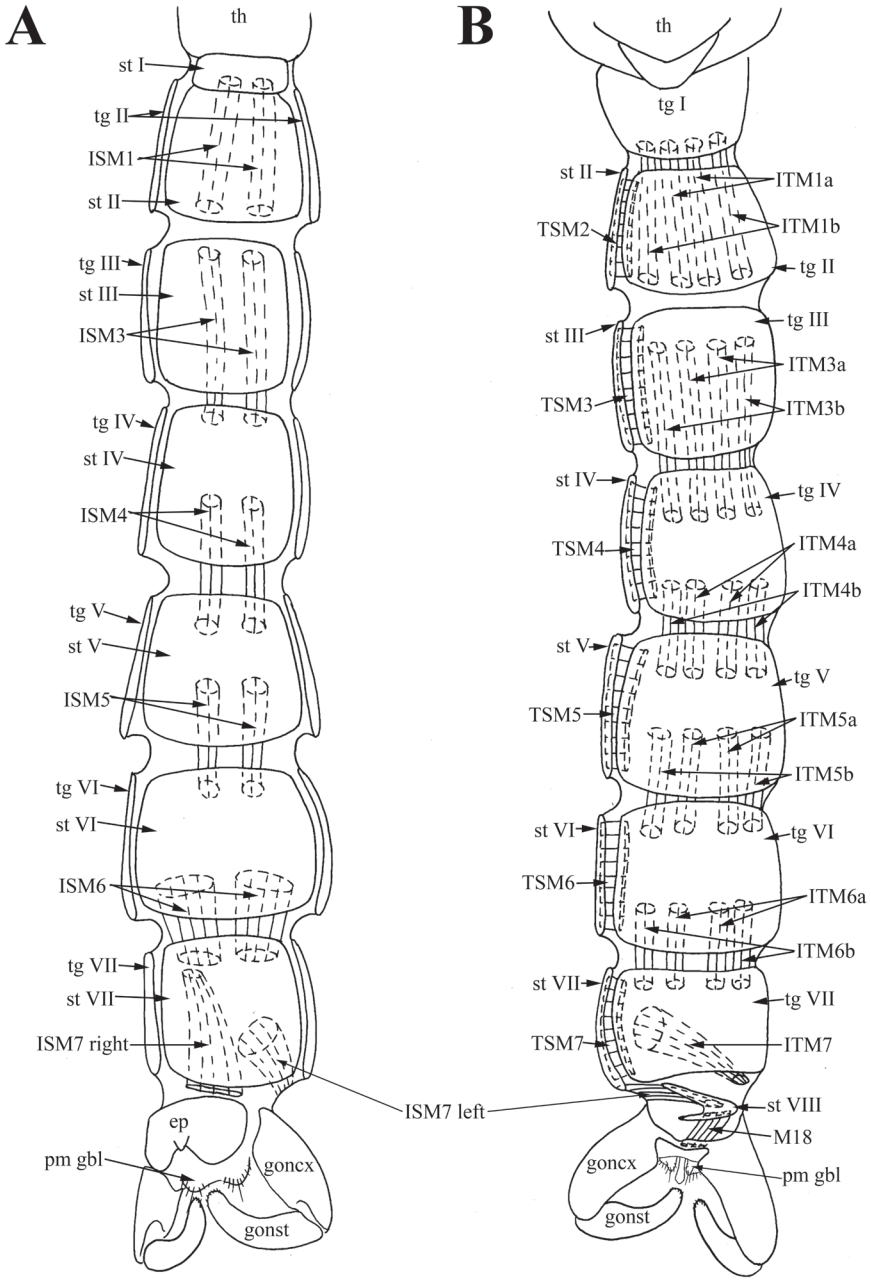

Figure 5. Male of *Nothoderus australiensis*. **A** abdomen, ventral view **B** abdomen, dorsal view.

apically (Figures 1C, D, 5). Apparent hypandrium as narrow sclerotized stripe between gonocoxite bases (Figure 1E), according to muscle attachment sites (see musculature description). Epandrium slightly wider than long, with elongate setae along lateral

margins and robust closely set macrosetae on two large convex lobes; tiny bare medial lobe between lateral ones; cercus inconspicuous, unmodified, setose, with semicircular rim (Figures 1D, F, 6B). Hypoproct small, situated ventrad of epandrium (Figure 6E). Paramere subdivided into dorsal bridge (*pm db*), dorsomedial element (*pm dme*) and parameral lobe at gonocoxite base (*pm gbl*) (Figures 1D, F, H, 6B): dorsal bridge arch-shaped, with one pair of long projections anterolaterally; dorsomedial element "I-shaped", articulated with dorsal bridge basally and with lateral ejaculatory processes of aedeagus apically; parameral lobe at gonocoxite base bare inside and with group of elongated setae among shorter ones outside (Figure 1D, F, H). Ejaculatory apodeme extending anteriorly to segment VII, laterally compressed, clavate at base (Figure 6A, C); sperm sac balloon-like, surrounded by aedeagus posteriorly, attached to ejaculatory apodeme anteriorly; aedeagus relatively short, curved, with single trilobate phallotrema, placed between cerci when at rest (Figure 1F–H).

Musculature. *Abdominal muscles.* Tergosternal muscles *TSM1* of segment I not found. Segments II–VII with one pair of wide short tergosternal muscles (*TSM2–TSM7*) (Figure 5B). Two pairs of long symmetrical intersegmental tergal muscles (*ITM1a,b*) extending from posterior part of tergite I to posterior part of tergite II; paired medial *ITM1a* and paired lateral *ITM1b* with same thickness (Figure 5B). One pair of long intersegmental sternal muscles *ISM1* connecting posterior part of sternite I to posterior part of sternite II (Figure 5A). Intersegmental tergal and sternal muscles *ITM2* and *ISM2* connecting segment II and III not found. Intersegmental symmetrical tergal and sternal muscles *ITM3a,b–ITM5a,b* and *ISM3–ISM5* on segments III–VI with similar attachment sites as intersegmental muscles of segment I–II (Figure 5). Segments II–VII with wide short tergosternal muscles (*TSM2–TSM7*) (Figure 5B). Two pairs of intersegmental tergal muscles *ITM6a,b* extending from posterior part of tergite VI to anterior part of tergite VII. One pair of symmetrical wide intersegmental sternal muscles *ISM6* passing from posterior part of sternite VI to anterior part of sternite VII. Posterior sites of attachment of muscles *ITM6a,b* and *ISM6* slightly displaced clockwise (Figure 5). One pair of long asymmetrical muscles *ISM7* right extending from right anterior part of sternite VII to membrane between sternite VII and epandrium. *ISM7* left extending from left medial part of sternite VII to sternite VIII (Figure 5). Unpaired muscle *ITM7* connecting left medial part of tergite VII to membrane between tergite VII and sternite VIII (Figure 5B).

Pregenital muscles. Short unpaired muscle *M18* connecting sternite VIII to narrow sclerotized stripe or hypandrium between gonocoxite bases (Figure 5B). Narrow sclerotized stripe between gonocoxite bases interpreted as hypandrium, according to attachment sites of muscles *M18*. Muscles *M19* not found. Segment VIII decreased to one small dorsal sclerite; tergite VIII completely membranous, sternite VIII reduced to narrow sclerite.

Tergosternal muscles. Paired, wide symmetrical *M5* connecting anterolateral parts of epandrium to lateral thickenings of dorsal bridge of paramere in the point of connection of *pm db* with gonocoxites (= gonocoxal apodeme) (Figure 6B, C). Lateral thickenings of dorsal bridge of paramere interpreted as gonocoxites according to attachment sites of muscles *M5*.

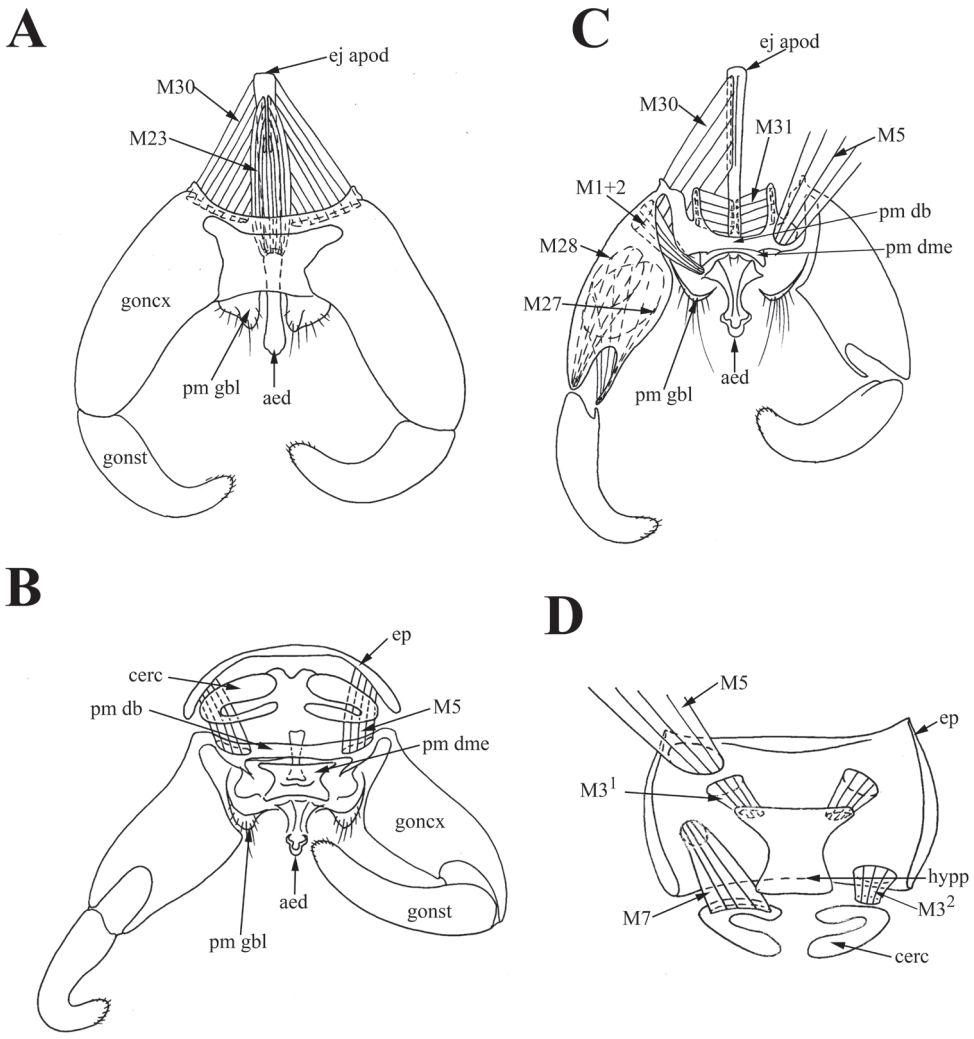

Figure 6. Male of *Nothoderus australiensis*. **A** genitalia, dorsal view **B** genitalia, posterior view **C** genitalia, inner view **D** epandrium, inner view.

Muscles of the hypandrial complex. Paired long retractors *M1+2* extending from anterior edges of gonocoxites to aedeagal condyle, and also several muscle filaments of *M1+2* extending from anterior edges of gonocoxites to posterior margin of dorsomedial element of paramere *pm dme* (Figure 6C). Paired long *M23* extending from posterior edge of ejaculatory apodeme (dorsally) to membrane near aedeagus (Figure 6A). Paired wide protractors *M30* extending from anterior half of ejaculatory apodeme (laterally) to anterior margin of gonocoxites (= gonocoxal apodeme) (Figure 6A, C). Paired wide retractors *M31* extending from posterolateral part of ejaculatory apodeme to medial anterolateral projections of dorsal bridge *pm db* (Figure 6C). Paired long wide muscles *M27* extending from anterior part of gonocoxites to ligament near anterior margin

of gonostyli (Figure 6C). Paired long wide *M28* extending from anteromedial part of gonocoxites to condyle of gonostyli (Figure 6C).

Muscles of the epandrial complex. Two pairs of *M3* muscles; *M3*[1] extending from lateral parts of epandrium to anterolateral parts of hypoproct (X sternite); *M3*[2] extending from posterolateral parts of epandrium to membrane between epandrium and cercus (Figure 6D, E). Paired thin *M7* extending from membrane near hypoproct to anterior lobe of cercus (Figure 6E). Hypoproct apparently partly membranous, according to site of attachment of muscles *M3*[2] and *M7*.

Discussion

Comparison of *Araucoderus* and *Nothoderus* sclerites and musculature

The sclerites and musculature of *Araucoderus* and *Nothoderus* are similar, but differ in several features. The overall pattern of male terminalia of both genera is similar to most of the Southern Hemisphere genera, with simple curved gonostyli, lobe-like setose parameres, and setose cerci inconspicuous under the epandrium. The terminalia of *Nothoderus* are distinct from genitalia of *Araucoderus* in shape of epandrium with tiny concave median lobe, absence of sclerotized protruding parameral elements and simple aedeagus. However, these differences in structure of terminalia in *Araucoderus* and *Nothoderus* are not associated with differences in musculature. Thus, in *Araucoderus* parameral elements are more diverse and developed and the structure of trifid and simple aedeagus is different; but the aedeagal muscles *M1+2* and ejaculatory muscles *M23*, *M30* and *M31* look very similar in both genera.

We have found different degrees of sclerotization of the hypoproct in *Araucoderus* and *Nothoderus*, and correlated differences in muscles of the epandrial complex. The hypoproct is recessed deeply within the genitalia; its location is possibly the reason why the hypoproct was not mentioned by some previous researchers (Krzemiński and Judd 1997). *Araucoderus* is characterized by the well-developed hypoproct connection to the wide muscles *M3*, whereas the hypoproct of *Nothoderus* is partly membranous, according to the site of attachment of muscles *M3*[2] and *M7* (both attached not to hypoproct but to a membrane near it). The weakening and division of muscles *M3* into two pairs of muscles in *Nothoderus* is probably associated with this membranization.

One interesting difference associated with rotation was found in the abdominal structure. *Nothoderus* is characterized by the 180° rotation of segments VII–IX, of the six specimens examined, four males demonstrated clockwise rotation (two of them only 160°; Figure 5) and two counterclockwise rotation; one of them had its terminalia rotated only 90°. In other families of nematocerous Diptera, this rotation often occurs several days after emergence, so probably it was a young male captured during its first days of activity (for details see Lukashevich 2018).

Araucoderus is also characterized by 180° rotation of segments VII–IX. However, of the 12 males of *Araucoderus* examined by us, seven had partially rotated terminalia (about 90°) and five males had terminalia with 180° rotation; eight specimens had

clockwise rotation and 4 males had counterclockwise rotation (such males are illustrated in Figures 1A, 2). Three males were collected by one of us during one hour on the same beach (Lenca River, Alerce Andino NP, 12.i.2015); one male had terminalia with 90° clockwise rotation, two others with 90° and 180° counterclockwise. Madriz and Courtney (2016, fig. 1) also recorded 90° and 180° rotation for *Araucoderus gloriosus* and figured clockwise rotation on the total view without any mention of reverse cases. The difference of rotation direction is common among nematocerous Diptera; e.g. the rotated genitalia were randomly oriented and similar numbers of clockwise and counterclockwise events were observed in sufficiently large samples within the same species in Culicidae and Psychodidae (Chevone and Richards 1976, Curler et al. 2015, Votypka et al. 2015). We believe that Tanyderidae are not exceptions and both genera have similar rotated terminalia with 180° (and 90° as an intermadiate stage), rotation may be either clockwise or counterclockwise in a 1:1 ratio. However, in spite of the similar results, this rotation is carried out in different ways in *Araucoderus* and *Nothoderus*.

Araucoderus is characterized by the narrow segment VIII, but not reduction of the separate sternite and tergite VIII. *Nothoderus* has segment VIII strongly reduced, with tergite VIII totally membranous and sternite VIII as a narrow sclerite. Accordingly, attachment sites and thickness of pregenital muscles are greatly different between the genera: reduction of muscles *M19* and unpaired *M18* was found in *Nothoderus*, whereas *Araucoderus* has paired symmetrical *M18* and *M19* (see below, Table 1).

The attachment sites of muscles *ISM7* and *M18* confirm the origin of sternite VIII, and the attachment sites of muscles *ITM7* confirm the entire membranization of tergite VIII of *Nothoderus* (Figure 5). Moreover, attachment sites of muscles *M18* (between sternites VIII and IX) confirm the homology of the hypandrium (sternite IX) as the narrowly sclerotized stripe between gonocoxite bases of both *Araucoderus* and *Nothoderus* (Figures 1E, 4A, 5B). Localization of these muscle attachment sites is reliable evidence of the hypandrial origin of the sclerites, as it was revealed by us for Diptera Cyclorrhapha (Galinskaya and Ovtshinnikova 2015a, b, Ovtshinnikova and Galinskaya 2016a). Merging of dorsal bridge with gonocoxites is confirming according to attachment sites of muscles *M5* (*M5* connecting anterolateral parts of epandrium to lateral thickenings of dorsal bridge of paramere in the point of connection of *pm db* with gonocoxites) (Figure 6B, C).

The reduction and asymmetry of segment VIII is noted for Tanyderidae for the first time. Such reduction of segment VIII contradicts Alexander's opinion of *Nothoderus* as "the most generalized of the living Tanyderidae" (Alexander 1928). Moreover, the free tip of Sc which was the reason for his conclusion, is not yet known in the fossil record (pers. obs. EDL), so we assume that it is also a derived character.

One more interesting difference was found in the structure of abdominal intersegmental muscles of VII sclerites. These muscles are asymmetrical and the sternal muscles *ISM7* are paired in both genera, whereas the tergal muscles *ITM7* are paired in *Araucoderus* but in *Nothoderus* only one unpaired *ITM7* was found (Table 1; Figures 2, 5). The position of these muscles as well as their symmetry in Ptychopteridae (the family without rotation of male terminalia) indicates that they probably provide the rotational force for inversion of the terminalia in Tanyderidae and Psychodidae.

Table 1. Musculature of male terminalia of Tanyderidae, Psychodidae, Blephariceridae and Ptychopteridae.

Taxa	Muscle Groups									
	Abdominal muscles	Pregenital muscles		Tergosternal muscles	Muscles of the hypandrial complex				Muscles of the epandrial complex	
	Muscles of VII sclerite	Hypandrial muscles	Epandrial muscles		Ejaculator muscles	Aedeagal muscles	Gonocoxal muscles	Gonostylar muscles	Muscles of hypoproct	Muscles of cercus
Tanyderidae										
Araucoderus gloriosus (present study)	Paired asymmetrical *ISM7*; Paired asymmetrical *ITM7*	Paired asymmetrical *M18*	Paired asymmetrical *M19*	*M5*	*M23*; *M30*; *M31*	*M1+2*	not found	*M27*; *M28*	*M3*	*M7*
Nothoderus australiensis (present study)	Paired asymmetrical *ISM7*; Unpaired *ITM7*	Unpaired *M18*	not found	*M5*	*M23*; *M30*; *M31*	*M1+2*	not found	*M27*; *M28*	*M3*$^{l-2}$	*M7*
Psychodidae										
Pericoma sp. (after Hennig 1936) *Pneumia palustris* (after Just 1973)	Paired slightly asymmetrical *ISM7* (*VLM1*, *VLM2* sensu Just 1973); Paired slightly asymmetrical *ITM7* (*DLM1*, *DLM2* sensu Just 1973)	*M18* (*VLM1a*, *VLM1b* sensu Just 1973)	*M19* (*JM8–9* sensu Hennig 1936; *DLM1*, *VLM2* sensu Just 1973)	*M5*$^{l-2}$ (*M6*, *M6a* sensu Hennig 1936; *M7*, *M9* sensu Just 1973)	*M30* (*MS1*, *MS2* sensu Hennig 1936; *M4* sensu Just 1973); *M31* (*MS3* sensu Hennig 1936; *M5* sensu Just 1973)	*M1* (MS4 sensu Hennig 1936; *M6* sensu Just 1973); *M2* (*M4* sensu Hennig 1936; *M1* sensu Just 1973)	not found	*M27* (*M3* sensu Hennig 1936; *M2* sensu Just 1973); *M28* (*M5* sensu Hennig 1936; *M3* sensu Just 1973)	*M3* (*M1* sensu Hennig 1936; *M8* sensu Just 1973)	*M7* (*M2a*, *M2b* sensu Hennig 1936; *M10* sensu Just 1973)
Phlebotomus garnhami (after Just 1973)	Paired asymmetrical *ISM7* (*VLM* sensu Just 1973); Paired asymmetrical *ITM7* (*DLM* sensu Just 1973)	*M18* (*VLM* sensu Just 1973)	*M19*$^{l-2}$ (*DLM*$^{l-2}$sensu Just 1973)	not found	*? M31*$^{l-2}$ (*M5, M6* sensu Just 1973)	*M1* (*M4* sensu Just 1973)?; *M2* (*M1* sensu Just 1973)	not found	*M27* (*M2*, *M2*^{l} sensu Just 1973); *M28* (*M3*, *M3*^{l} sensu Just 1973)	*M3* (*M7* sensu Just 1973)	*M7* (*M8* sensu Just 1973)
Blephariceridae										
Edwardsina gigantea (after Zwick 1977)	not examined	*M18* (described without numbering Zwick 1977: p.8 (1))	*M19* (described without numbering Zwick 1977: p.8 (1))	*M5*$^{l-2}$ (described without numbering Zwick 1977: p.8 (2))	*? M30* (*M7* sensu Zwick 1977); *M31*$^{l-2}$ (*M5*, *M6* sensu Zwick 1977)	*M1* (*M1* sensu Zwick 1977); *M2* (*M2* sensu Zwick 1977)	not examined	*M27* (*M3* sensu Zwick 1977); *M28* (*M4* sensu Zwick 1977)	*M3* (described without numbering Zwick 1977: p.8 (2))	*M7* (described without numbering Zwick 1977: p.8 (2))
Ptychopteridae										
Ptychoptera lacustris (after Just 1973)	Paired symmetrical *ISM7* (*VLM* sensu Just, 1973); Paired symmetrical *ITM7* (*DLM* sensu Just, 1973)	Paired symmetrical *M18* (*VLM2* sensu Just, 1973)	Paired symmetrical *M19* (*DLM2* sensu Just, 1973)	*M5* (*M1* sensu Just, 1973)	*M31* (*M11* sensu Just, 1973)	*M1*$^{l-4}$ (*M3*, *M8*, *M9*, *M7* sensu Just, 1973); *M2*$^{l-2}$ (*M6*, *M10* sensu Just, 1973)	*M33* (*M2*, sensu Just, 1973);	*M27* (*M4* sensu Just, 1973); *M28* (*M5* sensu Just, 1973)	*M3*$^{l-3}$ (*M12*, *M13*, *M14* sensu Just, 1973)	*M7*$^{l-2}$ (*M15*, *M16* sensu Just, 1973)

Relationship of Tanyderidae and their supposed relatives: male terminalia evidences

As it was discussed in the introduction, different authors cluster Tanyderidae with Blephariceridae, Ptychopteridae or Psychodidae. Data on skeleton and musculature of male terminalia in Tanyderidae, Psychodidae, Blephariceridae and Ptychopteridae are compared in Tables 1, 2 and illustrate the noticeable peculiarity of Tanyderidae.

Among these families only Tanyderidae are characterized by ejaculator muscles *M23* (in addition to muscles *M30* and *M31*, present in other families). Muscles *M23* connect only sclerites or membranes of aedeagal complex consisting of ejaculatory apodeme and aedeagus. Up to now these muscles were recorded in the only one nematocerous family, Trichoceridae, and in Brachycera (as *M32* in Ovtshinnikova 1989). Based on our data one can suppose that muscles *M23* are present in the groundplan of the Diptera.

It can be assumed that muscles *M30* and *M31* of Tanyderidae, attached to different parts of the ejaculatory apodeme, have the opposite functions of muscles *M30* and *M31* of Blephariceridae and Bibionidae and most of Brachycera, muscles *M31* of Psychodidae and Ptychopteridae. Muscles *M30* of Tanyderidae are, probably, protractors, muscles *M31* of Tanyderidae are, probably, retractors as in Trichoceridae (Ovtshinnikova 1989). Protractor muscles in these families are usually wide and fan-shaped, their attachment sites occupy a wide surface of the ejaculatory apodeme, regardless of the origin of the muscles (muscles *M30* or *M31*). At the same time, the other side of the protractor muscles of Tanyderidae is attached to the gonocoxites, therefore the muscles are designated as *M30*, as well as in the most other families (including Brachycera). Retractors are narrower and often connect to the base of the ejaculatory apodeme. In the Tanyderidae these muscles are connected to parameres, and are designated as *M31*, in other families these muscles are associated with gonocoxite apodemes or gonocoxites and are designated as *M30*. Therefore, in this case we assume a complete changing of the functions of these paired antagonist muscles.

Only Tanyderidae are characterized by the merging of aedeagal muscles *M1* and *M2*. Psychodidae, Blephariceridae, and Ptychopteridae are characterized by separate aedeagal muscles: the protractors *M1* and retractors of aedeagus *M2* and two pairs of aedeagal muscles are part of the dipteran groundplan (one pair *M1* and one pair of *M2*). Tanyderidae are characterized only by retractors *M1+2* that should lead to changing in mechanism of aedeagus functioning.

The examined tanyderids are characterized by muscles *M1+2* connecting gonocoxites partly to the aedeagus, partly to the dorsomedial element of the parameres *pm dme*, and by muscles *M31* connecting posterior part of ejaculatory apodeme to medial part of dorsal bridge of paramere *pm db*. Tanyderidae as well as Psychodidae and Blephariceridae are characterized by a sclerotized bridge forming through medial merging of parameres and "connecting the gonocoxites dorsally via the gonocoxal apodemes" (Sinclair 2000). It can be the initial stage of the aedeagal sheath forming: the fused parameres with attached powerful muscles provides protection of the aedeagus and increases the pulling of the aedeagus during copulation, whereas the aedeagus remains well sclerotized and independent. Therefore, the presence of the bridge could be a derived state for Tanyderidae, Psychodidae and Blephariceridae, however, the parameres are fused dorsally in many lineages, e.g. in Trichoceridae, Limoniidae and

Table 2. Characters of male terminalia of Tanyderidae, Psychodidae, Blephariceridae and Ptychopteridae, discussed in the text (1 – after Just 1973; 2 – after Zwick 1977).

	Rotation	Trifid aedeagus	Sperm pump hypertrophied	Aedeagal muscles		Tergosternal muscles M5	Ejaculator muscles			Gonocoxal muscles M33
				M1	M2		M23	M30	M31	
Tanyderidae										
Araucoderus gloriosus	+	+	–	one pair		one pair	one pair	one pair	one pair	–
Nothoderus australiensis	+	–	–	one pair		one pair	one pair	one pair	one pair	–
Psychodidae										
Pneumia palustris [1]	+	–	–	one pair	one pair	two pairs	–	one pair	one pair	–
Phlebotomus garnhami [1]	+	–	–	one pair	one pair	–	–	–	two pairs	–
Blephariceridae										
Edwardsina gigantea [2]	–	+	–	one pairs	one pair	two pairs	–	one pair	two pairs	–
Ptychopteridae										
Ptychoptera lacustris [1]	–	–	+	four pairs	two pairs	one pair	–	–	one pair	one pair

Axymyiidae (Wood 1991, Sinclair 2000; Paramonov 2004; Sinclair et al. 2013) and it is possible that the dorsal bridge connecting the gonocoxites dorsally via the gonocoxal apodemes is a part of the dipteran groundplan.

Blephariceridae are distinct from Tanyderidae in tergosternal muscles *M5* divided into two pairs and the absence of terminalia rotation (Table 2). Within the discussed families only Blephariceridae and Tanyderidae are characterized by a trifid aedeagus with three slender filaments, each with separate openings. There are currently two opinions on the number of aedeagal openings in the dipteran groundplan: three (based on basal number of spermathecae; e.g. Downes 1968, Petersen et al. 2010) or one (based on outgroup comparison, e.g. Wood 1991, Ribeiro 2008). Following the view of Wood (1991) we consider the trifid aedeagus as an apomorphic state, which evolved independently and repeatedly in different families (in Cylindrotomidae and some Brachycera besides Tanyderidae and Blephariceridae). It is obvious that a shift from single to multiple openings has occurred multiple times (Wood 1991) and Tanyderidae is one more example in this sequence (with the single opening in *Nothoderus* and three phallothremata in *Araucoderus*). Taking into account a bifid aedeagus (*Peringueyomyina* and several extinct genera, Madriz 2017, Lukashevich 2018), we can infer that the disparity of the aedeagus structure in tanyderids appears to be the most extreme in the order, which makes it impossible to draw any conclusions on relatives in the absence of an established phylogeny of Tanyderidae.

Ptychopteridae are also distinct from Tanyderidae in the absence of terminalia rotation, and share plesiomorphic characters only, such as tergosternal muscles *M5* not divided (Table 2). Ejaculatory-aedeagal complex of Ptychopteridae is very specialized, e.g. the spherical sperm pump is hypertrophied as compared with other dipteran families (including the discussed ones), with only one pair of ejaculator muscles *M31* and with six pairs of aedeagal muscles $M1^{1–3}$ and $M2^{1–2}$ (Tanyderidae

are characterized by one pair of merged *M1+2*). Ptychopteridae are characterized by one pair of hypandrial muscles of gonocoxite *M33* which is a feature of the groundplan of the Diptera (Paramonov 2004), whereas in Tanyderidae, Psychodidae, and Blephariceridae *M33* is absent. We did not find obvious male terminalia synapomorphies grouping Tanyderidae with Ptychopteridae.

Psychodidae is the single family under discussion with male terminalia rotation (for details see in Lukashevich 2018) although genera with unrotated male terminalia are known in Sycoracinae and Horaiellinae (Duckhouse 1972, Curler and Priyadarsanan 2015). In *Phlebotomus*, the rotation begins with segment VII as in both tanyderids described here. The genus has asymmetrically paired abdominal intersegmental muscles of VII sclerites as in *Araucoderus* and posterior sites of attachment of muscles *ITM7* and *ISM7* are slightly moved clockwise (Just 1973), similar to *Nothoderus*, but unpaired abdominal or pregenital muscles were not found in Psychodidae. We believe that Tanyderidae is closely related to Psychodidae, but the musculature of male terminalia offers rather little confirmation of this relatedness: we did not find any important similarities in the musculature of Psychodidae and Tanyderidae. The absence of *M33* in both families is not such an important similarity, although *M33* was found in Ptychopteridae, Trichoceridae, Pediciidae, Tipulidae and in some Bibionomorpha and Brachycera and is a considered part of the dipteran groundplan (Ovtshinnikova 1989, Paramonov 2004). However, *M33* is also absent in Limoniidae and some Bibionidae (Ovtshinnikova 1989, Paramonov 2004), so its loss seems to have occurred several times independently.

It is worth noting that Psychodidae are extremely diverse and the scarce data on their musculature confirms this diversity: e.g., Psychodinae are characterized by tergosternal muscles *M5* divided into two pairs, whereas Phlebotominae are characterized by absence of muscles *M5* (Just 1973, Jobling 1987, figure 111). At the same time, muscles *M5* are usually very stable within different families of Diptera (Ovtshinnikova 1989, 1993, 2000); e.g., Limoniidae has *M5* but *M5* is absent in Tipulidae and this character is considered an autapomorphy of the latter family by Paramonov (2004). Due to such diversity within Psychodidae, it is impossible to make serious conclusions based on only two examined derived genera, *Pneumia* and *Phlebotomus,* while data on more basal subfamilies are absent. Bruchomyiinae has been referred to as the sister group to the remaining Psychodidae by some authors (Quate and Alexander 2000) and earlier this subfamily was even included in Tanyderidae (Alexander 1927), whereas other authors hypothesized a more basal position for Sycoracinae and Horaiellinae (Curler and Moulton 2012), but the musculature of these subfamilies has not been studied.

Conclusions

The Tanyderidae are characterized by very specialized sclerites and muscles of male terminalia; these structures provide no evidence of relationship with previously studied members of Psychodidae, Blephariceridae and Ptychopteridae. Within these three families, only Psychodidae have obligatory 180° male terminalia rotation and only

Blephariceridae have a trifid aedeagus. Although our initial hypothesis was the similarity of Tanyderidae and Psychodidae and we looked for evidence using the analysis of musculature characters that had not previously been investigated; the musculature of male terminalia offers little confirmation of this relatedness. The absence of evidence is probably connected with the absence of data on musculature of the primitive psychodid subfamilies Bruchomyiinae, Sycoracinae and Horaiellinae.

Acknowledgements

E.D. Lukashevich is grateful to Dmitry Shcherbakov (Borissiak Paleontological Institute RAS, Moscow) for the opportunity to collect Tanyderidae in Chile and Tasmania. E.D. Lukashevich is also grateful to Cathy Byrne and Simon Grove (both Tasmanian Museum and Art Gallery, Hobart) for their hospitality and invaluable help in facilitating field work of the Russian team in Tasmania and to Mario Elgueta (National Museum of Natural History, Santiago) for facilitating fieldwork in Chile. We also thank Roman Rakitov (Borissiak Paleontological Institute of Russian Academy of Sciences, Moscow) for helping in taking scanning electron images and for other assistance. We are deeply indebted to Rolf G. Beutel (Institut für Spezielle Zoologie und Evolutionsbiologie, Jena) and Bradley J. Sinclair (Canadian National Collection of Insects and Canadian Food Inspection Agency, Ottawa) for insightful comments on the manuscript and linguistic advice.

The work of O.G. Ovtshinnikova was supported by the Zoological Institute of Russian Academy of Sciences (State Research Program AAAA-A17-117030310205-9) and the Russian Foundation for Basic Research (project no. 18-04-00354-a). The work of T.V. Galinskaya was supported by the Russian Science Foundation (project no. 14-14-00208). The research of E.D. Lukashevich was partly supported by grants from the Russian Foundation for Basic Research, projects no. 13-04-01839 and 16-04-01498.

References

Alexander CP (1920) A new genus and species of net-winged midge (Blepharoceridae) and an undescribed species of Tanyderidae (Diptera). Arkiv för Zoologi 13(7): 1–7.

Alexander CP (1921) A new genus and species of Tanyderid (*Peringueyomina barnardi*) in the South African Museum (Diptera). Annals of the South African Museum 18: 231–234.

Alexander CP (1922) Undescribed crane-flies (Tanyderidae and Tipulidae) in the South Australian museum. Records of the South Australian Museum 2: 223–270.

Alexander CP (1927) Diptera fam. Tanyderidae. Genera Insectorum 189: 1–13.

Alexander CP (1928) Tanyderidae of Australia (Diptera). Proceedings of the Linnean Society of New South Wales 53: 367–374.

Alexander CP (1929) Diptera of Patagonia and South Chile. Part I. Crane-flies (Tipulidae, Trichoceridae, Tanyderidae). British Museum (Natural History), London, 240 pp.

Ansorge J (1994) Tanyderidae and Psychodidae (Insecta: Diptera) from the Lower Jurassic of northeastern Germany. Paläontologisches Zeitschrift 68 (1–2): 199–209. https://doi.org/10.1007/BF02989440

Bertone MA, Courtney GW, Wiegmann BM (2008) Phylogenetics and temporal diversification of the earliest true flies (Insecta: Diptera) based on multiple nuclear genes. Systematic Entomology 33: 668–687. https://doi.org/10.1111/j.1365-3113.2008.00437.x

Borkent A, Sinclair BJ (2012) The male genital tract of Axymyiidae and Tanyderidae (Diptera). The Canadian Entomologist 144: 266–272. https://doi.org/10.4039/tce.2012.26

Chevone BI, Richards AG (1976) Ultrastructure of the atypic muscles associated with terminalial inversion in male *Aedes aegypti* (L). The Biological Bulletin 151: 283–296. https://doi.org/10.2307/1540661

Colless DH, McAlpine DK (1970) Chapter 34. Diptera. In: Waterhouse DF (Ed.) Insects of Australia. Melbourne University Press, Melbourne, 656–740.

Crampton GC (1926) A phylogenetic study of the thoracic sclerites of the Psychodoid Diptera, with remarks on the interrelationships of the Nematocera. Entomological News 37(3): 33–39, 65–70.

Cumming JM, Wood DM (2009) Adult morphology and terminology. In: Brown BV, Borkent A, Cumming JM, Wood DM, Woodley NE, Zumbado M (Eds) Manual of Central American Diptera. Volume 1. Research Press, Ottawa, 9–50.

Curler GR, Moulton JK (2012) Phylogeny of psychodid subfamilies (Diptera: Psychodidae) inferred from DNA sequences with a review of morphological evidence for relationships. Systematic Entomology 37: 603–616. https://doi.org/10.1111/j.1365-3113.2012.00634.x

Curler GR, Moulton JK, Madriz RI (2015) Redescription of *Aposycorax chilensis* (Tonnoir) (Diptera, Psychodinae, Sycoracinae) with the first identification of a blood meal host for the species. Zootaxa 4048(1): 114–126. https://doi.org/10.11646/zootaxa.4048.1.7

Curler GR, Priyadarsanan DR (2015) Descriptions of Psychodidae (Diptera) from the Western Ghats of India. Acta Entomologica Musei Nationalis Pragae 55(2): 473–483.

Downes JA (1968) Notes on the organs and processes of sperm-transfer in the lower Diptera. The Canadian Entomologist 100 (6): 608–617. https://doi.org/10.4039/Ent100608-6

Duckhouse DA (1972) Psychodidae (Diptera, Nematocera) of South Chile, subfamilies Sycoracinae and Trichomyiinae. Transactions of the Royal Entomological Society of London 124(3): 231–268. https://doi.org/10.1111/j.1365-2311.1972.tb00365.x

Eskov KY, Lukashevich ED (2015) On the history of ranges of two relict nematoceran families, Ptychopteridae and Tanyderidae (Insecta: Diptera): a biogeographical puzzle. Russian Entomological Journal 24: 257–270.

Friedrich F, Beutel RG (2008) The thorax of *Zorotypus* (Hexapoda, Zoraptera) and a new nomenclature for the musculature of Neoptera. Arthropod Structure & Development 37: 29–54. https://doi.org/10.1016/j.asd.2007.04.003

Galinskaya TV, Gafurova D, Ovtshinnikova OG (2018) X-ray microtomography (microCT) of male genitalia of *Nothybus kuznetsovorum* (Nothybidae) and *Cothornobata* sp. (Micropezidae). ZooKeys 744: 139–147. https://doi.org/10.3897/zookeys.744.22347

Galinskaya TV, Ovtshinnikova OG (2015a) Musculature of the male genitalia in the tribe Ulidiini (Diptera, Ulidiidae). Entomological Review 95(1): 31–37. https://doi.org/10.1134/S0013873815010042

Galinskaya TV, Ovtshinnikova OG (2015b) Musculature of the male genitalia in *Rivellia* (Diptera: Platystomatidae). ZooKeys 545: 149–158. https://doi.org/10.3897/zookeys.545.6702

Handlirsch A (1909) Zur Phylogenie und Flügelmorphologie der Ptychopteriden (Dipteren). Annalen des k.k. Naturhistorischen Hofmuseum in Wien 23: 263–272.

Heisch RB, Guiggsberg CAW, Teesdale C (1956) Studies in leishmaniasis in Eastern Africa. II. The sandflies of the Kuiti Kala-Azar area in Kenya, with descriptions of six new species. Transactions of the Royal Society of Tropical Medicine and Hygiene 50: 209–226. https://doi.org/10.1016/0035-9203(56)90025-6

Hennig W (1936) Der männliche Kopulationsapparates der Dipteren. III, Psychodidae und Asilidae. Zoologischer Anzeiger 114(7–8): 177–186.

Hennig W (1973) Ordnung Diptera (Zweiflügler). Handbuch der Zoologie 4(2, 2/31): 1–337.

Jobling B (1987) Anatomical drawings of biting flies, British Museum (Natural History). British Museum (Natural History) and the Wellcome Trust, London, 119 pp.

Just JP (1973) Die Anatomie der Postabdomina von *Phlebotomus garnhami* Heisch, Guiggsberg and Teesdale, *Pericoma palustris* Meigen und *Liriope lacustris* Meigen (Diptera, Nematocera). Zoologishe Jahrbücher, Abteilung für Anatomie und Ontogenie der Tiere 91(3): 305–388.

Krzemiński W, Azar D, Skibińska K (2013) *Nannotanyderus ansorgei* sp. n., the first member of the family Tanyderidae fromthe Lebanese amber (Lower Cretaceous). In: Azar D, Engel M, Jarzembowski E, Krogmann L, Santiago-Blay J (Eds) Insect Evolution in an Amberiferous and Stone Alphabet: Proceedings of the 6th International Congress on Fossil Insects, Arthropods and Amber. Brill, Leiden-Boston, 131–143.

Krzemiński W, Judd DD (1997) Family Tanyderidae. In: Papp L, Darvas B (Eds) Contributions to a Manual of Palaearctic Diptera (with special reference to flies of economic importance). Volume 2. Nematocera and Lower Brachycera. Science Herald, Budapest, 281–289.

Lambkin CL, Sinclair BJ, Pape T, Courtney GW, Skevington JH, Meier R, Yeates DK, Blagoderov V, Wiegmann BM (2013) The phylogenetic relationships among infraorders and superfamilies of Diptera based on morphological evidence. Systematic Entomology 38: 164 –179. https://doi.org/10.1111/j.1365-3113.2012.00652.x

Lukashevich ED (2018) Male terminalia and their rotation in Tanyderidae (Diptera, Nematocera) since the Mesozoic. Historical Biology. https://doi.org/10.108/08912963.2018.1500568 [published online]

Madriz RI (2017) 15. Tanyderidae. In: Kirk-Spriggs AH, Sinclair BJ (Eds) Manual of Afrotropical Diptera. Volume 2. Nematocerous Diptera and lower Brachycera. Suricate 5. South African National Biodiversity Institute, Pretoria, 479–485.

Madriz RI, Astorga A, Lindsay T, Courtney GW (2018) A new species of *Neoderus* Alexander, 1927 (Diptera: Tanyderidae) from southern Chile, with a first description of a male and key to extant genera of the family. Aquatic Insects. https://doi.org/10.1080/01650424.2018.1456665

Madriz RI, Courtney GW (2016) The Neotropical tanyderid *Araucoderus gloriosus* (Alexander) (Diptera, Tanyderidae), with description of the egg, larva and pupa, redescription of adults, and notes on natural history. Zootaxa 4158(3): 325–351. https://doi.org/10.11646/zootaxa.4158.3.2

Matsuda R (1976) Morphology and Evolution of the Insect Abdomen. Pergamon Press Ltd., Headington Hill, 534 pp.

Meigen JW (1804) Klassifikazion und Beschreibung der europäischen zweiflügeligen Insekten (Diptera Linn.). Erster Band. Reichard, Braunschweig, 314 pp.

Meigen JW (1830) Systematische Beschreibung der bekannten europäischen zweiflügeligen Insekten. Sechster Theil. Schulz, Hamm, 401 pp.

Oosterbroek P, Courtney G (1995) Phylogeny of the nematocerous families of Diptera (Insecta). Zoological Journal of the Linnean Society 115: 267–311. https://doi.org/10.1006/zjls.1995.0080

Osten-Sacken CR (1860) New genera and species of North American Tipulidae with short palpi, with attempt at a new classification of the tribe. Proceedings of the Academy of Natural Sciences of Philadelphia 1859: 197–256.

Osten-Sacken CR (1880) Die Tanyderina, eine merkwürdige Gruppe der Tipuliden. Verhandlungen der kaiserlich-kongiglichen zoologish-botanischen Gesellschaft in Wien 29: 517–522.

Ovtshinnikova OG (1989) Muscles of the male genitalia of Brachycera–Orthorrhapha (Diptera). Trudy Zoologicheskogo Instituta Akademii Nauk SSSR 190: 1–166. [in Russian]

Ovtshinnikova OG (1993) Homologies of the male genital sclerites of Diptera Brachycera based on the study of the muscles. Entomological Review 72(4): 737–746.

Ovtshinnikova OG (2000) Muscles of the Male Genitalia of Syrphidae (Diptera). NA Kholodkovsky Memorial Lectures: a Report to the 52nd Annual Meeting, April 1, 1999. St. Petersburg, 70 pp. [in Russian]

Ovtshinnikova OG, Galinskaya TV (2016b) Musculature of the male genitalia of a member of the genus *Teleopsis* Rondani, 1875 (Diopsidae, Diptera). Oriental Insects 50(2): 61–68. https://doi.org/10.1080/00305316.2016.1227733

Ovtshinnikova OG, Galinskaya TV (2016a) Musculature of the abdomen and male genitalia of a member of Celyphidae (Diptera, Cyclorrhapha). Oriental Insects 50(4): 178–186. https://doi.org/10.1080/00305316.2016.1227733

Ovtshinnikova OG, Galinskaya TV (2017) The male abdominal, genital and pregenital sclerites and musculature in *Neria commutata* (Czerny, 1930) (Diptera, Micropezidae). Entomological Review 97(3): 282–287. https://doi.org/10.1134/S0013873817030022

Ovtshinnikova OG, Yeates DK (1998) Male genital musculature of Therevidae and Scenopinidae (Diptera: Asiloidea): structure, homology and phylogenetic implications. Australian Journal of Entomology 37(1): 27–33. https://doi.org/10.1111/j.1440-6055.1998.tb01539.x

Paramonov NM (2004) Taxonomic position of the families Tipulidae and Limoniidae in Nematocera (Diptera) with account of characters of the male genital skeleton and muscles. Entomological Review 84(1): 15–30.

Petersen MJ, Bertone MA, Wiegmann BM, Courtney GW (2010) Phylogenetic synthesis of morphological and molecular data reveals new insights into the higher-level classification of Tipuloidea (Diptera). Systematic Entomology 35: 526–545. https://doi.org/10.1111/j.1365-3113.2010.00524.x

Quate LW, Alexander B (2000) Synopsis of the New World *Nemapalpus* (Diptera, Psychodiddae, Bruchomyiinae) with description of four new species. Annals of the Entomological Society of America 93: 185–193. https://doi.org/10.1603/0013-8746(2000)093[0185:SOTNWN]2.0.CO;2

Ribeiro GC (2008) Phylogeny of the Limnophilinae (Limoniidae) and early evolution of the Tipulomorpha (Diptera). Invertebrate Systematics 22: 627–694. https://doi.org/10.1071/IS08017

Savchenko EN (1971) On the discovery of tanyderids (Diptera, Tanyderidae) in Mongolia. Entomologicheskoye obozreniye (Entomological Review) 50(1): 167–170.

Savchenko EN (1974) The second species of the primitive crane-flies (Diptera, Tanyderidae) from the Soviet Middle Asia. Zoologicheskiy zhurnal (Zoological Journal) 53(12): 1892–1894.

Savchenko EN (1978) Tanyderid-flies (Diptera, Tanyderidae) of the USSR fauna. Report AS UkrSSR 1: 74–77.

Scopoli JA (1786) Deliciae florae et faunae Insubricae seu novae, aut minus cognitae species plantarum et animalium quas in Insubria Austriaca tam spontaneas, quam exoticas vidit, descripsit, et aeri incidi curavit. Pars II. S.Salvatoris, Ticini, 115 pp.

Shcherbakov DE, Lukashevich ED, Blagoderov VA (1995) Triassic Diptera and initial radiation of the order. International Journal of Dipterological Research 6: 75–115.

Sinclair BJ (2000) 1.2. Morphology and terminology of Diptera male terminalia. Manual of Palearctic Diptera 53–74.

Sinclair BJ, Cumming JM, Brooks SE (2013) Male terminalia of Diptera (Insecta): a review of evolutionary trends, homology and phylogenetic implications. Insect Systematict & Evolutions 44: 373–415. https://doi.org/10.1163/1876312X-04401001

Skibińska K, Krzemiński W, Coram RA (2014) Discovery of the most ancient member of family Tanyderidae (Diptera) from the Lower Jurassic (Sinemurian) of England. Zootaxa 3857: 125–130. https://doi.org/10.11646/zootaxa.3857.1.6

Spangenberg R, Hünefeld F, Schneeberg K, Beutel RG (2012) The male postabdomen and reproductive system of Bibio marci Linnaeus, 1758 (Hexapoda: Diptera: Bibionidae). Journal of Zoological Systematics and Evolutionary Research 50(4): 264–288. doi: 10.1111/j.1439-0469.2012.00669.x

Votypka J, Pavlasova M, Volfova V, Volf P (2015) Rotation of male genitalia in various species of phlebotomine sandfly. Medical and Veterinary Entomology 29: 355–360. https://doi.org/10.1111/mve.12132

Wiegmann BM, Trautwein MD, Winkler IS, Barr NB, Kim J-W, Lambkin C, Bertone MA, Cassel BK, Bayless KM, Heimberg AM, Wheeler BM, Peterson KJ, Pape T, Sinclair BJ, Skevington JH, Blagoderov VV, Caravas J, Kutty SN, Schmidt-Ott U, Kampmeier GE, Thompson FC, Grimaldi DA, Beckenbach AT, Courtney GW, Friedrich M, Meier R, Yeates DK (2011) Episodic radiation in the fly tree of life. Proceedings of the Natural Academy of Sciences 108: 5690–5695. https://doi.org/10.1073/pnas.1012675108

Williams IW (1933) The external morphology of the primitive tanyderid dipteron *Protoplasa fitchii* O.S., with notes on the other Tanyderidae. Journal of the New York Entomological Society 41: 1–35.

Wood DM (1991) Homology and phylogenetic implications of male genitalia in Diptera. The ground plan. In: Weisman L, Orsragh I, Pont AC (Eds) Proceedings of the Second International Congress of Dipterology. The Hague, 255–284.

Wood DM, Borkent A (1989) Phylogeny and classification of the Nematocera. In: McAlpine JF (Ed.) Manual of Nearctic Diptera Volume 3. Research Branch, Agriculture Canada, Ottawa, 1333–1370.

Zwick P (1977) Australian Blephariceridae (Diptera). Australian Journal of Zoology Supplement Series 46: 1–121. https://doi.org/10.1071/AJZS046

ZooKeys 809: 79–95 (2018)
doi: 10.3897/zookeys.809.29280
http://zookeys.pensoft.net

RESEARCH ARTICLE

A peer-reviewed open-access journal
ZooKeys
Launched to accelerate biodiversity research

A new species of *Lipogramma* from deep reefs of Roatan, Honduras (Teleostei, Grammatidae)

Luke Tornabene[1], D. Ross Robertson[2], Carole C. Baldwin[3]

1 *School of Aquatic and Fishery Sciences, Burke Museum of Natural History and Culture, University of Washington, Seattle, WA, USA* **2** *Smithsonian Tropical Research Institute, Balboa, Republic of Panama* **3** *Department of Vertebrate Zoology, National Museum of Natural History, Smithsonian Institution, Washington, DC, 20560, USA*

Corresponding author: *Luke Tornabene* (luke.tornabene@gmail.com)

Academic editor: *D. Bloom* | Received 28 August 2018 | Accepted 12 November 2018 | Published 19 December 2018

http://zoobank.org/4696B156-1BF8-4BA0-8DA7-33C73D915192

Citation: Tornabene L, Robertson DR, Baldwin CC (2018) A new species of *Lipogramma* from deep reefs of Roatan, Honduras (Teleostei, Grammatidae). ZooKeys 809: 79–95. https://doi.org/10.3897/zookeys.809.29280

Abstract

A new species of *Lipogramma* is described from submersible collections at 122–165 m depth off the coast of Roatan, Honduras, in the western Caribbean. The new species is distinguished from all other species in the genus by its bright blue coloration on the head, nape, and dorsal portion of the trunk beneath the spinous dorsal fin, a prominent round black blotch below the origin of the spinous dorsal fin, and a high number of gill rakers. A molecular phylogeny based on mitochondrial and nuclear genes shows that the new species belongs to a clade containing *L. levinsoni*, *L. regia*, and *L. anabantoides*. At Roatan, submersible observations of this and other *Lipogramma* species indicate clear, interspecific habitat partitioning by depth and substrate.

Keywords

systematics, phylogeny, Caribbean, basslet, species delimitation, submersible

Introduction

Manned submersibles have proven to be highly effective for collecting fishes from deep-reef habitats (Gilmore 2016), particularly in the rariphotic zone (below ~130 m; Baldwin et al. 2018), where divers using closed-circuit rebreathers, which are lim-

ited to depths less than ~ 150 m, are incapable of sampling for extended periods of time. This is especially true for cryptobenthic fishes such as grammatids and gobiids, many of which are associated with structurally complex reef and rocky habitats and are unlikely to be sampled using trawls or dredges. Partially because they are difficult to sample, cryptobenthic reef fishes as a whole are an understudied group, and recent studies suggest that they comprise nearly half of all fish diversity on coral reefs and possess a large number of undescribed species (Brandl et al. 2018). In recent years, researchers from the Smithsonian Deep Reef Observation Project (DROP) have used the manned submersible *Curasub*, located on the island of Curaçao in the southern Caribbean and capable of descending to 300 m, to collect and describe a cache of new species of reef fishes, including many species of cryptobenthic fishes (e.g. gobiids, Baldwin and Robertson 2015, Tornabene et al. 2016a, 2016b, Tornabene and Baldwin 2017; labrisomids, Baldwin and Robertson 2013; and grammatids, Baldwin et al. 2016, 2018).

In 2017, DROP operations expanded to Roatan, Honduras, where the *Idabel* manned submersible is located. On the first dive capturing specimens with *Idabel* off Halfmoon Bay, West End, Roatan, the authors collected a specimen of an undescribed species of *Lipogramma* (Grammatidae) at 165 m depth. Subsequent dives around this depth revealed that the species is relatively common, despite never having been collected before nor observed in more than 150 submersible dives throughout the Caribbean by us or others using *Curasub*, *Idabel,* or the *Johnson Sea-Link* subs. Four additional specimens, including one juvenile, were subsequently collected on later dives off Roatan.

The description of the new species from Roatan brings the total number of species in *Lipogramma* to 13, all of which occur in the tropical western Atlantic Ocean. *Lipogramma* and *Gramma* are currently classified in the family Grammatidae based on a single synapomorphy in the arrangement of cheek musculature (Gill and Mooi 1993). This relationship is not supported by molecular data, although the relationships between genera in the diverse Ovalentaria have proven to be difficult to resolve with traditional molecular markers, a combination of molecular markers and morphological characters, and phylogenomic data (Betancur-R et al. 2013; Mirande 2016; Eytan et al. 2015). Nearly all species of *Lipogramma* occur on deep reefs. *Lipogramma trilineata* and *L. anabantoides* are the only two species known to routinely occur above 50 m, which is approximately the limit of recreational scuba diving. Including the new species described here, five species of *Lipogramma* have been described from specimens collected using *Curasub* and *Idabel*. Several species are rare in collections, owing to the difficulties of collecting fishes from structurally complex deep-reef habitats. Currently *L. haberorum*, *L. barrettorum, L. schrieri*, *L. robinsi*, *L. flavescens*, *L. regia*, *L. rosea,* and the new species described here are each known from fewer than 10 specimens, although this may not accurately reflect an actual rarity in the wild. Increased sampling from Roatan and other localities across the Caribbean are certain to uncover additional undescribed species of *Lipogramma* and other cryptobenthic fishes.

Materials and methods

Specimens were collected using the *Idabel* submersible. The *Idabel* can accommodate a pilot and two scientists and is capable of diving to ~700 m. This sub was recently outfitted with a fish-catching system capable of delivering an anesthetic solution (5% quinaldine sulphate in seawater) and capturing specimens with a suction system powered by one of the submersible's vertical thrusters (Fig. 1). Four of the five type specimens were brought to the surface alive where they were photographed prior to euthanasia in MS222 and preservation. Tissue samples were taken and stored in 95% ethanol, and voucher specimens were fixed in 10% formalin and later transferred to 70–75% ethanol. Measurements were made weeks to months after preservation, and were taken to the nearest 0.1 mm with digital calipers. Counts and measurements follow Hubbs and Lagler (1947). Specimens were x-rayed with a digital radiography system. Type specimens were deposited at the University of Washington (**UW**), the National Museum of Natural History, Smithsonian Institution (**USNM**), the Florida Natural History Museum (**UF**) and the National History Museum of the National Autonomous University of Honduras in the Sula Valley (**MUVS-V**). Cephalic pores were viewed and photographed using a Zeiss Discovery V20 SteREO microscope with an attached Axiocam 503 digital camera. In addition to comparing our morphological data to those from original species descriptions, our comparative material examined here included several specimens (including types) of *L. evides*, *L. levinsoni*, *L. barrettorum*, *L. schrieri*, *L. haberorum*, as well as the voucher specimens from our phylogenetic analysis. Catalog numbers of these specimens are listed in the appendices of Baldwin et al. (2016) and Baldwin et al. (2018).

DNA was extracted from tissue samples using a Qiagen DNeasy Blood and Tissue kit. Four loci were sequenced for three specimens of the new species for phylogenetic analysis. A partial segment of the mitochondrial gene cytochrome c oxidase subunit I (COI), and three nuclear genes (TMO-4C4, Rag1, Rhodopsin) were amplified via PCR and sequenced using primers and PCR conditions from Weigt et al. (2012) and Lin and Hastings (2011, 2013). GenSeq nomenclature (Chakrabarty et al. 2013) and GenBank accession numbers are listed in Appendix 1: Table A1. The sequence data was aligned from the Roatan samples with data from our past studies (Baldwin et al. 2016, 2018). The alignments were concatenated and phylogeny was inferred using Bayesian Inference (BI), partitioning by gene. For the BI analysis, the substitution models and the partitioning scheme were chosen using PartitionFinder (Lanfear et al. 2012) according to Bayesian Information Criterion scores. The BI phylogeny was inferred in the program MrBayes v. 3.2 (Ronquist et al. 2012) using two Metropolis-coupled Markov Chain Monte Carlo (MCMC) runs, each with four chains. The analyses ran for 10 million generations sampling trees and parameters every 1000 generations. Burn-in, convergence and mixing were assessed using Tracer (Rambaut and Drummond 2007) and by visually inspecting consensus trees from both runs. The ML analysis was done in the program RAxML v.8.2.9 (Stamatakis 2014), using 20 initial random searches,

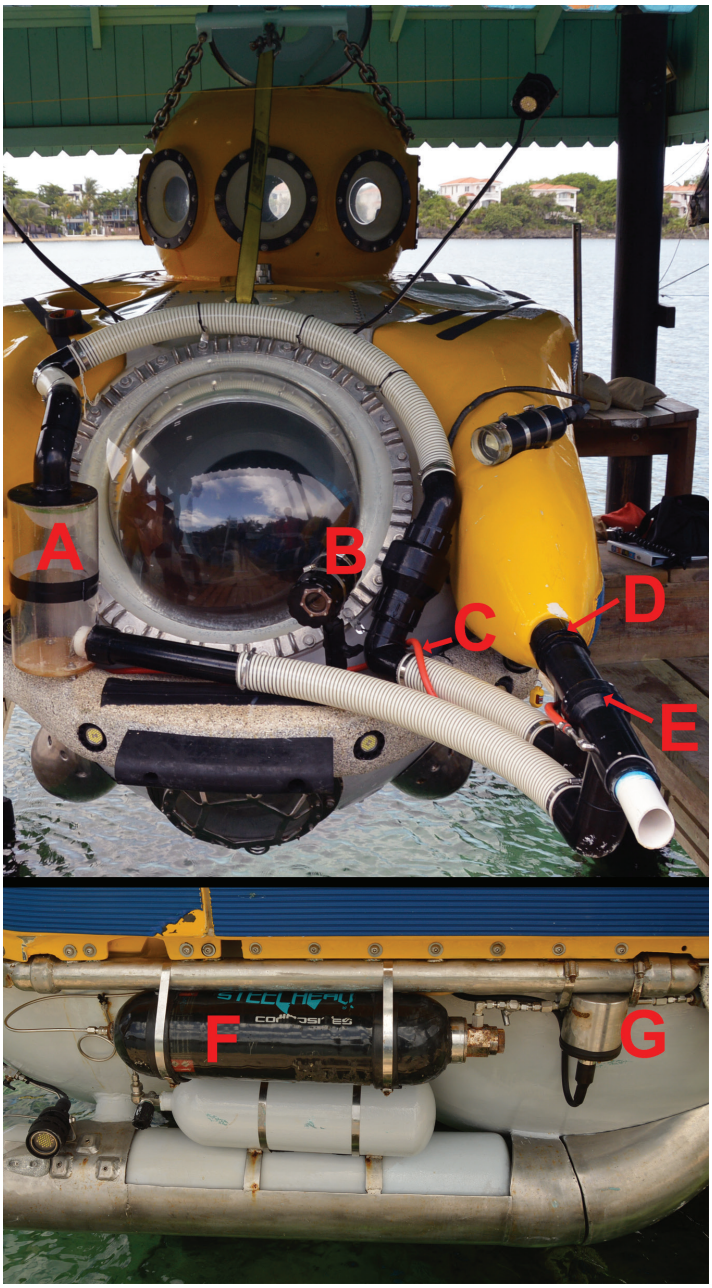

Figure 1. *Idabel* submersible outfitted with fish-catching system. **A** acrylic holding tank **B** housing for HD video camera **C** quinaldine sulphate delivery hose **D** suction for the system is powered by a PVC hose connecting to one of the submersible's vertical thrusters **E** two-way valve to allow for differential suction/blowing of water and or anesthetic **F** carbon-fiber compensator holding up to 2.5 gallons of anesthetic solution, powered by pressurized air from a SCUBA cylinder (not shown, lower tank in image is oxygen for life support systems) **G** housing for solenoid valve, enabling scientists to control the flow of anesthetic from a switch inside the submersible.

and topological support was assessed using 1000 bootstrap replicates. Outgroups for the phylogenetic analysis included two species of *Gramma* and several other genera from the Ovalentaria *sensu* Wainwright et al. (2012), i.e. *Acanthemblemaria* (Chaenopsidae), *Blenniella* (Blenniidae), and *Tomicodon* (Gobiesocidae).

A coalescent-based Bayesian species-delimitation analysis was also conducted (Yang and Rannala 2010, 2014) using the program BP&P ver 3.2 (Yang and Rannala 2010; Yang 2015). This program analyzes multi-locus sequence alignments under the multispecies coalescent model (Rannala and Yang 2003). Each individual was assigned to one of ten groups (nominal species) a priori, based on the potentially diagnostic morphological and pigmentation characters. BP&P was then used to infer a species tree and calculate and compare the posterior probabilities of different species-delimitation models that comprised ten species versus alternative models with fewer than ten (lumping "morpho-species") or more than ten (splitting "morpho-species").

Taxonomy

***Lipogramma idabeli* sp. n.**
http://zoobank.org/FC54BAB6-F303-48EC-8F03-E13BAE5534FA
Figures 2–4
English: Blue-backed Basslet; Spanish: Cabrilleta de Dorso Azul

Type locality. Roatan, Honduras, western Caribbean.

Holotype. USNM 444940, 26.2 mm SL, tissue ROA17002, 165 m depth, station IDABEL17-01, reef slope off Halfmoon Bay, West End, Roatan, Honduras, 16.305557, -86.597669, *Idabel* Submersible, Luke Tornabene, D. Ross Robertson, Karl Stanley, 24 July 2017. **Paratypes.** Locality data same as that of holotype: UW 158090, 26.3 mm SL, tissue ROA17020, 137 m depth, station IDABEL17-05, Luke Tornabene, Rachel Manning, Karl Stanley, 29 July 2017; UW 158096, 10 mm SL, tissue ROA17026, 152 m depth, station IDABEL17-05, Luke Tornabene, Rachel Manning, Karl Stanley, 29 July 2017; MUVS-V-137, 24.0 mm SL, tissue ROA18041, 125–152 m depth, station IDABEL18-03, Luke Tornabene, Rachel Manning, Karl Stanley, 6 June 2018; UF 240986, 22.5 mm SL, tissue ROA18042, 125–152 m depth, station IDABEL18-03, Luke Tornabene, Rachel Manning, Karl Stanley, 6 June 2018.

Diagnosis. A species of *Lipogramma* with pectoral-fin rays 15–16 (modally 16); gill rakers 18–20 total (10–11 elongate rakers plus 2–4 short, stout rudiments on lower limb, 3–4 elongate rakers plus 1–3 rudiments on upper limb); in life, body mostly yellow to tan with bright iridescent blue coloration on eye, dorsal portion of head, nape and dorsal portion of trunk beneath spinous-dorsal fin, oblique yellow bar from tip of snout to orbit and below eye, large, round, black blotch outlined with blue below anterior origin of dorsal fin, and dark ocellus outlined in blue with yellow or dark center at rear insertion of dorsal fin that extends onto body.

Description. Counts and measurements of type specimens given in Table 1. Dorsal-fin rays XII, 9, last ray composite; anal-fin rays III, 7–8 (four specimens including holotype with 8, one with 7), last ray composite; pectoral-fin rays 15–16 (four specimens including holotype with 16, one with 15); pelvic-fin rays I,5; total caudal-fin rays 24 (13 upper, 12 lower), principal rays 17 (9 + 8), procurrent rays 6 (III+III), and an additional 2 unbranched rays (i+i) between principal and procurrent rays that are sometimes segmented; vertebrae 25 (10+15); pattern of supraneural bones, anterior dorsal-fin pterygiophores, and dorsal-fin spines 0/0/0+2/1+1/1/; ribs on vertebrae 3–10, epineurals visible in x-rays on vertebrae 1–13; gill rakers (counted from two specimens, UF 240986, MUVS-V-137) 18–20, upper limb with 3–4 elongate rakers plus 1–2 short rudiments, lower limb with 10–11 moderate-to-elongate rakers plus 2–4 small rudiments present only as nubs, all elongate rakers possess tooth-like secondary rakers, as in *L. evides* (Baldwin et al. 2016: fig. 3); pseudobranchia 6–7, filaments stout and highly branched; branchiostegals 6.

Spinous and soft sections of dorsal fin confluent, several soft rays in posterior portion of fin forming slightly elevated lobe that extends posteriorly beyond base of caudal fin. Pelvic fin, when depressed, extending at least to origin of first soft ray of anal fin, and to origin of penultimate anal-fin ray in holotype. Dorsal profile from snout to origin of dorsal fin convex. Diameter of eye contained 2.8–3.0 times in head length. Pupil tear-shaped, with small aphakic space anteriorly. Scales extending anteriorly onto top of head, ending at a vertical just behind posterior margin of eye. Scales present on cheeks, operculum, and isthmus, absent on snout, jaws, and branchiostegals. Scales large and deciduous, missing on anterodorsal flank of several specimens. Approximately 22–25 lateral scales between shoulder and base of caudal fin (24 in holotype), 4–6 cheek rows, 11 rows across body from above anal-fin origin. Scales on nape and along dorsal midline with reduced or absent cteni, those on cheek and opercula lacking cteni. Fins naked except base of posteriormost dorsal-fin rays, which possess 1 or 2 small embedded scales. No modified lateral-line scales present on body, but faint indication of a lateral line present superficially in fresh photographs.

Margins of bones of opercular series smooth, opercle without spines. Single row of teeth on premaxilla posteriorly, broadening to 2 or 3 rows anteriorly, teeth in innermost row smallest, some teeth in outer row enlarged into small canines. Dentary similar with 3 or 4 enlarged teeth in outer row near symphysis. Vomer with chevron-shaped patch of teeth that extends posterolaterally nearly length of premaxilla, palatine with long series of small teeth.

Cephalic head pores arranged as in Fig. 2, with conspicuous pores present in infraorbital canal (2), dentary canal (2), supraorbital canal (2 pores above each eye plus one median coronal pore), preopercular canal (7), posttemporal canal (3), plus a single pore in canal above post-temporal canal in line with preopercle. Anterior naris in elongate tube above upper lip, posterior naris a wide opening with slightly raised rim immediately anterior to supraorbital canal.

Coloration in fresh specimens (Fig. 3): **Head:** top of snout, top of head, and nape bright blue; lower part of head yellow brown, with faint blue overtone; eye with bright blue iris, black pupil; top and bottom lips with pale blue overtone; yellow oblique bar,

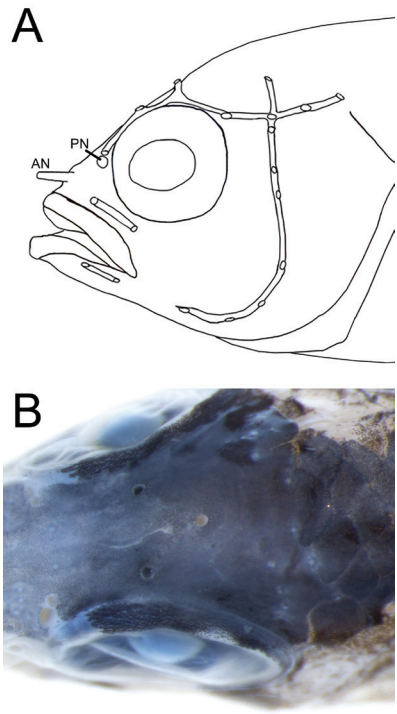

Figure 2. Cephalic sensory-canal pore system **A** composite pattern from entire type series **B** Supraorbital and median coronal pores, MUVS-V-137. Abbreviations: AN anterior naris, PN posterior naris.

Table 1. Counts and measurements from type series. All measurements except SL are in % SL. Abbreviations: CP = caudal peduncle; PFO = pelvic-fin origin; P1 = pectoral fin; P2 = pelvic fin; DXII = twelfth dorsal-fin spine. Other caudal rays include i, a slender, flexible, non-spinous, sometimes segmented ray, and I, a spinous procurrent ray.

	USNM 444940 Holotype	MUVS-V-137 Paratype	UF 240986 Paratype	UW 158090 Paratype	UW 158096 Paratype
Tissue number	ROA17003	ROA18041	ROA18042	ROA17020	ROA17026
SL (mm)	26.2	24	22.5	26.3	10
Dorsal-fin rays	XII, 9	XII, 9	XII, 9	XII, 9	XII, 9
Anal-fin rays	III, 8	III, 7	III, 8	III, 8	III, 8
Principal caudal rays	9+8	9+8	9+8	9+8	9+8
Other caudal rays	IIIi+iIII	IIIi+iIII	IIIi+iIII	IIIi+iIII	IIIi+iIII
Pectoral-fin rays	16	15	16	16	16
Gill rakers - upper limb	not counted	11+4 rudiments	10+2 rudiments	not counted	not counted
Gill rakers - lower limb	not counted	4+1 rudiment	3+3 rudiments	not counted	not counted
Head length	37.4	37.9	38.2	37.3	40.0
Eye diameter	13.0	14.6	14.2	12.9	2.0
Snout length	8.8	9.2	8.9	6.8	7.0
Depth at CP	20.2	17.9	19.1	19.0	17.1
Depth at PFO	36.3	30.8	35.6	33.4	35.5
Length P1 Fin	24.8	24.2	23.1	24.7	22.1
Length P2 Fin	50.4	45.4	44.9	46.4	35.0
Length DXII	14.8	13.7	12.0	14.1	13.0

bordered with blue, extending from tip of snout to mid orbit and continuing below orbit towards lower corner of preopercle; opercle with lavender hue from bright red gills and blood vessels visible through gill cover. **Trunk:** yellowish to yellow-brown, paler and sometimes with faint bluish cast on isthmus and abdomen; large, eye-size round black blotch on upper back under the origin of dorsal fin, surrounded by thin bright blue ring; blue coloration on nape extends along the upper back to end of spinous dorsal. **Spinous dorsal fin:** bright blue anteriorly, fading to blue-grey posteriorly on basal half; outer edge blue-grey, with thin submarginal yellow stripe formed by series of close-set, horizontally elongate yellow spots; row of yellow spots (each on and just behind a spine), beginning at base of the first 2–3 spines, then continuing as row along other 1/3 of the fin**. Soft dorsal fin**: rays blue-grey anteriorly, with the last several posterior rays blue; upper margin whitish-blue, with a submarginal row of vertically elongate, inter-radial yellow spots, and 3–4 rows of vertically oval, inter-radial yellow spots, those at rear forming thin, yellow lines along the membranes between last 2 or 3 rays; pupil-sized, round, yellow-brown blotch containing darker scales ringed with bright blue at rear insertion of fin, with half of blotch covering base of last 6 or 7 rays and half on upper back. **Anal fin***:* bluish grey, with brownish cast on scaled base of fin; 3 or 4 irregular rows of yellow spots along fin elements, central spots oval, basal and outer spots forming streaks along fin elements; outer margin of fin whitish-blue. **Caudal fin:** base translucent yellow; center of fin with rows of yellow spots along fin rays; outer part of fin translucent, with thin whitish-blue rear margin; vertical rows of pale blue spots on rays in center of fin. **Pectoral fins:** pectoral rays tinged with yellow, membranes translucent; base of fin paler than adjacent body. **Pelvic fins:** pale bluish grey, with elongate yellowish spots along fin rays, that yellow coloration strongest at base of fin.

Juvenile coloration: Coloration of the single small juvenile is essentially the same as in the adult, except that the posterior portion of the body is more noticeably yellow, the entire center of the anal fin, and, apparently, much of the soft dorsal and caudal fins are yellow, and the dark center of the ocellus at the lower rear corner of the dorsal fin is solid black.

Comments about live coloration: As can be seen in the video of the holotype being captured (https://doi.org/10.5281/zenodo.1334518, or https://zenodo.org/record/1334518#.W89WsSPMyFU), live fish have the upper third of the head and body bright blue, the lower 2/3 yellow, and a prominent large round black blotch on the shoulder.

Color in preservation (Fig. 4): Overall pigmentation pattern largely similar to that of fresh individuals, except iridescent blue coloration replaced by dark brown pigment; oblique bar on head below eye pale in preservation versus yellow in life; dark ocelli below spinous and soft dorsal fins less distinct, with no clearly defined ring or margin; background body coloration darkest on head and below origin of spinous dorsal fin, gradually fading from brownish-tan anteriorly to pale-yellow posteriorly.

Distribution. Known only from specimens collected off Roatan, Honduras (Fig. 5).

Habitat. The species was frequently observed in the mid-to-upper rariphotic zone between 122–165 m depth, in or around small rock crevices, rock piles, or caves situ-

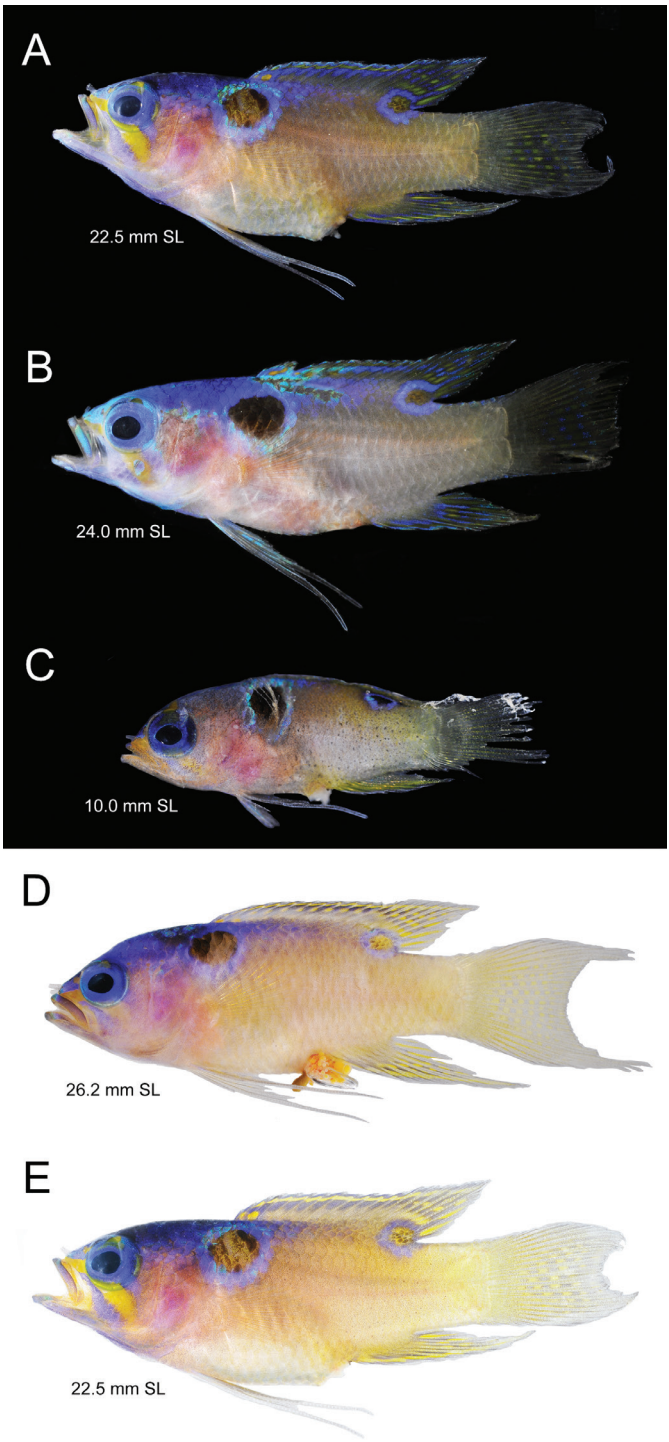

Figure 3. *Lipogramma idabeli*, fresh specimens on dark (**A–C**) and light (**D, E**) backgrounds. **A** UF 240986 **B** MUVS-V-137 **C** UW 158096 **D** USNM 444940, holotype **E** MUVS-V-137.

Figure 4. *Lipogramma idabeli*, preserved **A** USNM 444940, holotype **B** UW 158090.

ated on steep limestone walls covered with coarse sediment and fine rubble composed of dead sections of the green macroalga *Halimeda* (Fig. 5). A video showing the collection of the holotype is available online (https://doi.org/10.5281/zenodo.1334518, or https://zenodo.org/record/1334518#.W89WsSPMyFU).

Etymology. The specific epithet *idabeli* refers to the *Idabel* submersible, which was used to collect the type series, and recognizes of the efforts of its owner-designer and pilot Karl Stanley and engineer Thomas Trudel, who made these and other collections of fishes possible by constructing a fish-catching system that converted *Idabel* from an observation-only vessel to one capable of collecting scientific specimens. The name *idabeli* is to be treated as a patronym (adjective) formed from the female name Idabel. The generic name *Lipogramma* is feminine and is formed from *lipo* (without) and *gramma* (a line of text, feminine), referring to the absence of a well-developed lateral line. The common name Cabrilleta de Dorso Azul (Blue-backed Basslet in English) refers to its distinctive coloration.

Comparisons. *Lipogramma idabeli* is easily distinguished from all other species of *Lipogramma* by the bright blue coloration on the head and eye, and by the pair of blue-margined ocelli below the anterior origin of the dorsal fin and at the posterior insertion of the dorsal fin. There are only two other species of *Lipogramma* in which the head is a markedly different color than the body; *L. klayi* and *L. anabantoides* both

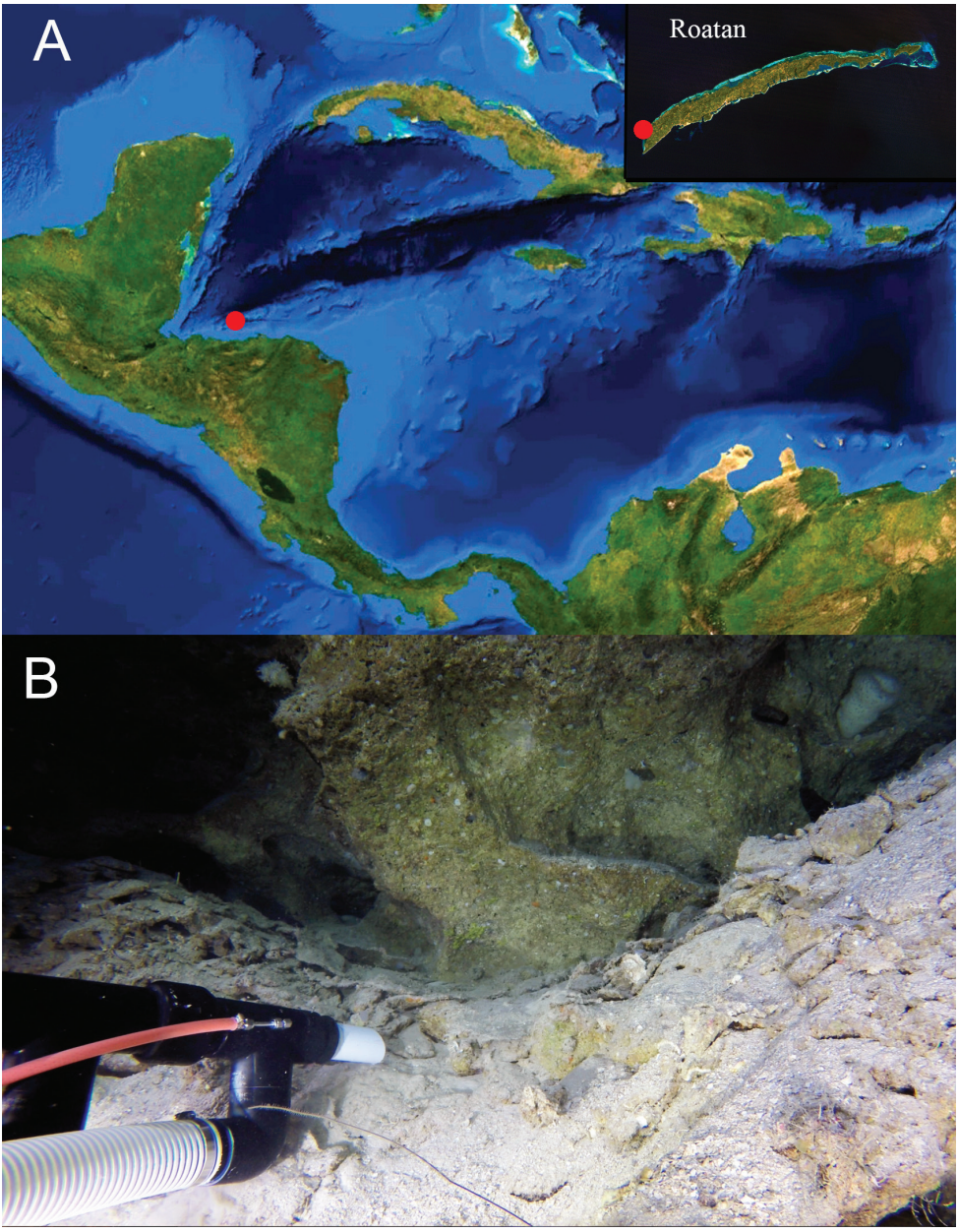

Figure 5. Type locality. **A** Halfmoon Bay, Roatan, Honduras. **B** Habitat where holotype was collected 165 m depth. The rock pile immediately in front of the suction tube is where the fish was sheltered. Maps courtesy of NASA.

have rose, pink, or purple heads with tan or yellow bodies. No other known species has bright blue coloration on the dorsal portion of the head, nape, and dorsal portion of the trunk. All species of *Lipogramma* except *L. klayi*, *L. rosea*, and *L. trilineata* possess an ocellus on the posterior portion of the dorsal fin, but the pattern of barring and

shading on the head and body differ among all of those species (Fig. 6). In addition to the differences, none have the ocellus with a blue margin except *L. idabeli*. Furthermore, in *L. idabeli*, the ocellus varies from having a dark center as a juvenile to a yellow or dusky center as an adult, whereas in the other species, the ocellus is always black. The absence of prominent vertical barring on the body distinguishes *L. idabeli* from *L. robinsi*, *L. barretorum*, *L. haberorum*, *L. evides*, *L. levinsoni*, *L. schrieri*, and *L. regia* (Fig. 6). *Lipogramma idabeli* has more total gill rakers (18–20) than all other species except *L. evides* (19–22), *L. klayi* (19), and *L. levinsoni* (17–20); all other species have 16 or fewer. The combination of XII, 9 dorsal-fin elements and III, 8 anal-fin elements present in *L. idabeli* is shared among most species in the genus, except *L. rosea* (XI, 6 and III, 6), *L. trilineata* (XII, 10 and III, 7), and *L. anabantoides* (XIII, 8 and III, 8).

Phylogenetics and eco-evolutionary relationships. Coloration unambiguously diagnoses *L. idabeli* and supports its recognition as a distinct species. Molecular data from the ten species of *Lipogramma* for which tissue samples were available also support this distinction. The molecular phylogenies from the Bayesian and Maximum Likelihood analyses (Fig. 7; Suppl. material 1: Figure S1), which were identical in topology to that from the BP&P coalescent species-tree analysis, show that the three specimens of *L. idabeli* form a monophyletic group with strong support (1.0 posterior probability; 100 bootstrap). The BP&P species delimitation analysis had overwhelming support for a 10-species model (posterior probability 0.997) versus models with fewer or more species, indicating perfect congruence between morphological and molecular delimitation approaches.

Our analyses show *L. idabeli* as part of a well-supported clade containing *L. regia*, *L. levinsoni*, and *L. anabantoides*, with the relationships within this clade being less resolved. All of these species occur from the mid-to-upper rariphotic zone and shallower (20–165 m). Similar to our observations of species of *Lipogramma* occurring off Curacao and other localities in the Caribbean (Baldwin et al. 2016, 2018), species off Roatan appear to be partitioning the reef by depth and microhabitat association. The known depth range for *L. idabeli* off Roatan, based on collected specimens and visual observations, is 122–165 m. At Roatan, its depth range broadly overlaps with that of *L. levinsoni*, but the two species occupy very different microhabitats. *Lipogramma levinsoni* is typically found hovering around and above limestone rubble and small cobble habitats on gradual slopes, whereas *L. idabeli* is found around larger rocks, caves, and outcroppings on steeper slopes and vertical walls. In addition to *L. idabeli* and *L. levinsoni*, other nominal species of *Lipogramma* observed at Roatan include *L. klayi*, *L. evides*, and *L. flavescens*. Like *L. idabeli*, *L. klayi* also occurs around steep walls but at depths considerably shallower than *L. idabeli* (~65–120 m versus 122–165 m), where the reef wall is generally covered with more extensive growth of *Halimeda*, encrusting sponges, gorgonians, and other sessile habitat-forming organisms. Both *L. flavescens* and *L. evides* were observed deeper than *L. idabeli* at 213–250 m, with *L. evides* usually occurring on gradual rocky slopes with a heavy layer of cobbles (similar to the habitat of *L. levinsoni*), and *L. flavescens* found out in the open on bottoms of coarse sand with small, low, scattered piles of rock and rubble, far from the wall.

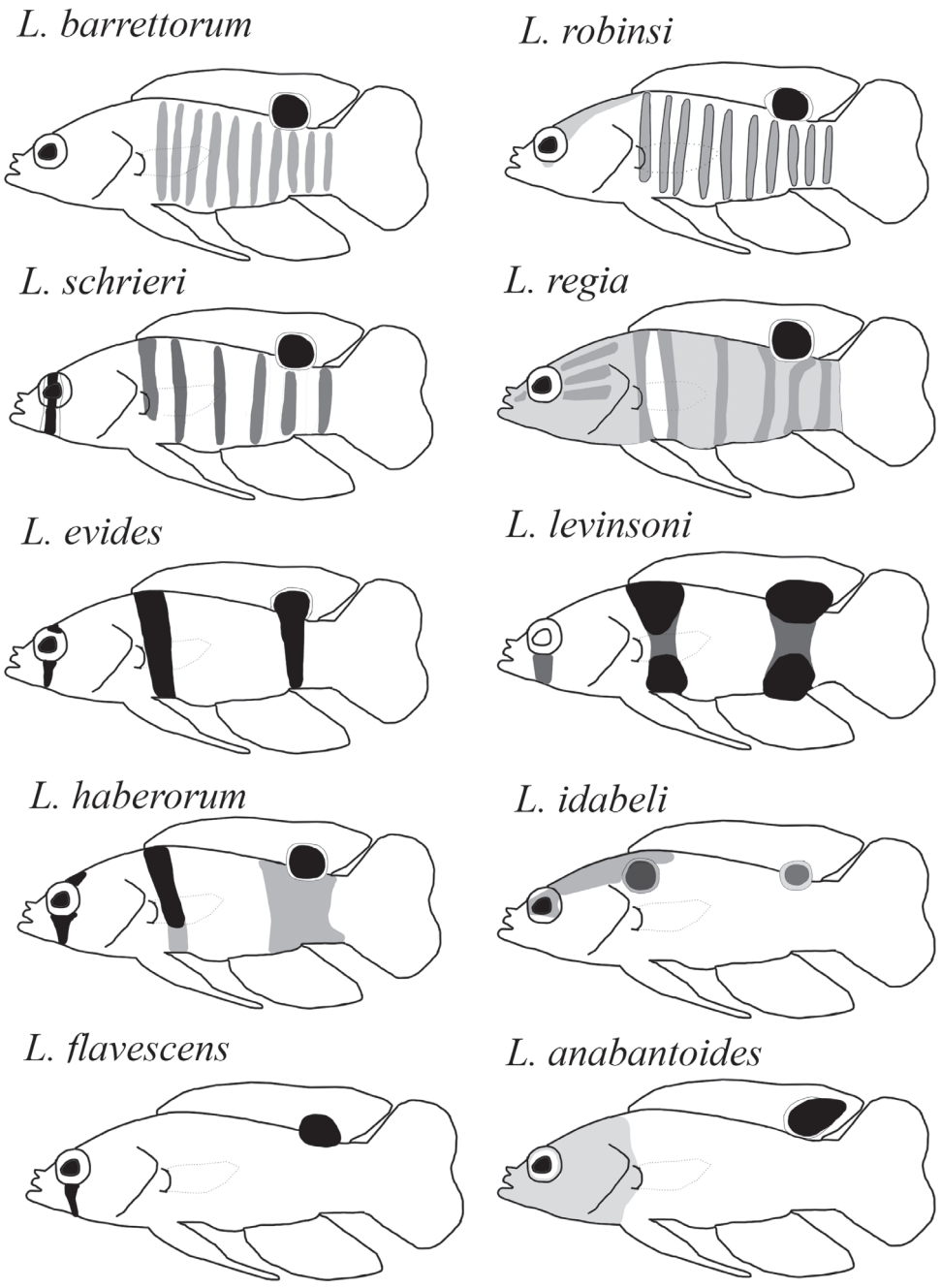

Figure 6. Schematic showing the barring and shading patterns of the ten species of *Lipogramma* that possess a dark ocellus on the posterior portion of the dorsal fin.

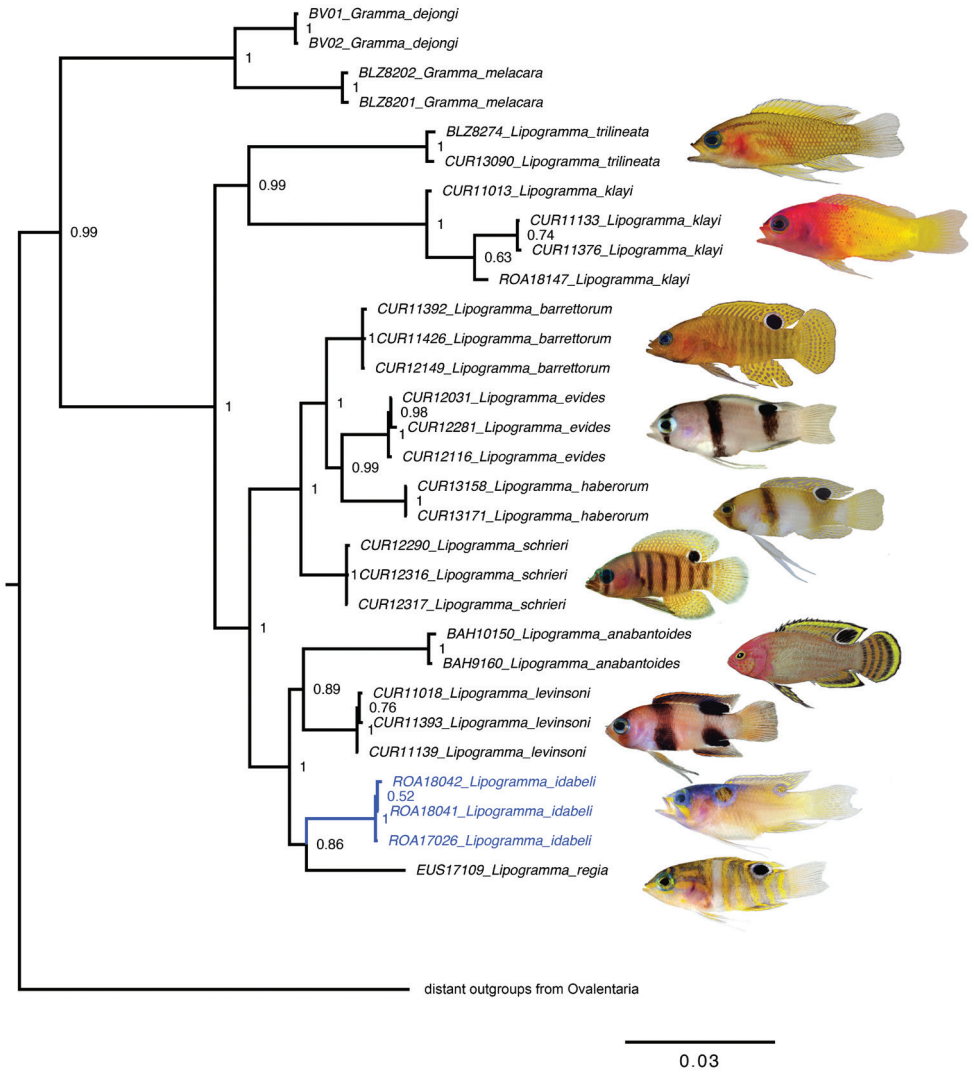

Figure 7. Bayesian inference molecular phylogeny of *Lipogramma*. Numbers at nodes are posterior probabilities. Photographs and illustrations by CC Baldwin, DR Robertson, L Tornabene, RG Gilmore, and CR Robins.

Acknowledgements

We thank Karl Stanley and Thomas Trudel of the Roatan Institute of Deep-sea Exploration for their support with piloting *Idabel* and designing, building, and maintaining the fish-catching system and other research tools for *Idabel*. We thank Rachel Manning for her assistance in the field, and Sam Ghods for his help with molecular work. We are grateful for the help of Katherine Maslenikov, who assisted in the field and with cataloging specimens. Funding for the Deep Reef Observation Project was provided by the Herbert R. and Evelyn Axelrod Endowment Funding for systematic ichthyology to CCB, STRI funds to

DRR, and funds from the University of Washington School of Aquatic and Fishery Sciences to LT. Rob Robins at UF, and Diane Pitassy and Jeff Williams at USNM assisted with cataloging specimens. We are indebted to Claudia Lardizabal and Alex Vallejo at Universidad Nacional Autónoma de Honduras – Valle de Sula for helping with research permits and deposition of specimens in the MUVS collection. This is Ocean Heritage Foundation/Curacao Sea Aquarium/Substation Curacao (OHF/SCA/SC) contribution #35.

References

Baldwin CC, Robertson DR (2013) A new *Haptoclinus* blenny (Teleostei, Labrisomidae) from deep reefs off Curacao, southern Caribbean, with comments on relationships of the genus. ZooKeys 306: 71–81. https://doi.org/10.3897/zookeys.306.5198

Baldwin CC, Robertson DR (2015) A new, mesophotic *Coryphopterus* goby (Teleostei: Gobiidae) form the southern Caribbean, with comments on relationships and depth distributions within the genus. ZooKeys 513: 123–142. https://doi.org/10.3897/zookeys.513.9998

Baldwin CC, Robertson DR, Nonaka A, Tornabene L (2016) Two new deep-reef basslets (Teleostei, Grammatidae, *Lipogramma*), with comments on the eco-evolutionary relationships of the genus. ZooKeys 638: 45–82. https://doi.org/10.3897/zookeys.638.10455

Baldwin CC, Tornabene L, Robertson DR (2018) Below the mesophotic. Scientific Reports 8: 4920. https://doi.org/10.1038/s41598-018-23067-1

Betancur-R R, Broughton RE, Wiley EO, Carpenter K, López JA, Li C, Holcroft NI, Arcila D, Sanciangco M, Cureton II JC, Zhang F, Buser T, Campbell MA, Ballesteros JA, Roa- Varon A, Willis S, Borden WC, Rowley T, Reneau PC, Hough DJ, Lu G, Grande T, Arratia G, Ortí G (2013) The tree of life and a new classification of bony fishes. PLoS Currents Tree of Life. 2013 Apr 18. Edition 1. https://doi.org/10.1371/currents.tol.53ba26640df0ccaee75bb165c8c26288 [Last modified: 2013 Apr 18]

Brandl SJ, Goatley CHR, Bellwood DR, Tornabene L (2018) The hidden half: ecology and evolution of cryptobenthic fishes on coral reefs. Biological Reviews. https://doi.org/10.1111/brv.12423

Chakrabarty P, Warren M, Page LM, Baldwin CC (2013) GenSeq: An updated nomenclature and ranking for genetic sequences from type and non-type sources. ZooKeys 346: 29–41. https://doi.org/10.3897/zookeys.346.5753

Eytan RI, Evans BR, Dornburg A, Lemmon AR, Lemmon EM, Wainright PC, Near TJ (2015) Are 100 enough? Inferring Acanthomorph teleost phylogeny using Anchored Hybrid Enrichment. BMC Evolutionary Biology 15: 113. https://doi.org/10.1186/s12862-015-0415-0

Gill AC, Mooi RD (1993) Monophyly of the Grammatidae and of the Notograptidae, with evidence for their phylogenetic positions among perciforms. Bulletin of Marine Science 25: 327–350.

Gilmore RG (2016) You can't catch a fish with a robot. Gulf and Caribbean Research 27(1): 2–14. https://doi.org/10.18785/gcr.2701.11

Lanfear R, Calcott B, Ho SYW, Guindon S (2012) PartitionFinder: Combined selection of partitioning schemes and substitution models for phylogenetic analyses. Molecular Biology and Evolution 29: 1695–1701. https://doi.org/10.1093/molbev/mss020

Lin H-C, Hastings PA (2011) Evolution of a Neotropical marine fish lineage (Subfamily Chaenopsinae, Suborder Blennioidei) based on phylogenetic analysis of combined molecular and morphological data. Molecular Phylogenetics and Evolution 60: 236–248. https://doi.org/10.1016/j.ympev.2011.04.018

Lin H-C, Hastings PA (2013) Phylogeny and biogeography of a shallow water fish clade (Teleostei: Blenniiformes). BMC Evolutionary Biology 13: 210. https://doi.org/10.1186/1471-2148-13-210

Mirande JM (2016) Combined phylogeny of ray-finned fishes (Actinopterygii) and the use of morphological characters in large-scale analyses. Cladistics 2016: 1–18. https://doi.org/10.1111/cla.12171

Rambaut A, Drummond AJ (2007) Tracer. http://beast.bio.ed.ac.uk/Tracer

Ronquist F, Teslenko M, van der Mark P, Ayres DP, Darling A, Höhna S, Larget B, Liu L, Suchard MA, Huelsenbeck JP (2012) MrBayes 3.2: efficient Bayesian phylogenetic inference and model choice across a large model space. Systematic Biology 61: 539–542. https://doi.org/10.1093/sysbio/sys029

Stamatakis A (2014) RAxML Version 8: A tool for phylogenetic analysis and post-analysis of large phylogenies. Bioinformatics 30: 1312–1313. https://doi.org/10.1093/bioinformatics/btu033

Tornabene L, Baldwin CC (2017) A new mesophotic goby, *Palatogobius indendius* (Teleostei: Gobiidae), and the first record of invasive lionfish preying on undescribed biodiversity. PLoS ONE 12(5): e0177179. https://doi.org/10.1371/journal.pone.0177179

Tornabene L, Robertson DR, Baldwin CC (2016a) *Varicus lacerta*, a new species of goby (Teleostei, Gobiidae, Gobiosomatini, *Nes* subgroup) from a mesophotic reef in the southern Caribbean. ZooKeys 596: 143–156. https://doi.org/10.3897/zookeys.596.8217

Tornabene L, Van Tassell JL, Gilmore RG, Robertson DR, Young F, Baldwin CC (2016b) Molecular phylogeny, analysis of character evolution, and submersible collections enable a new classification for a diverse group of gobies (Teleostei: Gobiidae: *Nes* subgroup), including nine new species and four new genera. Zoological Journal of the Linnean Society 177(4): 764–812. https://doi.org/10.1111/zoj.12394

Wainwright PC, Smith WL, Price SA, Tang KL, Sparks JS, Ferry LA, Kuhn KL, Eytan RI, Near TJ (2012) The evolution of pharyngognathy: a phylogenetic and functional appraisal of the pharyngeal jaw key innovation in labroid fishes and beyond. Systematic Biology 61: 1001–1027. https://doi.org/10.1093/sysbio/sys060

Weigt LA, Driskell AC, Baldwin CC, Ormos A (2012) DNA barcoding fishes. Chapter 6 In: Kress WJ, Erickson DL (Eds) DNA Barcodes: Methods and Protocols, Methods in Molecular Biology 858: 109–126. https://doi.org/10.1007/978-1-61779-591-6_6

Yang Z (2015) The BPP program for species tree estimation and species delimitation. Current Zoology 61(5): 854–865. http://dx.doi.org/10.1093/czoolo/61.5.854

Yang Z, Rannala B (2010) Bayesian species delimitation using multilocus sequence data. Proceedings of the National Academy of Sciences of United States of America 107: 9264–9269. https://doi.org/10.1073/pnas.0913022107

Yang Z, Rannala B (2014) Unguided species delimitation using DNA sequence data from multiple loci. Molecular Biology and Evolution 31: 3125–3135. https://doi.org/10.1093/molbev/msu279

Appendix 1

Table A1. DNA voucher specimens, GenBank numbers, and GenSeq nomenclature for new sequences generated in this study.

Catalog number	Tissue number	Type	Species	GenBank COI	GenBank TMO-4c4	GenBank Rag1	GenBank Rhodopsin	GenSeq Designation
MUVS-V-137	ROA18041	paratype	*Lipogramma idabeli*	MK227831	MK227821	MK227827	MK227824	genseq-2
UF 240986	ROA18042	paratype		MK227830	MK227822	MK227826	MK227825	genseq-2
UW 158096	ROA17026	paratype		MK227829	MK227820	MK227828	MK227823	genseq-2

Supplementary material 1

Figure S1

Authors: Luke Tornabene, D. Ross Robertson, Carole C. Baldwin

Data type: statistical data

Explanation note: Maximum likelihood inference molecular phylogeny of *Lipogramma*. Numbers at nodes are bootstrap support values.

Link: https://doi.org/10.3897/zookeys.809.29280.suppl1

ZooKeys 809: 97–124 (2018)
doi: 10.3897/zookeys.809.25207
http://zookeys.pensoft.net

RESEARCH ARTICLE

A peer-reviewed open-access journal
ZooKeys
Launched to accelerate biodiversity research

A new treefrog from Cordillera del Cóndor with comments on the biogeographic affinity between Cordillera del Cóndor and the Guianan Tepuis (Anura, Hylidae, *Hyloscirtus*)

Santiago R. Ron[1], Marcel A. Caminer[1], Andrea Varela-Jaramillo[1], Diego Almeida-Reinoso[1]

1 *Museo de Zoología, Escuela de Biología, Pontificia Universidad Católica del Ecuador, Av. 12 de Octubre y Roca, Aptdo. 17-01-2184, Quito, Ecuador*

Corresponding author: *Santiago R. Ron* (santiago.r.ron@gmail.com)

Academic editor: *Angelica Crottini* | Received 22 March 2018 | Accepted 28 September 2018 | Published 19 December 2018

http://zoobank.org/17A46360-8038-4385-A995-1168357B08A3

Citation: Ron SR, Caminer MA, Varela-Jaramillo A, Almeida-Reinoso D (2018) A new treefrog from Cordillera del Cóndor with comments on the biogeographic affinity between Cordillera del Cóndor and the Guianan Tepuis (Anura, Hylidae, *Hyloscirtus*). ZooKeys 809: 97–124. https://doi.org/10.3897/zookeys.809.25207

Abstract

The *Hyloscirtus larinopygion* group is a clade of 16 species of large hylids that inhabit cascading Andean streams. They have brown coloration that, in most species, contrasts with bright marks. Herein morphological and genetic evidence is used to describe a new species of the group from Cordillera del Cóndor, a sub-Andean mountain chain that has phytogeographic affinities with the Guianan Tepuis. The new species is characterized by dark-brown coloration with contrasting bright orange flecks and by the presence of an enlarged and curved prepollex protruding as a spine. The new species is closely related to *H. tapichalaca* and an undescribed species from the southern Andes of Ecuador. The genetic distance between *H. hillisi* **sp. n.** and its closest relative, *H. tapichalaca*, is 2.9% (gene 16S mtDNA). Our phylogeny and a review of recently published phylogenies show that amphibians from Cordillera del Cóndor have close relationships with either Andean or Amazonian species. Amphibians do not show the Condor-Guianan Tepuis biogeographic link that has been documented in plants.

Keywords

Biodiversity, *Colomascirtus*, Ecuador, *H. larinopygion* group, Peru, prepollical spine, phylogeny

Introduction

Hyloscirtus Peters 1882, is a genus of 37 species of treefrogs distributed from Costa Rica to the Andes of Bolivia, Colombia, Ecuador, Peru, and Venezuela (AmphibiaWeb 2018; Frost 2018). They reproduce along streams and share, as a synapomorphy, the presence of wide lateral fringes on fingers and toes (Faivovich et al. 2005 but see Coloma et al. 2012). A well-supported clade within *Hyloscirtus* is the *Hyloscirtus larinopygion* species group (Almendáriz et al. 2014; Coloma et al. 2012; Duellman and Hillis 1990; Rivera-Correa et al. 2016). It is composed of 16 species characterized by large size (SVL < 60 mm) and gray or brown coloration that in many species contrast with bright marks. Species of this group were transferred to the genus *Colomascirtus* by Duellman et al. (2016). A recent phylogeny showed that the recognition of *Colomascirtus* rendered *Hyloscirtus* paraphyletic (Rojas-Runjaic et al. 2018). To maintain taxonomic stability, *Colomascirtus* was synonymized under *Hyloscirtus* by Rojas-Runjaic et al. (2018).

The *Hyloscirtus larinopygion* group is composed of two well-supported clades that replace each other latitudinally with a small area of sympatry in central Ecuador (Almendáriz et al. 2014a). The northern clade is distributed in the Andes of central and northern Ecuador and southern Colombia; the southern clade is distributed in the eastern Andean slopes of central and southern Ecuador and northern Peru (Rivera-Correa et al. 2016). The southern clade is composed of three species: *H. condor* Almendáriz et al. 2014a, *H. tapichalaca* (Kizirian et al. 2003), and an undescribed species previously reported as *H. lindae* (Almendáriz et al. 2014a). *Hyloscirtus diabolus* Rivera-Correa et al. 2016 is also a putative member of this clade (Rivera-Correa et al. 2016). The four species differ from species in the northern clade by having an enlarged prepollex with the shape of a spine that protrudes below the thumb (Almendáriz et al. 2014; Rivera-Correa et al. 2016). Recent fieldwork in Cordillera del Cóndor by a field team from the Museum of Zoology, Pontificia Universidad Católica del Ecuador, resulted in the discovery of an undescribed species of the southern clade which also shares a spine-shaped prepollex. Cordillera del Cóndor is a sub-Andean mountain chain with phytogeographic affinities to the Tepuis in the Guiana Region (e.g., Neill 2005). Herein we present morphological and genetic evidence to describe the new species and provide a new phylogeny for the genus *Hyloscirtus*. We also review recent amphibian phylogenies to explore the existence of biogeographic links between Cordillera del Cóndor and the Guianan Tepuis.

Materials and methods

DNA extraction, amplification, and sequencing

DNA was extracted from muscle or liver tissue preserved in 95% alcohol following standard phenol-chloroform extraction protocols (Sambrook et al. 1989). Standard polymerase chain reaction (PCR) was performed to amplify two mitochondrial genes (12S rRNA + $tRNA^{Val}$ and 16S rRNA), using primers listed in Goebel et al. (1999), Heinicke et al.

(2007), Hedges et al. (2008), and Heinicke et al. (2009) under standard protocols. PCR products were sequenced in both directions by Macrogen (Macrogen Inc., Seoul, Korea).

Sequences were edited and assembled with Geneious 10.2.3 software (Gene Matters Corp, Kearse et al. 2012). The obtained sequences were compared with those available in GenBank (http://www.ncbi.nlm.nih.gov/genbank/) for the *Hyloscirtus larinopygion* and *bogotensis* groups (published by Almendáriz et al. 2014; Coloma et al. 2012; Darst and Cannatella 2004; Elmer and Cannatella 2008; Faivovich et al. 2004; Faivovich et al. 2005; Guayasamin et al. 2015; Rojas-Runjaic et al. 2018; Wiens et al. 2005; Wiens et al. 2006) (Table 1). For the outgroup we added sequences of *Aplastodiscus weygoldti*, *Bokermannohyla circumdata*, *Boana crepitans*, *B. lundii*, *B. marianitae*, *B. riojana*, *Itapotihyla langsdorfii*, *Myersiohyla kanaima*, and *Pseudacris nigrita*.

Sequences were aligned using the Geneious extension MAFFT Multiple Alignment with the algorithm LINS-I (Katoh and Standley 2013). Alignments were imported into Mesquite (version 3.04; Maddison and Maddison 2018) for final visual adjustments. The final matrix included 2497 characters. The best partition strategy and best-fit model of nucleotide evolution for our data were obtained in PartitionFinder v.2.1.1 (Lanfear et al. 2012) under the corrected Akaike Information Criterion (AICc).

Phylogeny

Phylogenetic relationships were inferred using maximum-likelihood and Bayesian inference. Maximum likelihood analysis were conducted with GARLI 2.0 (Zwickl 2006) using default values, except for the number of generations without topology improvement required for termination (genthreshfortopoterm = 30000) and the maximum number of generations to run and maximum search time (stopgen and stoptime = 5000000). A total of 40 independent searches were run, 20 started from random trees (streefname = random) and 20 from stepwise addition trees (streefname = stepwise). Likelihood values of the 40 searches were within 0.1 likelihood units of each other indicating that all searches converged on similar optimal trees. Support was assessed using 200 bootstrap pseudoreplicates. Bayesian phylogenetic analyses were carried out in MrBayes 3.2.6 (Ronquist et al. 2012). We made four parallel runs of the Metropolis-coupled Monte Carlo Markov for 20 million generations. Each run had five chains, sampled every 1000 generations and with a temperature of 0.1. Convergence into a stationary distribution was measured with software Tracer version 1.4 (Rambaut and Drummond 2007). The search was finished when the average standard deviations of split frequencies was < 0.05 between runs and ESS values were > 200 for all parameters. The consensus tree was generated after discarding 10% of the initial generations as burn-in. Bayesian analyses were carried out at Cipres Science Gateway (available at https//www.phylo.org; Miller et al. 2010).

Pairwise genetic distances between-species (uncorrected-*p*) were calculated with MEGA 5 (Tamura et al. 2011) for genes 16S (886 bp) and 12S (773 bp). Genetic distances for gene 16S are the most widely used standard to identify candidate species (e.g., Coloma et al. 2012; Fouquet et al. 2007; Janzen and Hallwachs 2011; Vieites et al. 2009).

Table 1. Genbank accession numbers for DNA sequences included in the phylogenetic analysis.

Species	Museum Number	GenBank Accession Number		Source
		12S	16S	
Hyloscirtus alytolylax	QCAZ 24376	JX155799	JX155826	Coloma et al. 2012
	QCAZ 24377	JX155798	JX155825	Coloma et al. 2012
H. armatus	KU 173222	AY819423	–	Wiens et al. 2005
	AMNH 165163	AY549321	AY549321	Faivovich et al. 2004
H. callipeza	UIS-A 5947	MG596780	MG596780	Rojas-Runjaic et al. 2018
H. charazani	AMNH 165132	AY843618	AY843618	Faivovich et al. 2005
H. colymba	SIU 6926	DQ380353	–	Wiens et al. 2006
	SIUC H-7079	AY843620	AY843620	Faivovich et al. 2005
H. condor	MEPN 14754	KF756939	KF756939	Almendáriz et al. 2014a
	MEPN 14758	KF756938	KF756938	Almendáriz et al. 2014a
H. criptico	QCAZ 43421	JX155812	JX155839	Coloma et al. 2012
	QCAZ 43422	JX155814	JX155841	Coloma et al. 2012
	QCAZ 45466	JX155813	JX155840	Coloma et al. 2012
H. hillisi sp. n.	QCAZ 68646	MH883792	MH883796	This study
	QCAZ 68647	–	MH883797	This study
	QCAZ 68648	MH883793	MH883798	This study
	QCAZ 68649	MH883794	MH883799	This study
	QCAZ 68651	MH883795	MH883800	This study
H. jahni	MHNLS 20318	MG596776	MG596776	Rojas-Runjaic et al. 2018
	MHNLS 20319	MG596777	MG596777	Rojas-Runjaic et al. 2018
	MHNLS 20324	MG596779	MG596779	Rojas-Runjaic et al. 2018
H. japreria	MHNLS 18888	MG596766	MG596766	Rojas-Runjaic et al. 2018
	MHNLS 19235	MG596769	MG596769	Rojas-Runjaic et al. 2018
	UIS-A 5496	MG596770	MG596770	Rojas-Runjaic et al. 2018
H. larinopygion	QCAZ 41826	JX155817	JX155844	Coloma et al. 2012
	QCAZ 45462	JX155818	JX155845	Coloma et al. 2012
H. lascinius	KU 181086	DQ380359	–	Wiens et al. 2006
	MHNLS 19163	MG596762	MG596762	Rojas-Runjaic et al. 2018
	MHNLS 19164	MG596763	MG596763	Rojas-Runjaic et al. 2018
H. lindae	QCAZ 41232	JX155821	JX155848	Coloma et al. 2012
	QCAZ 45342	JX155824	JX155851	Coloma et al. 2012
	QCAZ 45346	JX155822	JX155849	Coloma et al. 2012
	QCAZ 45463	JX155823	JX155850	Coloma et al. 2012
H. mashpi	MZUTI 614	KT279526	KT279511	Guayasamin et al. 2015
H. pacha	KU 202760	AY326057	AY326057	Darst and Cannatella 2004
	WED 53493	AY326057	AY326057	Darst and Cannatella 2004
H. palmeri	MZUTI 608	KT279549	KT279520	Guayasamin et al. 2015
	SIUC H-6924	AY843650	AY843650	Faivovich et al. 2005
H. pantostictus	QCAZ 45435	JX155820	JX155847	Coloma et al. 2012
	QCAZ 45438	JX155819	JX155846	Coloma et al. 2012
	KU 202732	AY326052	–	Darst and Cannatella 2004
H. phyllognathus	QCAZ 23938	JX155800	JX155827	Coloma et al. 2012
	QCAZ 32271	JX155802	JX155829	Coloma et al. 2012
	QCAZ 41032	JX155801	JX155828	Coloma et al. 2012
	KU 212119	DQ380369	–	Wiens et al. 2006
	MHNLS 20321	MG596772	MG596772	Rojas-Runjaic et al. 2018
	MHNLS 20325	MG596774	MG596774	Rojas-Runjaic et al. 2018
H. psarolaimus	QCAZ 42165	JX155806	JX155833	Coloma et al. 2012
	QCAZ 43654	JX155807	JX155834	Coloma et al. 2012
	QCAZ 27049	JX155808	JX155835	Coloma et al. 2012
	QCAZ 46095	JX155809	JX155836	Coloma et al. 2012
H. ptychodactylus	QCAZ 46030	JX155804	JX155831	Coloma et al. 2012
	QCAZ 46031	JX155805	JX155832	Coloma et al. 2012
H. simmonsi	KU 181167	DQ380376	–	Wiens et al. 2006
H. staufferorum	QCAZ 45962	JX155816	JX155843	Coloma et al. 2012
	QCAZ 45967	JX155815	JX155842	Coloma et al. 2012

Species	Museum Number	GenBank Accession Number		Source
		12S	16S	
H. tapichalaca	QCAZ 15083	JX155803	JX155830	Coloma et al. 2012
	QCAZ 16704	AY563625	AY563625	Faivovich et al. 2004
H. tigrinus	QCAZ 31550	JX155811	JX155838	Coloma et al. 2012
	QCAZ 41351	JX155810	JX155837	Coloma et al. 2012
Hyloscirtus sp.	MZUTI 3262	KT279503	KT279544	Guayasamin et al. 2015
	KU 202728	DQ380361	–	Wiens et al. 2006

Morphology

Specimens of the new species were compared to published descriptions and alcohol-preserved specimens of the *Hyloscirtus larinopygion* group from Museo de Zoología at Pontificia Universidad Católica del Ecuador, Quito (QCAZ). Examined specimens are listed as Appendix 1. Webbing formulae of hand and foot follow Savage and Heyer (1967) as modified by Myers and Duellman (1982). Morphological measurements were taken with digital calipers (± 0.01 mm) from specimens fixed in 10% formalin and preserved in 70% ethanol according to the methodology described in Duellman (1970). Measurements are: SVL (snout-vent length); HL (head length); HW (head width); ED (eye diameter); TD (tympanum diameter); TL (tibia length); FEL (femur length); and FL (foot length). Sex was determined by direct examination of gonads.

We also compared qualitative morphological characters between the new species and its closest relatives. Six characters were evaluated: (1) dorsal coloration; (2) ventral coloration; (3) marks on flanks and hidden surfaces of thighs; (4) iris coloration; (5) prepollex condition; and (6) in life, webbing coloration. Life coloration was obtained from color photographs.

Results

Phylogeny and genetic distances

According to PartitionFinder, the best partition strategy consisted of two partitions under model GTR + I + G. Maximum likelihood and Bayesian inference analyses resulted in similar topologies. Four species groups within *Hyloscirtus* (*H. jahni, H. bogotensis, H. armatus,* and *H. larinopygion* group) were recovered with strong support (posterior probability, pp = 1.0 and bootstrap = 100) in both analysis (Figure 1). However, phylogenetic relationships among these groups were weakly supported (pp < 0.71 and bootstrap < 50), as previously reported (Almendáriz et al. 2014; Coloma et al. 2012; Guayasamin et al. 2015; Rojas-Runjaic et al. 2018). The only exception was the strong support found for the clade *H. armatus* group + *H. larinopygion* group found in the Bayessian analysis (pp = 0.99). The phylogeny shows *Hyloscirtus hillisi* sp. n. sister to *Hyloscirtus* sp. + *H. tapichaca*. *Hyloscirtus* sp. (KU 202728) is an undescribed species previously referred as "*H. lindae*" (Almendáriz et al. 2014; Duellman and Hillis 1990).

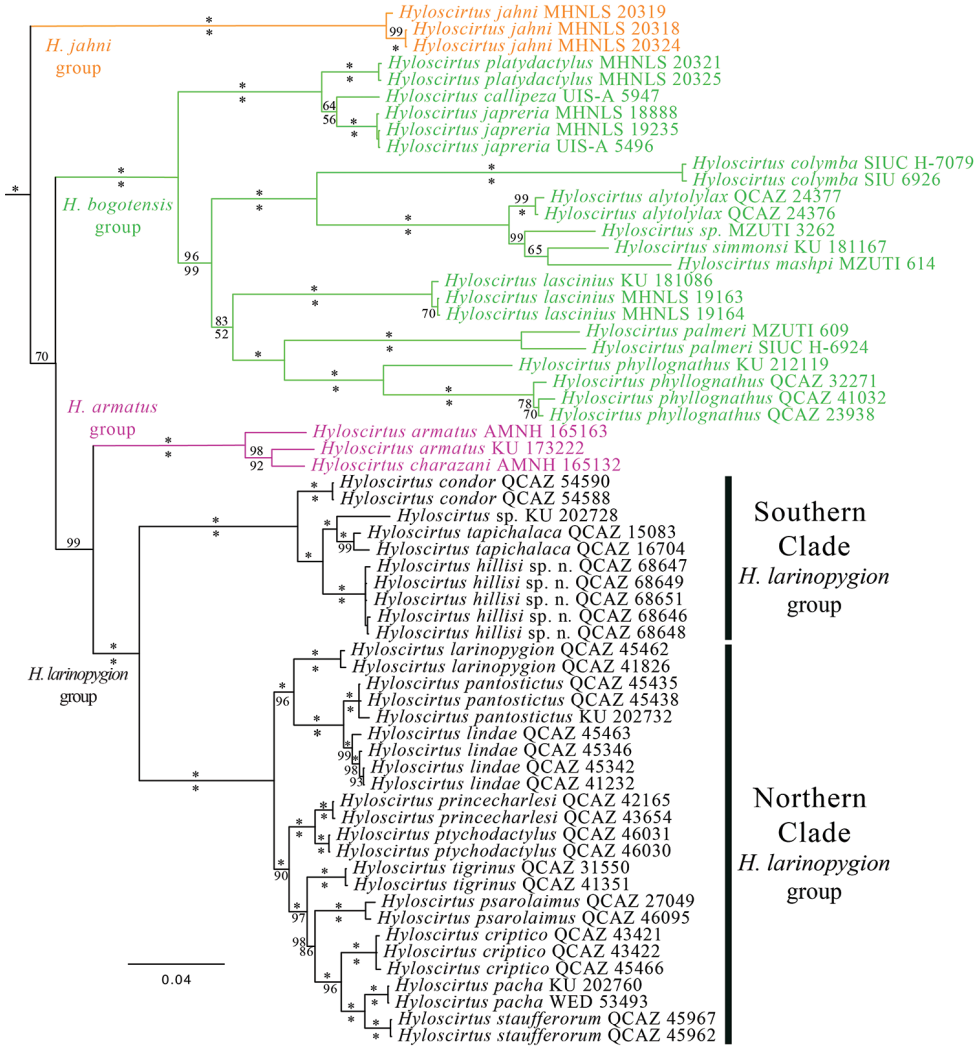

Figure 1. Strict consensus tree of *Hyloscirtus* species inferred with Bayesian inference. Museum numbers are shown for each sample. Bayesian posterior probabilities (pp × 100) are shown above the branches and bootstrap values below. Values of 100% are represented by an asterisk. Missing values indicate weakly supported nodes (pp and bootstrap < 50). Outgroup species are not shown. For locality data see Table 1 and Appendix 1.

Hyloscirtus condor is sister to a clade conformed by these three species. All together form a strongly supported clade distributed in the eastern slopes of the Andes of central and southern Ecuador and northern Peru (Southern Clade; Figs. 1, 2). The Southern Clade is sister to a clade distributed to the north and confirmed by the remaining species of the *Hyloscirtus larinopygion* group (Northern Clade; Figs. 1, 3). The Northern and Southern clades have a narrow zone of sympatry in central Ecuador (Figure 2).

Genetic distances between the new species and its closest relatives are characteristic of interspecific distances for the *H. larinopygion* group. For gene 12S, distances with

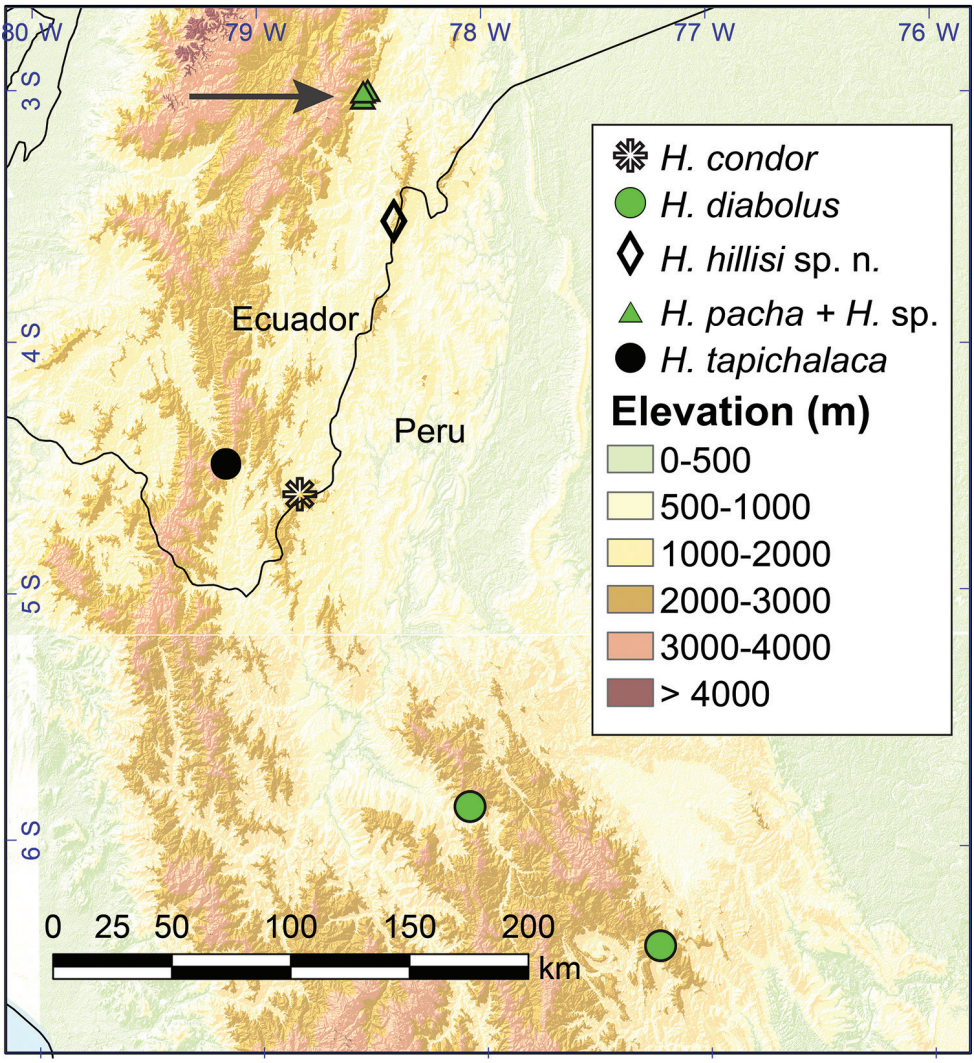

Figure 2. Records of the Southern Clade of the *Hyloscirtus larinopygion* group. Locality data were obtained from specimens deposited at Museo de Zoología, Pontificia Universidad Católica del Ecuador (QCAZ), Duellman and Hillis (1990), Almendáriz et al. (2014a), and Rivera-Correa et al. (2016). The arrow indicates the locality where the Northern and Southern clades are sympatric. See text for details.

H. tapichalaca are 0.031 to 0.038 and with *H.* sp. (KU 202728) are 0.031 to 0.033. These distances are higher than those observed for the same gene between *H. pacha* and *H. staufferorum* (0.014–0.018), *H. princecharlesi* and *H. ptychodactylus* (0.004–0.020) and *H. criptico* and *H. psarolaimus* (0.022–0.026; Almendáriz et al. 2014). Genetic distances for gene 16S range from 0.029 and 0.040 (Table 2). The genetic divergence between *H. hillisi* sp. n. and its closest relatives and its unique morphology indicates that it is a new species that we describe below.

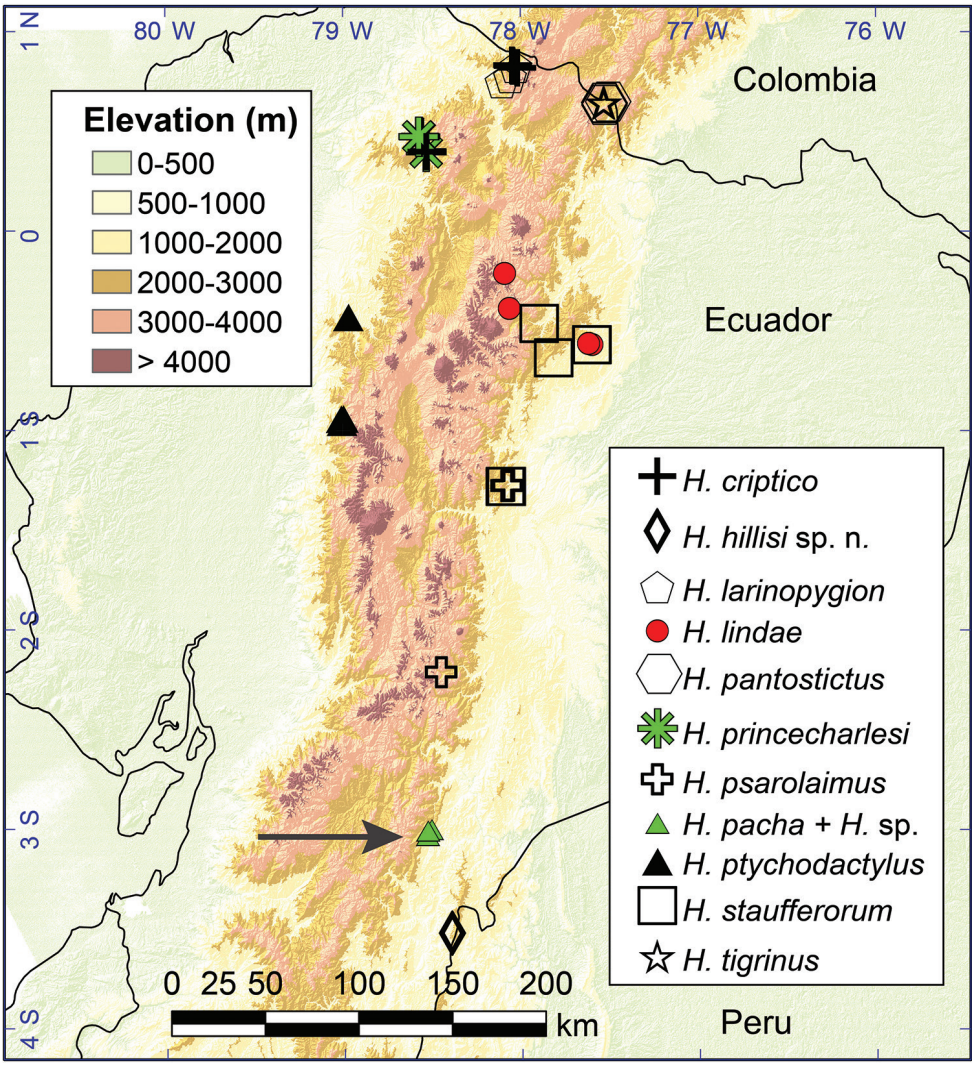

Figure 3. Records of the Northern Clade of the *Hyloscirtus larinopygion* group. Locality data were obtained from specimens deposited at Museo de Zoología, Pontificia Universidad Católica del Ecuador (QCAZ) and Duellman and Hillis (1990). The arrow indicates the locality where the Northern and Southern clades are sympatric. See text for details.

Table 2. Pairwise genetic distances (uncorrected-*p*) between *Hyloscirtus hillisi* sp. n. and its closest relatives, based on sequences of 16S mtDNA. Mean and ± standard deviation are given with range in parentheses. Diagonal values are intraspecific distances.

	***H. hillisi* sp. n. (*n* = 5)**	***H. tapichalaca* (*n* = 2)**	***H. condor* (*n* = 2)**
H. hillisi sp. n.	0.001 ± 0.0007 (0–0.002)	–	–
H. tapichalaca	0.029 ± 0.0005 (0.029–0.030)	0.009	–
H. condor	0.04 ± 0.0005 (0.039–0.040)	0.041 ± 0.002 (0.039–0.043)	0

***Hyloscirtus hillisi* sp. n.**
http://zoobank.org/95C54DD9-297E-471D-8E5F-2B96BE740147

Holotype. QCAZ 68649 (Figs. 5–7), field no. SC 59176, adult female from Ecuador, Provincia Morona Santiago, Caverns-cascade trail, Reserva Biológica El Quimi, on the slopes of flat-topped mountain on the eastern side of the Río Quimi valley (3.5190S, 78.3788W), 2128 m above sea level, collected by Diego Almeida, Darwin Núñez, Kunam Nucirquia, Alex Achig, and Ricardo Gavilanes on 8 July 2017.

Paratopotypes. QCAZ 68646, 72549 subadult females, 68651–54, 72552, tadpoles, 69001, metamorphs, 72550, 72553, adult males, 2112–2134 m of elevation. Collected on 7–14 July 2017 and 12–19 April 2018 by Diego Almeida, Darwin Núñez, Kunam Nucirquia, Alex Achig, Ricardo Gavilanes, and María del Mar Moretta.

Paratypes. All specimens from Reserva Biológica el Quimi, eastern side of the Río Quimi valley, Provincia Morona Santiago, Ecuador. Base camp surroundings, near Río Cristalino (3.5183S, 78.3914W), 1992 m, QCAZ 68647, juvenile, 68648, 68650, metamorphs, 68655–56, 71182, tadpoles collected on 4, 8–9 July 2017; second plateau, near limestone cave (3.5189S, 78.3815W), 2121 m, QCAZ 72551, adult male, collected on 19 April 2018. Collected by Diego Almeida, Darwin Núñez, Kunam Nucirquia, Alex Achig, and Ricardo Gavilanes.

Diagnosis. The diagnosis and comparisons are based on one adult female, three adult males, and two subadult females. The new species is diagnosed by the following characters: mean SVL 70.3 mm in adult males (range 66.7–72.3; n = 3), 65.8 mm in one adult female; vomerine odontophores conic-shaped with a gap medially, each process with three to five prominent teeth; supracloacal flap ill-defined; supratympanic fold present; finger webbing formula: I basal II2$^-$—3$^-$III2½—2IV, toe webbing formula: I2$^-$—2II1$^+$—2$^+$III1½—2½IV2½—1$^+$V; forelimbs hypertrophied in males; enlarged and curved prepollex protruding as a spine in both sexes; fleshy calcar absent; dorsum, flanks, and dorsal areas of limbs dark grayish brown with tiny orange marks varying from abundant to sparse; venter dark grayish brown; iris bronze or yellowish with dark brown reticulation.

Comparisons. *Hyloscirtus hillisi* is most similar to *H. condor*, *H. diabolus,* and *H. tapichalaca* (Figure 4). They share the presence of an enlarged claw-like prepollex. *Hyloscirtus condor* differs in ventral coloration (light gray to light salmon in *H. condor* vs. dark brown in *H. hillisi*) and dorsal coloration (brown dorsum with diffuse yellow speckling in *H. condor* vs. dark brown dorsum with contrasting orange round marks in *H. hillisi*). *Hyloscirtus diabolus* differs from *H. hillisi* by having a red iris (bronze or yellowish with brown reticulations in *H. hillisi*) and a fleshy calcar (calcar absent in *H. hillisi*; Rivera-Correa et al. 2016). *Hyloscirtus tapichalaca* differs from *H. hillisi* by having a brown dorsum without orange marks (orange marks present in *H. hillisi*) and white disks on fingers and toes (disks are dark brown in *H. hillisi*). The remaining species of the *H. larinopygion* group lack the enlarged claw-like prepollex (Ardila-Robayo et al. 1993; Mueses-Cisneros and Anganoy-Criollo 2008; Mueses-Cisneros and Perdomo-Castillo 2011; Ruiz-Carranza and Lynch 1982; Rivera-Correa et al. 2016).

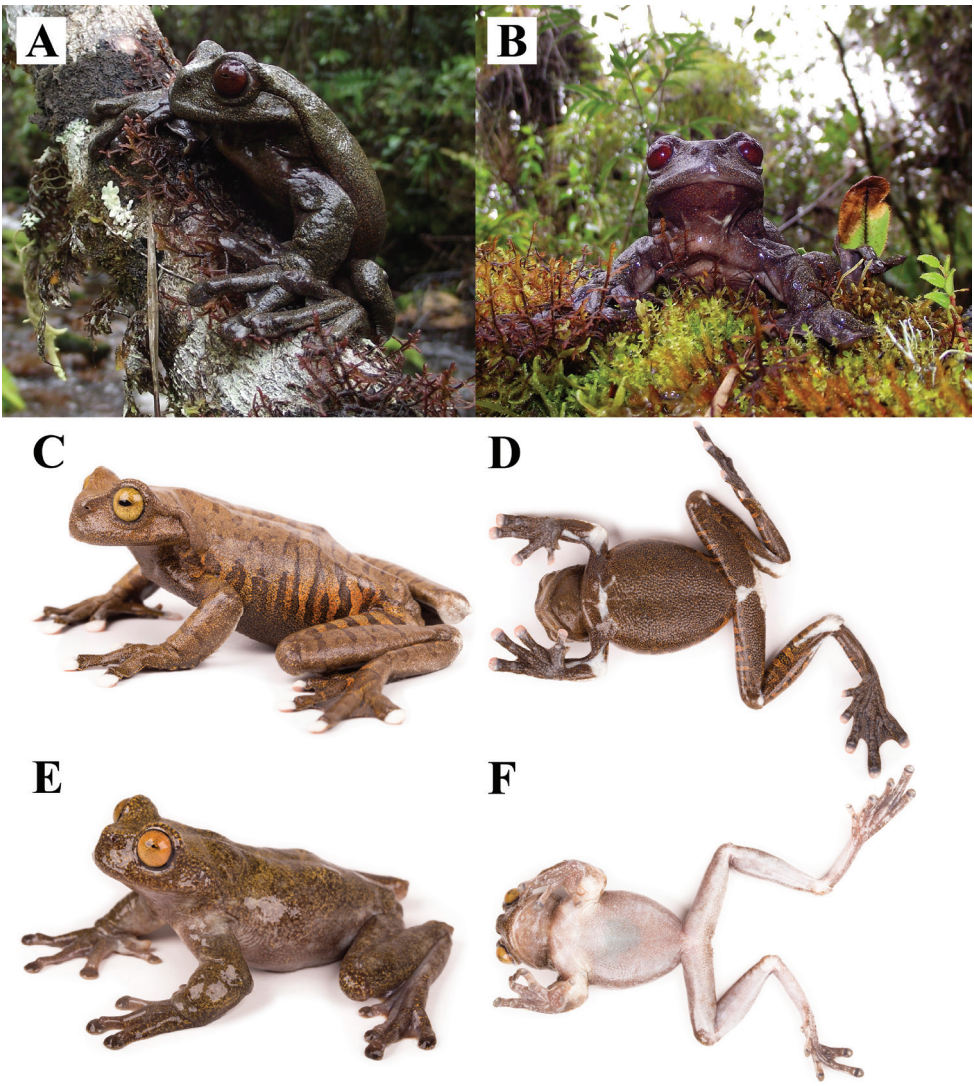

Figure 4. Live individuals of *Hyloscirtus*. **A, B** *Hyloscirtus diabolus* (CORBIDI 12885, adult male, holotype, SVL = 82.3 mm); **C, D** *H. tapichalaca* (QCAZ 63872, adult female, SVL = 76.19 mm); **E, F** *H. condor* (QCAZ 65237, adult male, SVL = 67.18 mm). Photographs: Karla García-Burneo, Diego Quirola, and Santiago Ron.

Description of the holotype. An adult female (Figs. 5–7), 65.78 mm SVL. Head round in dorsal view, wider than long; snout nearly truncate in lateral and dorsal views; distance from nostril to eye shorter than diameter of eye; canthus rostralis rounded; loreal region slightly concave; internarial region nearly flat; top of head slightly concave; nostrils slightly protruding anterolaterally; lips rounded, not flared; interorbital area

Figure 5. Variation in life of *Hyloscirtus hillisi* sp. n. from Reserva Biológica El Quimi. **A** QCAZ 68649 (adult female, holotype, SVL = 65.78 mm) **B** QCAZ 68646 (subadult female, SVL = 48.55 mm) **C** not collected.

slightly convex; eye large, protuberant; diameter of eye 1.85 times diameter of tympanic annulus; supratympanic fold thick, curved, covering posterodorsal edge of tympanum, extending from eye to posterior end of mandible and to shoulder; tympanum rounded; tympanic annulus distinct, rounded, separated from eye by ca. 1.43 times its diameter.

Forearms robust compared to upper arms but not hypertrophied; axillary membrane absent; ulnar tubercles absent; relative length of fingers I < II < IV < III; fingers bearing large, oval discs, wider than finger; subarticular tubercles prominent, round to ovoid, single; supernumerary tubercles present, small and rounded; thenar tubercle, elliptical; palmar tubercle round; prepollical tubercle large, elliptical; prepollex enlarged, claw shaped; webbing formula of fingers I basal II2^{-}—3^{-}III2½—2IV (Fig. 7).

Toes bearing discs broadly expanded, rounded and slightly smaller than those of fingers; relative length of toes I < II < III < V < IV; inner metatarsal tubercle large,

Figure 6. Variation of preserved specimens of *Hyloscirtus hillisi* sp. n. From left to right, first and second rows: QCAZ 68649 (holotype, adult female), QCAZ 68646 (subadult female); third and fourth rows: QCAZ 68647 (juvenile), QCAZ 69001**,** 68650, 68648 (metamorphs).

oval; outer metatarsal tubercle absent; subarticular tubercles single, round, large, and protuberant; supernumerary tubercles present; toes webbing formula I2^{-}—2II1^{+}—2^{+}III1½—2½IV2½—1^{+}V (Fig. 7).

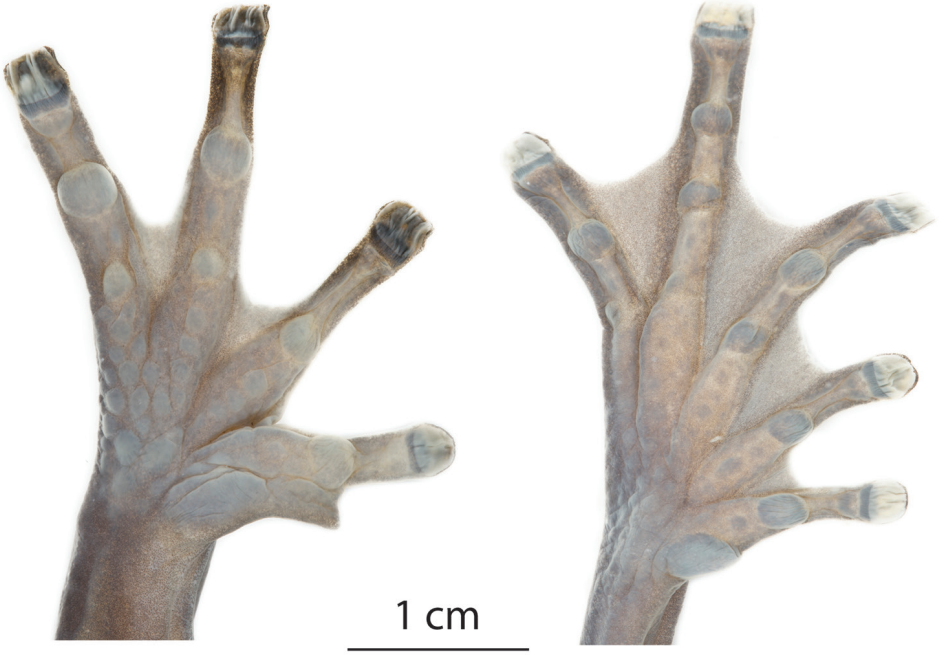

Figure 7. Ventral views of the left hand and foot of *Hyloscirtus hillisi* sp. n. Holotype (QCAZ 68649).

Skin on dorsum, flanks, dorsal surfaces of limbs, throat, chest, dorsal, and inner surfaces of thighs smooth; belly and ventral surfaces of thighs areolate, those of shanks smooth. Cloacal opening directed posteriorly at upper level of thighs, round tubercles below and of vent. Tongue slightly cordiform, widely attached to mouth floor; vomerine odontophores conic-shaped, separated medially, behind level of ovoid choana; each bearing 3–5 vomerine teeth. Additional measurements of the holotype are listed in Table 3.

Color of holotype in preservative. (Figure 6). Dorsal surfaces of head, body, and limbs, including fingers, dark grayish-brown densely stippled with minute, cream flecks. Ventral surfaces of limbs and belly grayish-brown, ventral surfaces of discs, webbing, chest, and throat paler.

Color of holotype in life. (Figure 5A). Based on digital photographs. Dorsal surfaces same as above except that flecks are bright orange. Ventral surfaces are dark grayish-brown. Ventral pads of digital discs on fingers and toes are gray. Iris is yellowish-cream.

Variation. Dorsal and ventral variation of preserved individuals is depicted in Figure 6. Morphometric variation is shown in Table 3. In preservative, dorsum varies from dark grayish-brown (e.g., QCAZ 68646) in adults to pale grayish-brown (e.g., QCAZ 68647, 68650) or pale gray (e.g., QCAZ 68648) in juveniles and metamorphs. Scattered minutes cream flecks can be present on dorsal surfaces (e.g., QCAZ 68646, 68647). Specimen QCAZ 68647 (juvenile) has cream transverse bars on the dorsal surfaces of the limbs (two to four on the forearm and five to seven on the thigh, shank, and foot). Ventral surfaces vary from pale grayish-brown (e.g., QCAZ 68646) to pale

Table 3. Descriptive statistics for measurements of *Hyloscirtus hillisi* sp. n. Abbreviations: SVL = snout-vent length; FL = foot length; HL = head length; HW = head width; ED = eye diameter; TD = tympanum diameter; TL = tibia length; FEL = femur length. All measurements in mm.

	Adult female (holotype)	Adult males (n = 3)	Subadult females (n = 2)	Juveniles (n = 1)
SVL	65.8	70.3 ± 3.1 (66.7–72.3)	48.6–56.8	40.2
FL	29.9	30.3 ± 0.1 (30.1–30.4)	21.4–27.6	17.6
HL	14.9	14.3 ± 2.7 (11.4–16.6)	11.9–12.9	9.4
HW	22.7	24.5 ± 0.9 (23.7–25.5)	18.4–20.5	13.1
ED	6.3	6.5 ± 0.1 (6.4–6.6)	5.1–5.2	5.4
TD	3.4	4.3 ± 0.2 (4.1–4.3)	2.9–3.2	2.1
TL	32.3	33.9 ± 0.6 (33.4–34.6)	25.6–28.1	21.2
FEL	35.2	35.9 ± 1.7 (34.3–37.7)	25.7–32.36	20.9

brown or cream (e.g., QCAZ 68648, 68650). Coloration of webbing and discs vary from dark grayish-brown to pale grayish-brown or gray.

In life, (Figure 5), the adult specimens are very similar to the holotype except for the density of bright orange flecks (bright yellow *in situ*; Figure 11A) on the dorsal surfaces. Background dorsal coloration in juveniles and metamorphs (Figure 8) varies from mottled or uniformly brown (e.g., SC 59268, QCAZ 68650) to light brown (e.g., QCAZ 68648) with or without orange-brown transversal bars on the dorsal surfaces of the limbs. Ventral surfaces vary from dark grayish-brown to cream (e.g., SC 59268). Iris varies from bronze (e.g., SC 59268) to yellowish-cream (e.g., QCAZ 68648).

Tadpole description. The following description is based on a tadpole of series QCAZ 68651 in Stage 25 (Gosner 1960). The specimen was collected in a slow-moving pool along the margins of a stream (Figure 9; 3.5187S, 78.3919W; 1991 m) at the type locality on 7 July 2017. All measurements are in mm. Total length 86.7; body length 29.1 (33.6% of total length). Body ovoid and depressed; width at the level of spiracle 19.2, height at same position 14.7; head width at level of the eyes 17.9; anterior margin of snout uniformly rounded in dorsal view and sloping at level of nares in lateral view; lateral-line system evident with supraorbital, infraorbital, mandibular, angular, postorbital, dorsal body, and ventral body lines. The arrangement of the lateral-line system is symmetrical; the supra and infra orbital lines begin at the tip of the snout and join behind the eye, continuing as a single longitudinal line extending along the anterior half of the tail. The dorsal lines extend along the posterior half of the dorsum until reaching the anterior edge of the tail, at the base of the upper fin. The angular line starts behind the orbit and extends longitudinally, contouring the spiracle, to the posterior end of the body, down towards the venter and ending at the base of the vent tube. The postorbital line starts behind the intersection of the supra and infraorbital lines and continues obliquely towards the venter, joining the anteroventral line. The mandibular line originates at the lateral border of the oral disc and runs obliquely until joining the anteroventral line. The posteroventral line forms a V whose vertex is directed towards the midposterior venter ending at the lateral edge of the venter, at the base of the spiracle. The nostrils are ovoid, not protruding and directed anterolaterally,

Figure 8. Color variation in life of juvenile and metamorphs of *Hyloscirtus hillisi* sp. n. **A** SC 59268 (SVL = 39.52 mm, not preserved) **B** QCAZ 68648 (SVL = 35.6 mm) **C** QCAZ 68650 (SVL = 40.73 mm).

6.8 from tip of snout; internarial distance 8.6. Eyes positioned and directed dorsolaterally; eye length 2.8, eye width 2.5; interorbital distance 9.9. Spiracle sinistral, located at midbody and oriented posterodorsally, inner wall free from body; tube length 2.8, tube width 2.6; spiracular opening directed posterodorsally, diameter 1.6; distance from tip of snout to spiracular opening 22.5. Vent tube medial, opening directed posteriorly; tube length 3.8, tube width 2.6. Tail length 57.5; caudal musculature robust, narrowing gradually until tail terminus. At tail-body junction, tail muscle width 9.6, tail muscle height 11.7; maximum height of tail 17.7. Oral disc located anteroventrally; transverse width 11.6; bordered by two rows of small and rounded papillae; upper jaw sheath forming an arch, unpigmented, transverse width including lateral processes 4.0 (34.4% of transverse width of oral disc); oral apparatus well preserved, showing complete teeth rows. Labial tooth row formula 8(8)/11(1). Only A-8 and P-1 have gaps. Tadpoles were gregarious and fled to the bottom of the pool when disturbed.

Color in preservative of tadpoles. In dorsal view, the body is gray, lighter on the tip of snout and towards the base of the tail, grayish cream belly, mouth cream; tail

Figure 9. Variation in life of tadpoles of *Hyloscirtus hillisi* sp. n. **A** QCAZ 68651 (photograph taken 5 days after capture on 19 July 2017) **B** QCAZ 71182 (photograph taken 16 days after capture, on 20 July 2017) **C** QCAZ 71182 (photograph taken 8 months and 4 days after capture on 08 March 2018). Note change in color between (**B**) and (**C**). Gosner Stage 25. Photographs by Gustavo Pazmiño.

musculature grayish cream with irregular gray spots, upper and lower fins transparent, light gray with irregular dark gray spots.

Color in life of tadpoles. In dorsal view, body brown, including head and snout; in lateral view body dark-brown. Small bronze dots concentrate in the anterior edge of the eye, become diffuse at level of the base of the spiracle. Venter cream, becoming darker medially as result of intestines being dimly visible; oral disc light brown becoming dark brown posteriorly. Iris bronze. Vent tube cream. Muscle tail light brown with gray irregular spots; lower fin transparent cream with a combination of brown and gray irregular spots; upper fin transparent light brown with light brown spots and few scattered dark gray spots. The brown coloration and the pattern of dark gray and brown spots in several individuals is maintained; however, an individual kept in captivity (QCAZ 71182) during 8 months presents an evident change in its coloration, becoming much clearer with a combination of light brown on the back and greenish brown on the flanks; muscles of tail light brown with gray spots; lower fin cream with brown spots, upper fin greenish cream becoming transparent in the distal third with dark brown spots. The differences in coloration after 8 months in captivity may be due to the effects of diet.

Figure 10. Oral disc of preserved tadpole of *Hyloscirtus hillisi* sp. n. QCAZ 68651, Gosner Stage 25. Photograph by Gustavo Pazmiño.

Tadpoles variation. Based on a series of five individuals in stage 25 and two in stages 37 and 40. Meristic variation of tadpoles in Stages 25–40 is shown in Table 4. Seven tadpoles in Stages 25–40 varied in total length, ranging from 57.4 to 101 mm; body length ranged from 20.4 to 34.2 mm; tail length ranged from 37.0 to 67.6 mm. Inter orbital distance from 6.27 to 10.43 mm. Labial tooth row formula varied from 8(8)/11(1) to 7(7)/12(1) (Figure 10).

Etymology. The specific name is a noun in the genitive case and is a patronym for David Hillis, an evolutionary biologist who has made significant contributions to the study of the evolution of amphibians and reptiles. During the 1980s, David Hillis carried out fieldwork in Ecuador that resulted in the discovery of three undescribed species of the *H. larinopygion* group. In 1990, in collaboration with WE Duellman, he published the first phylogeny for the *H. larinopygion* group using allozyme data (Duellman and Hillis 1990). Currently he is professor at the University of Texas in Austin.

Distribution and natural history. *Hyloscirtus hillisi* is only known from two nearby sites (airline distance = 1.7 km) on the slopes of a flattop limestone mountain in the Río Quimi basin, Provincia Zamora Chinchipe, at elevations between 1991 and 2134 m (Figure 2). Biogeographic region is Eastern Montane Forest according to Ron et al. (2018) classification. Vegetation at the type locality (Figure 11B, C) was dominated by shrubs (1.5 m tall) with sparse trees (10–15 m tall). The ground had cushioned consistency and was covered by roots and bare soil. Mosses and ground-bromeliads were abundant. This type of ground cover is locally known as *bamba*. Two adults and

Table 4. Measurements (in mm) of tadpoles of *Hyloscirtus hillisi* sp. n. Mean ± SD is given with range in parentheses. Abbreviations: TL (total length), BL (body length), TAL (tail length), TAL/TL (ratio tail length/total length), MHT (Maximum Height of Tail, including dorsal and ventral fins), IOD (inter orbital distance), WOD (transverse width of oral disc), WUJ (transverse width of upper jaw sheath, including lateral processes), WUJ/WOD (ratio width of upper jaw sheath/width of oral disc), TUW (tube transverse width), TUL (tube length spiracle).

Character	Stage 25 (*n* = 5)	Stage 37 (*n* = 1)	Stage 40 (*n* = 1)
TL	79.2 ± 12.4 (57.4–86.7)	99.5	101
BL	26.1 ± 3.6 (20.4–29.1)	34.2	33.4
TAL	53 ± 9.02 (37–58)	65.3	67.6
TAL/TL	0.7 ± 0.04 (0.6–0.7)	0.7	0.7
MHT	15.4 ± 1.7 (13.7–17.7)	19	19.4
IOD	8.4 ± 1.5 (6.3–9.9)	10.2	10.4
WOD	9.3 ± 1.7 (7–11.6)	11.7	11.7
WUJ	3.9 ± 0.1 (3.8–4)	5.2	5.5
WUJ/WOD	2.8 ± 0.4 (2.3–3.3)	2.2	2.1
TUW	1.9 ± 0.5 (1.4–2.6)	2.7	3.6
TUL	2.4 ± 0.4 (1.7–2.8)	3.2	4.3

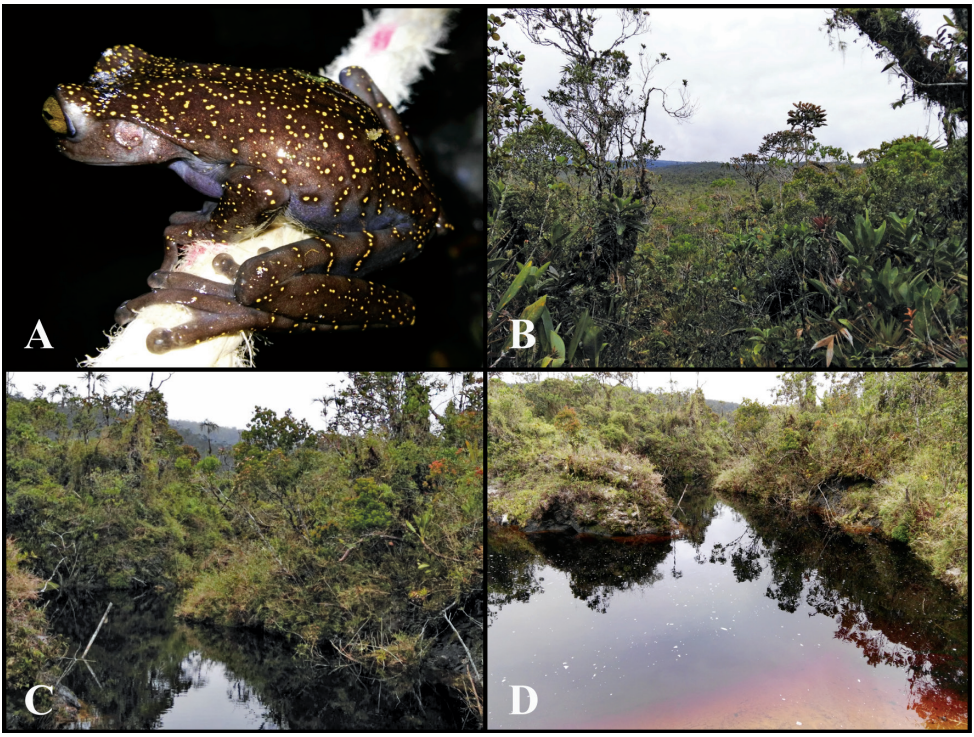

Figure 11. Habitat of *Hyloscirtus hillisi* sp. n. **A** *Hyloscirtus hillisi* sp. n. *in situ* **B** vegetation at the type locality, Reserva Biológica El Quimi, Ecuador **C** habitat where the adults were found **D** habitat where the tadpoles and metamorphs were found. Photographs by Diego Almeida.

one juvenile were found on shrubs next to small streams on the Río Cristalino basin, at an elevation of 2134 m. The tadpoles and juveniles were found in ponds on the margin of Río Cristalino, at an elevation of 1991 m (Figure 11D). Collections took place in July 2017 and April 2018. The site where the adults were collected is ~500 m from the border between Peru and Ecuador. Therefore, the occurrence of *H. hillisi* in Peru is almost certain.

Conservation status. *Hyloscirtus hillisi* is only known from two nearby sites in Cordillera del Cóndor. Population size is unknown, but the scant evidence suggests low abundances. In 2017, at the site where the tadpoles and juveniles were found, five hours of nocturnal search by five experienced herpetologists yielded no adults. At the site where the adults were found, ten hours of nocturnal search, for two nights, by two experienced herpetologists, yielded two adults and one subadult. Habitat destruction and fragmentation is evident at a distance of 3.5 km from one of the collection sites (according to Ministerio de Ambiente del Ecuador 2013 map). Cordillera del Cóndor is threatened by large and small-scale mining which has already affected amphibian populations (Valencia et al. 2017). Because of its small known distribution and nearby habitat destruction and mining activities, we suggest to assign *H. hillisi* to the Critically Endangered category under criteria B1a, b(iii), according to IUCN (2001) guidelines.

Discussion

Our phylogeny is consistent with previous phylogenies of *Hyloscirtus* (e.g., Almendáriz et al. 2014; Coloma et al. 2012; Faivovich et al. 2005; Rojas-Runjaic et al. 2018). The sister clade of the *H. larinopygion* group appears to be the *H. armatus* group (e.g., Rojas-Runjaic et al. 2018, Duellman et al. 2016, herein). A close relationship between the *H. armatus* group and *H. larinopygion* group is also supported by the shared presence of an enlarged prepollex protruding as a spine in the *H. armatus* group and in the Southern Clade of the *H. larinopygion* group. Under Duellman et al. (2016) topology, the absence of the spine in the Northern Clade would result from a secondary loss.

Hyloscirtus hillisi is the second species of the *Hyloscirtus larinopygion* group to be discovered in Cordillera del Cóndor, a sub-Andean mountain chain with unique geology. While the main Andes are composed of igneous and metamorphic rocks, Cordillera del Cóndor is composed predominantly by sedimentary rocks, specially limestone and sandstone (Neill 2005). Although much younger, Cordillera del Cóndor is geologically similar to the Tepuis in the Guianan region. Remarkably, surveys of the plant communities of Cordillera del Cóndor have recorded at least 10 genera that otherwise are endemic or nearly endemic to the Guianan Tepuis (Ulloa and Neill 2006).

The biogeographic affinity between the biotas of Cordillera del Cóndor and the Guianan Tepuis can be tested with phylogenies. Close relationships between biotas from El Cóndor and the Guianan Tepuis are expected under that biogeographic scenario. However, a review of recently published phylogenies is inconsistent with a Cón-

dor-Guianan link. Our phylogeny, for example, shows that both species of *Hyloscirtus* from el Cóndor are closely related to Andean species from southern Ecuador and northern Peru. Similar results are evident in *Pristimantis muranunka* (closely related to *Pristimantis* from the Andes of southern Ecuador; Brito et al. 2017), *Pristimantis yantzaza* (closely related to *Pristimantis* from the Andes and adjacent Amazonian lowlands of Peru and Ecuador; Valencia et al. 2017), *Excidobates condor* (closely related to *Excidobates* from Cordillera del Cóndor and adjacent Amazonian lowlands; Almendáriz et al. 2012), *Centrolene condor* (sister to a large clade of *Centrolene* with species from the Andes of Venezuela, Colombia, Ecuador and Peru; Castroviejo-Fisher et al. 2014), and *Chiasmocleis parkeri* (closely related to *Chiasmocleis* from the Amazonian lowlands; Almendáriz et al. 2017). The combined evidence indicates that the biogeographic link between Cordillera del Cóndor and the Tepui region is not discernable in amphibians.

We suspect that the difference in biogeographic pattern observed between plants and amphibians may result from differences in the ecological factors that influence their geographic distribution. In plants, a key factor is soil type (e.g., Clark et al. 1999). The similarity in soil type between Cordillera del Cóndor and the Tepui region (Neill 2005) may explain the biogeographic connection observed in plants. In amphibians, in contrast, edaphic conditions appear to be of minor importance explaining the lack of biogeographic affinity between both regions.

As result of its historic inaccessibility, the organismal diversity of Cordillera del Cóndor is poorly known. During the last two decades, after armed conflicts between Ecuador and Peru ended, roads began to be built and biodiversity surveys became more frequent. These surveys have revealed a large number of unknown species of amphibians, several of which have been recently described (e.g., Almendáriz et al. 2014; Almendáriz et al. 2017; Almendáriz et al. 2012; Almendáriz et al. 2014; Brito et al. 2017; Brito et al. 2014; Terán-Valdez and Guayasamín 2010; Valencia et al. 2017). Additional expeditions to Cordillera del Cóndor are likely to result in more discoveries since it remains largely unexplored.

Acknowledgments

Field and laboratory work in Ecuador were funded by grants from Secretaría Nacional de Educación Superior, Ciencia, Tecnología e Innovación (SENESCYT, Arca de Noé Initiative; Omar Torres and SRR principal investigators) and PUCE-DGA (SRR principal investigator). Ana Carrillo and Claudia Terán carried out laboratory work. Fernando Rojas-Runjaic provided early access to unpublished sequences of *Hyloscirtus*. Gustavo Pazmiño and Valeria Chasiluisa helped making photographs of preserved specimens. Karla García-Burneo provided photographs of *H. diabolus*. For field assistance we thank María del Mar Moretta, Darwin Núñez, Kunam Nucirquia, Alex Achig, and Ricardo Gavilanes. Ministerio de Ambiente del Ecuador issued collecting permit 003-17-IC-FAU-DNB/MA. The park rangers fro Ministerio de Ambiente del Ecuador, Morona Santiago Province, provided field assistance.

References

Almendáriz A, Brito J, Batallas D, Ron SR (2014) Una nueva especie de rana arbórea del género *Hyloscirtus* (Amphibia: Anura: Hylidae) de la Cordillera del Cóndor. Papeis Avulsos de Zoologia 54: 33–49. https://doi.org/10.1590/0031-1049.2014.54.04

Almendáriz A, Brito MJ, Batallas D, Vaca-Guerrero J, Ron SR (2017) Una especie nueva de rana del género *Chiasmocleis* (Microhylidae: Gastrophryninae) de la Cordillera del Cóndor, Ecuador. Papeis Avulsos de Zoologia 57: 119–136. https://doi.org/10.11606/0031-1049.2017.57.10

Almendáriz A, Ron SR, Brito J (2012) Una especie nueva de rana venenosa de altura del género *Excidobates* (Dendrobatoidea: Dendrobatidae) de la Cordillera del Cóndor). Papeis Avulsos de Zoologia (Sao Paulo) 52: 387–399. https://doi.org/10.1590/S0031-10492012021200001

Almendáriz A, Simmons JE, Brito J, Vaca-Guerrero J (2014) Overview of the herpetofauna of the unexplored Cordillera del Cóndor of Ecuador. Amphibian & Reptile Conservation 8: 45–64.

AmphibiaWeb (2018) AmphibiaWeb: information on amphibian biology and conservation. http://amphibiaweb.org/. University of California Berkeley.

Ardila-Robayo MC, Ruiz-Carranza PM, Roa-Trujillo SH (1993) Una nueva especie de *Hyla* del grupo *larinopygion* (Amphibia: Anura: Hylidae) del sur de la Cordillera Central de Colombia. Revista de la Academia Colombiana de Ciencias Exactas, Físicas y Naturales 18: 559–566.

Brito J, Almendáriz A, Batallas D, Ron SR (2017) Nueva especie de rana bromelícola del género *Pristimantis* (Amphibia: Craugastoridae), meseta de la cordillera del Cóndor, Ecuador. Papeis Avulsos de Zoologia (Sao Paulo) 57: 177–195. https://doi.org/10.11606/0031-1049.2017.57.15

Brito J, Batallas D, Velalcázar D (2014) Nueva especie de rana terrestre del género *Pristimantis* (Amphiibia: Craugastoridae), meseta de la cordillera del Cóndor. Papeis Avulsos de Zoologia (Sao Paulo) 54: 435–446. https://doi.org/10.1590/0031-1049.2014.54.30

Castroviejo-Fisher S, Guayasamin JM, Gonzalez-Voyer A, Vila C (2014) Neotropical diversification seen through glassfrogs. Journal of Biogeography 41: 66–80. https://doi.org/10.1111/jbi.12208

Clark DB, Palmer MW, Clark DA (1999) Edaphic factors and the landscape-scale distributions of tropical rain forest trees. Ecology 80: 2662–2675. https://doi.org/10.1890/0012-9658(1999)080[2662:EFATLS]2.0.CO;2

Coloma LA, Carvajal-Endara S, Dueñas JF, Paredes-Recalde A, Morales-Mite M, Almeida-Reinoso D, Tapia EE, Hutter CR, Toral E, Guayasamín JM (2012) Molecular phylogenetics of stream frogs of the *Hyloscirtus larinopygion* group (Anura: Hylidae), and description of two new species from Ecuador. Zootaxa 3364: 1–78.

Darst CR, Cannatella DC (2004) Novel relationships among hyloid frogs inferred from 12S and 16S mitochondrial DNA sequences. Molecular Phylogenetics and Evolution 31: 462–475. https://doi.org/10.1016/j.ympev.2003.09.003

Duellman WE (1970) Hylid frogs of Middle America. Monograph of the Museum of Natural History University of Kansas 1: 1–753.

Duellman WE, Hillis DM (1990) Systematics of frogs of the *Hyla larinopygion* group. Occasional Papers of the Museum of Natural History of the University of Kansas 134: 1–23.

Duellman WE, Marion AB, Hedges SB (2016) Phylogenetics, classification, and biogeography of the treefrogs (Amphibia: Anura: Arboranae). Zootaxa 4104: 1–109. https://doi.org/10.11646/zootaxa.4104.1.1

Elmer KR, Cannatella DC (2008) Three new species of leaflitter frogs from the upper Amazon forests: cryptic diversity within *Pristimantis* "*ockendeni*" (Anura: Strabomantidae) in Ecuador. Zootaxa 1784: 11–38.

Faivovich J, Garcia PC, Ananias F, Lanari L, Basso NG, Wheeler WC (2004) A molecular perspective on the phylogeny of the *Hyla pulchella* species group (Anura, Hylidae). Molecular Phylogenetics and Evolution 32: 938–950. https://doi.org/10.1016/j.ympev.2004.03.008

Faivovich J, Haddad CFB, Garcia PCA, Frost DR, Campbell JA, Wheeler WC (2005) Systematic review of th frog family Hylidae, with special reference to Hylinae: phylogenetic analysis and taxonomic revision. Bulletin of the American Museum of Natural History 294: 6–228. https://doi.org/10.1206/0003-0090(2005)294[0001:SROTFF]2.0.CO;2

Fouquet A, Gilles A, Vences M, Marty C, Blanc M, Gemmell NJ (2007) Underestimation of species richness in neotropical frogs revealed by mtDNA analyses. Plos Biology 2: e1109. https://doi.org/10.1371/journal.pone.0001109

Frost DR (2018) Amphibian Species of the World: an Online Reference. http://research.amnh.org/vz/herpetology/amphibia/ [accessed 06 March 2018]

Goebel AM, Donnelly MA, Atz M (1999) PCR primers and amplification methods for 12S ribosomal DNA, the control region, cytochrome oxidase I, and cytochrome b in bufonids and other frogs, and an overview of PCR rimers which have amplified DNA in amphibians successfully. Molecular Phylogenetics and Evolution 11: 163–199. https://doi.org/10.1006/mpev.1998.0538

Gosner KL (1960) A simplified table for staging anuran embryos and larvae with notes on identification. Herpetologica 16: 183–190.

Guayasamin JM, Rivera-Correa M, Arteaga A, Culebras J, Bustamante L, Pyron RA, Peñafiel N, Morochz C, Hutter CR (2015) Molecular phylogeny of stream treefrogs (Hylidae: *Hyloscirtus bogotensis* group), with a new species from the Andes of Ecuador. Neotropical Biodiversity 1: 2–21. https://www.doi.org/10.1080/23766808.2015.1074407

Hedges SB, Duellman WE, Heinicke MP (2008) New World direct-developing frogs (Anura: Terrana): molecular phylogeny, classification, biogeography, and conservation. Zootaxa 1737: 1–181.

Heinicke MP, Duellman WE, Hedges SB (2007) Major Caribbean and Central American frog faunas originated by ancient oceanic dispersal. Proceedings of the National Academy of Sciences of the United States of America 104: 10092–10097. https://doi.org/10.1073/pnas.0611051104

Heinicke MP, Duellman WE, Trueb L, Means DB, MacCulloch RD, Hedges B (2009) A new frog family (Anura: Terrarana) from South America and an expanded direct-developing clade revealed by molecular phylogeny. Zootaxa 2211: 1–35.

IUCN (2001) Red list categories: version 3.1. UICN Species Survival Comission, Gland.

Janzen DH, Hallwachs W (2011) Joining inventory by parataxonomists with DNA barcoding of a large complex tropical conserved wildland in northwestern Costa Rica. PLoS One 6: e18123.

Katoh K, Standley DM (2013) MAFFT multiple sequence alignment software version 7: improvements in performance and usability. Molecular Biology and Evolution 30: 772–780. https://doi.org/10.1093/molbev/mst010

Kearse M, Moir R, Wilson A, Stones-Havas S, Cheung M, Sturrock S, Buxton S, Cooper A, Markowitz S, Duran C, Thierer T, Ashton B, Meintjes P, Drummond A (2012) Geneious Basic: an integrated and extendable desktop software platform for the organization and analysis of sequence data. Bioinformatics 28: 1647–1649. https://doi.org/10.1093/bioinformatics/bts199

Kizirian D, Coloma LA, Paredes-Recalde A (2003) A new treefrog (Hylidae: *Hyla*) from southern Ecuador and a description of its antipredator behavior. Herpetologica 59: 339–349. https://doi.org/10.1655/02-41

Lanfear R, Calcott B, Ho SYW, Guindon S (2012) PartitionFinder: combined selection of partitioning schemes and substitution models for phylogenetic analyses. Molecular Biology and Evolution 29: 1695–1701. https://doi.org/10.1093/molbev/mss020

Maddison WP, Maddison DR (2018) Mesquite: a modular system for evolutionary analysis. Version 3.04. http://mesquiteproject.org [accessed June 08 2015]

Miller MA, Pfeiffer W, Schwartz T (2010) Creating the CIPRES science gateway for inference of large phylogenetic trees. 2010 Gateway Computing Environments Workshop (GCE), 8 pp. https://doi.org/10.1109/GCE.2010.5676129

Ministerio de Ambiente del Ecuador (2013) Sistema de Clasificación de los Ecosistemas del Ecuador Continental. Subsecretaría de Patrimonio Natural, Quito.

Mueses-Cisneros JJ, Anganoy-Criollo MA (2008) Una nueva especie del grupo *Hyloscirtus larinopygion* (Amphibia: Anura: Hylidae) del Suroccidente de Colombia. Papeis Avulsos de Zoologia (Sao Paulo) 48: 129–138. https://doi.org/10.1590/S0031-10492008001500001

Mueses-Cisneros JJ, Perdomo-Castillo IV (2011) *Hyloscirtus tigrinus* Mueses-Cisneros y Anganoy-Criollo, 2008: una especie amenazada, con comentarios sobre su distribución geográfica e historia natural. Herpetotropicos 5: 93–103.

Myers CW, Duellman WE (1982) A new species of *Hyla* from Cerro Colorado, and other tree frog records and geographical notes from Western Panama. American Museum Novitates 2752: 1–32.

Neill D (2005) Cordillera del Cóndor: botanical treasures between the Andes and the Amazon. PlantTalk 41: 17–21.

Peters WCH (1882) Der namen der Batrachiergattung Hylonomus in Hyloscirtus zu Ändern und legte zwei neue Arten von Schlangen, Microsoma notatum und Liophis Ygraecum. Sitzungsberichte der Gesellschaft Naturforschender Freunde zu Berlin 1882: 127–129. https://doi.org/10.5962/bhl.part.15223

Rambaut A, Drummond AJ (2007) Tracer v1.4. University of Edinburgh. http://beast.bio.ed.ac.uk/Tracer

Rivera-Correa M, García-Burneo K, Grant T (2016) A new red-eyed of stream frog of *Hyloscirtus* (Anura: Hylidae) from Peru, with comments on the taxonomy of the genus. Zootaxa 4061: 29–40. https://doi.org/10.11646/zootaxa.4061.1.3

Rojas-Runjaic JM, Infante-Rivero EE, Salerno PE, Meza-Joya FL (2018) A new species of *Hyloscirtus* (Anura, Hylidae) from the Colombian and Venezuelan slopes of Sierra de Perijá, and the phylogenetic position of *Hyloscirtus jahni* (Rivero, 1961). Zootaxa 4382: 121–146. https://doi.org/10.11646/zootaxa.4382.1.4

Ron SR, Merino-Viteri A, Ortiz DA (2018) Anfibios del Ecuador. Version 2018.0. https://bioweb.bio/faunaweb/amphibiaweb/ [accessed March 8, 2018]

Ronquist F, Teslenko M, van der Mark P, Ayres DL, Darling A, Höhna S, Larget B, Liu L, Suchard MA, Huelsenbeck JP (2012) MrBayes 3.2: efficient bayesian phylogentic inference and model choice across a large model space. Systematic Biology 61: 539–542. https://doi.org/10.1093/sysbio/sys029

Ruiz-Carranza PM, Lynch JD (1982) Dos nuevas especies de *Hyla* (Amphibia: Anura) de Colombia, con aportes al conocimiento de *Hyla bogotensis*. Caldasia 13: 647–671.

Sambrook J, Fritsch EF, Maniatis T (1989) Molecular Cloning: a Laboratory Manual. Cold Spring Harbor Laboratory Press, New York.

Savage JM, Heyer WR (1967) Variation and distribution on the tree-frog genus *Phyllomedusa* in Costa Rica, Central America. Beiträge zur Neotropischen Fauna 2: 111–131. https://doi.org/10.1080/01650526709360400

Tamura K, Peterson D, Peterson N, Stecher G, Nei M, Kumar S (2011) MEGA5: molecular evolutionary genetics analysis using maximum likelihood, evolutionary distance, and maximum parsimony methods. Molecular Biology and Evolution 28: 2731–2739. https://doi.org/10.1093/molbev/msr121

Terán-Valdez A, Guayasamín JM (2010) The smallest terrestrial vertebrate of Ecuador: A new frog of the genus *Pristimantis* (Amphibia: Strabomantidae) from the Cordillera del Cóndor. Zootaxa 2447: 53–68.

Ulloa C, Neill D (2006) *Phainantha shuariorum* (Melastomataceae), una especie nueva de la Cordillera del Cóndor, Ecuador, disyunta de un género guayanés. Novon 16: 281–285. https://doi.org/10.3417/1055-3177(2006)16[281:PSMUEN]2.0.CO;2

Valencia JH, Dueñas MR, Székely P, Batallas D, Pulluquitín F, Ron SR (2017) A new species of direct-developing frog of the genus *Pristimantis* (Anura: Terrarana: Craugastoridae) from Cordillera del Cóndor, Ecuador, with comments on threats to the anuran fauna in the region. Zootaxa 4353: 447–466. https://doi.org/10.11646/zootaxa.4353.3.3

Vieites DR, Wollenberg KC, Andreone F, Kohler J, Glaw F, Vences M (2009) Vast underestimation of Madagascar's biodiversity evidenced by an integrative amphibian inventory. Proceedings of the National Academy of Sciences of the United States of America 106: 8267–8272. https://doi.org/10.1073/pnas.0810821106

Wiens JJ, Fetzner JW, Parkinson CL, Reeder TW (2005) Hylid frog phylogeny and sampling strategies for speciose clades. Systematic Biology 54: 778–807. https://doi.org/10.1080/10635150500234625

Wiens JJ, Graham CH, Moen DS, Smith SA, Reeder TW (2006) Evolutionary and ecological causes of the latitudinal diversity gradient in hylid frogs: treefrog trees unearth the roots of high tropical diversity. American Naturalist 168: 579–596. https://doi.org/10.1086/507882

Zwickl DL (2006) Genetic algorithm approaches for the phylogenetic analysis of large biological sequence dataset under the maximum likelihood criterion. PhD Thesis, University of Texas, Austin.

Appendix 1

Examined specimens. All specimens were collected in Ecuador and are deposited at the Museum of Zoology, Pontificia Universidad Católica del Ecuador (QCAZ).

Species	Museum Number	Province	Locality
Hyloscirtus condor	QCAZ 65235	Zamora Chinchipe	Reserva Biológica Cerro Plateado, 2200 m; 4.6045S, 78.8227W
H. condor	QCAZ 65236	Zamora Chinchipe	Reserva Biológica Cerro Plateado, 2243 m; 4.6044S, 78.8226W
H. condor	QCAZ 65237	Zamora Chinchipe	Reserva Biológica Cerro Plateado, 2219 m; 4.6044S, 78.8238W
H. condor	QCAZ 65240	Zamora Chinchipe	Reserva Biológica Cerro Plateado, 2320 m; 4.6050S, 78.8166W
H. condor	QCAZ 65241	Zamora Chinchipe	Reserva Biológica Cerro Plateado, 2320 m; 4.6050S, 78.8166W
H. criptico	QCAZ 4161	Carchi	22 km E Maldonado, Maldonado-Tulcán Road, 2560 m; 0.8301N, 78.0456W
H. criptico	QCAZ 4168	Carchi	22 km E Maldonado, Maldonado-Tulcán Road, 2560 m; 0.8301N, 78.0456W
H. criptico	QCAZ 4169	Carchi	22 km E Maldonado, Maldonado-Tulcán Road, 2560 m; 0.8301N, 78.0456W
H. criptico	QCAZ 4170	Carchi	22 km E Maldonado, Maldonado-Tulcán Road, 2560 m; 0.8301N, 78.0456W
H. criptico	QCAZ 10487	Imbabura	Cuellaje, 1813 m; 0.4N, 78.525W
H. criptico	QCAZ 11989	Carchi	22 km E Maldonado, Maldonado-Tulcán Road, 2560 m; 0.8260N, 78.0420W
H. criptico	QCAZ 41467	Imbabura	Seis de Julio de Cuellaje, 2800 m; 0.3968N, 78.5273W
H. criptico	QCAZ 42149	Imbabura	Cuellaje, San Antonio, Reserva Ecológica Cotacachi Cayapas, 2720 m; 0.4775N, 78.5626W
H. criptico	QCAZ 42150	Imbabura	Cuellaje, San Antonio, Reserva Ecológica Cotacachi Cayapas, 2720 m; 0.4775N, 78.5626W
H. criptico	QCAZ 42152	Imbabura	Cuellaje, San Antonio, Reserva Ecológica Cotacachi Cayapas, 2720 m; 0.4775N, 78.5626W
H. criptico	QCAZ 42153	Imbabura	Cuellaje, San Antonio, Reserva Ecológica Cotacachi Cayapas, 2720 m; 0.4775N, 78.5626W
H. criptico	QCAZ 42156	Imbabura	Cuellaje, San Antonio, Reserva Ecológica Cotacachi Cayapas, 2720 m; 0.4775N, 78.5626W
H. criptico	QCAZ 42157	Imbabura	Cuellaje, San Antonio, Reserva Ecológica Cotacachi Cayapas, 2720 m; 0.4775N, 78.5626W
H. criptico	QCAZ 42168	Imbabura	Cuellaje, San Antonio, Reserva Ecológica Cotacachi Cayapas, 2720 m; 0.4775N, 78.5626W
H. criptico	QCAZ 43421	Imbabura	Cuellaje, San Antonio, Reserva Ecológica Cotacachi Cayapas, 2560 m; 0.4747N, 78.5550W
H. criptico	QCAZ 43422	Imbabura	Cuellaje, San Antonio, Reserva Ecológica Cotacachi Cayapas, 2560 m; 0.4747N, 78.5550W
H. criptico	QCAZ 43500	Imbabura	Cuellaje, San Antonio, Reserva Ecológica Cotacachi Cayapas, 2794 m; 0.4732N, 78.5702W
H. criptico	QCAZ 43503	Imbabura	Cuellaje, San Antonio, Reserva Ecológica Cotacachi Cayapas, 2830 m; 0.4758N, 78.5679W
H. criptico	QCAZ 43516	Imbabura	Cuellaje, San Antonio, 2760 m; 0.4724N, 78.5660W
H. criptico	QCAZ 43517	Imbabura	Cuellaje, San Antonio, 2760 m; 0.4724N, 78.5660W
H. criptico	QCAZ 43518	Imbabura	Cuellaje, San Antonio, 2765 m; 0.4724N, 78.5660W
H. criptico	QCAZ 43528	Imbabura	Cuellaje, San Antonio, 2885 m; 0.4724N, 78.5660W
H. criptico	QCAZ 44894	Imbabura	Cuellaje, San Antonio, Reserva Ecológica Cotacachi Cayapas, 2720 m; 0.4775N, 78.5626W
H. criptico	QCAZ 44895	Imbabura	Cuellaje, San Antonio, Reserva Ecológica Cotacachi Cayapas, 2720 m; 0.4775N, 78.5626W

Species	Museum Number	Province	Locality
H. criptico	QCAZ 45466	Carchi	Tulcán-Maldonado Road, Quebrada Centella, 2806 m; 0.8179N, 78.016W
H. criptico	QCAZ 50320	Imbabura	Seis de Julio de Cuellaje, 1858 m; 0.3968N, 78.5273W
H. criptico	QCAZ 57951	Imbabura	Cuellaje, San Antonio, Reserva Ecológica Cotacachi Cayapas, 2720 m; 0.4775N, 78.5626W
H. criptico	QCAZ 57952	Imbabura	Cuellaje, San Antonio, Reserva Ecológica Cotacachi Cayapas, 2720 m; 0.4775N, 78.5626W
H. larinopygion	QCAZ 29211	Carchi	24 km Maldonado, Tulcán Road, 2664 m; 0.8231N, 78.0253W
H. larinopygion	QCAZ 29212	Carchi	24 km Maldonado, Tulcán Road, 2664 m; 0.8231N, 78.0253W
H. larinopygion	QCAZ 38418	Carchi	Cerro Centella, Tulcán-Maldonado Road, 2788 m; 0.8143N, 78.0149W
H. larinopygion	QCAZ 41826	Carchi	Cañón de Morán, 2452 m; 0.7467N, 78.1038W
H. larinopygion	QCAZ 45462	Carchi	Tulcán-Tufiño-Maldonado Road, Quebrada Centella, 2806 m; 0.8179N, 78.0160W
H. larinopygion	QCAZ 55574	Carchi	Morán, 2800 m; 0.7729N, 78.0559W
H. larinopygion	QCAZ 55575	Carchi	Morán, 2800 m; 0.7729N, 78.0559W
H. lindae	QCAZ 7593	Napo	10 Km E Oyacachi, 2510 m; 0.2322S, 78.0072W
H. lindae	QCAZ 10483	Napo	Oyacachi, 3217 m; 0.2128S, 78.0876W
H. lindae	QCAZ 41232	Napo	Pacto Sumaco, Parque Nacional Sumaco, 2479 m; 0.5696S, 77.5941W
H. lindae	QCAZ 41294	Napo	Pacto Sumaco, Pabayacu, 2775 m; 0.5639S, 77.6154W
H. lindae	QCAZ 41295	Napo	Pacto Sumaco, Pabayacu, 2775 m; 0.5639S, 77.6154W
H. lindae	QCAZ 41296	Napo	Pacto Sumaco, Pabayacu, 2775 m; 0.5639S, 77.6154W
H. lindae	QCAZ 41297	Napo	Pacto Sumaco, Pabayacu, 2775 m; 0.5639S, 77.6154W
H. lindae	QCAZ 41298	Napo	Pacto Sumaco, Pabayacu, 2775 m; 0.5639S, 77.6154W
H. lindae	QCAZ 45342	Napo	11-12 km E Papallacta, 2700 m; 0.3884S, 78.0605W
H. lindae	QCAZ 45345	Napo	Papallacta, Papallacta-Cuyuja Road, 2600 m; 0.3884S, 78.0605W
H. lindae	QCAZ 45346	Napo	Papallacta, Papallacta-Cuyuja Road, 2600 m; 0.3884S, 78.0605W
H. lindae	QCAZ 45463	Sucumbíos	11 km S Santa Bárbara, La Bonita Road, 2341 m; 0.6159N, 77.4879W
H. pacha	QCAZ 10489	Morona Santiago	Gualaceo-Limón Road, 2120 m; 3.0310S, 78.5270W
H. pacha	QCAZ 48237	Morona Santiago	Plan de Milagro, 8 km Plan de Milagro, 2152 m; 3.0011S, 78.5052W
H. pacha	QCAZ 48238	Morona Santiago	Plan de Milagro, 9 km Plan de Milagro, 2300 m; 3.0079S, 78.5253W
H. pacha	QCAZ 48239	Morona Santiago	Plan de Milagro, 9 km Cuenca Road, 2300 m; 3.0079S, 78.5253W
H. pacha	QCAZ 48240	Morona Santiago	Plan de Milagro, 9 km Cuenca Road, 2300 m; 3.0079S, 78.5253W
H. pacha	QCAZ 48241	Morona Santiago	Plan de Milagro, 9 km Plan de Milagro, 2300 m; 3.0079S, 78.5253W
H. pacha	QCAZ 57944	Morona Santiago	Limón Indanza, 2300 m; 3.0079S, 78.5253W
H. pantostictus	QCAZ 731	Sucumbíos	3.5 km Santa Bárbara-La Bonita Road, 2690 m; 0.6490N, 77.5040W
H. pantostictus	QCAZ 2721	Sucumbíos	6.1 km Santa Bárbara-La Bonita Road, 2760 m; 0.6410N, 77.4989W
H. pantostictus	QCAZ 3753	Sucumbíos	Santa Bárbara, 2656 m; 0.6437N, 77.5257W
H. pantostictus	QCAZ 4505	Sucumbíos	Santa Bárbara, 2656 m; 0.6437N, 77.5257W
H. pantostictus	QCAZ 4506	Sucumbíos	Santa Bárbara, 2656 m; 0.6437N, 77.5257W
H. pantostictus	QCAZ 6596	Sucumbíos	Santa Bárbara, 2710 m; 0.6437N, 77.5257W

Species	Museum Number	Province	Locality
H. pantostictus	QCAZ 10661	Sucumbíos	Santa Bárbara, 2700 m; 0.64373N, 77.5257W
H. pantostictus	QCAZ 10671	Sucumbíos	Santa Bárbara, 2700 m; 0.6437N, 77.5257W
H. pantostictus	QCAZ 11660	Sucumbíos	Santa Bárbara, 2656 m; 0.6437N, 77.5257W
H. pantostictus	QCAZ 11661	Sucumbíos	Santa Bárbara, 2656 m; 0.6437N, 77.5257W
H. pantostictus	QCAZ 11662	Sucumbíos	Santa Bárbara, 2656 m; 0.6437N, 77.5257W
H. pantostictus	QCAZ 11663	Sucumbíos	Santa Bárbara, 2656 m; 0.6437N, 77.5257W
H. pantostictus	QCAZ 11664	Sucumbíos	Santa Bárbara, 2656 m; 0.6437N, 77.5257W
H. pantostictus	QCAZ 11665	Sucumbíos	Santa Bárbara, 2656 m; 0.6437N, 77.5257W
H. pantostictus	QCAZ 11666	Sucumbíos	Santa Bárbara, 2656 m; 0.6437N, 77.5257W
H. pantostictus	QCAZ 11667	Sucumbíos	Santa Bárbara, 2656 m; 0.6437N, 77.5257W
H. pantostictus	QCAZ 12171	Sucumbíos	Santa Bárbara, 2800 m; 0.6437N, 77.5257W
H. pantostictus	QCAZ 14084	Sucumbíos	Santa Bárbara, 2710 m; 0.6415N, 77.5218W
H. pantostictus	QCAZ 30529	Sucumbíos	Santa Bárbara, 2656 m; 0.6437N, 77.5257W
H. pantostictus	QCAZ 30530	Sucumbíos	Santa Bárbara, 2656 m; 0.6437N, 77.5257W
H. pantostictus	QCAZ 30531	Sucumbíos	Santa Bárbara, 2656 m; 0.6437N, 77.5257W
H. pantostictus	QCAZ 42350	Sucumbíos	Santa Bárbara, 2709 m; 0.6445N, 77.5228W
H. pantostictus	QCAZ 45435	Sucumbíos	Santa Bárbara, 2709 m; 0.6444N, 77.5522W
H. pantostictus	QCAZ 45438	Sucumbíos	Santa Bárbara, 2656 m; 0.6437N, 77.5257W
H. pantostictus	QCAZ 45440	Sucumbíos	Santa Bárbara, 2586 m; 0.6436N, 77.5323W
H. pantostictus	QCAZ 45449	Sucumbíos	Santa Bárbara, Quebrada Santa Bárbara, La Bonita, 2341 m; 0.6159N, 77.4879W
H. pantostictus	QCAZ 46587	Sucumbíos	3 km Santa Bárbara, 2600 m; 0.6328N, 77.5231W
H. pantostictus	QCAZ 46588	Sucumbíos	3 km Santa Bárbara, 2600 m; 0.6328N, 77.5231W
H. princecharlesi	QCAZ 41465	Imbabura	Seis de Julio de Cuellaje, 2800 m; 0.3968N, 78.5273W
H. princecharlesi	QCAZ 41466	Imbabura	Seis de Julio de Cuellaje, 2800 m; 0.3968N, 78.5273W
H. princecharlesi	QCAZ 42165	Imbabura	Cuellaje, San Antonio, 2720 m; 0.4775N, 78.5626W
H. princecharlesi	QCAZ 43654	Imbabura	Cuellaje, San Antonio, 2760 m; 0.4724N, 78.5660W
H. princecharlesi	QCAZ 44893	Imbabura	Cuellaje, San Antonio, Reserva Ecológica Cotacachi Cayapas, 2794 m; 0.4732N, 78.5702W
H. psarolaimus	QCAZ 13252	Napo	11 km SE Papallacta, 2800 m; 0.3870S, 78.0600W
H. psarolaimus	QCAZ 27049	Sucumbíos	Santa Bárbara, 0.8 km Julio Andrade Road, 2600 m; 0.6422N, 77.5264W
H. psarolaimus	QCAZ 31671	Morona Santiago	San Vicente, Parque Nacional Sangay, 15 km Lagunas de Atillo, 2815 m; 2.2102S, 78.4487W
H. psarolaimus	QCAZ 46095	Napo	60 km E Salcedo, 2748 m; 0.9709S, 78.2413W
H. psarolaimus	QCAZ 46096	Napo	60 km E Salcedo, 2748 m; 0.9709S, 78.2413W
H. psarolaimus	QCAZ 46097	Napo	60 km E Salcedo, 2748 m; 0.9709S, 78.2413W
H. psarolaimus	QCAZ 46098	Napo	60 km E Salcedo, 2748 m; 0.9709S, 78.2413W
H. pantostictus	QCAZ 46808	Sucumbíos	Santa Bárbara, El Corazón, 2670 m; 0.6437N, 77.5321W
H. pantostictus	QCAZ 46811	Sucumbíos	Santa Bárbara, 2589 m; 0.6437N, 77.5321W
H. psarolaimus	QCAZ 46890	Napo	Salcedo-Tena Road, km 60, 2748 m; 0.9719S, 78.2413W
H. pantostictus	QCAZ 46894	Sucumbíos	Santa Bárbara, 2709 m; 0.6445N, 77.5522W
H. pantostictus	QCAZ 46896	Sucumbíos	Santa Bárbara, 2709 m; 0.6445N, 77.5522W
H. pantostictus	QCAZ 46929	Sucumbíos	Santa Bárbara, 2709 m; 0.6445N, 77.5228W
H. pantostictus	QCAZ 50358	Sucumbíos	Santa Bárbara, 2589 m; 0.6437N, 77.5321W
H. pantostictus	QCAZ 50389	Sucumbíos	Santa Bárbara, 2589 m; 0.6437N, 77.5321W
H. pantostictus	QCAZ 50390	Sucumbíos	Santa Bárbara, 2586 m; 0.6436N, 77.5323W
H. pantostictus	QCAZ 50415	Sucumbíos	Santa Bárbara, 2709 m; 0.6445N, 77.5228W
H. psarolaimus	QCAZ 66563	Pastaza	Reserva Comunitaria Ankaku, Parque Nacional Llanganates, 2165 m; 1.2752S, 78.0657W
H. psarolaimus	QCAZ 66564	Pastaza	Reserva Comunitaria Ankaku, Parque Nacional Llanganates, 2315 m; 1.2764S, 78.0759W

Species	Museum Number	Province	Locality
H. psarolaimus	QCAZ 66565	Pastaza	Reserva Comunitaria Ankaku, Parque Nacional Llanganates, 2334 m; 1.2771S, 78.0768W
H. psarolaimus	QCAZ 66566	Pastaza	Reserva Comunitaria Ankaku, Parque Nacional Llanganates, 2322 m; 1.2767S, 78.0763W
H. psarolaimus	QCAZ 66568	Pastaza	Reserva Comunitaria Ankaku, Parque Nacional Llanganates, 2216 m; 1.2770S, 78.0698W
H. ptychodactylus	QCAZ 46030	Cotopaxi	Pilaló, Quebrada 2, 2500 m; 0.9424S, 78.9956W
H. ptychodactylus	QCAZ 46031	Cotopaxi	Pilaló, Quebrada 2, 2500 m; 0.9424S, 78.9956W
H. staufferorum	QCAZ 3701	Napo	Volcán Sumaco, Lago Sumaco, 2463 m; 0.5689S, 77.5948W
H. staufferorum	QCAZ 3704	Napo	Codillera de Guacamayos, 31 km Baeza, Archidona Road, 2210 m; 0.6505S, 77.7907W
H. staufferorum	QCAZ 3705	Napo	Baeza, 2040 m; 0.4634S, 77.8915W
H. staufferorum	QCAZ 3706	Napo	Baeza, 2040 m; 0.4634S, 77.8915W
H. staufferorum	QCAZ 11150	Napo	13.4 km S Río Cosanga, 2040 m; 0.6560S, 77.9129W
H. staufferorum	QCAZ 36278	Napo	Volcán Sumaco, Lago Sumaco, 2470 m; 0.5689S, 77.5948W
H. staufferorum	QCAZ 36279	Napo	Volcán Sumaco, Lago Sumaco, 2470 m; 0.5689S, 77.5948W
H. staufferorum	QCAZ 45962	Pastaza	Reserva Comunitaria Ankaku, Río Challuwa Yacu, Parque Nacional Llanganates, 2250 m; 1.2792S, 78.0779W
H. staufferorum	QCAZ 45963	Pastaza	Reserva Comunitaria Ankaku, Río Challuwa Yacu, Parque Nacional Llanganates, 2250 m; 1.2792S, 78.0779W
H. staufferorum	QCAZ 45965	Pastaza	Reserva Comunitaria Ankaku, Río Challuwa Yacu, Parque Nacional Llanganates, 2250 m; 1.2792S, 78.0779W
H. staufferorum	QCAZ 45966	Pastaza	Reserva Comunitaria Ankaku, Río Challuwa Yacu, Parque Nacional Llanganates, 2250 m; 1.2792S, 78.0779W
H. staufferorum	QCAZ 45967	Pastaza	Reserva Comunitaria Ankaku, Río Challuwa Yacu, Parque Nacional Llanganates, 2250 m; 1.2792S, 78.0779W
H. staufferorum	QCAZ 56807	Pastaza	Reserva Comunitaria Ankaku, Río Challuwa Yacu, Parque Nacional Llanganates, 2250 m; 1.2792S, 78.0779W
H. staufferorum	QCAZ 64480	Pastaza	Reserva Comunitaria Ankaku, Río Challuwa Yacu, Parque Nacional Llanganates, 2250 m; 1.2792S, 78.0779W
H. staufferorum	QCAZ 66567	Pastaza	Reserva Comunitaria Ankaku, Parque Nacional Llanganates, 2434 m; 1.2799S, 78.0826W
H. tapichalaca	QCAZ 15083	Zamora Chinchipe	Yangana-Valladolid Road, Reserva Tapichalaca, 2625 m; 4.4816S, 79.1491W
H. tapichalaca	QCAZ 15084	Zamora Chinchipe	Yangana-Valladolid Road, Reserva Tapichalaca, 2625 m; 4.4816S, 79.1491W
H. tapichalaca	QCAZ 15085	Zamora Chinchipe	Yangana-Valladolid Road, Reserva Tapichalaca, 2625 m; 4.4816S, 79.1491W
H. tapichalaca	QCAZ 16704	Zamora Chinchipe	Yangana-Valladolid Road, Reserva Tapichalaca, 2697 m; 4.4816S, 79.1491W
H. tapichalaca	QCAZ 16705	Zamora Chinchipe	Yangana-Valladolid Road, Reserva Tapichalaca, 2697 m; 4.4816S, 79.1491W
H. tapichalaca	QCAZ 16706	Zamora Chinchipe	Yangana-Valladolid Road, Reserva Tapichalaca, 2697 m; 4.4816S, 79.1491W
H. tapichalaca	QCAZ 17776	Zamora Chinchipe	Yangana-Valladolid Road, Reserva Tapichalaca, 2697 m; 4.4816S, 79.1491W
H. tapichalaca	QCAZ 17777	Zamora Chinchipe	Yangana-Valladolid Road, Reserva Tapichalaca, 2697 m; 4.4816S, 79.1491W
H. tapichalaca	QCAZ 46887	Zamora Chinchipe	Reserva Tapichalaca, 1637 m; 4.4730S, 79.1930W
H. tapichalaca	QCAZ 63872	Zamora Chinchipe	Parque Nacional Podocarpus, Tapichalaca, 2605 m; 4.4876S, 79.1479W
H. tigrinus	QCAZ 31550	Sucumbíos	Santa Bárbara, El Corazón, 2620 m; 0.6437N, 77.5321W
H. tigrinus	QCAZ 40331	Sucumbíos	Santa Bárbara, 2638 m; 0.6437N, 77.5321W
H. tigrinus	QCAZ 41351	Sucumbíos	0.7 km SW Santa Bárbara, Quebrada El Corazón, 2638 m; 0.6437N, 77.5321W

ZooKeys 809: 125–148 (2018)
doi: 10.3897/zookeys.809.28743
http://zookeys.pensoft.net

RESEARCH ARTICLE

A peer-reviewed open-access journal
ZooKeys
Launched to accelerate biodiversity research

Phylogeography indicates incomplete genetic divergence among phenotypically differentiated montane forest populations of *Atlapetes albinucha* (Aves, Passerellidae)

Alberto Rocha-Méndez[1], Luis A. Sánchez-González[1], Enrique Arbeláez-Cortés[2], Adolfo G. Navarro-Sigüenza[1]

1 *Museo de Zoología, Facultad de Ciencias, Universidad Nacional Autónoma de México, Apartado Postal 70-399, México City 04510, México* **2** *Grupo de Estudios en Biodiversidad, Escuela de Biología, Facultad de Ciencias, Universidad Industrial de Santander. Carrera 27 Calle 9. Bucaramanga, Santander, Colombia*

Corresponding author: *Adolfo G. Navarro-Sigüenza* (adolfon@ciencias.unam.mx)

Academic editor: *Knud Jønsson* | Received 1 August 2018 | Accepted 19 September 2018 | Published 19 December 2018

http://zoobank.org/5DE5C0C5-669F-427A-9965-A91E70FF3F17

Citation: Rocha-Méndez A, Sánchez-González LA, Arbeláez-Cortés E, Navarro-Sigüenza AG (2018) Phylogeography indicates incomplete genetic divergence among phenotypically differentiated montane forest populations of *Atlapetes albinucha* (Aves, Passerellidae). ZooKeys 809: 125–148. https://doi.org/10.3897/zookeys.809.28743

Abstract

The White-naped Brushfinch (*Atlapetes albinucha*) comprises up to eight allopatric subspecies mainly identified by the color of the underparts (gray vs. yellow belly). Yellow and gray bellied forms were long considered two different species (*A. albinucha* and *A. gutturalis*), but they are presently considered as one polytypic species. Previous studies in the genus *Atlapetes* have shown that the phylogeny, based on molecular data, is not congruent with characters such as coloration, ecology, or distributional patterns. The phylogeography of *A. albinucha* was analyzed using two mitochondrial DNA regions from samples including 24 different localities throughout montane areas from eastern Mexico to Colombia. Phylogeographic analyses using Bayesian inference, maximum likelihood and haplotype network revealed incomplete geographic structure. The genetic diversity pattern is congruent with a recent process of expansion, which is also supported by Ecological Niche Models (ENM) constructed for the species and projected into three past scenarios. Overall, the results revealed an incomplete genetic divergence among populations of *A. albinucha* in spite of the species' ample range, which contrasts with previous results of phylogeographic patterns in other Neotropical montane forest bird species, suggesting idiosyncratic evolutionary histories for different taxa throughout the region.

Keywords
allotypy, coalescent, Last Glacial Maximum, mtDNA, montane forest, Pleistocene, phylogeography, plumage differentiation

Introduction

Phylogeographic analyses of widespread Neotropical montane forest bird species have indicated different levels of geographic structure in the variation of mitochondrial DNA (mtDNA) among populations (Bonaccorso et al. 2008, Navarro-Sigüenza et al. 2008, Barrera-Guzmán et al. 2012, Ortíz-Ramírez et al. 2016). Deep genetic divergence may suggest a long history of geographic isolation, usually accompanied by phenotypic divergence, whereas a shallow genetic differentiation has been attributed to possible scenarios of either recent range expansions or recent divergence (Cortés-Rodríguez et al. 2008, Arbeláez-Cortés et al. 2010).

The genus *Atlapetes* comprises a group of Neotropical finches inhabiting mainly humid montane forests from Mexico to northern Argentina (Paynter 1972, 1978), and has been considered one of the most species-rich clades (nearly 30 recognized species) among the New World passerines (Paynter 1972, 1978, Sánchez-González et al. 2015). Diversification in this group started about 5.2–3.2 Mya, and has probably occurred mainly due to changes in the range of montane forests related to the Pleistocene glacial cycles (Ricklefs and Latham 1992, Hooghiemstra et al. 2006, Sánchez-González et al. 2015). *Atlapetes* also provides a complex and intriguing case of evolutionary differentiation in plumage color (Paynter 1972, 1978, Remsen and Graves 1995). Most *Atlapetes* species have either yellow or gray underparts, which has led to the distinction of two main plumage patterns distributed in a "leapfrog" fashion along the Andes (Remsen 1984). Paynter (1972, 1978) included yellow and gray taxa in two different phylogenetic groups; a third group included yellow-plumaged species with bicolored crowns (*A. albinucha*, *A. gutturalis*, and *A. pallidinucha*). This phenotypically-based arrangement suggested that similarly plumaged species may have shared a common ancestor. However, Remsen and Graves (1995) proposed that some yellow and gray taxa may be representatives of the same species, suggesting that plumage differentiation patterns may be adaptive, as species with pale gray colors are generally found in drier and higher elevation habitats, whereas yellow-colored taxa are generally found in humid and lower elevations (Remsen and Graves 1995, García-Moreno and Fjeldså 1999).

Atlapetes albinucha (White-naped Brushfinch) is a widely distributed species found in montane regions from eastern Mexico to Colombia (AOU 1998, del Hoyo et al. 2011, Gill and Donsker 2015, Remsen et al. 2015). This species inhabits mainly humid and temperate montane forests (900 to 3000 m), as well as upper tropical zones and edges of clearings of cloud forests (Dwight and Griscom 1921, Paynter 1978, Howell and Webb 1995, del Hoyo et al. 2011). Up to eight allopatric subspecies showing two well-differentiated plumage coloration patterns with clear geographic structure have been recognized (Figure 1, del Hoyo et al. 2011, Remsen et al. 2015, Gill and Donsker 2018). Phenotypic differentiation in this taxon led some researchers to consider such differenti-

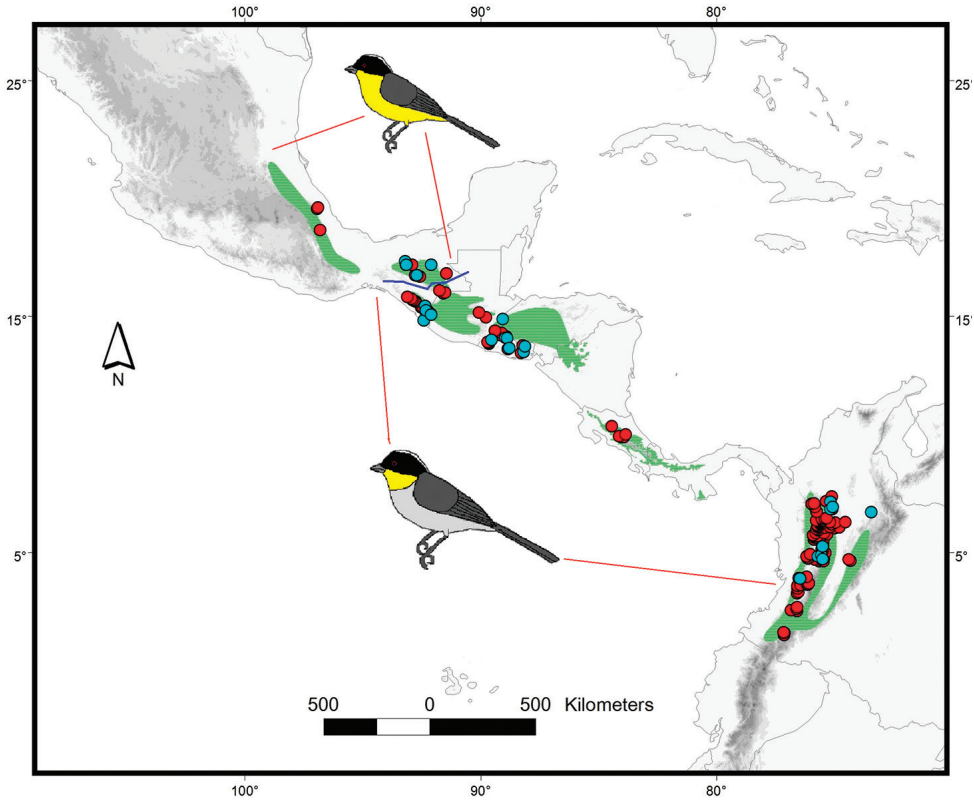

Figure 1. *Atlapetes albinucha* distribution shown in green stapled lines, based on Sánchez-González et al. (2015) and Natureserve (http://natureserve.org). Blue dots depict tissue samples used in the present study. Red dots depict records of the species used to construct the distribution model. Bird pictures depict the geographic regions where color morphs are found. Blue line depicts the location of the putative distribution barrier of the morphs in Chiapas.

ated populations as two species (Dwight and Griscom 1921, Howell and Webb 1995, Navarro-Sigüenza and Peterson 2004) or as part of a polytypic species (Paynter 1978, Remsen and Graves 1995, AOU 1998, del Hoyo et al. 2011, Gill and Donsker 2015, Remsen et al. 2015). Differences between subspecies with pale-gray underparts are apparently largely clinal, and are based in subtle variations of size and color (Paynter 1978); while color morphs with yellow- and pale-gray underparts are allopatric (Figure 1), and their ranges are separated by the low valley of Río Grijalva (1000 m) in Chiapas (southeastern Mexico), where the two morphotypes are less than 100 km apart (Paynter 1978).

Paynter (1972, 1978) reviewed extensively the taxonomy and geographic variation in *A. albinucha* complex and suggested that plumage differentiation in these nearly parapatric populations were not indicative of a high genetic differentiation nor the product of ecological exclusion, but the result of a low river barrier, therefore implying isolation due to environmental factors as the main cause for this phenotypic differentiation. Current taxonomic schemes have adopted the proposal that *A. albinucha* represents a single

polytypic species (Paynter 1978, Remsen and Graves 1995, AOU 1998, del Hoyo et al. 2011, Gill and Donsker 2015, 2018, Remsen et al. 2015). A study using mtDNA genetic analyses (Sánchez-González et al. 2015) at the genus level showed a phylogenetic reconstruction in which both yellow- and gray-plumaged birds in the *A. albinucha* complex were recovered mixed in a monophyletic group, sister to *A. pileatus* and well separated from the rest of *Atlapetes*, partially supporting the conclusions of Paynter (1978).

Here, using an extensive sampling for *A. albinucha* (39 individuals from 24 localities in four countries), we tested: a) if yellow- and gray-plumaged groups are reciprocally monophyletic, b) if there is phylogeographic structure in this widespread taxon across their range, and c) if past reconstructions of the environmental conditions were *A. albinucha* ranges at present indicate distributional changes that may be related with their genetic-geographic variation. These questions were approached using a mtDNA assessment of populations included within this complex, as well as environmental niche modelling analyses based on records of voucher specimens in biological collections.

Materials and methods

Taxon sampling

Tissue and blood samples of *A. albinucha* were obtained from different museum collections in Mexico, USA, and Colombia, spanning the whole distribution of the species (Table1, see Acknowledgements), except from two subspecies endemic to Panama (*brunnescens* and *azuerensis*). We also supplemented our study with two published sequences of *Atlapetes pileatus*, and two from *Arremon brunneinucha* to be used as outgroups (Klicka et al. 2007, DaCosta et al. 2009). Overall, we analyzed 39 samples from *A. albinucha* representing 24 localities from four countries, and four subspecies (Figure 1, Table 1).

Laboratory procedures

Extraction of DNA from tissue samples was carried out in two laboratory facilities in Mexico and Colombia using the DNeasy Blood & Tissue Kit (Qiagen Inc., Valencia, CA) following manufacturer's protocols. We amplified two mtDNA genes fragments comprising the NADH dehydrogenase subunit 2 (ND2) and Cytochrome b (Cyt b), which have been shown to successfully assess phylogenetic relationships due to its high probability for tracking recent diversification events (Ball and Avise 1992, Avise 2000). We used primers L5215 (Hackett 1996) and H1064 (Drovetsky et al. 2004) for ND2. The Cyt b was amplified using primers L14990 (Kocher et al. 1989) and H15646 (Sorenson et al. 1999). PCR amplification reactions were performed in 12 to 25 µl reaction mix containing 2 µl of each primer, 2 µl (~10 ng) of DNA and 6 µl Readymix Redtaq (Sigma-Aldrich), or 6 µl of Taq polymerase. PCR products were observed in a

1% agarose gel stained with Ethidium Bromide (EtBr) or EZ-Vision. DNA sequencing was performed at the High Throughput Genomics Center of the University of Washington (USA), Macrogen Inc., Korea, and at the *Servicio de Secuenciación y Análisis Molecular Universidad Nacional* (SSiGMol, Colombia). Sequences were edited and aligned by eye using SEQUENCHER 5.4.6 (Gene Codes Corporation, Ann Arbor, MI USA). Mitochondrial origin for all of our sequences was corroborated in BLAST, through the NCBI server (https://blast.ncbi.nlm.nih.gov/Blast.cgi). Afterwards sequences were aligned using CLUSTALX 2.1 (Thompson et al. 1997) and inspected by eye. Newly generated sequences have been deposited in Gen Bank under accession numbers MH938455 to MH938526.

Phylogeographic analyses

We conducted analyses using an alignment with both mtDNA loci (ND2 and Cyt B) concatenated. Nucleotide substitution model parameters and partition schemes were estimated for each gene in PARTITIONFINDER (Lanfear et al. 2012), using the Bayesian Information Criterion (BIC) for model selection. Resultant partition schemes and model parameters were used for conducting a phylogenetic reconstruction using the Bayesian inference approach (BI) implemented in MR. BAYES 3.2 (Ronquist et al. 2011) using two independent searches running four Markov-Chains Montecarlo (temperature 0.2) for 10^6 generations sampling every 1000 generations. Convergence across runs was evaluated using two methods: I) the examination of the standard deviation of split frequencies (with acceptance values <0.01); and II) by verification of parameter estimates in TRACER v1.6 (Rambaut et al. 2014), based on acceptable effective sample sizes (ESS values > 200). After checking for convergence, the first 25 % of the generated trees were discarded as burn-in and the remaining 75 % were kept to calculate posterior probabilities. In addition, we also conducted phylogenetic analyses using maximum likelihood (ML) criteria as implemented in RAXMLGUI 1.5b1 (Stamatakis 2006, 2014, Silvestro and Michalak 2012), using the GTRCAT model for nodal support via 1000 bootstrap iterations using the selected partitions. We considered nodes highly supported when bootstrap values were > 70 % (ML) or when posterior probability values were > 90 % (BI).

Divergence times were estimated through calculation of a maximum clade credibility tree (MCCT) using a Yule speciation process (Yule 1925, Gernhard 2008). Calibration of divergence time estimates was based on mutation rates proposed for the ND2 (0.013 subs/site/lineage/My, Arbogast et al. 2006) and Cyt b (0.01 subs/site/lineage/My, Lovette 2004) loci. To test whether our dataset fits to a strict clock model or to a relaxed clock model, we performed selection tests through the stepping-stone method (Xie et al. 2011) as implemented in MrBAYES 3.2 (Ronquist et al. 2011). Given our partitioning model, the mean marginal likelihood of the strict clock (-Ln 5845.98) performed better than the relaxed clock (-Ln 5913.55). Therefore, chains were run under a strict clock with substitution models according to PARTITIONFINDER for

Table 1. Tissue and blood samples used in this study. Samples of *A. albinucha* species were grouped in five geographic groups: Northern Chiapas (NC, n = 11), Southern Chiapas (SC, n = 11), El Salvador (Sal, n = 7), Honduras (Hon, n = 1), and Colombia (Col, n = 9). One sample of *Atlapetes pileatus* tissue was also obtained and added to the analysis.

Sample source	Catalog number	Voucher specimen	State/ Department	Locality	Latitude	Longitude	GenBank Accession Number		Geographic Group
							ND2	Cyt b	
Museo de Zoología "Alfonso L. Herrera", Facultad de Ciencias, UNAM	BONA 33	BONA 33	Chiapas	Carretera estatal Coapilla-Ocotepec km 29 a 5.4 km N de Coapilla	17.31388	-93.2	MH938475	MH938514	NC
	BONA 39	BONA 39	Chiapas	Volcán Tacaná ladera, vereda a Tapalapa, Rancho Chiquihuite	15.0666	-92.08333	MH938476	MH938515	SC
	BONA 52	BONA 52	Chiapas	Volcán Tacaná ladera, vereda a Tapalapa, Rancho Chiquihuite	15.0666	-92.08333	MH938474	MH938513	SC
	BONA 89	BONA 89	Chiapas	Volcán Tacaná ladera, vereda a Tapalapa, Rancho Chiquihuite	15.0666	-92.08333	MH938479	–	SC
	BONA 94	BONA 94	Chiapas	Volcán Tacaná ladera, vereda a Tapalapa, Rancho Chiquihuite	15.0666	-92.08333	MH938477	MH938516	SC
	BMM 577	BMM 577	Chiapas	6 km NE de Pueblo Nuevo; camino a Aurora-Ermita	17.18333	-92.08333	MH938478	MH938517	NC
	BMM 582	BMM 582	Chiapas	6 km NE de Pueblo Nuevo; camino a Aurora-Ermita	17.18333	-92.08333	MH938464	MH938503	NC
	BMM 834	BMM 834	Chiapas	Volcán Tacaná ladera, vereda a Tapalapa, Rancho Chiquihuite	15.0666	-92.08333	KM360517	MH938498	SC
	MOL 13001	MOL 13001	Chiapas	San Nicolás Buenavista, Cerro Huitepec	16.73805	-92.68805	MH938468	MH938507	NC
	MOL 13061	MOL 13061	Chiapas	San Nicolás Buenavista, Cerro Huitepec	16.73805	-92.68805	MH938467	MH938506	NC
	MOL 13130	MOL 13130	Chiapas	San Nicolás Buenavista, Cerro Huitepec	16.73805	-92.68805	MH938466	MH938505	NC
	SIT 105	SIT 105	Chiapas	CarreteraCopainalá-Ocotepec km 38 a 95.5 km N de Coapilla	17.16891	-93.14533	MH938481	MH938519	NC
	SIT 146	SIT 146	Chiapas	Coapilla a 6.5 km N	17.17413	-93.14636	MH938463	MH938502	NC
	SIT 147	SIT 147	Chiapas	Coapilla a 6.5 km N	17.17413	-93.14636	MH938472	MH938511	NC
	SIT 157	SIT 157	Chiapas	Coapilla a 6.5 km N	17.17413	-93.14636	MH938462	MH938501	NC
	SIT 158	SIT 158	Chiapas	Coapilla a 6.5 km N	17.17413	-93.14636	MH938480	MH938518	NC
	EAGT 806	EAGT 806	Chiapas	Cerro Mozotal, en la cima	15.4294	-92.3411	MH938458	MH938495	SC
	EAGT 817	EAGT 817	Chiapas	Cerro Mozotal, en la cima	15.4294	-92.3411	MH938457	MH938494	SC
	EAGT 844	EAGT 844	Chiapas	Cerro Boqueron, en la cima	15.23541	-92.30463	MH938473	MH938512	SC
	ZRH 407	ZRH 407	Chiapas	Cerro Mozotal, en la cima	15.4294	-92.3411	MH938460	MH938499	SC
Museo de Zoología Facultad de Ciencias "Alfonso L. Herrera" UNAM	130332	130332	Chiapas	Reserva Ecológica el Triunfo	14.81278	-92.40594	MH938456	MH938492	SC
	130345	130345	Chiapas	Reserva Ecológica el Triunfo	14.81278	-92.40594	KM360516	MH938493	SC
	QRO0272	QRO0272	Querétaro	El Pemoche	21.2263	-99.109694	MH938455	MH938491	
	OVMP227	OVMP227	Jalisco	–	–	–	FJ547292	FJ547251	

Sample source	Catalog number	Voucher specimen	State/ Department	Locality	Latitude	Longitude	GenBank Accession Number		Geographic Group
							ND2	Cyt b	
University of Kansas, Natural History Museum	EAGT 21	KU 4907	San Miguel	San Miguel	13.48138	-88.1775	GU377050	MH938497	Sal
	EAGT 74	KU 5017	Chalatenango	Concepción Quezaltepec	14.08333	-88.95	MH938459	MH938496	Sal
	OK 56	KU 4961	Morazan	Chilanga	13.71666	-88.11666	MH938465	MH938504	Sal
	CMZF 120	KU 6448	San Vicente	Nuevo Tepetitán	13.64527	-88.78416	MH938471	MH938510	Sal
	LR 58	KU 7704	Chalatenango	La Laguna	14.0666	-88.8666	MH938470	MH938509	Sal
	SLA 165	KU 7775	San Vicente	Nuevo Tepetitán	13.64527	-88.78416	MH938461	MH938500	Sal
	MBR 6584	KU 9400	Santa Ana	Metapán	13.98333	-89.5333	MH938469	MH938508	Sal
Instituto de Investigación de Recursos Biológicos "Alexander von Humboldt"	IAvH-CT-01158	IAvH-11694	Pereira	Parque regional Ucumarí Entre Peña Bonita y Peñas Blancas	4.709233	-75.4907	MH938483	MH938521	Col
	IAvH-CT-01726	IAvH-11946	Aranzazu	Vereda El Laurel, Cuenca Alta del Río Hacienda Termopilas	5.230944	-75.48841	MH938484	–	Col
	IAvH-CT-02391	IAvH-12363	Yotoco	Yotoco	3.87975	-76.443	MH938485	MH938522	Col
	IAvH-CT-04519	IAvH-13101	Santa Rosa de Cabal	Vereda La Linda, Parque Municipal de Campoalegre	4.8675	-75.54666	MH938486	MH938523	Col
	IAvH-CT-04835	IAvH-CT-04835	Anorí	Vereda Santa Gertrudis, Finca La Estrella margen derecha de la Quebrada Santa Gertrudis	7.135444	-75.15527	MH938487	–	Col
	IAvH-CT-07844	IAvH-CT-07844	Amalfi	Vereda Cajamarca, Finca Canales Cuenca de la quebrada Cajamarca	6.8235	-75.15527	MH938488	MH938524	Col
	IAvH-CT-09344	ICN 34591	Amalfi	Vereda El Encanto, La Secreta	6.909167	-75.0766	MH938489	MH938525	Col
	IAvH-CT-09695	IAvH-CT-09695	Pereira	P. Ucumarí, La Pastora	4.814278	-75.69455	MH938490	MH938526	Col
	IAvH-CT-18248	ICN 38086	Santander	Serranía de los Yariguies, Carmen de Chucurí	6.68333	-73.4333	MH938482	MH938520	Col
Marjorie Barrick Museum of Natural History	GAV 1374	MBM 6640	Copán	Copán Ruinas, 10 km ENE	14.86667	-89.05	GU377047	DQ459625	Hon
	DAB1706	MBM 4600	Managua	Chocoyero, Volcán Mombacho, 48km SE Managua	11.829	-85.963	EF529823	EF529932	

10^6 generations and discarded the first 25 % as burn-in. Stationarity was analyzed with TRACER v1.6 (Rambaut et al. 2014). Mean heights and 95 % credibility interval values for node estimates were generated in TREEANNOTATOR v1.8.4 (Drummond et al. 2012) with a posterior probability limit of 0.6. Trees were visualized in FIGTREE v1.4.2 (http://tree.bio.ed.ac.uk/software/figtree/).

Finally, to complement the visualization of the relationships among haplotypes, a haplotype network was constructed using NETWORK 4.6.1.1 (Fluxus Engineering, www.fluxus-engineering.com), through a Median-joining method, assigning equal weights to all variable sites and an epsilon parameter with default values ($\varepsilon = 0$). This method estimates evolutionary relationships among sequences when divergences are recent (Crandall and Templeton 1996, Bandelt et al. 1999).

Population genetic structure and historical demographic analyses

To analyze the molecular information in the framework of population genetics, we clustered individuals of *A. albinucha* into four groups considering subspecific membership as well as geographic proximity and evidence of montane forest continuity (Table 1): (I) Northern Chiapas (NCh, n = 11; subspecies *albinucha*), (II) Southern Chiapas (SCh, n = 11; subspecies *griseipectus*), (III) El Salvador (Sal, n = 7; subspecies *griseipectus*), Honduras (Hon, n = 1; subspecies *fuscipygius*), and (IV) Colombia (Col, n = 9; subspecies *gutturalis*). For each group, genetic diversity was assessed through the estimation of haplotype diversity (Hd), and nucleotide diversity (π) in ARLEQUIN 3.1 (Excoffier et al. 2005).

To test if there is evidence of genetic structure among the four geographic groups, we performed a hierarchical analysis of molecular variance (AMOVA) using pairwise differences. In addition, to test if phenotypic divergence is related to genetic structure we also performed an AMOVA between gray-plumaged subspecies and yellow-plumaged subspecies. Genetic divergence between groups was also measured using F_{ST} fixation index values (Wright 1931, 1978), which were interpreted following the guidelines in Hartl and Clark (1997). All tests were performed with ARLEQUIN 3.1 (Excoffier et al. 2005); and their significance was assessed using 1000 permutations.

To test for evidence of recent demographic changes in *A. albinucha*, we estimated demographic dynamics experienced by the whole taxon through the calculation of neutrality tests corresponding to Fu's F_S statistic (Fu 1997) and Tajima's D statistic (Tajima 1989). Significance of these tests ($p < 0.02$ in the case of the F_S statistic) was calculated by developing 1000 simulations using ARLEQUIN 3.1. Evidence of historical signatures of fluctuations in population size was also examined through a Bayesian skyline plot model on the Maximum Clade Credibility Tree (MCCT), as implemented in BEAST v1.8.4 (Drummond et al. 2012), using a coalescent-based estimation of population size changes over time with MCMC sampling procedure (Ho and Shapiro 2011, Houston et al. 2014).

Analysis of the historic range using ecological niche models

We tested the hypotheses that the ecological/environmental conditions in which *A. albinucha* ranges at present may have allowed for population connectivity at least since the Last Interglacial (120,000 ya) using ecological niche models (ENM). We compiled a total of 475 geographical records, representing 176 localities, of the species through the Global Biodiversity Information Facility (GBIF, http://www.gbif.org) and museum vouchers (see Acknowledgements). GBIF records were filtered for elimination of both duplicates and records lacking geographic data. ENMs were obtained using 19 bioclimatic variables with a cell resolution of 2.5 arc-minutes (ca. 4.5 km^2) generated by the Community Climate System Model (CCSM) downloaded through WorldClim (http://

www.worldclim.org/bioclim; Hijmans et al. 2005). ENM models were obtained and evaluated in MAXENT 3.3.3 (Phillips et al. 2006), whose algorithms have been used to transfer present niche space conditions into past scenarios (120,000 ya–present). Past ENM reconstructions were based on the CCSM scenarios for the LIG (ca. 120,000 ya), Mid-Holocene (MHCO, ca. 6,000 ya), and LGM (ca. 22,000 ya). CCSM scenarios were preferred over other models as it has been proposed that global cooling conditions are not overestimated (Fernández-Mazuecos and Vargas 2013, Harrison et al. 2014), therefore representing a conservative hypotheses of humid montane forests connectivity. MAXENT parameters were run as follows: Ten-thousand random points within extreme coordinates 22N–105W, 20S–62W were generated to serve as background data to encompass mostly montane habitats in the Neotropics, 50 bootstrap replicates with a maximum iteration value of 5000, and a random test percentage of 25 with a 10 percentile training presence threshold rule (Warren and Seifert 2011, Baldwin 2009). To evaluate the predictive ability of the generated distribution models we implemented two model validations using the ROC plot method. As a first evaluation measure, we used the value for the area under the receiver operating characteristic curve (AUC), which can be used as a measure of the model's overall performance; for a second model validation we used PARTIAL-ROC (P-ROC) analysis (Barve 2008, Peterson et al. 2008), which generates ratios that provide a measurement of the correct identification of presences against the total area predicted (Mendoza-González et al. 2016). ENM models were visualized in ARCMAP 10 (ESRI 2010).

Results

Phylogeography

Phylogenetic reconstruction analyses were conducted using the substitution models HKY+I+G for the first position of ND2 and the second position of Cyt b, F81+I for ND2 second position and third Cyt b position and HKY+G for the third and first positions of ND2 and Cyt b respectively. Both phylogenetic reconstruction methods (ML and IB) rendered similar topologies. The Bayesian tree topology (Figure 2A) recovered all of the *A. albinucha* samples in a monophyletic group (as suggested previously by Sánchez-González et al. 2015) showing two major well-supported clades (0.99 and 1.00) but moderate bootstrap support (0.56 and 0.66). One clade, including only gray-plumaged birds, grouped all of the individuals from the Central Andes of Colombia, as well as two individuals from southern Chiapas, in Mexico (Reserva Ecológica El Triunfo). The other clade included both yellow- and gray-plumaged birds from Mexico and Central American, as well as one Colombian sample from Serranía de los Yariguies, Santander (IAvH-CT 18248). No one of the four subspecies included was monophyletic according to the two mtDNA loci analyzed, and the yellow- and gray-plumaged groups were neither reciprocally monophyletic. Therefore, no clear phylogeographic structure was recovered from our analysis (Figure 2).

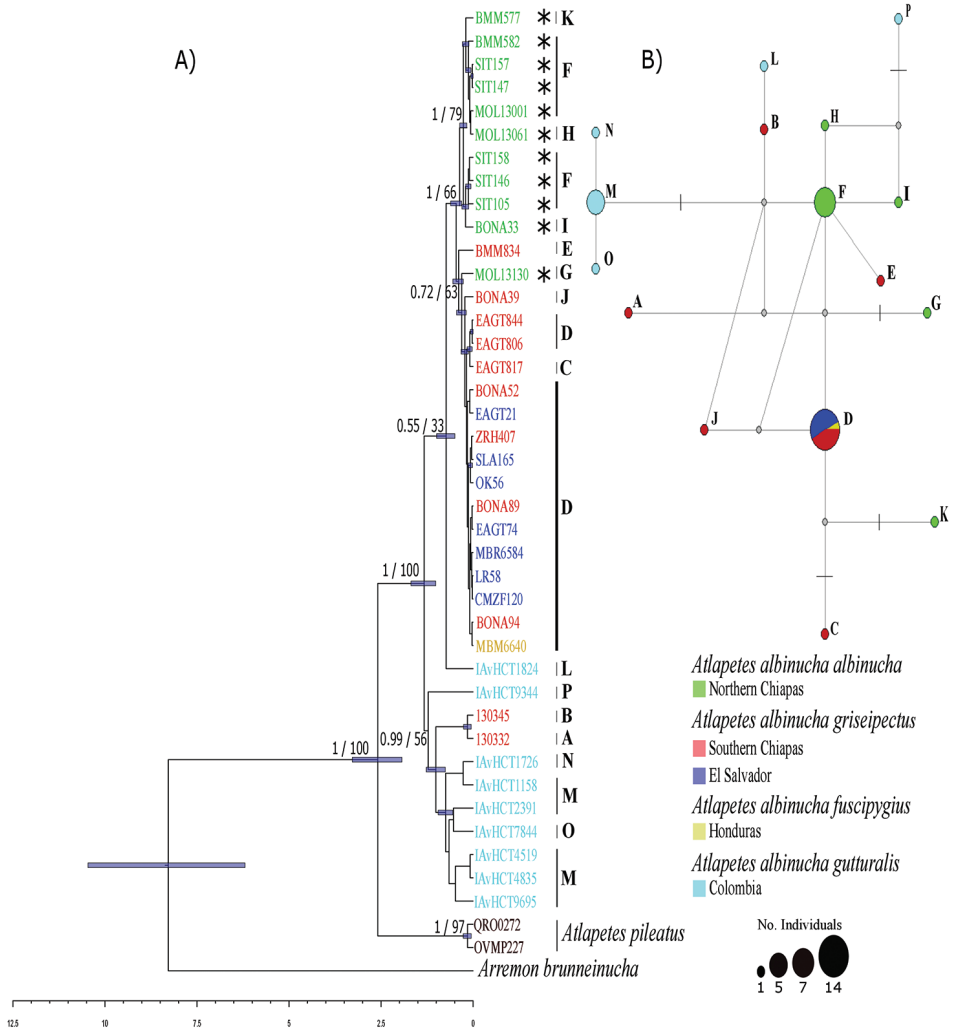

Figure 2. A Dated Bayesian maximum clade credibility tree showing phylogenetic relationships among members of *Atlapetes albinucha* species. Node bars depict 95% HDP interval, scale bar represents millions of years. Nodal values above branches indicate posterior probabilities/ bootstrap supports of BI/ML. Capital letters depict haplotypes. An asterisk (*) indicate birds representing yellow morphs **B** Median-joining haplotype network for the concatenated dataset. Each color depicts the geographic provenance of samples: green-northern Chiapas (subspecies *albinucha*), red-southern Chiapas (subspecies *griseipectus*), blue-El Salvador (subspecies *griseipectus*), yellow-Honduras (subspecies *fuscipygius*) and light blue-Colombia (subspecies *gutturalis*). Each branch represents a single nucleotide change, transversal black lines along branches depict the occurrence of three mutations. Gray dots indicate median vectors inferred for the data.

Population genetic structure and demographic history

Overall, genetic diversity values for the geographic groups showed a low nucleotide diversity ($\pi < 0.008$), but high haplotype diversity (Hd > 0.71; Table 2). The AMOVA between geographic groups indicated that genetic variation was explained (almost equally) by both differences among populations (50.7%), as well as by variation within groups (49.2%, Table 3). Comparisons among pairs of geographic groups using F_{ST} values revealed very high genetic differentiation between El Salvador and northern Chiapas (F_{ST} = 0.71412), but lower differentiation was among El Salvador and southern Chiapas (F_{ST} = 0.04556); the remaining F_{ST} values indicated moderate genetic differentiation (F_{ST} between 0.4 and 0.7). AMOVA between gray- and yellow-plumaged morphs showed that most of the variance occurs within groups (64.5%), paralleling the results of the phylogenetic analysis that showed that both phenotypes are not reciprocally monophyletic.

The haplotype network showed three non-shared high frequency haplotypes: one including most samples from Colombia (*gutturalis*); a second one where most samples from northern Chiapas (*albinucha*) are located; and a third high frequency haplotype that was shared by most samples corresponding to northern Central America, which includes subspecies *griseipectus* and *fuscipygius* (Figure 2B).

Despite relatively low bootstrap values, molecular dating of the divergence between *A. albinucha* and *A. pileatus* yielded a time estimate during the Late Pliocene-Early Pleistocene about 2.5 Mya (HPD range 1.94–3.28 Mya), whereas differentiation between major clades of *A. albinucha* apparently occurred around 1.5 Mya (HDP range 1.01–1.61 Mya), during the Early Pleistocene (Figure 2A).

Historical demography in *A. albinucha* as estimated from the Tajima's D and Fu's F_S tests showed in most cases negative values, except for the F_S in the Colombian population. Both demographic tests did not depart from neutrality given that values were not significant neither at the species nor at the geographic group level; therefore, demographic fluctuations are difficult to suggest based on these values (Table 2). Bayesian skyline plot indicated an overall pattern of population stability throughout the Pleistocene at the species level, however, a fluctuation near the present (ca. 100,000 ya), suggests a population bottleneck followed by rapid population expansion (Figure 3), thus paralleling results from the genetic diversity analyses.

Table 2. Genetic diversity measures and demographic fluctuation measured at the species and population level within the concatenated data set. Abbreviations: N Sample size, Hd Haplotype diversity, π nucleotide diversity, SD standard deviation.

	N	Hd (SD)	π (SD)	Tajima's D	Fu's F_s
Northern Chiapas	11	0.982 (0.046)	0.00264 (0.0015)	-1.49107	-2.654
Southern Chiapas	11	0.727 (0.144)	0.007674 (0.0041)	-1.037	-0.905
El Salvador	7	0.714 (0.181)	0.00077 (0.00028)	-1.023	-0.538
Colombia	9	0.722 (0.159)	0.004313 (0.0026)	-1.37093	0.81161
Honduras	1	–	–	–	–
Total	39	0.835 (0.047)	0.00652 (0.0007)	-1.267	-5.08

Table 3. Analyses of molecular variance (AMOVA) between gray- and yellow-plumaged morphs and between geographical groups.

AMOVA: gray- and yellow-plumaged morphs				
Source of variation	**Sum of squares**	**Variance components**	**Percentage of variation**	***P***
Among morphs	70.621	4.00944	35.48	0.001
Within morphs	269.815	7.29230	64.52	0.00098
AMOVA: geographic groups				
Source of variation	**Sum of squares**	**Variance components**	**Percentage of variation**	***P***
Among geographic groups	170.961	5.13057	50.72	0.001
Within geographic groups	169.475	4.98455	49.28	0.001

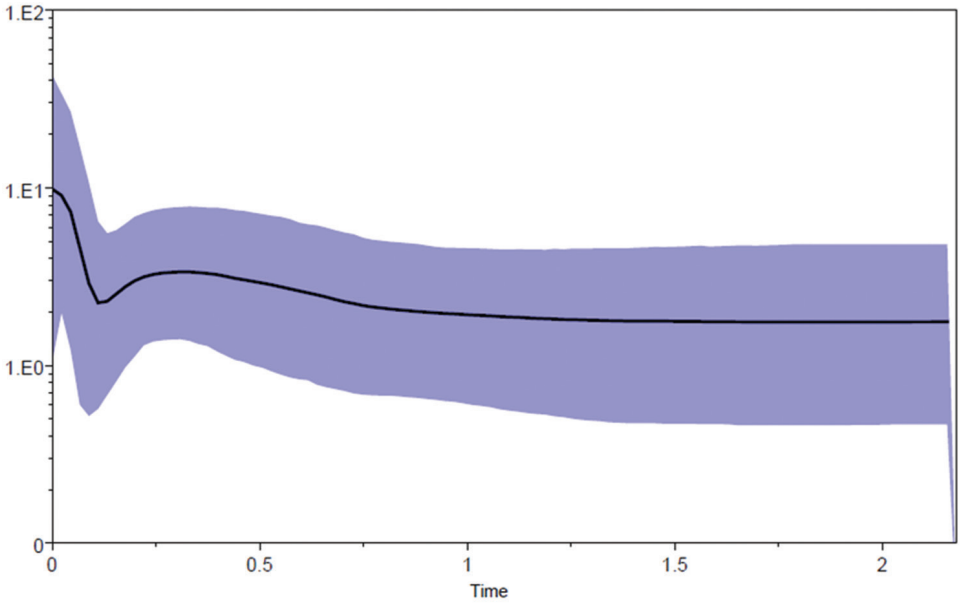

Figure 3. Bayesian skyline plot derived from the concatenated gene dataset of *Atlapetes albinucha* species. Time in millions of years. Population size change (Ne*generation time) in the Y axis. Mean estimate is shown as a thick solid line, and the 95% HDP limits are shown in solid purple color area surrounding the mean estimate.

Ecological niche models

All of our ENM analyses performed better (AUC > 0.94) than a random non-predictive model (AUC = 0.5), indicating that the models obtained may reflect, relatively well, the past distribution of environmental conditions where *A. albinucha* inhabits at present. ENMs suggested a scenario of geographically fragmented environmental conditions for populations in Mexico, Central America, and Colombia during three of the modeled timeframes: LIG (ca. 120,000 ya, P-ROC, min = 0.998, max = 1.972; Figure 4d), Mid-Holocene (MH, ca. 6,000 ya, P-ROC, min = 0.997, max = 1.907; Figure 4b), and for the present (Figure 4a). Present, LIG, and MH timeframes showed four main environmentally suitable areas for *A. albinucha* separated by lowlands such as the Isthmus of

Tehuantepec, the Nicaragua Depression, and the Isthmus of Panama. In contrast, ENM for the LGM (ca. 22,000 ya, P-ROC, min = 1.1404, max = 1.532) suggested these same lowland areas as corridors, which may have served for the dispersal between previously isolated populations (Figure 4c), thus supporting the scenario suggested by phylogeographic patterns.

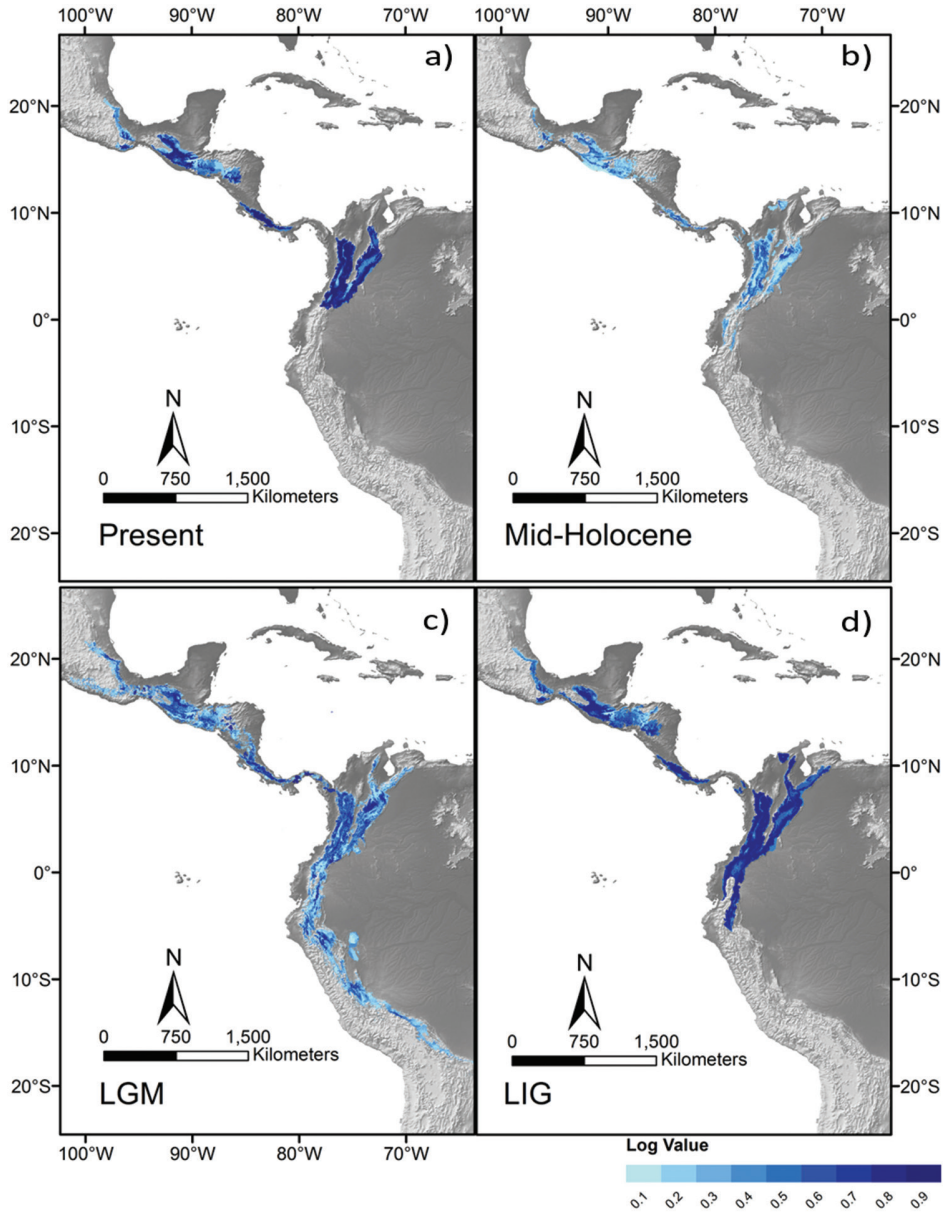

Figure 4. Maxent ENMs for *A. albinucha* species projected into present and past scenarios. Darker blue areas depict higher logistic prediction values. ENM projected in the **a** present **b** the Mid-Holocene Climatic Optimum (MH) **c** the Last Glacial Maximum (LGM) and **d** the Last Interglacial (LIG).

Discussion

The major result of our analyses using mtDNA sequence data for individuals of *A. albinucha* is that this taxon exhibits an incomplete genetic differentiation along their range in the Neotropical Montane Forest. The lack of clear phylogeographic structure in this montane bird taxon is in sharp contrast with expectations based on plumage differentiation which has resulted in the recognition of up to eight subspecies (Gill and Donsker 2018) as well as to the genetic divergence found in other birds from other naturally fragmented environments throughout the Neotropics (García-Moreno et al. 2004, Cadena et al. 2007, Navarro-Sigüenza et al. 2008, Weir et al. 2008, Pérez-Emán et al. 2010, Arbeláez-Cortés and Navarro-Sigüenza 2013). Despite not recovering a clear phylogeographic structure, the geographic distribution of the genetic variation in the geography is not completely random (as indicated by AMOVA and F_{ST} values), suggesting a scenario in which two groups (South America and Mesoamerica) have been diverging in isolation followed by range expansion, allowing the mixture of the genetic variation in periods favoring habitat connectivity during the LIG. Signatures for this vicariant scenario of genetic differentiation may be found in the phylogeographic topology, in which two groups including mainly South American and mainly Mesoamerican individuals were recovered, and in the significant variation among geographic groups determined by the AMOVA analyses (Table 3), as well as in the gene flow values (Table 4). Moreover, the low nucleotide diversity, but high haplotype diversity we found for mtDNA of *A. albinucha*, is thought to be consistent with populations passing through genetic bottlenecks followed by rapid population growth (see Grant and Bowen 1998).

The phylogeographic pattern of *A. albinucha* is consistent with allotypy, a term used to denote a stage in intermediate polyphyly (Omland et al. 2006). Allotypy is a likely intermediate stage of divergence characterized by local fixation of haplotypes on the path to reciprocal monophyly (Hudson 1990). This genetic pattern has been found in other bird species such as ducks (Peters et al. 2005, Peters and Omland 2007) and ravens (Omland et al. 2006) in the Holarctic, a raptor species in Neotropical lowlands (Johnson et al. 2007), and in passerines from Australia (Joseph and Wilke 2007) and from the Neotropical montane forests (Arbeláez-Cortés et al. 2010). For most of these cases, present distribution of the genetic diversity may reflect the retention of the genetic diversity found in the ancestor for a long time after isolation, which may have had a larger population size, thus increasing the time for some polymorphisms to be retained (Joseph and Omland 2009). Similarly, population expansion derived from populations with high effective sizes may also explain the haplotype and nucleotide diversities observed (Harpending et al. 1998, Ray et al. 2003, Ng et al. 2013, Jezkova et al. 2015).

In the case of *A. albinucha*, BSP (Figure 4) suggests a long period of population stability, with a slight increase from 750,000 to 250,000 ya, after which a relatively slight decrease in population size occurred ca. 100,000 ya. This population decrease, followed by rapid population growth and range expansion is coincident with the Last Glacial Maximum during the Late Pleistocene (~21,000 ya), when colder conditions may have allowed the formation of corridors between previously isolated humid montane forest

Table 4. Population pairwise comparisons using the concatenated data set. Above the diagonal is found the number of migrants per generation estimates (Nm value). Below the diagonal FST index. FST values with * depict significant values p < 0.05. Numbers depict geographic group correspondence.

	1	2	3	4	5
1-Northern Chiapas		0.70586	0.20016	0.2547	0.45921
2-Southern Chiapas	0.41464*		10.47426	0.67099	–
3-El Salvador	0.71412*	0.04556		0.24878	–
4-Colombia	0.66252*	0.42699*	0.66775*		0.75137
5-Honduras	0.52126	0	0	0.39956	

patches (Figure 4a), likely enhanced by the downward altitudinal range changes of the forest belt (Hooghiemstra et al. 2006, Gutiérrez-Rodríguez et al. 2011, Rojas-Soto et al. 2012, Ornelas et al. 2010, 2013, Ramírez-Barahona and Eguiarte 2013). Such a scenario, probably promoted gene flow between previously isolated populations (e. g., Hewitt 2000, Zink and Blackwell-Rago 2000, Weir 2006, Hooghiemstra et al. 2006, Barber and Klicka 2010, Pérez-Emán et al. 2010, Wachowiak et al. 2013, Bagley and Johnson 2014, Ornelas et al. 2016). In addition, an interesting result emerging from our ENM is that regions inhabited by yellow-plumaged and grey-plumaged populations in Chiapas-Guatemala have apparently never been isolated, which seems to support conclusions by Paynter (1972, 1978) regarding the weakness of a low river valley as an effective barrier in separating these populations.

Causes of differentiation in plumage coloration in *A. albinucha* remain elusive in our analysis, as both plumage coloration patterns appeared intermixed in the tree topology, which suggest different processes for the configuration of the genetic variation and the phenotypic plumage differentiation. Therefore, the clear phenotypic differentiation between yellow-colored birds in northern Chiapas and gray-colored birds in the rest of the distributional range suggests that plumage may be under natural selection. Similar results have been obtained for other groups of birds in different geographical and ecological settings, such as in the Tropical Pacific islands (Filardi and Smith 2005, Uy et al. 2009), shorebirds (Rheindt et al. 2011), and Australian woodswallows (Joseph et al. 2006). In the case of *Atlapetes* brushfinches, yellow- and gray-plumage patterns are apparently ecologically segregated from each other at different elevations. Gray-plumaged birds tend to occupy high elevation, whereas yellow-plumaged birds tend to occupy lower elevations (Remsen and Graves 1995), thus suggesting that gray-plumages have evolved to deal with conditions on high elevations, but also some dry low-elevation environments (Sánchez-González et al. 2015). Similar changes in plumage patterns like the one detected in our study, and their correlation with environmental variables, have been also documented for other bird groups throughout the World (see Bowers 1960, Hall et al. 1966, Wunderle 1981, Galeotti and Cesaris 1996, Grunst et al. 2014, Reudnik et al. 2015). At the molecular level, plumage color changes are apparently a result of the concentration of lutein in the feather (Johnson and Brush 1972, Brush and Johnson 1976, McGraw and Hill 2006), however the specific mechanism in *Atlapetes* is unknown, although some studies point to single point mutations at the MCR-1 (melanocortin-1 receptor gene) as respon-

sible for similar plumage changes in birds (reviewed in Mundy 2005, but see Cadena et al. 2011). Consistent with previous molecular-based studies, this study also supported that mtDNA variation does not correspond to plumage pattern differentiation in this species (Sánchez-González et al. 2015), suggesting that plumage coloration pattern in *A. albinucha* may be taxonomically misleading because it doesn't reflect population history. In addition, it has been shown that vocal repertories are very similar and calls between color morphs cannot be reliably differentiated (Sánchez-González et al. 2015, Boesman 2016).

Results in this paper are not conclusive in terms of the currently accepted taxonomy for *A. albinucha*. Genetic divergence as a result of allotypy is apparent, suggesting that these taxa are likely at allotypy (Omland et al. 2006). Results in other bird taxa where allotypy has been found, show support to maintain recognized species, as genetic divergence is accompanied by morphological divergence (e. g., Peters and Omland 2007, Johnson et al. 2007), whereas others advocate to a single widespread (albeit genetically differentiated) species (e. g., Peters et al. 2005, Omland et al. 2006), lending an ambiguous support for species recognition. The study of Johnson et al. (2007) offered however, a threshold for species and subspecies recognition for a Neotropical raptor. The application of such a threshold for *A. albinucha* would support a subspecific status for all populations analyzed, thus maintaining the current taxonomic treatment (Paynter 1978, AOU 1998, Gill and Donsker 2015). However, further studies should be extended to include southern Central American populations and other genetic markers. Finally, results presented here underline that a general pattern for the evolution of montane bird taxa in Mesoamerica and Northern South America should consider several exceptions like the one depicted here for *A. albinucha*, as well as emphasize the role of idiosyncratic events in the recent evolution of bird taxa in this region, as it has been suggested for lowland bird taxa (Smith et al. 2014).

Conclusions

Genetic patterns found in *A. albinucha* were unexpected given previous findings in birds and other taxa codistributed in montane forests throughout the region (see Ornelas et al. 2013), which in general have showed corresponding patterns of genetic and morphological divergence (e. g., García-Moreno et al. 2004, Pérez-Emán et al. 2010).

The phylogeography of *A. albinucha* is consistent with allotypy, which has been suggested to represent an intermediate stage in the path to reciprocal monophyly (Omland et al. 2006). Most cases of allotypy have been reported in temperate birds from Eurasia (Peters et al. 2005, Omland et al. 2006, Peters and Omland 2007) as well as in the Eremian birds from Australia (Joseph and Wilke 2007), as well as in the Neotropics (see also Arbeláez-Cortés et al. 2010).

Environmental factors may have played a major role in shaping the evolution of morphological traits by natural selection that have been considered taxonomically relevant (Ball and Avise 1992), such as coloration pattern seen across the entire lineage (Paynter 1972, 1978, Remsen and Graves 1995, Sánchez-González et al. 2015), but that are not congruent with the genetic divergence indicated by mtDNA.

Acknowledgements

This contribution is part of AR-M Undergraduate Thesis and was supported by a scholarship from PAPIIT. Financial support was obtained from CONACyT 152060 and PAPIIT 215515 to AGN-S, and from Vicerrectoría de Investigación y Extensión of Universidad Industrial de Santander, Colombia, under Grant *Proyecto de investigación capital semilla* 2300 to EA-C. We thank the University of Kansas (M. B. Robbins & A. T. Peterson), the Colección de Tejidos del Instituto de Investigación de Recursos Biológicos "Alexander von Humboldt", and the Museo de Zoología de la Facultad de Ciencias "Alfonso L. Herrera" and their respective staff for kindly providing tissue samples used in this study; a special acknowledgment to all the scientific collectors that obtained and deposited samples and voucher specimens of *A. albinucha* in these collections. We thank Natural Earth (http://www.naturalearthdata.com) for providing the raster data that was used in this study to map our species distribution models. Logistic help was obtained from Jano Núñez, Fanny Rebón, and Alejandro Gordillo (at UNAM), and by Diana Espitia Reina and Claudia A. Medina Uribe (at IAvH). Comments to early versions of this paper were obtained from Laura Márquez, Leticia Ochoa, and Erick García-Trejo. We are deeply indebted to Jon Fjeldså and Knud Jønsson for their comments, which greatly improved our manuscript.

References

AOU (1998) Check-List of North American Birds (7th edn). American Ornithologists' Union, Washington, DC, 829 pp.

Arbeláez-Cortés E, Nyári ÁS, Navarro-Sigüenza AG (2010) The differential effect of lowlands on the phylogeographic pattern of a Mesoamerican montane species (*Lepidocolaptes affinis*, Aves: Furnariidae). Molecular Phylogenetics and Evolution 57: 658–68. https://doi.org/10.1016/j.ympev.2010.06.013

Arbeláez-Cortés E, Navarro-Sigüenza AG (2013) Molecular evidence of the taxonomic status of western Mexican populations of *Phaethornis longirostris* (Aves:Trochilidae). Zootaxa 3716: 81–97. https://doi.org/10.11646/zootaxa.3716.1.7

Arbogast BS, Drovetski SV, Curry RL, Boag PT, Seutin G, Grant PR, Grant RB, Anderson DJ (2006) The origin and diversification of Galapagos mockingbirds. Evolution 60 370–382. https://doi.org/10.1111/j.0014-3820.2006.tb01113.x

Avise JC (2000) Phylogeography. Harvard University Press, Cambridge, 447 pp.

Bagley JC, Johnson JB (2014) Phylogeography and biogeography of the Lower Central American Neotropics: diversification between two continents and between two seas. Biological Reviews 89: 767–790. https://doi.org/10.1111/brv.12076

Ball RM, Avise JC (1992) Mitochondrial DNA phylogeographic differentiation among avian populations and the evolutionary significance of subspecies. Auk 109(3): 626–636.

Baldwin RA (2009) Use of Maximum Entropy Modeling in Wildlife Research. Entropy 11: 854–866. https://doi.org/10.3390/e11040854

Bandelt HJ, Forster P, Röhl A (1999) Median-joining networks for inferring intraspecific phylogenies. Molecular Biology and Evolution 16(1): 37–48. https://doi.org/10.1093/oxfordjournals.molbev.a026036

Barber BR, Klicka J (2010) Two pulses of diversification across the Isthmus of Tehuantepec in a montane Mexican bird fauna. Proceedings of the Royal Society B 277(1694): 2675–2681. https://doi.org/10.1098/rspb.2010.0343

Barrera-Guzmán AO, Milá B, Sánchez-González LA, Navarro-Sigüenza AG (2012) Speciation in an avian complex endemic to the mountains of Middle America (Ergaticus, Aves: Parulidae). Molecular Phylogenetics and Evolution 62(3): 907–920. https://doi.org/10.1016/j.ympev.2011.11.020

Barve N (2008) Tool for Partial – ROC (ver 1.0). Biodiversity Institute, Lawrence.

Boesman P (2016) Notes on the vocalizations of White-naped Brush-finch (*Atlapetes albinucha*). HBW Alive Ornithological Note 364. Handbook of the Birds of the World Alive. Lynx Edicions, Barcelona. http://www.hbw.com/node/1252909 [8 February 2018]

Bonaccorso E, Navarro-Sigüenza AG, Sánchez-González LA, Townsend PA, García-Moreno J (2008) Genetic differentiation of the *Chlorospingus ophthalmicus* complex in Mexico and Central America. Journal of Avian Biology 39: 311–321. https://doi.org/10.1111/j.0908-8857.2008.04233.x

Bowers DE (1960) Correlation of variation in the wrentit with environmental gradients. Condor 62: 91–120. https://doi.org/10.2307/1365675

Brush AH, Johnson NK (1976) The evolution of colour differences between Nashville and Virginia's warblers. Condor 78: 412–414. https://doi.org/10.2307/1367707

Cadena CD, Klicka J, Ricklefs RE (2007) Evolutionary differentiation in the Neotropical montane region: Molecular phylogenetics and phylogeography of *Buarremon* brush-finches (Aves, Emberizidae). Molecular Phylogenetics and Evolution 44: 993–1016. https://doi.org/10.1016/j.ympev.2006.12.012

Cadena CD, Cheviron ZA, Funk WC (2011) Testing the molecular and evolutionary causes of a 'leapfrog' pattern of geographical variation in coloration. Journal of Evolutionary Biology 24: 402–14. https://doi.org/10.1111/j.1420-9101.2010.02175.x

Cortés-Rodríguez N, Hernández-Baños BE, Navarro-Sigüenza AG, Omland KE (2008) Geographic variation and genetic structure in the Streak-Backed Oriole: Low mitochondrial DNA differentiation reveals recent divergence. The Condor 110(4): 729–739. https://doi.org/10.1525/cond.2008.8578

Crandall KA, Templeton AR (1996) Applications of intraspecific phylogenetics. In: Harvey PH, Leigh Brown AJ, Maynard Smith J, Nee S (Eds) New Uses for New Phylogenies. Oxford University Press, Oxford, 81–99.

DaCosta JM, Spellman GM, Escalante P, Klicka J (2009) A molecular systematic revisión of two historically problematic songbird clades: *Aimophila* and *Pipilo*. Journal of Avian Biology 40: 206–216. https://doi.org/10.1111/j.1600-048X.2009.04514.x

del Hoyo J, Elliott A, Christie DA (2011) Handbook of the Birds of the World, Volume 16: Tanagers to New World Blackbirds. Lynx Editions, Barcelona, 800 pp.

Drovetsky SV, Zink RM, Fadeev IV, Nesterov EV, Koblik EA, Red'kin YA, Rohwer S (2004) Mitochondrial phylogeny of *Locustella* and related genera. Journal of Avian Biology 35(2): 105–110. https://doi.org/10.1111/j.0908-8857.2004.03217.x

Drummond AJ, Suchard MA, Xie D, Rambaut A (2012) Bayesian phylogenetics with BEAUTi and the BEAST 1.7. Molecular Biology and Evolution 29: 1969–1973. https://doi.org/10.1093/molbev/mss075

Dwight J, Griscom L (1921) A Revision of *Atlapetes gutturalis* with Descriptions of Three New Races. American Museum Novitates 16: 1–4.

ESRI (2010) ArcGIS Desktop. Environmental Systems Research Institute, Redlands.

Excoffier L, Laval G, Schneider S (2005) Arlequin ver 3.0: An integrated software package for population genetics data analysis. Evolutionary Bioinformatics Online 1: 47–50. https://doi.org/10.1177/117693430500100003

Fernández-Mazuecos M, Vargas P (2013) Congruence between distribution modelling and phylogeographical analyses reveals Quaternary survival of a toadflax species (*Linaria elegans*) in oceanic climate areas of a mountain ring range. New Phytologist 198: 1274–1289. https://doi.org/10.1111/nph.12220

Filardi CE, Smith CE (2005) Molecular phylogenetics of monarch flycatchers (genus *Monarcha*) with emphasis on Solomon Island endemics. Molecular Phylogenetics and Evolution 37(3): 776–788. https://doi.org/10.1016/j.ympev.2005.02.007

Fu YX (1997) Statistical Tests of Neutrality of Mutations Against Population Growth, Hitchhiking and Background Selection. Genetics 147: 915–925.

Galeotti P, Cesaris C (1996) Rufous and gray colour morphs in the Italian Tawny Owl: Geographical and environmental influences. Journal of Avian Biology 27: 15–20. https://doi.org/10.2307/3676956

García-Moreno J, Fjeldså J (1999) A re-evaluation of species limits in the genus *Atlapetes* based on mtDNA sequence data. Ibis 141: 199–207. https://doi.org/10.1111/j.1474-919X.1999.tb07542.x

García-Moreno J, Navarro-Sigüenza AG, Townsend-Peterson A, Sánchez-González LA (2004) Genetic variation coincides with geographic structure in the common Bush-tanager (*Chlorospingus ophthalmicus*) complex from Mexico. Molecular Phylogenetics and Evolution 33: 186–196. https://doi.org/10.1016/j.ympev.2004.05.007

GBIF Secretariat (2015) GBIF Backbone Taxonomy. http://www.gbif.org/species/2491453 [2015-07-10]

Gernhard T (2008) The conditioned reconstructed process. Journal of Theoretical Biology 253: 769–778. https://doi.org/10.1016/j.jtbi.2008.04.005

Gill F, Donsker D (2015) IOC Bird World List (Version 5.2). [updated 2015-04-23]

Gill F, Donsker D (2018) IOC World Bird List (Version 8.2). https://doi.org/10.14344/IOC.ML.8.2

Grant WS, Bowen BW (1998) Shallow population histories in deep evolutionary lineages of marine fishes: Insights from sardines and anchovies and lessons for conservation. Journal of Heredity 89(5): 415–426. https://doi.org/10.1093/jhered/89.5.415

Grunst AS, Salgado-Ortiz J, Rotenberry JT, Grunst ML (2014) Phaeomelanin-and carotenoid-based pigmentation reflect oxidative status in two populations of the yellow warbler (*Setophaga petechia*). Behavioral Ecology and Sociobiology 68: 669–80. https://doi.org/10.1007/s00265-013-1681-8

Gutiérrez-Rodríguez C, Ornelas JF, Rodríguez-Gómez F (2011) Chloroplast DNA phylogeography of a distylous shrub (*Palicourea padifolia*, Rubiaceae) reveals past fragmentation and

demographic expansion in Mexican cloud forests. Molecular Phylogenetics and Evolution 61: 603–615. https://doi.org/10.1016/j.ympev.2011.08.023

Hackett SJ (1996) Molecular phylogenetics and biogeography of tanagers in the genus *Ramphocelus* (Aves). Molecular Phylogenetics and Evolution 5(2): 368–382. https://doi.org/10.1006/mpev.1996.0032

Hall BP, Moreau RE, Galbraith CJ (1966) Polymorphism and parallelism in the african bush-shrikes of the genus *Malaconotus* (including *Chlorophoneus*). Ibis 108: 161–162. https://doi.org/10.1111/j.1474-919X.1966.tb07266.x

Harrison SP, Bartlein PJ, Brewer S, Prentice IC, Boyd M, Hessler L, Holmgren K, Izumi K, Willis K (2014) Climate model benchmarking with glacial and mid-Holocene climates. Climate Dynamics 43: 671–688. https://doi.org/10.1007/s00382-013-1922-6

Harpending HC, Batzer MA, Gurven M, Jorde LB, Rogers AR, Sherry ST (1998) Genetic traces of ancient demography. Proceedings of the National Academy of Sciences 95(4): 1961–1967. https://doi.org/10.1073/pnas.95.4.1961

Hartl DL, Clark AG (1997) Principles of Population Genetics (Vol. 116). Sinauer Associates, Sunderland, 542 pp.

Hewitt G (2000) The genetic legacy of the Quaternary Ice Ages. Nature 405(6789): 907–913. https://doi.org/10.1038/35016000

Hijmans RJ, Cameron SE, Parra JL, Jones PG, Jarvis A (2005) Very high resolution interpolated climate surfaces for global land areas. International Journal of Climatology 25: 1965–1978. https://doi.org/10.1002/joc.1276

Ho SY, Shapiro B (2011) Skyline-plot methods for estimating demographic history from nucleotide sequences. Molecular Ecology Resources 11(3): 423–434. https://doi.org/10.1111/j.1755-0998.2011.02988.x

Hooghiemstra H, Wijninga VM, Cleef AM (2006) The paleobotanical record of Colombia: implications for biogeography and biodiversity. Annals of the Missouri Botanical Garden 93(2): 297–325. https://doi.org/10.3417/0026-6493(2006)93[297:TPROCI]2.0.CO;2

Houston DD, Shiozawa DK, Tilston Smith B, Riddle BR (2014) Investigating the effects of Pleistocene events on genetic divergence within *Richardsonius balteatus*, a widely distributed western North American minnow. BMC Evolutionary Biology 14: 111. https://doi.org/10.1186/1471-2148-14-111

Howell SNG, Webb S (1995) A guide to The Birds of Mexico and Northern Central America. Oxford University Press, 1010 pp.

Hudson RR (1990) Gene genealogies and the coalescent process. Oxford Surveys in Evolutionary Biology 7: 1–44.

Jezkova T, Riddle BR, Card DC, Schield DR, Eckstut ME, Castoe TA (2015) Genetic consequences of postglacial range expansion in two codistributed rodents (genus *Dipodomys*) depend on ecology and genetic locus. Molecular Ecology 24: 83–97. https://doi.org/10.1111/mec.13012

Johnson NK, Brush AH (1972) Analysis of polymorphism in the Sooty-capped Bush-tanager. Systematic Zoology 21: 245–26. https://doi.org/10.2307/2412163

Johnson JA, Thorstrom R, Mindell DP (2007) Systematics and conservation of the hook-billed kite including the island taxa from Cuba and Grenada. Animal Conservation 10: 349–59. https://doi.org/10.1111/j.1469-1795.2007.00118.x

Joseph L, Wilke T, Ten Have J, Chesser TR (2006) Implications of mitochondrial DNA polyphyly in two ecologically undifferentiated but morphologically distinct migratory birds, the masked and white-browed woodswallows *Artamus* spp. of inland Australia. Journal of Avian Biology 37: 625–36. https://doi.org/10.1111/j.0908-8857.2006.03767.x

Joseph L, Wilke T (2007) Lack of phylogeographic structure in three widespread Australian birds reinforces emerging challenges in Australian historical biogeography. Journal of Biogeography 34: 612–24. https://doi.org/10.1111/j.1365-2699.2006.01635.x

Joseph L, Omland KE (2009) Rowley Review. Phylogeography: its development and impact in Australo-Papuan ornithology with special reference to paraphyly in Australian birds. Emu 2009 109: 1–23. https://doi.org/10.1071/MU08024

Klicka J, Burns K, Spellman GM (2007) Defining a monophyletic Cardonalini: A molecular perspective. Molecular Phylogenetics and Evolution 45: 1014–1032. https://doi.org/10.1016/j.ympev.2007.07.006

Kocher TD, Thomas WK, Meyer A, Edwards SV, Paabo S, Villablanca FX, Wilson AC (1989) Dynamics of Mitochondrial DNA Evolution in Animals: Amplification and Sequencing with Conserved Primers. Proceedings of the National Academy of Sciences 86: 6196–6200. https://doi.org/10.1073/pnas.86.16.6196

Lanfear R, Calcott B, Ho SYW, Guindon S (2012) PartitionFinder: Combined Selection of Partitioning Schemes and Substitution Models for Phylogenetic Analyses. Molecular Biology and Evolution 29(6): 1695–1701. https://doi.org/10.1093/molbev/mss020

Lovette IJ (2004) Mitochondrial dating and mixed support for the "2% rule" in birds. Auk 121: 1–6.

McGraw KJ, Hill GE (2006) Mechanics of carotenoid-based coloration. Bird coloration Vol 1: 177–242.

Mendoza-González G, Martínez ML, Rojas-Soto O, Téllez-Valdés O, Arias-Del Razo I (2016) Priority areas for conservation of beach and dune vegetation of the Mexican Atlantic coast. Journal for Nature Conservation 33: 25–34. https://doi.org/10.1016/j.jnc.2016.04.007

Mundy NI (2005) A window on the genetics of evolution: MC1R and plumage colouration in birds. Proceedings of the Royal Society B 272: 1633–1640. https://doi.org/10.1098/rspb.2005.3107

Navarro-Sigüenza AG, Peterson AT (2004) An Alternative Species Taxonomy of the Birds of Mexico. Biota Neotropica 4(2): 1–32.

Navarro-Sigüenza AG, Peterson AT, Nyari A, García-Deras GM, García-Moreno J (2008) Phylogeography of the *Buarremon* brush-finch complex (Aves, Emberizidae) in Mesoamerica. Molecular Phylogenetics and Evolution 47: 21–35. https://doi.org/10.1016/j.ympev.2007.11.030

Ng KW, Pointing SB, Dvornyk V (2013) Patterns of nucleotide diversity of the *IdpA* circadian gene in closely related species of cyanobacteria from extreme cold deserts. Applied and Environmental Microbiology 79(5): 1516–1522. https://doi.org/10.1128/AEM.03439-12

Omland KE, Baker JM, Peters JL (2006) Genetic signatures of intermediate divergence: population history of Old and New World Holarctic ravens (*Corvus corax*). Molecular Ecology 15: 795–808. https://doi.org/10.1111/j.1365-294X.2005.02827.x

Ornelas JF, Ruiz-Sánchez E, Sosa V (2010) Phylogeography of *Podocarpus matudae* (Podocarpaceae): pre-quaternary relicts in northern Mesoamerican cloud forests. Journal of Biogeography 37: 2384–2396. https://doi.org/10.1111/j.1365-2699.2010.02372.x

Ornelas JF, Sosa V, Soltis DE, Daza JM, González C, Soltis PS, Gutiérrez-Rodríguez C, Espinosa de los Monteros A, Castoe TA, Bell C, Ruiz-Sánchez E (2013) Comparative phylogeographic analyses illustrate the complex evolutionary history of threatened cloud forests of northern Mesoamerica. PLoS ONE 8: e56283 https://doi.org/10.1371/journal.pone.0056283

Ornelas JF, González C, Hernández-Baños BE, García-Moreno J (2016) Molecular and iridescent feather reflectance data reveal recent genetic diversification and phenotypic differentiation in a cloud forest hummingbird. Ecology and Evolution 6: 1104–1127. https://doi.org/10.1002/ece3.1950

Ortiz-Ramírez MF, Andersen MJ, Zaldívar-Riverón A, Ornelas JF, Navarro-Sigüenza AG (2016) Geographic isolation drives divergence of uncorrelated genetic and song variation in the Ruddy-capped Nightingale-Thrush (*Catharus frantzii*; Aves: Turdidae). Molecular Phylogenetics and Evolution 94(Pt A): 74–86. https://doi.org/10.1016/j.ympev.2015.08.017

Paynter RA (1972) Biology and evolution of the *Atlapetes schistaceus* species-group (Aves: Emberizinae). Bulletin of the Museum of Comparative Zoology 148: 297–320.

Paynter RA (1978) Biology and Evolution of the avian genus *Atlapetes* (Emberizinae). Bulletin of the Museum of Comparative Zoology 148: 323–369.

Pérez-Emán JL, Mumme RL, Jablonski PG (2010) Phylogeography and adaptive plumage evolution in Central American subspecies of the slate-throated Redstart (*Myioborus miniatus*). Ornithological Monographs 67: 90–102. https://doi.org/10.1525/om.2010.67.1.90

Peters JL, Gretes W, Omland KE (2005) Late Pleistocene divergence between eastern and western populations of wood ducks (*Aix sponsa*) inferred by the 'isolation with migration' coalescent method. Molecular Ecology 14: 3407–18. https://doi.org/10.1111/j.1365-294X.2005.02618.x

Peters JL, Omland KE (2007) Population structure and mitochondrial polyphyly in North American Gadwalls (*Anas strepera*). Auk 124: 444–462. https://doi.org/10.1642/0004-8038(2007)124[444:PSAMPI]2.0.CO;2

Peterson AT, Papes M, Soberón J (2008) Rethinking receiver operating characteristic analysis applications in ecological niche modeling. Ecological Modelling 213: 63–72. https://doi.org/10.1016/j.ecolmodel.2007.11.008

Phillips SJ, Anderson RP, Schapire RE (2006) Maximum entropy modeling of species geographic distributions. Ecological Modelling 190: 231–259. https://doi.org/10.1016/j.ecolmodel.2005.03.026

Rambaut A, Suchard MA, Xie D, Drummond AJ (2014) Tracer v1.6. http://beast.bio.ed.ac.uk/Tracer

Ramírez-Barahona S, Eguiarte LE (2013) The role of glacial cycles in promoting genetic diversity in the Neotropics: the case of cloud forests during the Last Glacial Maximum. Ecology and Evolution 3(3): 725–738. https://doi.org/10.1002/ece3.483

Ray N, Currat M, Excoffier L (2003) Intra deme Molecular Diversity in Spatially Expanding Populations. Molecular Biology and Evolution 20(1): 76–86.

Remsen JV (1984) High incidence of "leapfrog" pattern of geographic variation in Andean birds: implications for the speciation process. Science 224(4645): 171–173. https://doi.org/10.1126/science.224.4645.171

Remsen JV, White Solomon Graves IV (1995) Distribution patterns and zoogeography of *Atlapetes* brush-finches (Emberizinae) of the Andes. The Auk 112: 210–224. https://doi.org/10.2307/4088780

Remsen JV, Areta JIJr, Cadena CD, Jaramillo A, Nores M, Pacheco JF, Robbins MB, Stiles FG, Stotz DF, Zimmer KJ (2015) A Classification of the Bird Species of South America. American Ornithologists' Union. http://www.museum.lsu.edu/-Remsen/SACCBaseline.html

Rheindt FE, Székely T, Edwards SV, Lee PLM, Burke T, et al. (2011) Conflict between Genetic and Phenotypic Differentiation: The Evolutionary History of a "Lost and Rediscovered" Shorebird. PLoS ONE 6(11): e26995. https://doi.org/10.1371/journal.pone.0026995

Ricklefs RE, Latham RE (1992) Intercontinental correlation of geographical ranges suggests stasis in ecological traits of relict genera of temperate perennial herbs. The American Naturalist 139: 1305–1321. https://doi.org/10.1086/285388

Rojas-Soto O, Sosa V, Ornelas JF (2012) Forecasting cloud forest in eastern and southern Mexico: conservation insights under future climate change scenarios. Biodiversity Conservation 21: 2671–2690. https://doi.org/10.1007/s10531-012-0327-x

Ronquist F, Huelsenbeck J, Teslenko M (2011) MrBayes 3.2: Efficient Bayesian phylogenetic inference and model choice across a large model space. Systematic Biology 61(3): 539–542. https://doi.org/10.1093/sysbio/sys029

Sánchez-González LA, Navarro-Sigüenza AG, Krabbe NK, Fjeldså J, García-Moreno J (2015) Diversification in the Andes: the *Atlapetes* brush-finches. Zoologica Scripta 44(2): 135–152. https://doi.org/10.1111/zsc.12088

Silvestro D, Michalak I (2012) raxmlGUI: a graphical front-end for RAxML. Organisms Diversity & Evolution 12(4): 335–337. https://doi.org/10.1007/s13127-011-0056-0

Smith BT, McCormack JE, Cuervo AM, Hickerson MJ, Aleixo A, Cadena CD, Pérez-Emán J, Burney CW, Xie X, Harvey MG, Faircloth BC (2014) The drivers of tropical speciation. Nature 515: 406. https://doi.org/10.1038/nature13687

Sorenson MD, Ast JC, Dimcheff DE, Yuri T, Mindell DP (1999) Primers for a PCR-based approach to mitochondrial genome sequencing in birds and other vertebrates. Molecular Phylogenetics and Evolution 12: 105–114. https://doi.org/10.1006/mpev.1998.0602

Stamatakis A (2006) RAxML-VI-HPC: maximum likelihood-based phylogenetic analyses with thousands of taxa and mixed models. Bioinformatics 22(21): 2688–2690. https://doi.org/10.1093/bioinformatics/btl446

Stamatakis A (2014) RAxML version 8: a tool for phylogenetic analysis and post-analysis of large phylogenies. Bioinformatics 30(9): 1312–1313. https://doi.org/10.1093/bioinformatics/btu033

Tajima F (1989) Statistical Method for Testing the Neutral Mutation Hypothesis by DNA Polymorphism. Genetics 123: 585–595.

Thompson JD, Gibson TJ, Plewniak F, Jeanmougin F, Higgins DG (1997) The ClustalX windows interface: flexible strategies for multiple sequence alignment aided by quality analysis tools. Nucleic Acids Research 25: 4876–4882. https://doi.org/10.1093/nar/25.24.4876

Uy JA, Moyle RG, Filardi CE, Cheviron ZA (2009) Difference in plumage color used in species recognition between incipient species is linked to a single amino acid substitution in the melanocortin-1 receptor. American Naturalist 174: 244–54. https://doi.org/10.1086/600084

Wachowiak N, Boratynska K, Cavers S (2013) Geographic patterns of nucleotide diversity and population differentiation in three closely related European pine species from the *Pinus mugo* complex. Botanical Journal of the Linnean Society 172(2): 225–238. https://doi.org/10.1111/boj.12049

Warren DL, Seifert SN (2011) Ecological niche modeling in Maxent: the importance of model complexity and the performance of model selection criteria. Ecological Applications 21(2): 335–342. https://doi.org/10.1890/10-1171.1

Weir JT (2006) Divergent timing and patterns of species accumulation in lowland and highland neotropical birds. Evolution 60: 842–855. https://doi.org/10.1111/j.0014-3820.2006.tb01161.x

Weir JT, Bermingham E, Miller MJ, Klicka J, González MA (2008) Phylogeography of a morphologically diverse Neotropical montane species, the Common Bush-Tanager (*Chlorospingus ophthalmicus*). Molecular Phylogenetics and Evolution 47: 650–664. https://doi.org/10.1016/j.ympev.2008.02.004

Wright S (1931) Evolution in Mendelian populations. Genetics 16(2): 97–159.

Wright S (1978) Evolution and genetics of populations. Vol 4. Variability Within and Among Natural Populations. University of Chicago Press, 590 pp.

Wunderle J (1981) An analysis of morph ratio cline in the bananaquit (*Coereba flaveola*) on St. Vincent, West Indies. Evolution 35: 333–344.

Xie WG, Lewis PO, Fan Y, Kuo L, Chen MH (2011) Improving marginal likelihood estimation for bayesian phylogenetic model selection. Systematic Biology 60: 150–160. https://doi.org/10.1093/sysbio/syq085

Yule GU (1925) A Mathematical theory of evolution based on the conclusions of Dr. J C Willis. Philosophical Transactions of the Royal Society B 213: 21–87. https://doi.org/10.1098/rstb.1925.0002

Zink RM, Blackwell-Rago RC (2000) Species limits and recent population history in the curve-billed thrasher. The Condor 102: 881–886. https://doi.org/10.1650/0010-5422(2000)102[0881:SLARPH]2.0.CO;2